Polyethylenimine-based Nucleic Acid Delivery

Dissertation zur Erlangung des Doktorgrades der Naturwissenschaften
(Dr. rer. nat.)
der Fakultät Chemie und Pharmazie der Universität Regensburg

vorgelegt von
Miriam Breunig
aus Mudau
im Oktober 2005

Diese Doktorarbeit entstand in der Zeit von Januar 2002 bis Oktober 2005 am Lehrstuhl für Pharmazeutische Technologie an der Universität Regensburg.

Die Arbeit wurde von Prof. Dr. Achim Göpferich angeleitet.

Promotionsgesuch eingereicht am:	12. Oktober 2005	
Mündliche Prüfung am:	18. November 2005	
Prüfungsausschuss:	Prof. Dr. J. Heilmann	(Vorsitzender)
	Prof. Dr. A. Göpferich	(Erstgutachter)
	Prof. Dr. A. Kurtz	(Zweitgutachter)
	Prof. Dr. R. Witzgall	(Drittprüfer)

Meinen Eltern

in Liebe und Dankbarkeit gewidmet

Eine Theorie ist desto eindrucksvoller, je größer die Einfachheit ihrer Prämissen ist, je verschiedenartigere Dinge sie verknüpft und je weiter ihr Anwendungsbereich ist.

(Albert Einstein)

Table of Contents

Chapter 1

Introduction
and
Goals of the Thesis

Non-viral nucleic acid delivery

With recent advances in molecular biology and the sequencing of the human genome, nucleic acids (DNAs and RNAs) are expected to assume a pivotal position as drugs in the treatment of genetic and acquired diseases. The minimalist approach towards a gene therapy application is the use of 'naked' DNA without any carrier. However, due to limited uptake, rapid degradation by nucleases and fast clearance from the plasma [1-3], carrier systems are required for efficient nucleic acid delivery.

The carrier system has to overcome many obstacles: it has to transport the DNA to the proper cell type, mediate cell entry, avoid endo-lysosomal degradation, translocate the DNA to the nucleus and promote efficient gene expression (Figure 1).

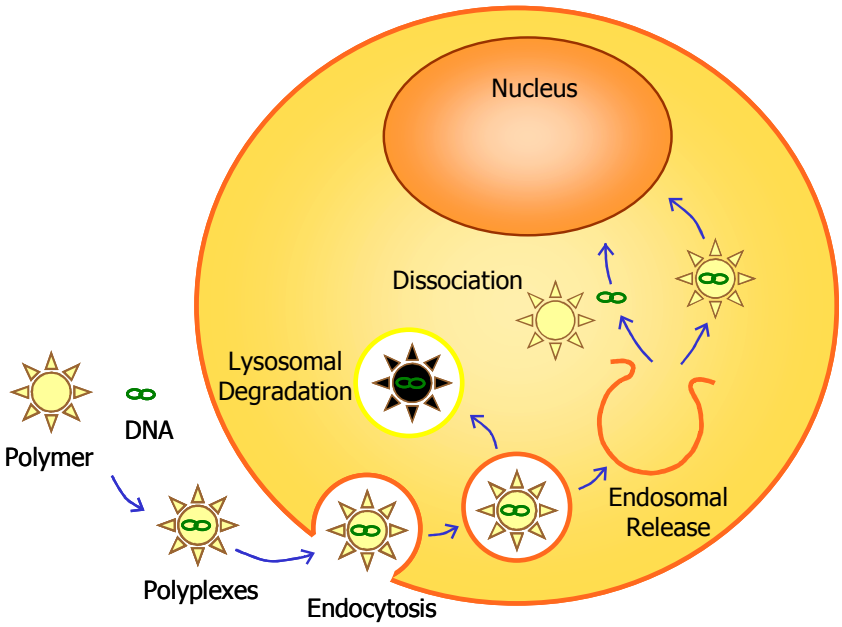

Figure 1: Obstacles in gene delivery following in vitro administration. The carrier system, here a cationic polymer, should efficiently condense DNA into polyplexes, bind to the plasma membrane, be internalized by a target cell, avoid endo-lysosomal degradation and transport the DNA to the nucleus to be transcribed.

Viral vectors have been engineering by evolution to wrapping DNA and embody many of the required characteristics for efficient gene transfer. The application of viruses as gene carriers has advanced to the stage of clinical trials for the treatment of cancer [4] and monogenetic hereditery diseases [5] as well as to treat vascular [6] and infectious diseases [7]. The cumulative number of clinical trials exceeded 1,000 by 2005 [8], however, progressed only moderately as several regulatory agencies put a temporary hold on new or ongoing trials [9],

due to severe safety risks based on the immunogenicity and oncogenic potential of the viral vectors [10,11].

In the light of these concerns, non-viral strategies have emerged as potential alternatives for nucleic acid-based therapeutics. Mechanical and physical methods such as the gene gun, electroporation, sonoporation or laser irradiation have been introduced [12], but their major disadvantage is that the target tissue must be surgically exposed for gene transfer. Cationic lipids have also been tested in various clinical trials, however, they lack adaquate efficacy, are toxic upon repeated use and bear a significant inflammatory toxicity *in vivo* [13,14]. Therefore, the attention has turned to a number of cationic polymers as carriers for nucleic acid delivery. Among several polymeric candidates, such as poly(L-lysine) (PLL), chitosan and poly(diethylaminoethyl methylacrylate) (pDEAEMA) that exhibit differences concerning their charge density, hydrophilicity and structure (for reviews see [15,16]), poly(ethylenimine) (PEI) has gained some prominence [17].

Although initially, polymer-mediated transfection efficacy had been relatively low compared to viral systems, significant progress has been made over the past decade regarding the carrier design, allowing transfection agents to perform multiple tasks, and the efficiency in cell lines cultured *in vitro* has steadily improved. The most potent polyplex formulations have reached efficiencies comparable to those of viral vectors, although far more particles are required per cell for successful transfection. However, the non-viral gene delivery systems still lack adequate efficiency in many primary cells both *in vitro* and *in vivo*.

Improvement of the transfection efficiency is one of the most important research subjects for non-viral gene delivery systems. Therefore, investigations into intracellular mechanism of gene expression have attracted interest.

PEI - polyplexes, structure, transfection and cytotoxicity

The ability of PEI to complex DNA into stable complexes, also termed polyplexes, via electrostatic interactions is a necessary prerequisite for efficient delivery into cells. The polyplex properties are not only dependent on the polymer characteristics, but also on other factors, such as the composition of the complexes, e.g. the ratio of nitrogens in polymer to phosphates in DNA (NP ratio) and the medium for polyplex building [18]. In the past, only limited attention has been given to the structure and composition of polyplexes. However, a recent study using fluorescence correlation spectroscopy (FCS) with two-photon-excitation showed that polyplexes contained on average about 3.5 plasmid DNAs and 30 PEI (25 kDa) molecules, while a high proportion of polymer (~86%) remained in its free, unbound form

[19]. The free polymer may play a significant part in cytotoxicity. Nevertheless, an excess of polycation is necessary, because the cationic surface charge of polyplexes mediates the interaction with the negatively charged cell membrane [20].

PEI exists as a branched polymer (BPEI), commercially available in a broad range of molecular weights (MWs), as well as in its linear form (LPEI). The transfection efficiency and cytotoxicity [21] of PEI-based transfection systems depends on the MW, the degree of branching, the cationic charge density and buffer capacity of the polymer [22-24]. High MW BPEI has been shown to have a superior transfection efficiency compared to BPEIs with lower MW [24], but unfortunately, the higher transfection efficiency was accompanied by a decrease in the cell viability. Therefore, among BPEIs, a MW of 25 kDa is commonly believed to be most suitable for gene transfer. Polyplexes containing LPEIs have recently been shown to have an improved transfection efficiency and cell viability compared to BPEI-based transfection systems [25-28].

Intracellular pathway

Binding and uptake

Early steps in transfection involve the binding of polyplexes to the cell surface and their internalization or uptake into the cell cytosol. Unmodified polyplexes interact non-specifically with the negatively charged cell membrane due to their positive surface charge. Heparan sulfate proteoglycans have been suggested to play a major role in this interaction of lipopolyamine/DNA complexes [20]. This hypothesis could be verified and extended to apply to both PLL and PEI as well as some lipids [29,30]. Kopatz *et al.* also corroborated these findings with drug inhibition experiments analyzed with flow cytomerty and confocal laser scanning microscopy (CLSM) by demonstrating that heparan sulfate proteoglycans, presumably syndecans, play a major role in the cell entry of non-viral vectors [31]. Passive targeting with unmodified polyplexes is the simplest approach for polyplex binding to the cell membrane.

Active targeting using receptor-mediated uptake of modified polyplexes may enhance their availability in specific cells. This strategy has been used to deliver nucleic acids to hepatocytes [32], tracheal epithelial [33] and dendritic cells [34] via carbohydrates. Tumor tissues have been targeted via the folate [35,36], integrin [37-39], or transferrin [40,41] receptors, and targeting to specific tissues has been accomplished with antibodies or their fragments [42,43].

Recently, protein transduction domains (PTDs) have gained interest as sequences that may enhance cellular uptake of polyplexes and circumvent the endo-lysosomal pathway. For example, the HIV-1 TAT derived peptide is a small basic peptide that has successfully been shown to deliver a variety of cargos, from small particles [44,45] to proteins and peptides ([46], for reviews see [47,48]) and nucleic acids [49] to the cytoplasm of cells. The 'transduction domain' or region containing cell penetration properties appears to be confined to a small stretch of basic amino acids with the sequence RKKRRQRRR [50,51]. The mechanism by which the TAT peptide associates with and crosses the plasma membrane is currently a topic of heated discussion in the literature (for reviews see [52-54]).

Endocytosis or endocytosis-like mechanisms have been proposed as main pathways for the internalization of polyplexes. Generally, endocytosis occurs by multiple mechanisms that fall into two broad categories, 'phagocytosis' (the uptake of large particles) and 'pinocytosis' (the uptake of fluid and solutes) (for reviews see [55,56]). Phagocytosis is typically restricted to specialized mammalian cells, whereas pinocytosis occurs in all cells by at least four basic mechanisms: macropinocytosis, clathrin-mediated endocytosis, caveolae-mediated endocytosis and clathrin- and caveolae-independent endocytosis. The exact nature of polyplex-containing endocytotic vesicles, the influence of serum, polymer type, polyplex size and cell type remains elusive. Various groups have tried to elucidate this pathway primarily using two different approaches: micoscopy analysis and endocytosis-interfering drugs. Using unmodified polyplexes consisting of fluorescently labeled jetPEI^{TM} (a LPEI type) and plasmid DNA, Kopatz *et al.* suggested the following mechanism: the electrostatic binding of DNA-containing cationic particles to syndecan heparan sulfate proteoglycans induces syndecan to cluster into rafts. Actin binding to the cytoplasmic tail of the syndecans then generates a cortical network that may pull the particle into a cell, like a kind of actin-filament-mediated 'phagocytosis' [31]. They used HeLa cells as a model cell line, the uptake of polyplexes was investigated by flow cytometry and the interaction of polyplexes with the actin skeleton by CLSM. An alternative path for uptake was described for histidylated PLL (His-PLL) - polyplexes into HepG2 cells. Blocking various pathways followed by flow cytometry indicated that polyplexes were internalized via clathrin-dependent and -independent pathways [57].

Binding and uptake seem to be a limiting step in differentiated primary cell culture using cationic lipids [58,59], it has yet to be demonstrated whether this is also true for cationic polymers. In contrast, the high endocytotic capacity of most cell lines favors the uptake of

polyplexes [33,60,61]. However, primary cells are more representative of the *in vivo* situation than transformed cell lines.

Endosomolysis

Polyplex-containing endosomes undergo a rapid maturation to late endosomes that are able to fuse with other late endosomes [62] and lysosomes [60]. DNase II is an acidic endonuclease active in lysosomes and may play a role in the destruction of DNA [63]. Therefore, the accumulation of polyplexes in lysosomes is not expected to be productive for transfection [3]. However, the chemical structure of the gene carrier plays a critical role for the endo-lysosomal escape of polyplexes: using fluorescein-labeled plasmid DNA and Texas Red Dextran as an endosome marker, Itaka *et al.* observed with CLSM that BPEI - and LPEI - polyplexes rapidly escape from endosomes, in sharp contrast to PLL - polyplexes [61]. For the endo-lysosomal escape of PEI-containing polyplexes, Behr postultated the so called 'proton sponge hypothesis' [64]: at physiolocical pH only 1 to 6 nitrogen atoms of PEI are protonated. Upon lowering the pH in endosomes, the proportion of protonated nitrogens increases and generates a charge gradient, which induces Cl^- influx. The increase in Cl^- concentration is followed by an influx of water, leading to endosomal swelling and rupture. The efficacy of the cationic PEI has been related to its extensive buffering capacity, provoking the swelling and disruption of endosomes. This hypothesis was directly supported by Sonawane *et al*. [65]. They compared the endosomal Cl^- concentration and pH after uptake of complexes containing PLL, a non-buffering polyamine, PEI or polyamidoamine (PAM), two strongly buffering polyamines, by CLSM. The polymers were labeled with pH or Cl^- sensitive fluorescent dyes. Substantially greater Cl^- accumulation and swelling were found in PEI- and PAM-containing endosomes compared to PLL-containing endosomes. In a time course, the pH of endosomes containing PEI - or PAM - polyplexes decreased slowly from 7.2 to ~5.9 over 60 minutes and then increased to 6.5 at 75 minutes. In contrast, the pH of PLL-containing endosomes decreased rapidly to 5.9, an increase was not observed.

Another mechanism for endo-lysosomal escape was suggested by Bieber *et al.* [60]: in electron microscopy studies, endosomal membrane holes have been observed and were related to the direct interaction of high MW BPEI (800 kDa) with the endosomal membrane in a non-acidic environment. The authors suggested that low MW PEIs (25kDa) also induce minor membrane damages, but that those holes may be quickly resealed. In another study, the membrane damage was found to occur in a dose dependent manner [66].

Furthermore, the endosomolytic activity seems also to depend on the particle size, suggesting that larger polyplexes entrapped in endosomes may facilitate endosomolysis compared to smaller particles [18,67]. In addition to direct membrane interaction, the release of polyplexes may also be attributed to the extension of the polymer network as a result of the increasing electrostatic repulsion of charged groups during acidification [68]. Moreover, the extent of osmotic swelling should also depend on the number of protons entering the vesicles, these may increase the swelling [69].

Regardless of the precise mechanism of escape, a large portion of DNA is trapped and eventually degraded in endo-lysosomes. The use of peptides that have fusogenic or endosome disrupting properties has been followed up to enhance cytoplasmic delivery. The benefit depends on the characteristics of the polymer: The transfection efficiency of PLL-based delivery systems, which were postulated to accumulate in the lysosomal compartment, was enhanced up to more than 1000-fold by endosomolytic compounds, while the supplementation of membrane-destabilising peptides such as INF, GALA or KALA to PEI - polyplexes that have their own potential to destabilize membranes has failed to significantly enhance transfection efficacy [42,70-73].

Several groups observed the pH environment of polymer and DNA during their trafficking through the cytosol. The pH microenvironment of polyplexes provides an indication of polyplex location, because the luminal pH decreases with the maturation of endocytotic vesicles from early endosomes (neutral pH to ~ pH 6), late endosomes (pH ~ 5-6) and lysosomes (pH ~ 4.5). Akinc *et al.* used a flow cytometry-based technique to measure the pH environment of the plasmid DNA, which was covalently double-labeled with fluorescein and Cy5. The ratio of fluorescence emission of fluorescein and Cy5 increased with the pH. Plasmid DNA complexed with PLL was trafficked to acidic lysosomes with a pH of 4.5; after condensation with BPEI and LPEI, plasmid DNA had a pH of 5.9 and 5.0, respectively, indicating that polyplexes were trafficked to less acidic organelles [74]. This would be consistent with Sonawane *et al.* [65], however, in one study the polymer was labeled and in the other one the DNA. Using a similar technique, but labeling either polymer or DNA in different experiments, Gonçalves *et al.* showed that polyplexes containing His-PLL dissociated, because His-PLL was found in a slightly acidic environment (pH 6.7) and plasmid DNA in an compartment with neutral pH (~7.4) [57]. Histidylated residues may improve the buffering capacity of PLL. This potential segregation was confirmed by double labeling the His-PLL - polyplexes and scoring the number of internalized and intact polyplexes, free DNA and polymer in CLSM pictures. A rapid segregation of plasmid DNA

from the polymer upon internalization was suggested [57]. Forrest *et al.* made observations not expected for PEI and PLL by measuring their pH environment with a similar method [75]. The data indicated that PEI does not prevent exposure of polyplexes to acidic environments in C2C12 and HepG2 cells, but were nevertheless accompanied by a rather efficient gene expression. On the contrary, avoiding pH < 6 as with PLL correlated with greatly reduced gene expression. They hypothized that their data were consistent with the proton sponge hypothesis, including swelling and rupture of the vesicles, but exposure to a highly acidic pH, perhaps within lysosomes, may be required for efficient PEI-mediated gene delivery. Some of the described results seem to be inconsistent, however, this may be due to the fact that in each study the fluorescence label was attached to different components of polyplexes, different methods for pH measurements were applied and different cell lines have been used.

The above-mentioned study with His-PLL and earlier investigations indicate that a portion of polyplexes may dissociate, although the time point is still unclear. Whether polymer and DNA are then transported in separate vesicles or if the dissociation actually occurs after vesicular transport has concluded is unknown. Some double labeled PEI/DNA complexes were intact for 18 h and a higher proportion of free polymer was also detected [60]. Godbey *et al.* showed by CLSM that a certain amount of DNA separated in the cytoplasm, but most DNA/PEI polyplexes found their way to the nucleus together [76]. Our own investigations revealed similar results: intact polyplexes were available in the cytosol and nucleus six hours after transfection and a certain amount of plasmid DNA and LPEI was freely dispersed through the cells [77]. However, due to the resolution limit of a light microscope, it remains possible that the fluorescently labeled molecules are observed colocalized without being associated. Fluorescence resonance energy transfer (FRET) between a donor fluorophore on the DNA and an acceptor fluorophore on the carrier could be a better alternative to study the complexation. Itaka *et al.* made observations concerning the conformational change of plasmid DNA after condensation with polymer, which would lead to a change in the distance between two fluorescent molecules attached to plasmid DNA [78]. Plasmid DNA complexed with LPEI showed a remarkable decrease in FRET efficiency due to disintegration of the polyplexes, while a high FRET efficiency indicated stability of BPEI - polyplexes [61]. In the same study, AFM confirmed the tighter complexation of plasmid DNA by BPEI. The dissociation of polyplexes is a critical point. If the affinity between DNA and polymer is too low, a premature dissociation may occur; however a strong affinity may prevent intracellular release. The factors influencing the potential for and velocity of polyplex dissociation have not been elucidated so far. Most likely, the dissociation depends on the polymer

characteristics as well as polyplex size. Otherwise, it has not yet been shown whether free polymer or DNA detected inside cells is due to incomplete packing into polyplexes, i.e. uptake of free polymer, or really due to polyplex disintegration inside the cell.

Nuclear entry

One of the major steps limiting non-viral gene transfer is the entry of plasmid DNA from the cytoplasm into the nucleus. CLSM observations confirmed the nuclear transport of plasmid DNA complexed to either LPEI or BPEI, but only a small portion of DNA had been transported to the nucleus [61]. The translocation efficacy of plasmid DNA has been estimated to be 1 of 1000 plasmids [79]. Complexation of plasmid DNA to PEI improved the plasmid trafficking to the nucleus and increased the access of plasmid DNA to the nucleus by 10-fold [80]. Three main reasons for the low transport rate into the nuclear compartment have been described so far. In comparison to a DNA fragment of 100 bp, which is fully mobile in cytoplasm with a diffusibility only 5 times slower than in water, the diffusion of larger DNA fragments (> 250 bp) in cytoplasm is remarkably slower, with little or no diffusion for DNAs larger than 2000 bp [81]. This is probably due to the actin skeleton restricting cytoplasmic transport of non-complexed DNA [82]. Furthermore, diffusion and nuclear uptake compete with degradation by cytosolic nucleases [1]. The half-life of DNA in the cytoplasm of HeLa and COS cells was estimated at 50 - 90 min when monitored by fluorescent in situ hybridzation (FISH) [1,83]. Regarding these two points, a possible role for endocytosis may be to transport DNA from the plasma membrane to the perinuclear region, thereby shortening the exposure time of plasmid DNA in cytoplasm. This would be in agreement with the results that DNA injected far from the nucleus resulting in less transgene expression than DNA microinjected near the nucleus [84]. Nonetheless, as the average velocity of actively transported PEI/DNA complexes was 0.2 µm/s as determined by real-time multiple particle tracking, an active gene carrier transport allows for perinuclear DNA accumulation within minutes [85]. Unfortunately, the most part of polyplexes is transported by diffusion or subdiffusion and, therefore, more perceptive to degradation. Third, the nucleus is surrounded by a double membrane, which contains highly regulated pores for transport. Typically, a mammalian cell nucleus posesses about 3,000 – 5,000 nuclear pore complexes (NPCs), which occupy about 10-25% of the nuclear surface. The pores of the nucleus, which can expand to 26 nm, serve as size exclusion barriers (for a review see [86]). Studies with protein-coated gold particles confirm this upper limit for a non-deformable cargo [87]. Small molecules enter the nucleus via passive diffusion, while macromolecules larger than 40-50 kDa only

permeate through NPCs via highly regulated active processes mediated by nuclear localization signals (NLSs) [86]. The NLS is recognized by a heterodimer protein complex of importin-α and importin-β. In the classical case of NLS-containing proteins, importin-α directly interacts with the cargo-NLS, which in turn interacts with the importin-β molecule that docks the complex to the NPC. The translocation of the cargo through the nuclear pore is energy dependent (for reviews see [88,89]).

After the disassembly of polyplexes, plasmid DNA may enter the nuclear compartment either by passive diffusion during mitosis when the nuclear envelope breaks down or active transport through the nuclear pore. The first hypothesis was supported by experiments that demonstrated a correlation between the stage of the cell cycle at the time of transfection and the final transgene expression [90,91]. To this end, cells were synchronized at various time points during the cell cycle. The transfection efficiency was much higher when cells were transfected at or near the M phase compared to tranfection in the G1 or early S phase. Brunner *et al.* showed that there are remarkable differences between various non-viral gene delivery systems. DNA electroporation and LPEI-containing polyplexes had very little cell cycle dependence in comparison to BPEI-based polyplexes or Lipofectamine-containing lipoplexes [90,91].

Into non-dividing, postmitotic cells such as neurons [92] or dendritic cells [93], the entry of plasmid DNA into the nucleus can only occur by active transport through the nuclear pores. As the translocation rate is much lower compared to cell lines, two general approaches are followed to enhance the nuclear import of plasmid DNA or polyplexes, respectively: either a sequence-specific nuclear import of plasmid DNA mediated by DNA nuclear targeting sequences (DTS) or the application of peptides carrying a NLS signal (Figure 2) [94].

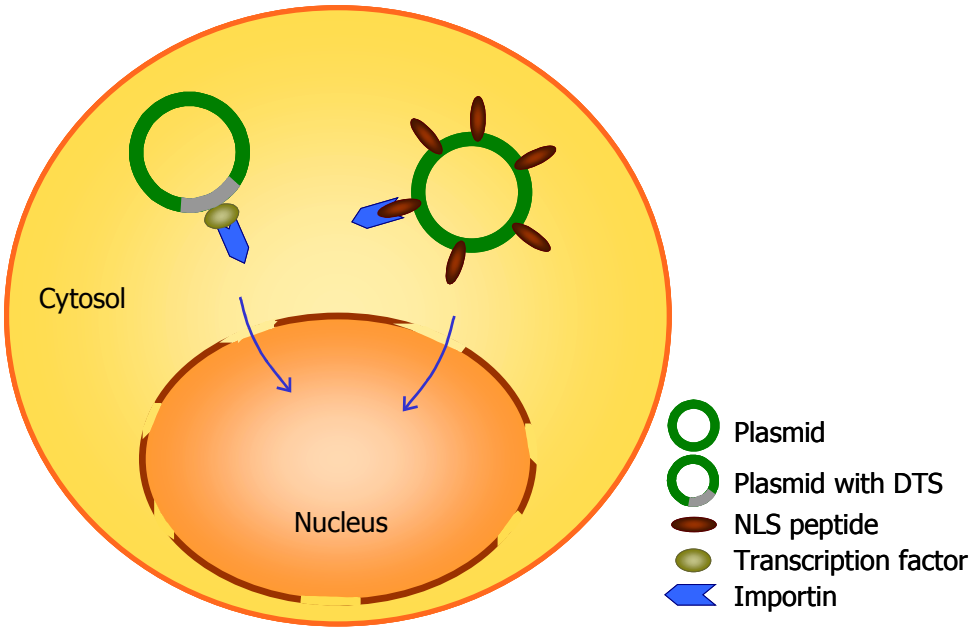

Figure 2: Approaches to increase the nuclear localization of transfected plasmids: Specific DTS incorporated in plasmid DNA allow for interaction with cytoplasmic transcription factors. As these transcription factors contain an NLS, they act as adaptors and home the plasmid DNA to the nucleus via the importin-mediated pathway. Other methods rely on the addition of NLS-peptides or NLS-containing proteins to the DNA by electrostatic, covalent or PNA clamps. By interaction with importin, the classical pathway is again followed (adapted from [94]).

Various studies provided evidence that the nuclear entry of plasmid DNA is sequence specific by applying the 72-bp enhancer repeat from the SV40 genome to support nuclear import of an otherwise cytoplasmically localized plasmid [95-97]. It is suggested that such sequences bind to NLS-containing cytoplasmic proteins, such as transcription factors. These proteins then act as adaptors between the plasmid DNA and the importin-dependent nuclear import machinery [98]. As the 72-bp element of the SV40 enhancer additionally increased CMV promotor-driven gene expression by as much as 20-fold in murine tibialis muscle *in vivo*, the SV40 DTS has two functions incorporated in one element, namely the facilitation of nuclear import and transcriptional activity. However, it remains unclear how plasmid DNA, even though it is larger in diameter, can cross a nuclear pore.

Coupling peptides containing the NLS to plasmid DNA or polymer is another approach towards enhancing nuclear uptake of cargo molecules. Coupling strategies have involved electrostatic interaction [99,100], PNA (peptide nucleic acid)-mediated hybridization [101,102] or covalent coupling to polymer or plasmid DNA [103-105]. Classical NLS peptides, such as the SV40 large T-antigen derived peptide [100,101,105], and non-classical NLS, such as the HIV-1 virus TAT derived peptide [106] and the M9 sequence from the

heterogeneous nuclear ribonucleoprotein [99,107], have been tested (for reviews see [108-110]). Despite the promising concept there is a lack of consensus concerning the potency of NLS-peptides in nucleic acid delivery. Zanta *et al.* prepared a linear, double-stranded DNA fragment encoding luciferase, endcapped to enhance the resistance against nucleases and coupled to a NLS peptide [104]. Transfection efficacy was enhanced by 10- to 30- fold in non-dividing cells such as macrophages or murine neurons and 1,000- fold in fast dividing cells such as HeLa or 3T3 when DNA was complexed to Transfectam®, BPEI 25 kDa or LPEI 22 kDa. However, in another study, linear DNA constructs containing a NLS complexed with cationic polymers failed to enhance gene expression [111]. It was also shown that a circular plasmid DNA covalently attached to NLS retained its transfection ability, but the reporter gene expression was not significantly increased [103,105,112]. Subramaniam *et al.* showed a 63-fold increase in the percentage of transfected cells in non-dividing confluent endothelial cells (83%) when plasmid was coupled to an M9-derived NLS and delivered via lipoplexes [99]. An up to 8- fold increase in the transfection efficiency was obtained when plasmid was coupled to an SV40-derived NLS and delivered into several cell lines via PEI-based polyplexes [101]. Seymour *et al.* followed up another approach by linking the adenovirus hexonprotein covalently to the polymer, namely PEI 800 kDa, and complexed it to plasmid DNA. The hexon-mediated nuclear entry enabled substantially better transgene expression compared to classical NLS in HepG2 cells, however, results were only elevated 10-fold compared to PEI/DNA complexes [113].

Concluding, success has been mixed so far, with some studies showing successful NLS-mediated nuclear delivery of oligonucelotides or linearized plasmids [101,104], but less efficient transfer of intact plasmids [103]. This is, however, not a general rule as shown by [99]. Perhaps non-dividing cells may benefit more from nuclear targeting strategies compared to cell lines, because they cannot use the breakdown of the nuclear envelope during mitosis. Furthermore, the amount of NLS per plasmid DNA required for efficient nuclear import is controversial. Both the addition of an excess [101] or only one NLS linked to DNA [104] has been successful.

Using the strategy of nuclear targeting, the specific targeting sequence should be accessible in polyplexes. However, it has been shown that compared to cationic lipids, PEI or PLL do not prevent gene expression when injected into the nucleus together with plasmid DNA [80]. Furthermore, it was also shown that DNA/PEI complexes can penetrate into the nucleus, suggesting that a complete dissociation may not be a necessary prerequisite for nuclear translocation [60,76].

Goals of the thesis

Non-viral, polymer-based nucleic acid delivery is increasingly acknowlegded to serve for both the development of novel therapeutic concepts and basic research. A functional design of polycationic carriers involves a material that enables efficient condensation of nucleic acids into polyplexes in terms of cellular uptake. Furthermore, the exposure of polyplexes to the acidic pH of the endo-lysosomal compartment requires an intrinsic ability of the polymer to facilitate endo-lysosomal release. Last, but not least, the DNA has to be transported to the nucleus to be transcribed.

A successful delivery system allows for a high transfection efficiency and is assembled from non-toxic components. However, existing polymers fail at least one of these requirements. Therefore, the work presented in this thesis aimed at testing the hypothesis that biodegradable polymers are an intelligent alternative as effective polymer-based nucleic acid delivery systems with low cytotoxicity for *in vitro* use. On the way to accomplish the overall objective, it was necessary to meet the following specific aims:

1. Investigation of low MW LPEI-based nucleic acid delivery systems

The first aim strove to overcome the frequent restriction that high transfection efficiency is limited by the cytotoxicity of the non-viral carrier. Therefore, the potential of utilizing LPEIs with a MW ranging from 1.0 to 9.5 kDa was investigated. Furthermore, it was tested whether the unique property of PEI, namely the intrinsic endo-lysosmal escape capacity, is also evident for low MW LPEIs. Finally, it was investigated if, by reducing the MW, LPEIs retain their improved nuclear import characteristics (Chapter 2).

In order to gain a more comprehensive insight into LPEI-mediated gene transfer, the uptake and stability of plasmid DNA during the transfection process were measured. As it is known that polyplexes are sensitive to changes in the ionic strength, the transfection efficiency of polyplexes generated in salt-free and -containing medium and in the presence or absence of serum was determined. The polycationic carrier should efficiently condense and protect the DNA extracellularly and release the DNA intracellularly. Therefore, the extra- and intracellular interaction of LPEIs with plasmid DNA was investigated by CLSM (Chapter 3). To measure the interaction of plasmid DNA and LPEI in a more precise distance range, Chapter 4 aimed at evaluating fluorescence resonance energy transfer (FRET) as a technique to determine the intracellular disintegration of double labeled LPEI - polyplexes. FRET was measured by different means, namely CLSM and flow cytometry, in living cells.

2. Investigation of biodegradable PEI-based nucleic acid delivery systems

The intention of Chapter 5 was to identify suitable biodegradable, high MW polymers to further decrease the toxicity of the non-viral carrier. It was hypothesized that a bioreversible crosslinking of low MW LPEIs would raise the polymer's efficacy, due to the higher MW and hence transfection efficiency, while the biodegradable linkages would undergo intracellular breakdown and hence not be toxic. In detail, various biodegradable PEIs originating from crosslinking LPEI with a MW of 2.4 kDa by bioreversible disulfide bonds were investigated concerning the transfection efficiency and cytotxicity.

Furthermore, the capacity of biodegradable PEIs for gene transfer was evaluated in human primary cells *in vitro* (Chapter 6). Two different test systems were chosen, namely non-dividing dendritic cells (DCs) and chondrocytes that have a limited mitogenic activity. As they are cheaper to maintain and more available than DCs, the HT-29 cell line was used as a model to test whether the uptake is a rate limiting step in the transfection of 'hard-to-transfet' cells using polymers.

3. Investigation of the influence of variation in the PEI backbone

Last, but not least, since it is postulated that the high cationic charge density of the PEI backbone is significantly responsible for efficient gene delivery, the impact of converting primary and secondary amines of PEI to tertiary ones on the transfection efficiency and cytotoxicity was investigated (Chapter 7).

References

1. Lechardeur D, Sohn KJ, Haardt M, Joshi PB, Monck M, Graham RW, Beatty B, Squire J, O'Brodovich H, Lukacs GL. Metabolic instability of plasmid DNA in the cytosol: a potential barrier to gene transfer. *Gene Ther* 1999; **6**: 482-497.

2. Nishikawa M, Takakura Y, Hashida M. Theoretical considerations involving the pharmacokinetics of plasmid DNA. *Adv Drug Deliv Rev* 2005; **57**: 675-688.

3. Pinto-Gonzalez Howell D, Krieser RJ, Eastman A, Barry MA. Deoxyribonuclease II is a lysosomal barrier to transfection. *Mol Ther* 2003; **8**: 957-963.

4. Merdan T, Kopecek J, Kissel T. Prospects for cationic polymers in gene and oligonucleotide therapy against cancer. *Adv Drug Deliv Rev* 2002; **54**: 715-758.

5. Ferrari S, Geddes DM, Alton EWFW. Barriers to and new approaches for gene therapy and gene delivery in cystic fibrosis. *Adv Drug Deliv Rev* 2002; **54**: 1373-1393.

6. Yla-Herttuala S, Markkanen JE, Rissanen TT. Gene therapy for ischemic cardiovascular diseases: some lessons learned from the first clinical trials. *Trends Cardiovasc Med* 2004; **14**: 295-300.

7. Buchschacher GL, Wong-Staal F. Approaches to gene therapy for human immunodeficiency virus infection. *Hum Gene Ther* 2001; **12**: 1013-1019.

8. Clinical trials. Available at: http://www.wiley.co.uk/genmed/clinical/; accessed: August 2005.

9. Edelstein ML, Abedi MR, Wixon J, Edelstein RM. Gene therapy clinical trials worldwide 1989-2004-an overview. *J Gene Med* 2004; **6**: 597-602.

10. Sadelain M. Insertional oncogenesis in gene therapy: how much of a risk? *Gene Ther* 2004; **11**: 569-573.

11. Marshall E. What to do when clear success comes with an unclear risk? *Science* 2002; **298**: 510-511.

12. Mehier-Humbert S, Guy RH. Physical methods for gene transfer: improving the kinetics of gene delivery into cells. *Adv Drug Deliv Rev* 2005; **57**: 733-753.

13. Hirko A, Tang F, Hughes JA. Cationic lipid vectors for plasmid DNA delivery. *Cur Med Chem* 2003; **10**: 1185-1193.

14. Zhang JS, Liu F, Huang L. Implications of pharmacokinetic behavior of lipoplex for its inflammatory toxicity. *Adv Drug Deliv Rev* 2005; **57**: 689-698.

15. De Smedt SC, Demeester J, Hennink WE. Cationic polymer based gene delivery systems. *Pharm Res* 2000; **17**: 113-126.

16. Han So, Mahato RI, Sung YK, Kim SW. Development of biomaterials for gene therapy. *Mol Ther* 2000; **2**: 302-317.

17. Boussif O, Lezoualc'h F, Zanta MA, Mergny MD, Scherman D, Demeneix B, Behr J. A versatile vector for gene and oligonucleotide transfer into cells in culture and in vivo: polyethylenimine. *Proc Natl Acad Sci U S A* 1995; **92**: 7297-7301.

18. Ogris M, Steinlein P, Kursa M, Mechtler K, Kircheis R, Wagner E. The size of DNA/transferrin-PEI complexes is an important factor for gene expression in cultured cells. *Gene Ther* 1998; **5**: 1425-1433.

19. Clamme JP, Azoulay J, Mely Y. Monitoring of the formation and dissociation of polyethylenimine/DNA complexes by two photon fluorescence correlation spectroscopy. *Biophys J* 2003; **84**: 1960-1968.

20. Labat-Moleur F, Steffan A-M, Brisson C, Perron H, Feugeas O, Furstenberger P, Oberling F, Brambilla E, Behr J-P. An electron microscopy study into the mechanism of gene transfer with lipopolyamines. *Gene Ther* 1996; **3**: 1010-1017.

21. Moghimi SM, Symonds P, Murray JC, Hunter AC, Debska G, Szewczyk A. A two-stage poly(ethylenimine)-mediated cytotoxicity: implications for gene transfer/therapy. *Mol Ther* 2005; **11**: 990-995.

22. Kunath K, Von Harpe A, Fischer D, Petersen H, Bickel U, Voigt K, Kissel T. Low-molecular-weight polyethylenimine as a non-viral vector for DNA delivery: comparison of physicochemical properties, transfection efficiency and in vivo distribution with high-molecular-weight polyethylenimine. *J Control Release* 2003; **89**: 113-125.

23. von Harpe A, Petersen H, Li Y, Kissel T. Characterization of commercially available and synthesized polyethylenimines for gene delivery. *J Control Release* 2000; **69**: 309-322.

24. Godbey WT, Wu KK, Mikos AG. Size matters: molecular weight affects the efficiency of poly(ethylenimine) as a gene delivery vehicle. *J Biomed Mater Res* 1999; **45**: 268-275.

25. Goula D, Becker N, Lemkine GF, Normandie P, Rodrigues J, Mantero S, Levi G, Demeneix BA. Rapid crossing of the pulmonary endothelial barrier by polyethylenimine/DNA complexes. *Gene Ther* 2000; **7**: 499-504.

26. Goula D, Benoist C, Mantero S, Merlo G, Levi G, Demeneix BA. Polyethylenimine-based intravenous delivery of transgenes to mouse lung. *Gene Ther* 1998; **5**: 1291-1295.

27. Bragonzi A, Boletta A, Biffi A, Muggia A, Sersale G, Cheng SH, Bordignon C, Assael BM, Conese M. Comparison between cationic polymers and lipids in mediating systemic gene delivery to the lungs. *Gene Ther* 1999; **6**: 1995-2004.

28. Ferrari S, Moro E, Pettenazzo A, Behr JP, Zacchello F, Scarpa M. ExGen 500 is an efficient vector for gene delivery to lung epithelial cells in vitro and in vivo. *Gene Ther* 1997; **4**: 1100-1106.

29. Mislick KA, Baldeschwieler JD. Evidence for the role of proteoglycans in cation-mediated gene transfer. *Proc Natl Acad Sci U S A* 1996; **93**: 12349-12354.

30. Ruponen M, Ronkko S, Honkakoski P, Pelkonen J, Tammi M, Urtti A. Extracellular glycosaminoglycans modify cellular trafficking of lipoplexes and polyplexes. *J Biol Chem* 2001; **276**: 33875-33880.

31. Kopatz I, Remy J, Behr J. A model for non-viral gene delivery: through syndecan adhesion molecules and powered by actin. *J Gene Med* 2004; **6**: 769-776.

32. Kunath K, Von Harpe A, Fischer D, Kissel T. Galactose-PEI-DNA complexes for targeted gene delivery: degree of substitution affects complex size and transfection efficiency. *J Control Release* 2003; **88**: 159-172.

33. Grosse S, Aron Y, Honore I, Thevenot G, Danel C, Roche AC, Monsigny M, Fajac I. Lactosylated polyethylenimine for gene transfer into airway epithelial cells: Role of the sugar moiety in cell delivery and intracellular trafficking of the complexes. *J Gene Med* 2004; **6**: 345-356.

34. Diebold SS, Kursa M, Wagner E, Cotten M, Zenke M. Mannose Polyethylenimine conjugates for targeted DNA delivery into dendritic cells. *J Biol Chem* 1999; **274**: 19087-19094.

35. Gottschalk S, Cristiano RJ, Smith LC, Woo SLC. Folate receptor-mediated DNA delivery into tumor cells: potosomal disruption results in enhanced gene expression. *Gene Ther* 2001; **1**: 185-191.

36. van Steenis JH, van Maarseveen EM, Verbaan FJ, Verrijk R, Crommelin DJA, Storm G, Hennink WE. Preparation and characterization of folate-targeted pEG-coated pDMAEMA-based polyplexes. *J Control Release* 2003; **87**: 167-176.

37. Erbacher P, Remy JS, Behr JP. Gene transfer with synthetic virus-like particles via the integrin-mediated endocytosis pathway. *Gene Ther* 1999; **6**: 138-145.

38. Woodle MC, Scaria P, Ganesh S, Subramanian K, Titmas R, Cheng C, Yang J, Pan Y, Weng K, Gu C, Torkelson S. Sterically stabilized polyplex: ligand-mediated activity. *J Control Release* 2001; **74**: 309-311.

39. Kunath K, Merdan T, Hegener O, Haeberlein H, Kissel T. Integrin targeting using RGD-PEI conjugates for in vitro gene transfer. *J Gene Med* 2003; **5**: 588-599.

40. Kircheis R, Wightman L, Schreiber A, Robitza B, Rossler V, Kursa M, Wagner E. Polyethylenimine/DNA complexes shielded by transferrin target gene expression to tumors after systemic application. *Gene Ther* 2001; **8**: 28-40.

41. Cotten M, Langle-Rouault F, Kirlappos H, Wagner E, Mechtler K, Zenke M, Beug H, Birnstiel ML. Transferrin-polycation-mediated introduction of DNA into human leukemic cells: stimulation by agents that affect the survival of transfected DNA or modulate transferrin receptor levels. *Proc Natl Acad Sci U S A* 1990; **87**: 4033-4037.

42. Kircheis R, Kichler A, Wallner G, Kursa M, Felzmann T, Buchberger M, Wagner E. Coupling of cell-binding ligands to polyethylenimine for targeted gene delivery. *Gene Ther* 1997; **4**: 409-418.

43. Merdan T, Callahan J, Petersen H, Kunath K, Bakowsky U, Kopeckova P, Kissel T, Kopecek J. Pegylated polyethylenimine-Fab' antibody fragment conjugates for targeted gene delivery to human ovarian carcinoma cells. *Bioconjug Chem* 2003; **14**: 989-996.

44. Torchilin VP, Rammohan R, Weissig V, Levchenko TS. TAT peptide on the surface of liposomes affords their efficient intracellular delivery even at low temperature and in the presence of metabolic inhibitors. *Proc Natl Acad Sci U S A* 2001; **98**: 8786-8791.

45. Tseng YL, Liu JJ, Hong RL. Translocation of liposomes into cancer cells by cell-penetrating peptides penetratin and Tat: a kinetic and efficacy study. *Mol Pharmacol* 2002; **62**: 864-872.

46. Schwarze SR, Ho A, Vocero-Akbani A, Dowdy SF. In vivo protein transduction: delivery of a biologically active protein into the mouse. *Science* 1999; **285**: 1569-1572.

47. Wadia JS, Dowdy SF. Transmembrane delivery of protein and peptide drugs by TAT-mediated transduction in the treatment of cancer. *Adv Drug Deliv Rev* 2005; **57**: 579-596.

48. Gupta B, Levchenko TS, Torchilin VP. Intracellular delivery of large molecules and small particles by cell-penetrating proteins and peptides. *Adv Drug Deliv Rev* 2005; **57**: 637-651.

49. Rudolph C, Plank C, Lausier J, Schillinger U, Muller RH, Rosenecker J. Oligomers of the arginine-rich motif of the HIV-1 Tat protein are capable of transferring plasmid DNA into cells. *J Biol Chem* 2003; **278**: 11411-11418.

50. Park J, Ryu J, Kim KA, Lee HJ, Bahn JH, Han K, Choi EY, Lee KS, Kwon HY, Choi SY. Mutational analysis of a human immunodeficiency virus type 1 Tat protein transduction domain which is required for delivery of an exogenous protein into mammalian cells. *J Gen Virol* 2002; **83**: 1173-1181.

51. Vives E, Brodin P, Lebleu B. A Truncated HIV-1 Tat protein basic domain rapidly translocates through the plasma membrane and accumulates in the cell nucleus. *J Biol Chem* 1997; **272**: 16010-16017.

52. Rothbard JB, Jessop TC, Wender PA. Adaptive translocation: the role of hydrogen bonding and membrane potential in the uptake of guanidinium-rich transporters into cells. *Adv Drug Deliv Rev* 2005; **57**: 495-504.

53. Zorko M, Langel U. Cell-penetrating peptides: mechanism and kinetics of cargo delivery. *Adv Drug Deliv Rev* 2005; **57**: 529-545.

54. Futaki S. Arginine-rich peptides: potential for intracellular delivery of macromolecules and the mystery of the translocation mechanisms. *Int J Pharm* 2002; **245**: 1-7.

55. Conner SD, Schmid SL. Regulated portals of entry into the cell. *Nature* 2003; **422**: 37-44.

56. Marsh M, McMahon HT. The structural era of endocytosis. *Science* 1999; **285**: 215-220.

57. Goncalves C, Mennesson E, Fuchs R, Gorvel JP, Midoux P, Pichon C. Macropinocytosis of polyplexes and recycling of plasmid via the clathrin-dependent pathway impair the transfection efficiency of human hepatocarcinoma cells. *Mol Ther* 2004; **10**: 373-385.

58. Matsui H, Johnson LG, Randell SH, Boucher RC. Loss of binding and entry of liposome-DNA complexes decreases transfection efficiency in differentiated airway epithelial cells. *J Biol Chem* 1997; **272**: 1117-1126.

59. Fasbender A, Zabner J, Zeiher BG, Welsh MJ. A low rate of cell proliferation and reduced DNA uptake limit cationic lipid-mediated gene transfer to primary cultures of ciliated human airway epithelia. *Gene Ther* 1997; **4**: 1173-1180.

60. Bieber T, Meissner W, Kostin S, Niemann A, Elsasser HP. Intracellular route and transcriptional competence of polyethylenimine-DNA complexes. *J Control Release* 2002; **82**: 441-454.

61. Itaka K, Harada A, Yamasaki Y, Nakamura K, Kawaguchi H, Kataoka K. In situ single cell observation by fluorescence resonance energy transfer reveals fast intra-cytoplasmic delivery and easy release of plasmid DNA complexed with linear polyethylenimine. *J Gene Med* 2004; **6**: 76-84.

62. Remy-Kristensen A, Clamme JP, Vuilleumier C, Kuhry JG, Mely Y. Role of endocytosis in the transfection of L929 fibroblasts by polyethylenimine/DNA complexes. *Biochim Biophys Acta* 2001; **1514**: 21-32.

63. Evans CJ, Aguilera RJ. DNase II: genes, enzymes and function. *Gene* 2003; **322**: 1-15.

64. Behr JP. Gene transfer with synthetic cationic amphiphiles: prospects for gene therapy. *Bioconjug Chem* 1994; **5**: 382-389.

65. Sonawane ND, Szoka FC, Verkman AS. Chloride accumulation and swelling in endosomes enhances DNA transfer by polyamine-DNA polyplexes. *J Biol Chem* 2003; **278**: 44826-44831.

66. Clamme JP, Krishnamoorthy G, Mely Y. Intracellular dynamics of the gene delivery vehicle polyethylenimine during transfection: investigation by two-photon fluorescence correlation spectroscopy. *Biochim Biophys Acta* 2003; **1617**: 52-61.

67. Wattiaux R, Laurent N, Wattiaux-De Coninck S, Jadot M. Endosomes, lysosomes: their implication in gene transfer. *Adv Drug Deliv Rev* 2000; **41**: 201-208.

68. Merdan T, Kunath K, Fischer D, Kopecek J, Kissel T. Intracellular processing of poly(ethylene imine)/ribozyme complexes can be observed in living cells by using confocal laser scanning microscopy and inhibitor experiments. *Pharm Res* 2002; **19**: 140-146.

69. Kichler A, Leborgne C, Coeytaux E, Danos O. Polyethylenimine-mediated gene delivery: a mechanistic study. *J Gene Med* 2001; **3**: 135-144.

70. Wagner E. Application of membrane-active peptides for nonviral gene delivery. *Adv Drug Deliv Rev* 1999; **38**: 279-289.

71. Midoux P, Kichler A, Boutin V, Maurizot JC, Monsigny M. Membrane permeabilization and efficient gene transfer by a peptide containing several histidines. *Bioconjug Chem* 2001; **9**: 260-267.

72. Lee H, Jeong JH, Park TG. A new gene delivery formulation of polyethylenimine/DNA complexes coated with PEG conjugated fusogenic peptide. *J Control Release* 2001; **76**: 183-192.

73. Lee H, Jeong JH, Park TG. PEG grafted polylysine with fusogenic peptide for gene delivery: high transfection efficiency with low cytotoxicity. *J Control Release* 2002; **79**: 283-291.

74. Akinc A, Langer R. Measuring the pH environment of DNA delivered using nonviral vectors: implications for lysosomal trafficking. *Biotechnol Bioeng* 2002; **78**: 503-508.

75. Forrest ML, Pack DW. On the kinetics of polyplex endocytic trafficking: implications for gene delivery vector design. *Mol Ther* 2002; **6**: 57-66.

76. Godbey WT, Wu KK, Mikos AG. Tracking the intracellular path of poly(ethylenimine)/DNA complexes for gene delivery. *Proc Natl Acad Sci U S A* 1999; **96**: 5177-5181.

77. Breunig M, Lungwitz U, Liebl R, Fontanari C, Klar J, Kurtz A, Blunk T, Goepferich A. Gene delivery with low molecular weight linear polyethylenimines. *J Gene Med* 2005; **7**: 1287-1298.

78. Itaka K, Harada A, Nakamura K, Kawaguchi H, Kataoka K. Evaluation by fluorescence resonance energy transfer of the stability of nonviral gene delivery vectors under physiological conditions. *Biomacromolecules* 2002; **3**: 841-845.

79. Pollard H, Remy JS, Loussouarn G, Demolombe S, Behr JP, Escande D. Polyethylenimine but not cationic lipids promotes transgene delivery to the nucleus in mammalian cells. *J Biol Chem* 1998; **273**: 7507-7511.

80. Pollard H, Remy JS, Loussouarn G, Demolombe S, Behr JP, Escande D. Polyethylenimine but not cationic lipids promotes transgene delivery to the nucleus in mammalian cells. *J Biol Chem* 1998; **273**: 7507-7511.

81. Lukacs GL, Haggie P, Seksek O, Lechardeur D, Freedman N, Verkman AS. Size-dependent DNA mobility in cytoplasm and nucleus. *J Biol Chem* 2000; **275**: 1625-1629.

82. Dauty E, Verkman AS. Actin cytoskeleton as the principal determinant of size-dependent DNA mobility in cytoplasm: a new barrier for non-viral gene delivery. *J Biol Chem* 2005; **280**: 7823-7828.

83. Pollard H, Toumaniantz G, Amos JL, Avet-Loiseau H, Guihard G, Behr JP, Escande D. Ca2+-sensitive cytosolic nucleases prevent efficient delivery to the nucleus of injected plasmids. *J Gene Med* 2001; **3**: 153-164.

84. Dowty ME, Williams P, Zhang G, Hagstrom JE, Wolff JA. Plasmid DNA entry Into postmitotic nuclei of primary rat myotubes. *Proc Natl Acad Sci U S A* 1995; **92**: 4572-4576.

85. Suh J, Wirtz D, Hanes J. Real-time intracellular transport of gene nanocarriers studied by multiple particle tracking. *Biotechnol Prog* 2004; **20**: 598-602.

86. Talcott B, Moore MS. Getting across the nuclear pore complex. *Trends Cell Biol* 1999; **9**: 312-318.

87. Feldherr CM, Akin D. The permeability of the nuclear envelope in dividing and nondividing cell cultures. *J Cell Biol* 1990; **111**: 1-8.

88. Gasiorowski JZ, Dean DA. Mechanisms of nuclear transport and interventions. *Adv Drug Deliv Rev* 2003; **55**: 703-716.

89. Stewart M. Structural biology: nuclear trafficking. *Science* 2003; **302**: 1513-1514.

90. Brunner S, Sauer T, Carotta S, Cotten M, Saltik M, Wagner E. Cell cycle dependence of gene transfer by lipoplex, polyplex and recombinant adenovirus. *Gene Ther* 2000; **7**: 401-407.

91. Brunner S, Furtbauer E, Sauer T, Kursa M, Wagner E. Overcoming the nuclear barrier: cell cycle independent nonviral gene transfer with linear polyethylenimine or electroporation. *Mol Ther* 2002; **5**: 80-86.

92. Guerra-Crespo M, Charli JL, Rosales-Garcia VH, Pedraza-Alva G, Perez-Martinez L. Polyethylenimine improves the transfection efficiency of primary cultures of post-mitotic rat fetal hypothalamic neurons. *J Neurosci Methods* 2003; **127**: 179-192.

93. Tan PH, Beutelspacher SC, Wang YH, McClure MO, Ritter MA, Lombardi G, George AJT. Immunolipoplexes: an efficient, nonviral alternative for transfection of human dendritic cells with potential for clinical vaccination. *Mol Ther* 2005; **11**: 790-800.

94. Dean DA, Strong DD, Zimmer WE. Nuclear entry of nonviral vectors. *Gene Ther* 2005; **12**: 881-890.

95. Dean DA. Import of plasmid DNA into the nucleus is sequence specific. *Exp Cell Res* 2001; **230**: 293-302.

96. Dean DA, Dean BS, Muller S, Smith LC. Sequence requirements for plasmid nuclear import. *Exp Cell Res* 1999; **253**: 713-722.

97. Li S, MacLaughlin FC, Fewell JG, Gondo M, Wang J, Nicol F, Dean DA, Smith LC. Muscle-specific enhancement of gene expression by incorporation of SV40 enhancer in the expression plasmid. *Gene Ther* 2001; **8**: 494-497.

98. Wilson GL, Dean BS, Wang G, Dean DA. Nuclear import of plasmid DNA in digitonin-permeabilized cells requires both cytoplasmic factors and specific DNA sequences. *J Biol Chem* 1999; **274**: 22025-22032.

99. Subramanian A, Ranganathan P, Diamond SL. Nuclear targeting peptide scaffolds for lipofection of nondividing mammalian cells. *Nat Biotechnol* 1999; **17**: 873-877.

100. Chan CK, Jans DA. Enhancement of polylysine-mediated transferrinfection by nuclear localization sequences: polylysine does not function as a nuclear localization sequence. *Hum Gene Ther* 1999; **10**: 1695-1702.

101. Branden LJ, Mohamed AJ, Smith CIE. A peptide nucleic acid-nuclear localization signal fusion that mediates nuclear transport of DNA. *Nature Biotechnol* 1999; **17**: 784-787.

102. Morris MC, Chaloin L, Choob M, Archdeacon J, Heitz F, Divita G. Combination of a new generation of PNAs with a peptide-based carrier enables efficient targeting of cell cycle progression. *Gene Ther* 2004; **11**: 757-764.

103. Ciolina C, Byk G, Blanche F, Thuillier V, Scherman D, Wils P. Coupling of nuclear localization signals to plasmid DNA and specific interaction of the conjugates with importin alpha. *Bioconjug Chem* 1998; **10**: 49-55.

104. Zanta MA, Belguise-Valladier P, Behr JP. Gene delivery: A single nuclear localization signal peptide is sufficient to carry DNA to the cell nucleus. *Proc Natl Acad Sci U S A* 1999; **96**: 91-96.

105. Sebestyen MG, Ludtke JJ, Bassik MC, Zhang G, Budker V, Lukhtanov EA, Hagstrom JE, Wolff JA. DNA vector chemistry: The covalent attachment of signal peptides to plasmid DNA. *Nature Biotechnol* 1998; **16**: 80-85.

106. Sandgren S, Cheng F, Belting M. Nuclear targeting of macromolecular polyanions by an HIV-Tat derived peptide. Role for cell-surface proteoglycans. *J Biol Chem* 2002; **277**: 38877-38883.

107. Siomi H, Dreyfuss G. A nuclear localization domain in the hnRNP A1 protein. *J Cell Biol* 1995; **129**: 551-560.

108. Escriou V, Carriere M, Scherman D, Wils P. NLS bioconjugates for targeting therapeutic genes to the nucleus. *Adv Drug Deliv Rev* 2003; **55**: 295-306.

109. Munkonge FM, Dean DA, Hillery E, Griesenbach U, Alton EWFW. Emerging significance of plasmid DNA nuclear import in gene therapy. *Adv Drug Deliv Rev* 2003; **55**: 749-760.

110. Chan CK, Jans DA. Using nuclear targeting signals to enhance non-viral gene transfer. *Immunol Cell Biol* 2002; **80**: 119-130.

111. van der Aa MAEM, Koning GA, d'Oliveira C, Oosting RS, Wilschut KJ, Hennink WE, Crommelin DJA. An NLS peptide covalently linked to linear DNA does not enhance transfection efficiency of cationic polymer based gene delivery systems. *J Gene Med* 2005; **7**: 208-217.

112. Neves C, Escriou V, Byk G, Scherman D, Wils P. Intracellular fate and nuclear targeting of plasmid DNA. *Cell Biol Toxicol* 1999; **15**: 193-202.

113. Carlisle RC, Bettinger T, Ogris M, Hale S, Mautner V, Seymour LW. Adenovirus hexon protein enhances nuclear delivery and increases transgene expression of polyethylenimine/plasmid DNA vectors. *Mol Ther* 2001; **4**: 473-483.

Chapter 2

Gene Delivery with Low Molecular Weight Linear Polyethylenimines

Miriam Breunig[1], Uta Lungwitz[1], Renate Liebl[1], Claudia Fontanari[1], Juergen Klar[2], Armin Kurtz[2], Torsten Blunk[1], Achim Goepferich[1]

[1] Department of Pharmaceutical Technology, University of Regensburg, Universitaetsstrasse 31, 93040 Regensburg, Germany

[2] Department of Physiology, University of Regensburg, Universitaetsstrasse 31, 93040 Regensburg, Germany

Journal of Gene Medicine 7 (2005), 1287-1298

Abstract

Background

Linear polyethylenimine (LPEI) with a molecular weight (MW) of 22 kDa has been described as having a superior ability to induce gene transfer compared to its branched form. However, the transfection efficiency of the polymer cannot be enhanced beyond a certain limit due to cytotoxicity. We explored the potential of utilizing LPEIs with MWs ranging from 1.0 to 9.5 kDa to overcome this limitation.

Methods

Polyplexes of plasmid DNA encoding for enhanced green fluorescent protein (EGFP) and various LPEIs were compared concerning their transfection efficiency and cytotoxicity in CHO-K1 and HeLa cells by flow cytometry. The involvement of endolysosomes in LPEI – mediated gene transfer was investigated by applying the proton pump inhibitor bafilomycin A1 and the lysosomotropic agent sucrose. Confocal laser scanning microscopy was applied to assess the size and shape of polyplexes under cell culture conditions, to detect their endolysosomal localization and to observe their translocation to the nucleus.

Results

The transfection efficiency could be altered by varying the MW and the amount of the polymer available for polyplex formation. The highest transfection efficiency (about 44%), i.e. the fraction of EGFP positive cells, was obtained with LPEI 5.6 kDa, while the cytotoxicity remained low. The colocalization of polyplexes and endolysosomes was observed, and it appeared that the larger polyplexes escaped from the acidic organelles particularly quickly. For LPEI 5.0 and 9.0 kDa, the number of cells and nuclei that have taken up DNA after 6 hours was similar, as determined by flow cytometry.

Conclusions

Our study suggests that LPEIs with low MWs are promising candidates for non-viral gene delivery, because they are more efficient and substantially less toxic than their higher MW counterparts.

Introduction

Gene therapy has the potential to treat inherited and acquired diseases for which there is little hope of developing conventional medications. Significant progress has been made since the inception of gene therapy in the 1960s [1], but many hurdles remain before gene therapeutics could be used routinely in clinics. So far, gene therapy clinical trials have predominantly been based on viruses as gene vectors, because they are quite efficient in delivering DNA and initiating gene expression. However, their broad use is limited by the risk of insertional oncogenesis [2,3].

In the light of these concerns, non-viral gene delivery systems are gaining attention, as they are considered to be safer alternatives. However, their application is hampered by a low transfection efficiency compared to viruses. One non-viral gene delivery strategy involves the use of polycationic polymers such as polyethylenimine (PEI) as a DNA complexing agent for *in vitro* and *in vivo* use [4-9]. PEI/DNA complexes (polyplexes) are taken up by a variety of cells via endocytosis, enter the endolysosomal compartment, and are finally released due to their buffer capacity via the so-called ´proton sponge mechanism´ [9,10]. Subsequent to their successful escape from intracellular vesicles, the translocation of polyplexes to the nucleus remains the major barrier. A number of branched PEI (BPEI) – based transfection systems with varying molecular weight (MW) have been described, which accomplish a relatively high transfection efficiency [11], but are generally afflicted with a high cytotoxicity [6,12]. The situation demands better materials with a high transfection efficiency and low cytotoxicity.

Polyplexes containing linear PEI (LPEI) are larger (> 1000 nm) in salt-containing buffers compared to those prepared with its branched form (about 100 – 600 nm) [4,13,14], although the polyplex size not only depends on the polymer structure, but also on the MW and the NP ratio (indicates the ratio of nitrogens in polymer to phosphates in DNA). Larger particles sediment onto plated cells more quickly than smaller ones, which are limited to their Brownian molecular motion, and therefore result in an increase of particle uptake *in vitro* [7,15]. Furthermore, it has been suggested that large particles exhibit a higher intrinsic endolysosomal activity, which may enhance their escape from the acidic compartment [15]. Moreover, a particularly high gene expression was found with LPEI 22 kDa in non-dividing polarized cells [5], which implies that LPEI allows for a cell cycle independent gene transfer [16], and therefore may not be limited to fast-dividing cells.

Several studies revealed that polyplexes formed with LPEI 22 kDa reach a higher transfection efficiency than BPEI – polyplexes [17-20]. However, most studies have been confined to only a few commercially available LPEI derivatives, for example ExGen® 500 with a MW of 22 kDa. Moreover, even LPEI 22 kDa displays cytotoxic effects at a certain dose. In this study, we therefore explored the possibility and potential of utilizing LPEIs within the range of 1.0 to 9.5 kDa as carriers for gene delivery. First, as it is known for BPEI that the transfection efficiency correlates with the MW of the polymer [11], we wanted to determine the size limit of LPEI that still allows for gene transfer. In particular, we intended to verify for LPEIs, that low MW substances are substantially less toxic than their high MW counterparts [14], but still retain their ability for gene transfer. We sought to overcome the restriction that high transfection efficiency is limited by the cytotoxicity of the non-viral carrier. Furthermore, we wanted to gain some insight into the mechanism of transfection using LPEI – polyplexes and, therefore, investigated their nuclear entry and the involvement of endolysosomes.

Materials and Methods

All materials were purchased from Sigma-Aldrich Chemie GmbH (Germany) unless otherwise stated.

Cell lines and cell culture

CHO-K1 (ATCC No. CCL-61) and HeLa cells (ATCC No. CCL-2.1) were grown in 75 ml culture flasks in a 5% CO_2 atmosphere at 37°C as adherent culture to 90% confluency before seeding. Culture medium for CHO-K1 cells consisted of Ham´s F-12 supplemented with 10% FBS (Biochrom AG, Germany). HeLa cells were maintained in Dulbecco´s Medium (Invitrogen, Germany) supplemented with 10% FBS, 1 mM sodium pyruvate and 2 mM L-glutamine (both Invitrogen, Germany).

Non-viral carriers

Twelve LPEI derivates within the range of 1.0 to 9.5 kDa were synthesized by ring-opening polymerization of 2-ethyl-2-oxazoline and acidic hydrolysis of the corresponding poly(2-ethyl-2-oxazoline) as previously described [13]. The amine bases of the LPEIs were precipitated, recrystallized in ethanol and the average MW was estimated by ^{1}H-NMR spectroscopy. In the following, the notation of polymers was made without the unit kDa, for example LPEI 9.5 represents LPEI with a MW of 9.5 kDa. Polymer stock solutions were prepared with 150 mM NaCl, the pH of LPEI solutions was adjusted to 7 and then filtered

(0.2 µm filter, Corning GmbH, Germany). ExGen® 500 was obtained from MBI Fermentas GmbH (Germany). When indicated, polymers were labeled with 6-TAMRA- succinimidyl ester (Molecular Probes, The Netherlands). Briefly, the amine bases of the corresponding LPEIs and 6-TAMRA- succinimidyl ester were dissolved in DMSO and stirred for 24 hours at room temperature in the dark. The labeled polymers were dissolved in diluted hydrochloric acid, precipitated with sodium hydroxide solution and then washed extensively. The labeling reaction was controlled by thin layer chromatography.

Plasmid isolation and labeling

Plasmid encoding enhanced green fluorescent protein (EGFP) (Clontech, Germany) was used as reporter gene in this study. Plasmid was isolated from E. coli by using a Qiagen Plasmid Maxi Kit (Qiagen, Germany) according to the supplier´s protocol. For confocal laser scanning microscopy (CLSM), in cases when only the plasmid DNA was stained, it was labeled with fluorescein using the FluoroULS® Labeling Kit (MBI Fermantas GmbH, Germany) according to the manufacturer´s protocol. The labeled DNA was purified by ethanol precipitation. For uptake experiments by flow cytometry and other experiments by CLSM, plasmid DNA was stained with YOYO-1 (Molecular Probes, The Netherlands). The labeling reaction was carried out with a molar ratio of 1 dye molecule per 320 base pairs at room temperature in the dark.

Preparation of plasmid DNA / polymer complexes - polyplexes

Plasmid DNA / LPEI complexes were prepared at a NP ratio of 6, 12, 18, 24 and 30. Polyplexes were formed by mixing 2 µg DNA with the appropriate amount of polymer solution, while both components were diluted to 50 µl with 150 mM NaCl or 5% glucose, as indicated. The resulting LPEI - polyplexes were incubated for 20 minutes at room temperature before use. In the following, the notation of polyplexes was made without the unit kDa, for example LPEI 9.0 – polyplexes expresses that polyplexes were built with LPEI 9.0.

In vitro transfection and cytotoxicity experiments

For gene transfer studies, CHO-K1 cells were grown in 24-well plates at an initial density of 38,000 cells per well and HeLa cells at 40,000 cells per well. 18 hours after plating, the culture medium was removed, cells were washed with PBS (Invitrogen, Germany) and 900 µl serum-free medium was added (transfection medium). Thereafter, the prepared polyplexes

were added to the cells. After 4 hours, the medium was replaced with 1 ml of culture medium. When Bafilomycin A1, dissolved in ethanol (J.T. Baker, Holland), or sucrose were used, cells were pretreated for 15 min at 37°C, and the transfection was performed in the presence of the drug [21,22]. In experiments with sucrose, the transfection medium was replaced with culture medium containing the same concentration of sucrose to prevent osmotic lysis of the lysosomes and cells. 48 hours later, cells were prepared for flow cytometry analysis. Floating cells were collected and combined with adherent cells after trypsinization. The pooled cells were washed twice with PBS, resuspended in 500 µl PBS and propidium iodide was added at a concentration of 1 µg / ml to half of the samples. Measurements were taken on a FACSCalibur (Becton Dickinson, Germany) using CellQuest Pro software (Becton Dickinson, Germany) and WinMDI 2.8 (©1993-2000 Joseph Trotter). EGFP positive cells were detected using a 530/30 nm band-pass filter, whereas the propidium iodide emission was measured with a 670 nm longpass filter. Logarithmic amplification of EGFP and propidium iodide emission in green and red fluorescence was obtained with 20,000 cells counted for each sample. In a density plot representing forward scatter against sideward scatter, whole cells were gated out (this process allows to distinguish between the cell population and cell fragments) and depicted in two-parameter dot plots of EGFP versus propidium iodide to analyse the measurements. The EGFP positive region, which corresponds to the transfection efficiency, was drawn starting above cell autofluorescence, where EGFP positive cells were < 0.2%. The geometric mean fluorescence intensity was determined from the number of EGFP positive cells. Further, the number of propidium iodide negative cells was counted as a measure of cell viability [23].

Cellular and nuclear uptake of polyplexes

YOYO-1 - labeled DNA was used to monitor polyplex delivery and LPEI 2.0, 5.0 and 9.0 were applied for polyplex formation. As a negative control, mock transfected cells and cells transfected with unlabeled polyplexes were employed. 50,000 CHO-K1 cells per well were seeded in a 24-well plate and then treated as described in the previous section, but were detached after transfection for 6 hours with trypsin containing 20 mM sodium azide (Merck KGaA, Germany). Sodium azide depletes ATP and prevents further particle uptake [24], whereas trypsin cleaves surface bound proteins [25]. Briefly, the nuclei were isolated as follows: cells were incubated for 5 minutes in a buffer with low salt concentration containing 10 mM Tris-HCl, 60 mM sodium chloride (Merck KGaA, Germany) and 1 mM EDTA. Thereafter, cells were treated with the same buffer additionally containing Phenyl-

Methylsulphonylfluoride, 1,4-Dithio-DL-threitol, protease inhibitors (Roche Diagnostics, Germany) and 0.5% Tergitol Type NP 40 (nuclei isolation buffer). Nuclei were pelleted at 2,500 rpm, rinsed three times with nuclei isolation buffer without Tergitol Type NP 40, and then resuspended in PBS with 20 mM sodium azide. Whole cells were treated as described for in vitro transfection, but PBS was also supplemented with 20 mM sodium azide. The percentage of isolated nuclei was determined to be > 95% by propidium iodide incorporation measured by flow cytometry, and the absence of extracellular and nuclear associated polyplexes was confirmed by CLSM (data not shown). The percentage of cells and nuclei that had taken up polyplexes and their mean fluorescence intensity was determined by flow cytometry. The mean fluorescence intensity of cells and nuclei that have *incorporated* YOYO-1 - labeled DNA, cannot be regarded as absolute value for the number of polyplexes, because those are not homogeneous in size distribution, i.e. larger polyplexes display a higher fluorescence intensity than smaller ones. Furthermore, polyplexes may also show a different fluorescence intensity in various compartments of a cell or dissociate after uptake. Therefore, we used the mean fluorescence intensity only as an indirect measure or, rather, an indicator of the amount of the internalized polyplexes.

Intracellular trafficking - confocal laser scanning microscopy (CLSM)

A Zeiss Axiovert 200 M microscope coupled to a Zeiss LSM 510 scanning device (Carl Zeiss Co. Ltd., Germany) was used for CLSM experiments. The inverted microscope was equipped with a Plan – Apochromat 63x and Plan – Neofluar 100x objective. Cells were plated in 8 – well Lab-Tek^{TM} Chambered Coverglass (Nunc GmbH & Co. KG, Germany) at an initial density of 35,000 cells / chamber in a volume of 400 µl culture medium. For maintaining a pH of 7.4, 20 mM HEPES was supplied. After 18 hours, polyplexes were added and measurements were directly performed in each well at 37°C. The thickness of the optical sections was between 0.7 and 1.2 µm.

For the investigation of the intracellular trafficking of polyplexes, LPEI 22, 9.0, 2.0 and fluorescein - labeled DNA were used. An argon laser with 488 nm was used to excite fluorescein. Images were taken using a band-pass filter of 505 – 530 nm in the singletrack mode at the indicated times after the addition of the polyplexes. Values for the approximate size of the various polyplexes were acquired by measuring the extent of a representative collective of intracellular polyplexes in confocal images. In cases, when double – labeled polyplexes were observed, YOYO-1 – labeled DNA was excited with 488 nm and fluorescence was detected using a 505 – 530 nm band-pass filter, whereas the TAMRA –

labeled LPEI was excited with 543 nm and recorded with a 560 nm lonpass filter. Images were taken in the multitracking modus. For the detection of polyplexes in acidic compartments of the cell, TAMRA – labeled LPEI 9.0 or 5.0 were applied. Polyplexes and quinacrine mustard at a concentration 10^{-6} M were added to the cells at the same point of time. An argon laser with 458 nm was used to excite the quinacrine mustard and the fluorescence was imaged using a band-pass filter of 475 – 525 nm. TAMRA – labeled LPEI was excited at 543 nm and the fluoresecence was recorded with a 560 nm longpass filter. Images were taken in the multitracking modus.

Statistical analysis

All measurements were collected (n = 3 to 6) and expressed as means ± standard deviation (SD). Single factor of variance (ANOVA) was used in conjunction with a multiple comparison test (Tukey test) to assess the statistical significance.

Results

LPEI - mediated gene transfer and cytotoxicity

The transfection efficiency of polyplexes formed with LPEI 1.0 to 9.5 and plasmid DNA was evaluated in CHO-K1 cells (Figure 1). For polyplexes with LPEIs from 9.0 to 5.6 kDa, the transfection efficiency followed a certain profile: as the NP ratio was increased, the transfection efficiency first increased, plateaued and then decreased. Using LPEIs from 5.0 to 1.0 kDa, the transfection efficiency could be increased with the amount of polymer. Such a plateau or drop was not observed for LPEI 9.5. With increasing NP ratio, the maximum in transfection efficiency shifted to polyplexes made with a LPEI derivative with lower MW. The maximum transfection efficiency of about 44% was obtained with LPEI 5.6 at NP 18. LPEI 1.0 seemed to be the limit for gene transfer, because LPEI 1.0 - polyplexes displayed a minimal transfection efficiency (Figure 1). The mean fluorescence intensity of EGFP positive cells can serve as average expression of EGFP per cell. After transfection with LPEIs with a MW from 9.5 to 5.6 kDa at NP 6 to 30, no statistically significant differences could be found in the mean fluorescence intensity. Using LPEIs with a MW from 5.0 to 1.0 kDa, the mean fluorescence intensity of EGFP positive cells was only significantly ($p<0.05$) higher at NP 30 compared to NP 6 (data not shown). We confirmed our results by investigating the gene transfer ability of LPEI 9.0 - and 5.0 – polyplexes in HeLa cells (Figure 2).

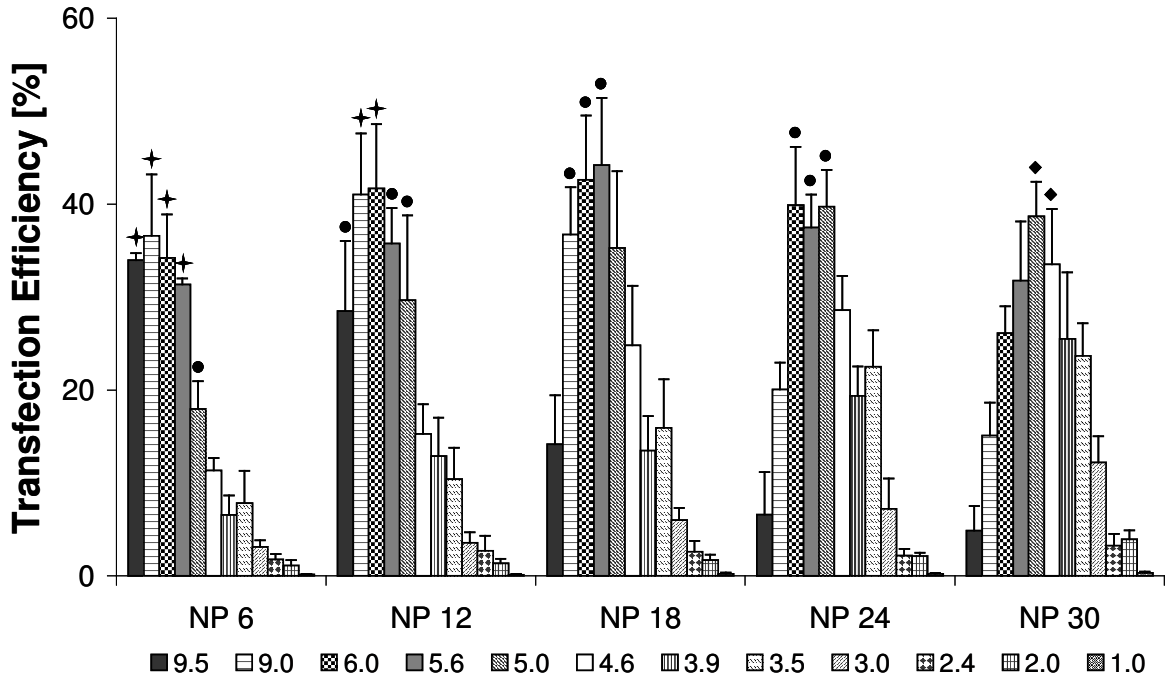

Figure 1: Transfection efficiency of LPEIs with various MW [kDa] (as indicated in the legend) complexed with pEGFP-N1 as reporter gene in CHO-K1 cells determined by flow cytometry. Experiments were performed in duplicate; values represent the EGFP positive cells as means ± SD of one representative experiment (n=6). Transfection efficiencies of LPEI - polyplexes within each NP ratio are significantly different from LPEI ≤ 5.0 – polyplexes, denoted by ✦, significantly different from LPEI ≤4.6 - polyplexes, denoted by ●, and significantly different from LPEI ≤3.5 – polyplexes, denoted by ◆ ($p < 0.01$).

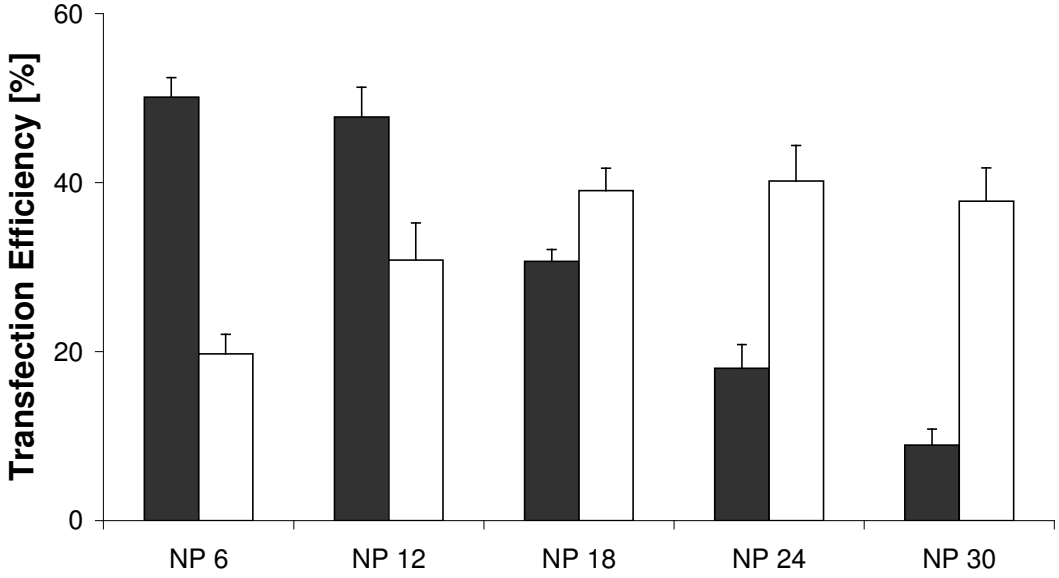

Figure 2: Transfection efficiency of LPEI 9.0 (■) - or 5.0 (□) - polyplexes with pEGFP-N1 as reporter gene, tested in HeLa cells. Experiments were performed in duplicate; values represent the EGFP positive cells as means ± SD of one representative experiment (n=4).

The polymers showed the same trend in both cell lines. Polyplexes built in glucose resulted in a reduced efficacy compared to those prepared in sodium chloride, but a dependency of the transfection efficiency on the MW could also be observed: LPEI 9.0 – polyplexes reached higher values than LPEI 5.0 – polyplexes (Figure 3).

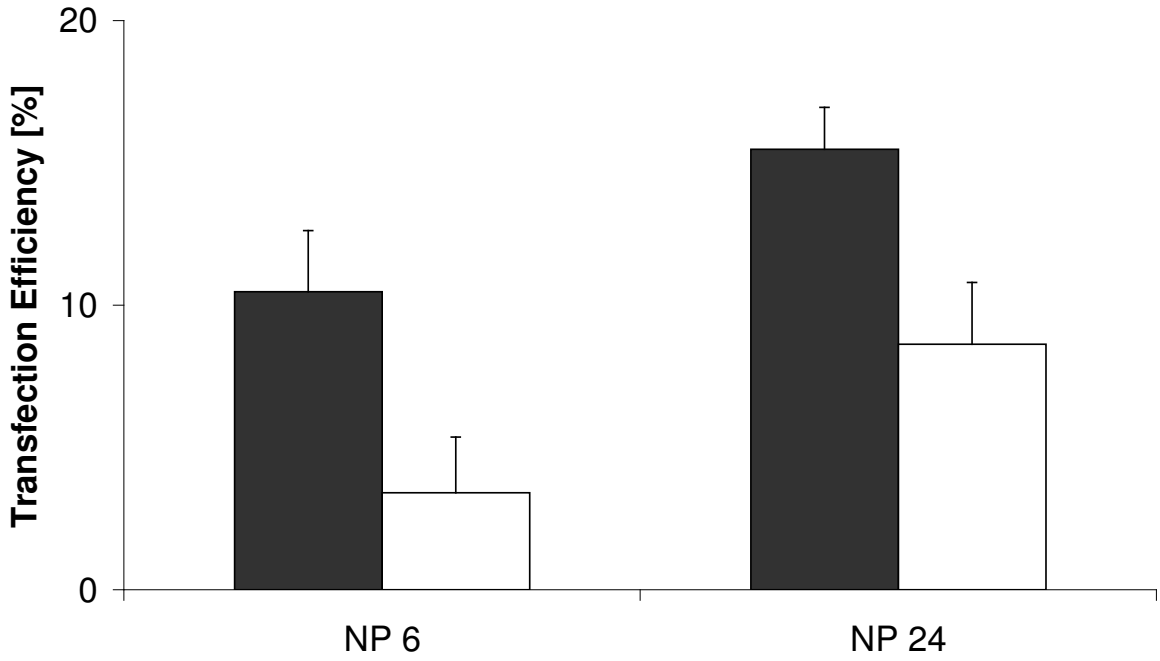

Figure 3: Transfection efficiency of LPEI 9.0 (■) - or 5.0 (□) - polyplexes with pEGFP-N1 as reporter gene, polyplexes were formed in glucose. Experiments were performed in duplicate; values represent the EGFP positive cells as means ± SD of one representative experiment (n=4).

The cell viability was evaluated by propidium iodide staining followed by flow cytometry analysis in the same experiment. Within a MW range of 4.6 to 9.5 kDa, the cell viability decreased with the MW of the polymer and the NP ratio in polyplexes (Figure 4). Using LPEIs with lower MW, the cell viability seemed to be unaffected compared to untreated cells.

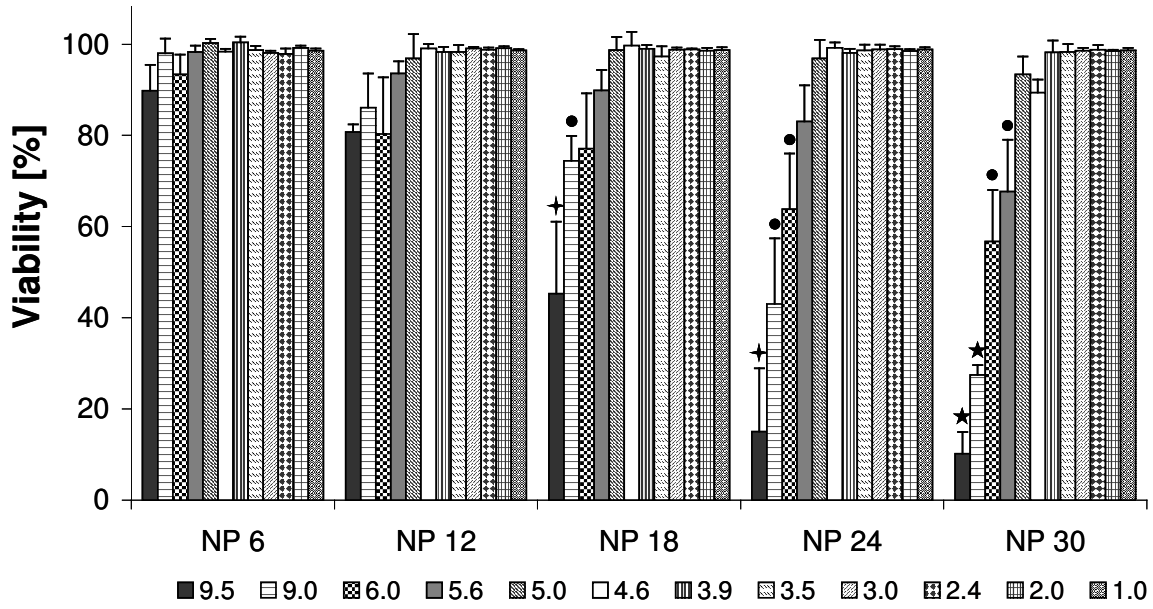

Figure 4: Relative viability of CHO-K1 cells after treatment with LPEI - polyplexes at various NP ratios determined with propidium iodide staining followed by flow cytometry, whereby the MW [kDa] of LPEI in polyplexes is indicated in the legend. Experiments were performed in duplicate, values are means ± SD of one representative experiment (n=3). Relative viability of cells within each NP ratio is significantly different from treatment with LPEI ≤ 9.0 kDa in polyplexes, denoted by ✦, significantly different from LPEI ≤ 6.0 kDa in polyplexes, denoted by ★, and significantly different from LPEI ≤ 5.0 kDa in polyplexes, denoted by ● ($p < 0.01$).

It was outstanding that within the same test system, LPEIs from 3.5 to 9.5 kDa obtained at certain NP ratios a higher transfection efficiency and cell viability compared to the commercially available LPEI 22 (ExGen® 500) (Figure 5).

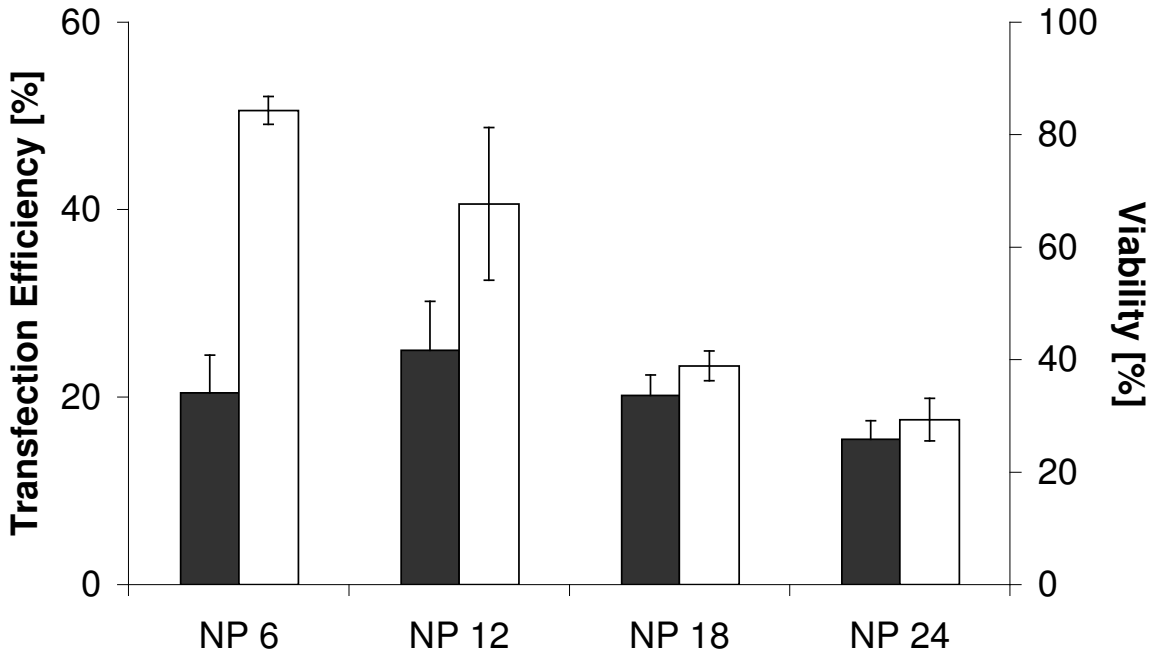

Figure 5: Transfection efficiency (■) and viability (□) of CHO-K1 cells after treatment with LPEI 22 – polyplexes as determined by flow cytometry. Values represent the EGFP positive or viable cells as means ± SD (n=4).

Mechanistic insights into LPEI – mediated gene transfer

Intracellular size and location of polyplexes

To understand the transfection efficiency of LPEI - polyplexes, we studied the intracellular fate of polyplexes with fluorescein – labeled DNA by CLSM. For this purpose, we chose two LPEI derivatives near opposite ends of our molecular weight spectrum (LPEI 9.0 and 2.0), and used the commercially available LPEI 22 as a control. The size distribution of intracellular LPEI 9.0 - polyplexes at NP 6 was not homogenous. There were many small and some large irregular aggregates ranging from about 1 to 5 µm (Table 1). At a NP 24, the polyplexes were somewhat smaller with a size of about 1 to 3.5 µm. Polyplexes formed with LPEI 2.0 seemed to be smaller than those prepared with LPEI 9.0, appeared almost spherical in shape and fewer aggregates were visible. At NP 6, they ranged from about 0.5 to 1.5 µm, slightly increasing in size at NP 24. LPEI 22 – polyplexes were smaller than those prepared with LPEIs with lower MW within the first hour of incubation, ranging from about 0.2 to 1.5 µm, but these polyplexes then grew to larger aggregates with sizes up to 5 µm.

Table 1: The approximate size [µm] of LPEI 9.0 -, 2.0 – and 22 - polyplexes at NP 6 and 24. The values were acquired from a representative collective of intracellular polyplexes in confocal images.

	LPEI 9.0 – polyplexes	LPEI 2.0 – polyplexes	LPEI 22 - polyplexes
NP 6	1.0 – 5.0	0.5 – 1.5	0.2 – 5.0
NP 24	1.0 – 3.5	1.0 – 2.0	0.2 – 5.0

After 2 hours of incubation, the number of internalized LPEI 2.0 – polyplexes reached a value of 1 to 2 at NP 6 and increased up to 4 at NP 24, whereas many more LPEI 22 – and 9.0 – polyplexes could be detected, irrespective of the NP ratio applied. LPEI 9.0 – polyplexes (NP 6) appeared inside the cells in less than 30 minutes. Within the second hour, polyplexes could be observed in almost every cell (Figure 6 A). Longer incubation times increased the number of polyplexes in the perinuclear region. The number of intracellular LPEI – 9.0 polyplexes at NP 24 was higher compared to NP 6 within the same time of incubation (Figure 6 B). Using LPEI 2.0 (NP 6), polyplexes could be seen in only a few cells within the first hour, but these polyplexes moved towards the nucleus (Figure 6 C). The number of intracellular LPEI 2.0 - polyplexes slightly increased with increasing NP ratio (Figure 6 D). LPEI 22 – polyplexes at NP 6 sedimented rapidly and could be detected inside cells within 30 minutes (Figure 6 E). The cytosol seemed to be flooded by LPEI 22 – polyplexes at NP 24 within 1 hour (Figure 6 F) and a slight contraction of the cells was observed. Polyplexes that have not been taken up by cells seemed to build larger aggregates in culture medium, irrespective of the MW and NP ratio (data not shown).

A

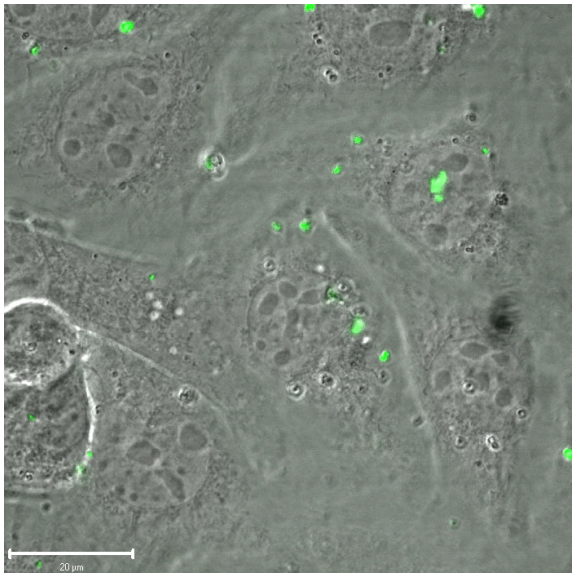

B

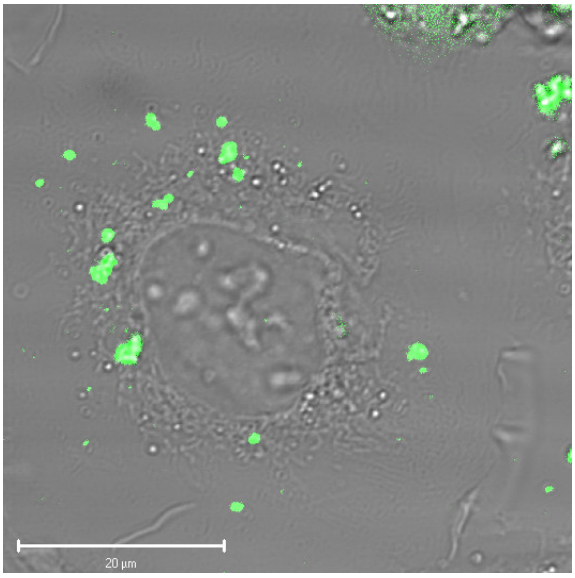

C

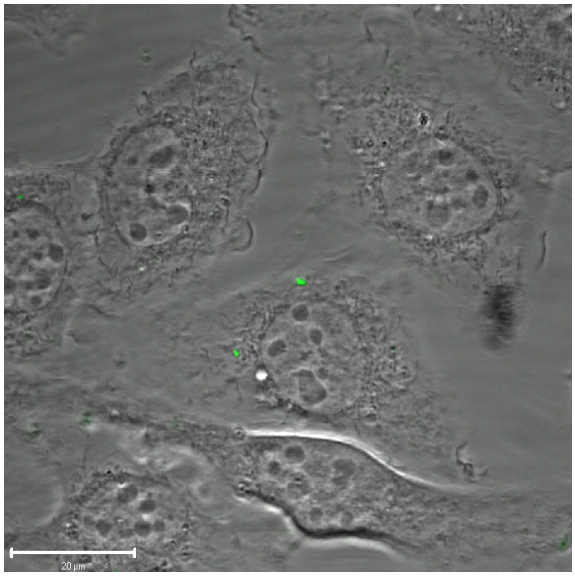

D

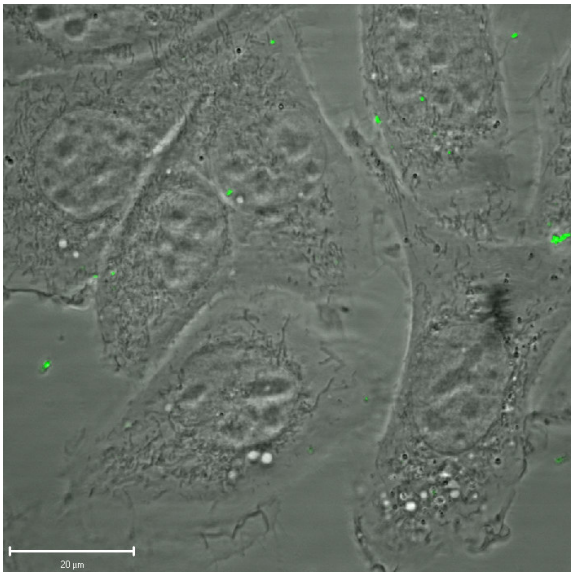

E

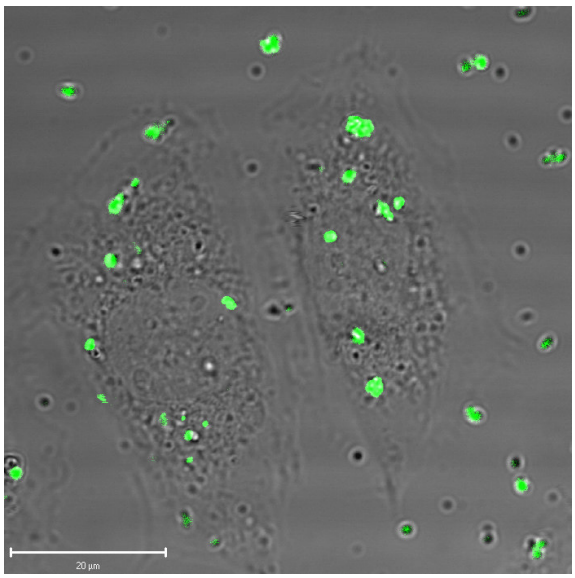

F

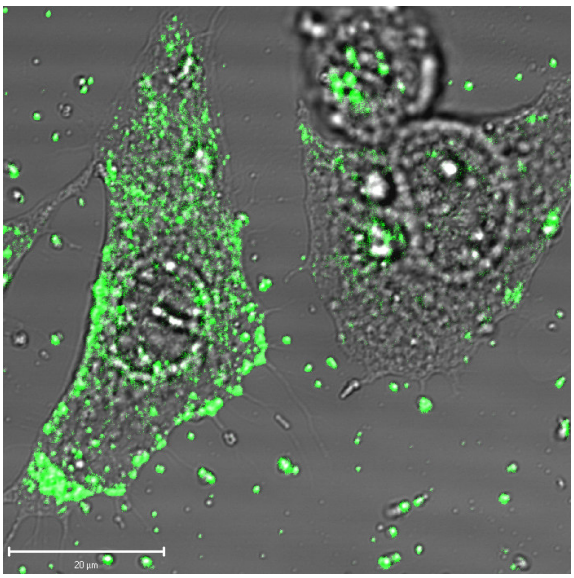

(continued on next page)

G H

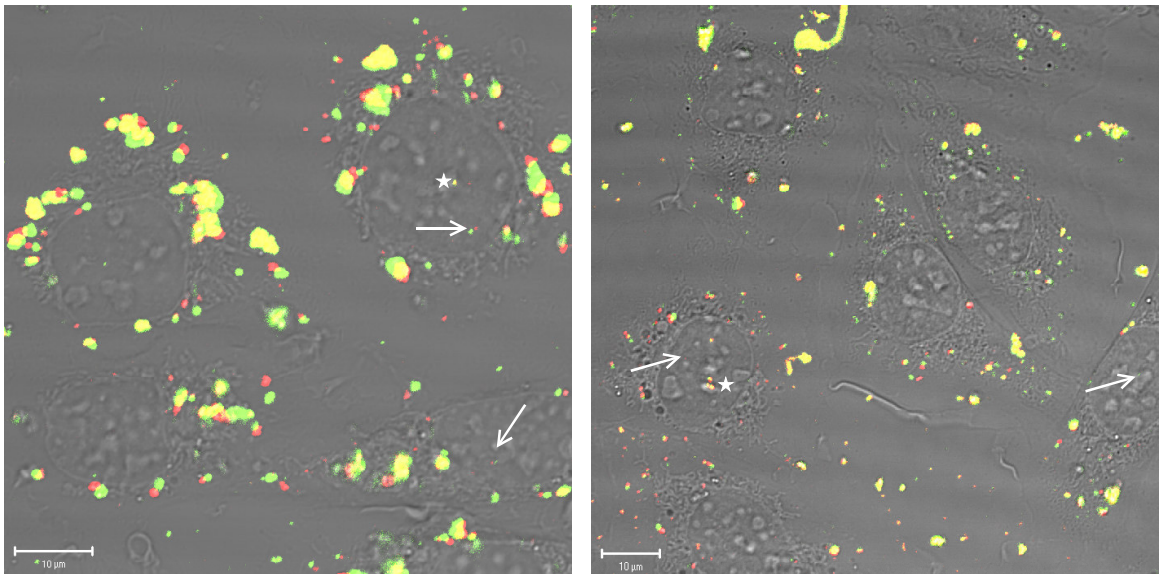

Figure 6: Intracellular distribution of fluorescein (A - F) - or YOYO-1 / TAMRA (G and H) - labeled polyplexes in CHO-K1 cells by CLSM. Times post transfection are as follows: A: 2h, LPEI 9.0 – polyplexes (NP 6) could be observed in nearly every cell; B: 2h, the number of intracellular polyplexes increased with increasing NP ratio (LPEI 9.0 – polyplexes, NP 24); C: 2h, LPEI 2.0 – polyplexes (NP 6) could be seen in only a few cells; D: 2h, the number of intracellular polyplexes only slightly increased with increasing NP ratio (LPEI 2.0 – polyplexes, NP 24); E: 2h, many LPEI 22 – polyplexes (NP 6) could be detected inside cells; D: 2h, cells seemed to be flooded by LPEI 22 – polyplexes (NP 24) and a slight contraction of cells was observed; G: 6h, double-labeled LPEI 9.0 – polyplexes at NP 24; H: double-labeled LPEI 5.0 – polyplexes at NP 24. DNA is represented by green dots and polymer by red dots. A colocalization of both would yield a mixture color of yellow. Intact polyplexes in nuclei are marked with a star, whereas disintegrated polyplexes and polymer or DNA only, are indicated with an arrow. Each bar indicates 20 µm (A – F) or 10 µm (G and H).

Polyplexes were double-labeled to investigate whether they remain intact or disintegrate inside cells. DNA was labeled with YOYO-1 and depicted in green, whereas TAMRA – labeled LPEIs 9.0 or 5.0, Figure 6 G or H, respectively, were represented by red dots. The larger extracellular polyplexes and polyplex aggregates exhibited a mixture of colors representing polyplexes consisting of polymer and DNA. The smaller intracellular polyplexes could be divided into red, green and yellow dots, corresponding to polymer only, DNA only and intact polyplexes. Inside the nucleus, intact (star, Figure 6 G and H) or disintegrated polyplexes (arrow, Figure 6 G and H) could also be detected.

Endosomolytic activity

First, the endolysosomolytic activity of LPEI 9.0 -, 5.0 - and 2.0 – polyplexes was tested by supplementing sucrose at concentrations of 5 mM [21] during the transfection process. Sucrose is a lysosomotropic agent and therefore accumulates in the lysosomal matrix,

inducing an osmotic imbalance with water penetrating into the organelles causing their swelling [26]. No statistically significant differences were found in terms of transfection efficiency and cell viability with LPEI 9.0 and 5.0 at every NP ratio tested compared to transfection without sucrose (Figure 7 A and B, respectively; cell viability data not shown). Using LPEI 2.0 – polyplexes, a slight increase in transfection efficiency could be observed with sucrose at NP 6 and a significant ($p < 0.05$) increase at NP 24 (Figure 7 C).

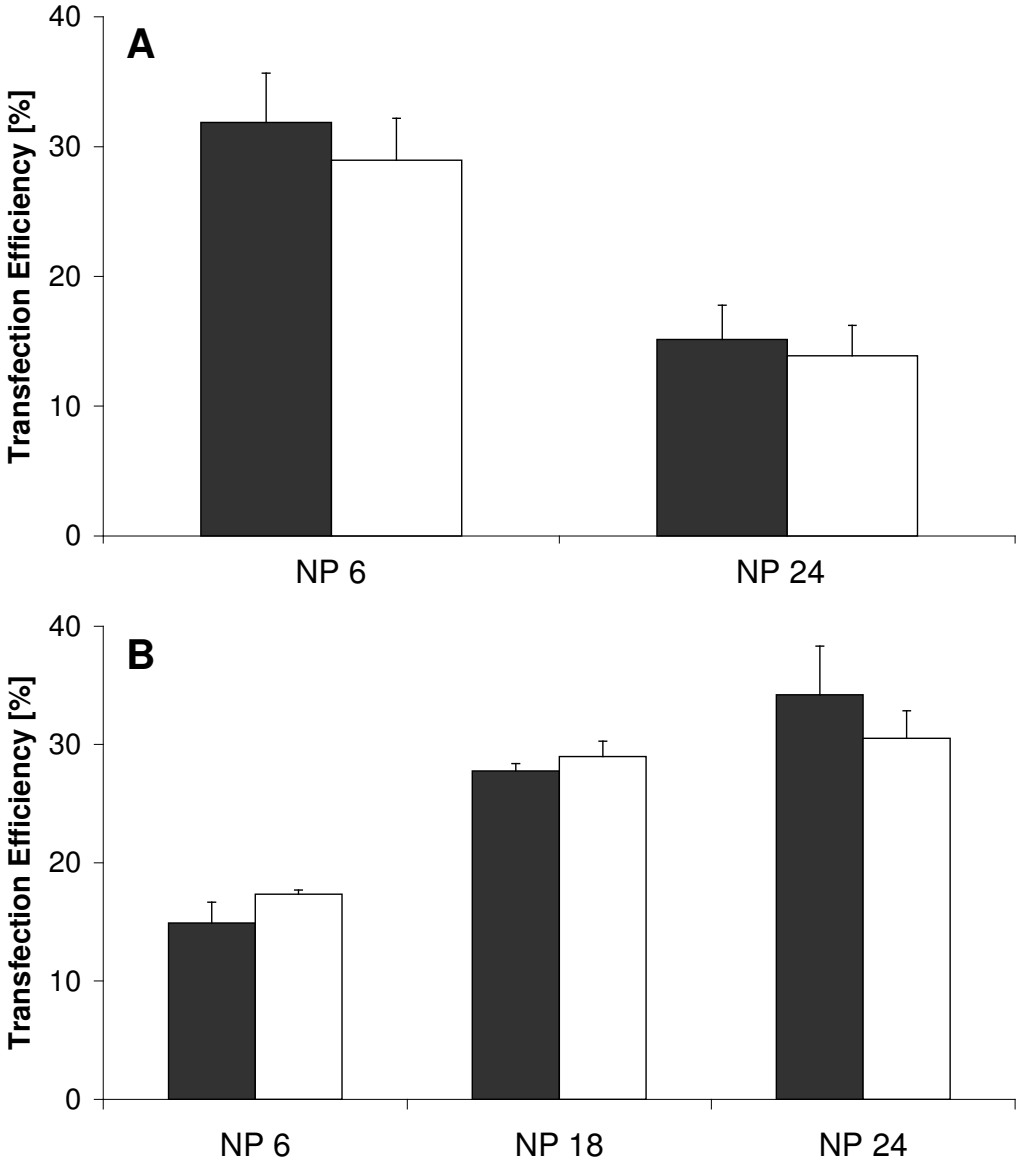

(continued on next page)

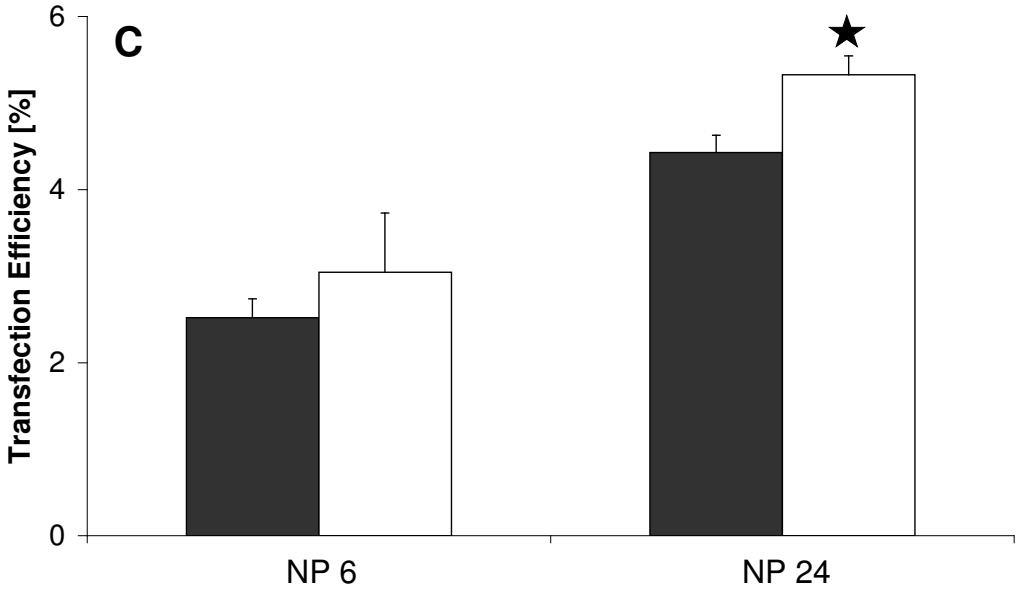

Figure 7: The effect of the lysosomotropic agent sucrose at 5 mM (□) on EGFP expression with LPEI 9.0 -, 5.0 – and 2.0 – polyplexes, respectively A, B and C, compared to transfection without sucrose (■) determined by flow cytometry. Experiments were performed in duplicate, values are means ± SD of one representative experiment (n = 4). No statistically significant differences could be found with LPEI 9.0 and 5.0, while transfection efficiency with LPEI 2.0 at NP 24 with and without sucrose was statistically significant different ($p < 0.05$), denoted by ★.

The involvement of acid-mediated endosomal escape was also assessed with Bafilomycin A1. This substrate prevents endosomal acidification by inhibiting the vacuolar ATPase proton pump [22]. If lysosomes are involved in LPEI – mediated gene transfer, a decrease in gene expression would be expected due to a lower polyplex concentration available in the cytoplasm. Applying bafilomycin A1 dissolved in ethanol at a concentration of 50 nM, the decrease in transfection efficiency of either LPEI 9.0 -, 5.0 or 2.0 – polyplexes at NP 6 was statistically significant ($p < 0.01$) compared to transfection with supplementation of the solvent ethanol alone [27] (Figure 8). The transfection efficiency of LPEI 9.0 was about 55 fold reduced upon the addition of bafilomycin, whereas the efficiency of LPEI 5.0 was 21 fold and of LPEI 2.0 was only 5 fold reduced.

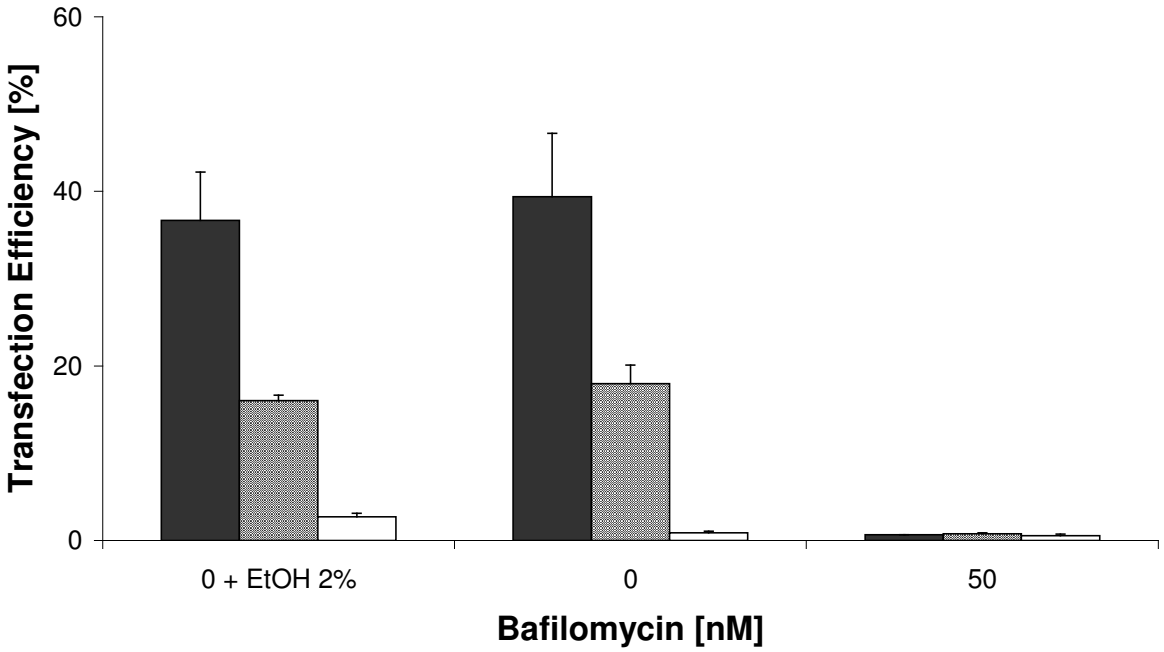

Figure 8: The effect of Bafilomycin A1, an inhibitor of vacuolar type H^+-ATPase, on EGFP expression with LPEI 9.0 (■)-, 5.0 (▩)- and 2.0 (□)– polyplexes at NP 6 in serum-containing transfection medium determined by flow cytometry. Experiments were performed in duplicate, values are means ± SD of one representative experiment (n = 3). The decrease in transfection efficiency of either LPEI 9.0 -, 5.0 - or 2.0 – polyplexes was statistically significant ($p < 0.01$) compared to transfection with supplementation of the solvent ethanol alone.

Lysosomal localization

CLSM was used to verify whether acidic vesicles and polyplexes ever colocalized. Recent studies used LysoTracker to investigate the involvment of lysosomes in the intracellular path of polyplexes [28,29]. However, it was shown that cationic amphiphilic drugs could displace this fluorescent dye from lysosomes [30]. Therefore, we chose the fluorescent dye quinacrine mustard as tag, as it is often used as an intracellular acidification marker [31] with pKa values of 7.8 and 9.72 [32]. LPEI 22 has an average pKa of 7.9 [33] and is less basic than quinacrine mustard. The acidic marker is likely not released from the lysosomes in presence of PEI. Acidic organelles, which were observed as turquoise patches, accumulated around the nucleus within 1.5 hours of exposure to the dye. A colocalization of acidic oranelles and polyplexes would yield a combination color of turquoise and red. The interaction of LPEI 9.0 - polyplexes with lysosomes was size and time dependent: after two hours, small polyplexes at NP 6 were observed trapped in acidic organelles (Figure 9 A, star); after 5 hours, these polyplexes were no longer associated with the acidic organelles (Figure 9 B, open arrow) or only partially colocalized (Figure 9 B, arrow). Large polyplexes at NP 6 were either only partially colocalized with acidic organelles (Figure 9 C; arrow) or completely unassociated

(Figure 9 C, open arrow) throughout the 6 hour observation period. At NP 24, similar results could be observed as for NP 6, despite the fact that fewer large polyplex - aggregates were present: Small polyplexes were associated with turquoise patches (Figure 9 D, star), and were released into the cytoplasm with further incubation time. Larger polyplexes were dispersed throughout the cytosol (Figure 9 D, open arrow). Using LPEI 5.0 – polyplexes, similar observations were made at NP 6. Most smaller polyplexes were combined with acidic organelles after 2 hours (Figure 9 E, star) and the larger ones only partially colocalized (Figure 9 E, arrow). With further incubation, most of the smaller polyplexes were no longer associated with acidic organelles (Figure 9 F, open arrow). At NP 24, already after 2 hours of incubation, many small polyplexes were dispersed in cytosol (Figure 9 G, open arrow). But we did not detect an increase of free polyplexes with further incubation (Figure 9 H).

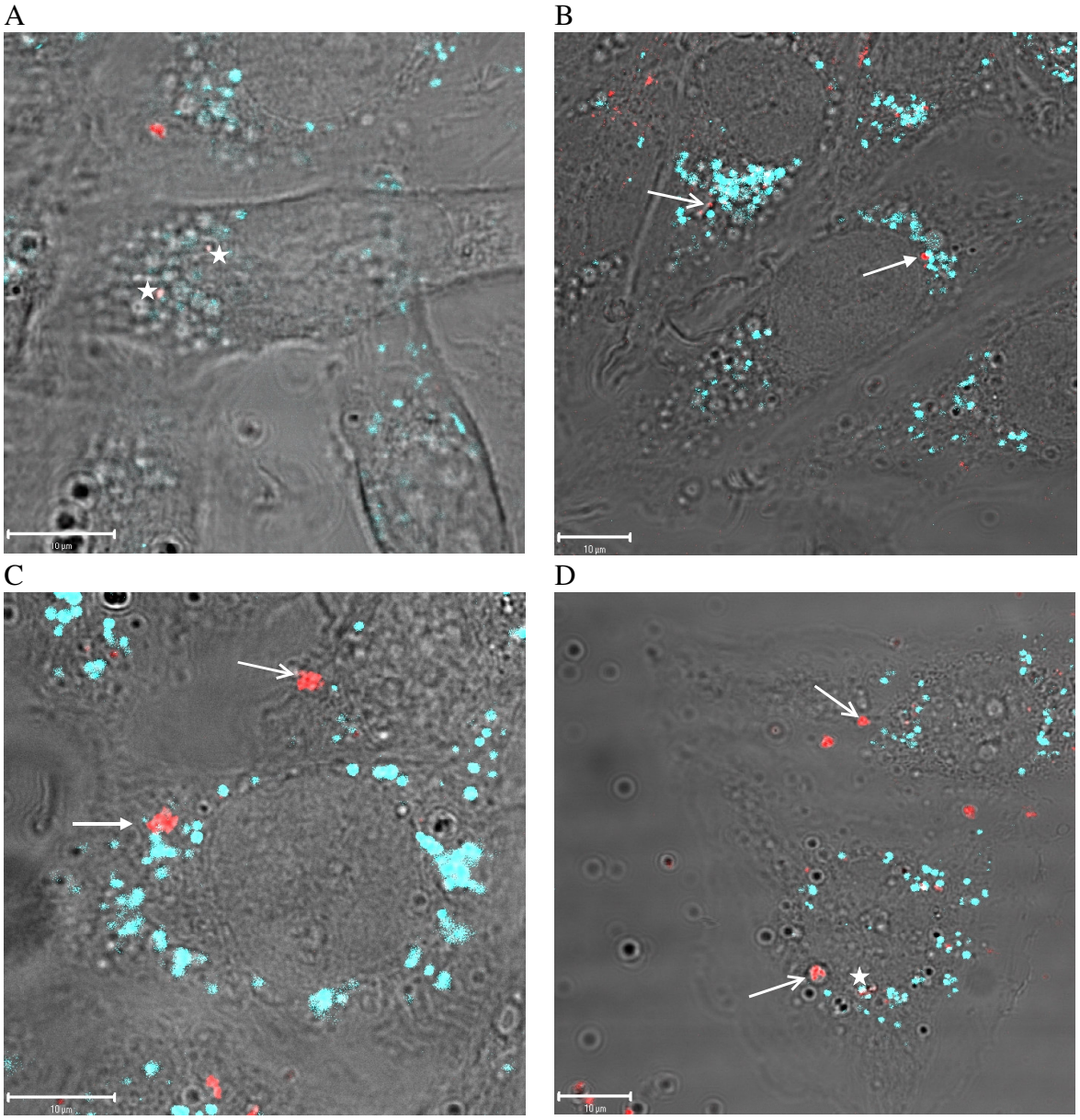

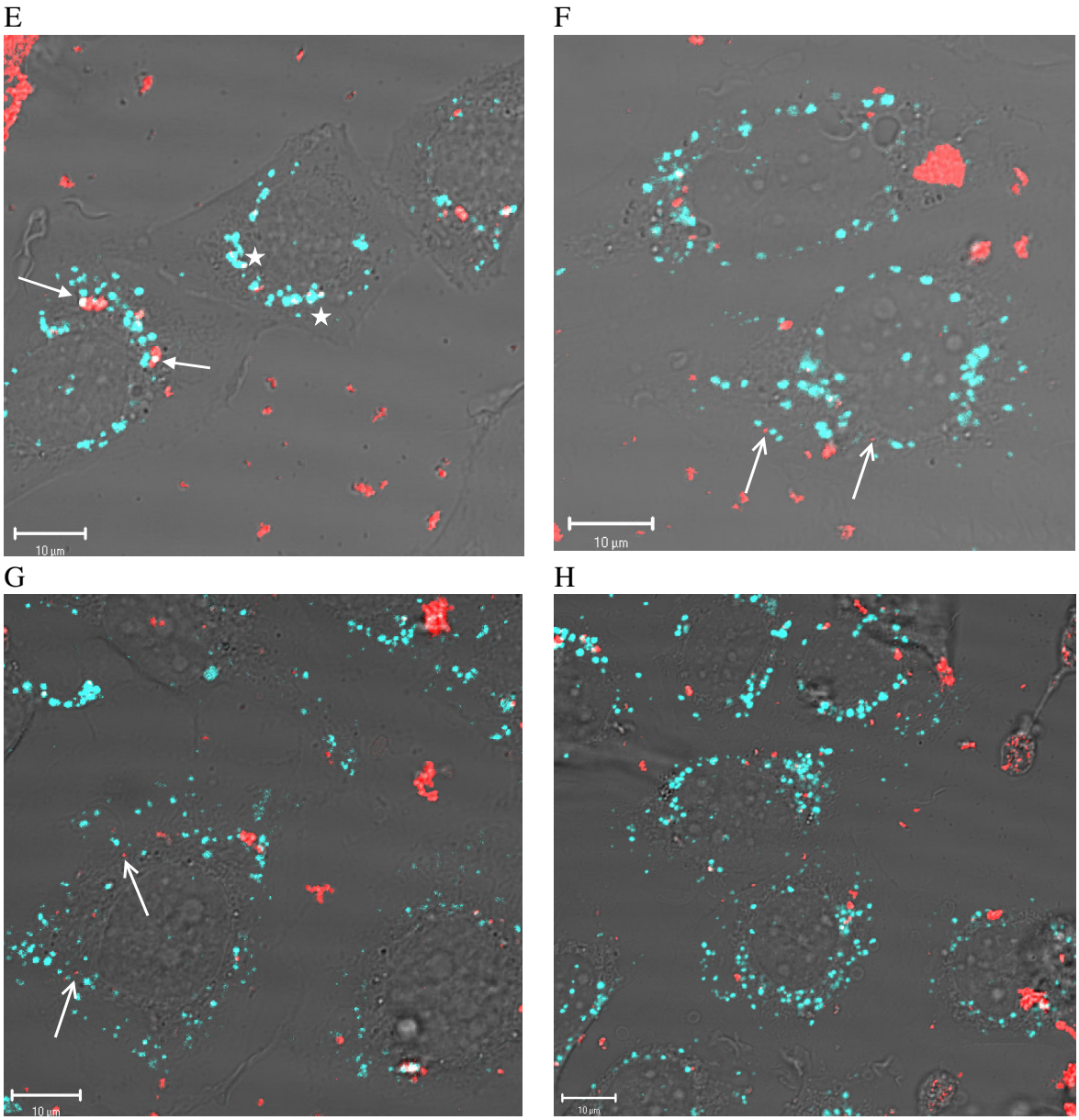

Figure 9: Tracking of TAMRA -labeled (red) LPEI 9.0 (A – D) and 5.0 (E – H) - polyplexes in CHO-K1 cells with labeled acidic organelles (turquoise) by CLSM. A mixture of both colors indicates a close proximity and therefore an interaction. Times post transfection are as follows: A: 2h, smaller polyplexes at NP 6 were trapped in acidic organelles (star); B: 5h, these polyplexes were released (open arrow) or only partially colocalized (arrow); C: 3h, larger polyplexes at NP 6 only partially colocalized with acidic organelles (arrow) or no colocalization could be observed (open arrow); D: 3h: smaller polyplexes at NP 24 were combined with turquoise patches (star), and the larger polyplexes at NP 24 were present free in the cytosol (open arrow). E: 2h: most of the smaller polyplexes were combined with acidic organelles after 2 hours (star), the larger ones only partially colocalized (arrow). F: 5h: with further incubation many smaller polyplexes at NP 6 were no longer associated with acidic organelles (open arrow). G: 2h: in comparison to NP 6, many small polyplexes at NP 24 were dispersed in cytosol (open arrow). H: 5h: an increase of free polyplexes with further incubation was not detected. Each bar indicates 10 µm.

Nuclear localization

Recently, it was suggested that LPEI 22 - polyplexes have improved nuclear import characteristics compared to other gene delivery systems due to their cell cycle independent entry into the nucleus [16]. To verify this for LPEIs with low MW, CHO-K1 cells were incubated with LPEI 2.0 -, 5.0 - and 9.0 - polyplexes with YOYO-1 - labeled DNA. The number of cells that showed fluorescence due to intracellular YOYO-1 - labeled DNA increased with the NP ratio. No statistically significant differences in the number of cells and nuclei that have taken up polyplexes could be found after 6 hours for LPEI 5.0 and 9.0, whereas significantly fewer nuclei showed fluorescence due to intranuclear DNA compared to whole cells after transfection with LPEI 2.0 – polyplexes (Figure 10 A).

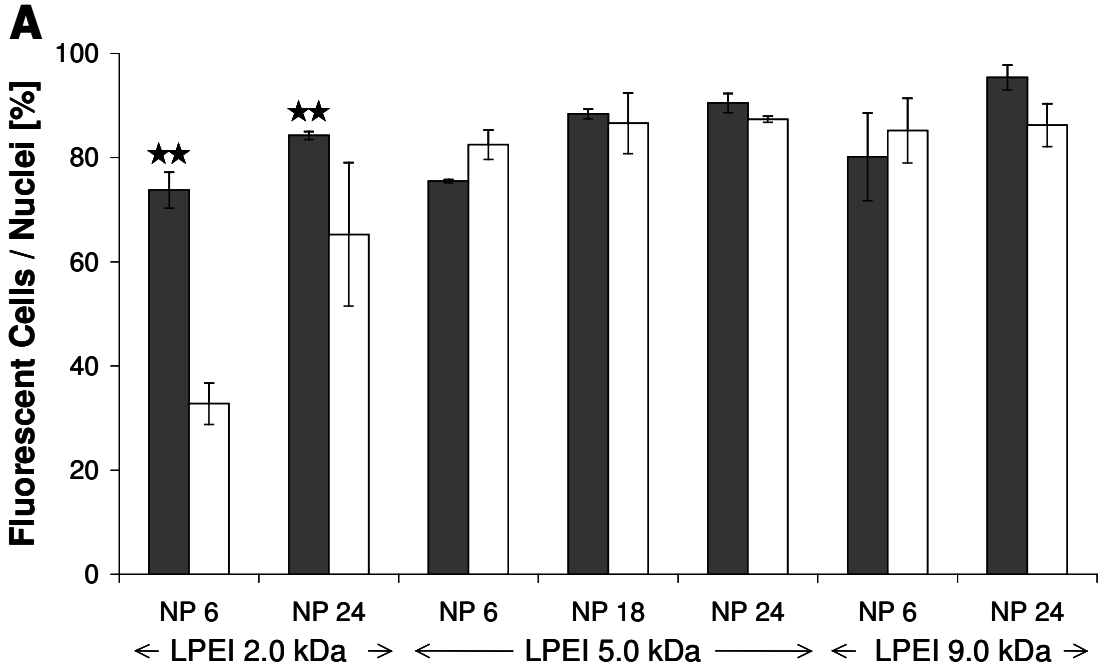

(continued on next page)

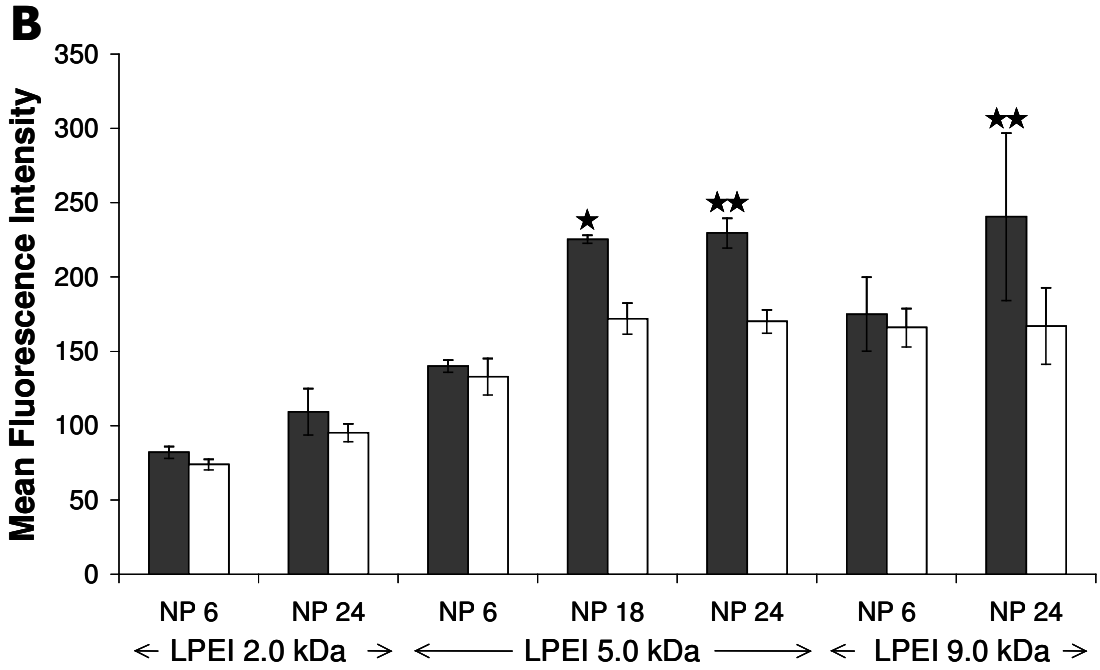

Figure 10: Uptake of polyplexes prepared with LPEI 2.0, 5.0 or 9.0 kDa and YOYO-1 – labeled DNA in whole cells (■) or intact nuclei (□) after 6 hours determined by flow cytometry. A: Fluorescent cells / nuclei indicates the percentage of cells / nuclei that show a fluorescence due to intracellular / intranuclear YOYO-1 – labeled DNA. Statistically significant differences between pairs are denoted by ★★ ($p < 0.01$). B: The mean fluorescence intensity is represented from those cells or nuclei that have incorporated YOYO-1 - labeled DNA. Statistically significant differences of pairs are denoted by ★ or ★★ ($p < 0.05$ or $p < 0.01$, respectively). Experiments were performed in duplicate, values are means ± SD of one representative experiment (n=3).

The mean fluorescence intensity of cells that have incorporated DNA increased with the MW of LPEI and the NP ratio, whereas the mean fluorescence intensity of isolated nuclei seems to have reached a limit at the value 170. The mean fluorescence intensity of whole cells with incorporated polyplexes was significantly higher than of the nuclei alone, when cells were transfected with LPEI 5.0 – polyplexes at NP 18 ($p<0.05$) and 24 ($p<0.01$) or with LPEI 9.0 – polyplexes at NP 24 ($p<0.01$). Other polyplexes showed no statistically significant differences in the mean fluorescence intensity between whole cells and the nuclei (Figure 10 B).

Discussion

A challenging demand in the field of non-viral gene therapy is to provide efficient delivery without significant toxicity. LPEI 22 has been described to have a superior ability to induce gene transfer compared to its branched form [17,20,34]. We explored the possibility and potential of utilizing LPEIs within the range of 1.0 to 9.5 kDa as carriers for gene delivery to verify our hypothesis that LPEIs with low MWs are substantially less toxic than their high MW counterparts, but still retain their ability for gene transfer. We sought to overcome the frequent restriction that high transfection efficiency is limited by the cytotoxicity of the non-viral carrier.

Experiments were performed with polyplexes at NP ratios from 6 to 30 in serum-free culture conditions. We found that LPEIs with MWs lower than 22 kDa are very efficient gene carriers. A maximal transfection efficiency of about 44% was obtained with LPEI 5.6 at NP 18. We could also show that a MW greater than 1.0 kDa is necessary for gene expression. The values are not easy to compare with other studies carried out with LPEI 22, because these are confined to the gene expression of luciferase [4,5,33] and do not report a percentage of transfected cells. Compared to our own investigations with LPEI 22 in the same test system, we could reach even higher transfection efficiencies with certain low MW LPEI derivatives and NP ratios. To interpret the results, it is reasonable to divide the applied polyplexes into two groups: LPEI – polyplexes with a MW from 9.5 to 5.6 kDa and from 5.0 to 1.0 kDa. Regarding the group with the higher MW LPEIs in polyplexes, generally, when increasing the MW of the polymer and the NP ratio, the transfection efficiency increases to a certain point, while the cell viability decreases. Cell viability may be reduced drastically due to a large excess of polymer infiltrating the cells. Probably, the cells are then metabolically inactive and not able to express the delivered gene. This could be the reason why the transfection efficiency also decreases with decreasing cell viability. In the second group with lower MW LPEIs in polyplexes, it is surprising to see that the transfection efficiency can be enhanced with the NP ratio without affecting cell viability. LPEI 5.0 – polyplexes yield a transfection efficiency of about 40% with only a slight reduction in cell viability. The average expression of EGFP per cell seems to be nearly uneffected by the MW of LPEI and the NP ratio applied. Recently, it was shown that large complexes lead to a higher transfection efficiency than smaller ones [15]. To demonstrate that the high transfection efficiency is not only an effect of sedimentation due to polyplex size, but also depends on the MW of LPEI, we examined the efficiency of small polyplexes formed in glucose solutions. These particles have roughly the same size independent of the MW of the polymer (about 200 nm [13]) and differences in

transfection efficiency should be independent of polyplex size and depend on MW of the polymer (and other factors). The fact that small LPEI 9.0 – polyplexes result in a higher transfection efficiency than the corresponding LPEI – 5.0 polyplexes affirms that the MW of LPEI plays a major role in transfection process. Notably, such a high transfection efficiency accompanied by such a high cell viability has not yet been reported. These results were achieved by reducing the chain length of the polymer while still retaining its overall amount.

As remarked before, polyplexes built in sodium chloride sediment onto the cells due to their size. Furthermore, polyplexes show a strong tendency towards aggregation after sedimentation onto the cells. Even though polyplexes built with various LPEIs have different sedimentation profiles due to varying size, and are therefore taken up by cells faster or slower, the uptake of polyplexes seems not to be a limiting step in the transfection process, because after 6 hours a large fraction of cells has taken up polyplexes irrespective of the MW and the NP ratio applied.

The endolysosmolytic activity is due to the ability of PEI to increase the ionic strength in endosomes by capturing protons and chloride ions during endosomal acidification, which causes osmotic swelling and subsequent endosome disruption [10,35]. As demonstrated by the reduced efficacy in gene delivery of LPEI 2.0 -, 5.0 - and 9.0 – polyplexes in the presence of bafilomycin A1 [22], the ´proton sponge effect` is also applicable and necessary for the high transfection efficiency of these polymers. However, the suppression of gene expression after application of bafilomycin A1 declines with the MW of the polymer. This implies that these polyplexes may escape by another mechanism from lysosomes, such as direct membrane disruption [36], endosomal disruption by PEI swelling due to charge repulsion upon acidification, or may not escape from the acidic organelles. The results were confirmed in a complimentary experiment: sucrose, which is used as a lysosomotropic agent [21], produces no increase in transfection efficiency with LPEI 5.0 - and 9.0 – polyplexes. No increase in transfection efficiency results when sucrose is administered in conjunction with polyplexes with high intrinsic endosomolytic activity, as they can escape from endolysosomes without the addition of a lysosomotropic agent or rather because those polyplexes do not reach the lysosomes. However, a higher percentage of CHO-K1 cells express EGFP after the co-application of LPEI 2.0 – polyplexes and sucrose. This means that the buffer capacity and ability to escape from lysosomes depends on the MW of the polymer.

The involvement of acidic organelles could also be demonstrated by CLSM. Particularly small polyplexes are found in acidic organelles, and most of them are released into the cytoplasm. Larger polyplexes are often only partially colocalized with acidic organelles,

because they either do not completely fit into the organelles or more likely, because they rapidly escape due to their higher buffer capacity [15]. In accordance with the literature, we could show that small complexes reach the lysosomal compartment, whereas big complexes either do not reach these organelles [37] or, in our opinion, probably escape from them rapidly. It could be that the smaller ones escape from lysosomes via the proton sponge mechanism, whereas the larger ones reach the cytoplasm via membrane damage [36] or other non-osmotic effects [15]. It is remarkable that many LPEI 5.0 – polyplexes at NP 24, a combination of MW and NP ratio that leads to a high transfection efficiency, can be detected freely dispersed in cytosol after only 2 hours.

The largest hurdle to non-viral gene delivery is nuclear uptake. As shown by CLSM, some polyplexes reach the nuclei intact, some of these polyplexes may dissociate inside the nuclei or other polyplexes disintegrate in the cytosol and DNA or polymer reach the nucleus on their own. Therefore, to track the polyplexes, we preferentially used labeled DNA, as it is the component of the polyplexes that has to be transcribed in the nucleus. Regarding the CLSM pictures after 2 hours of incubation, it is not surprising to see that the nuclear membrane seems to be a barrier for polyplexes. But this difference in the amount of polyplexes in the cytosol and nucleus seems to equalize with further incubation. Comparing the number of cells and nuclei the have incorporated DNA, no differences could be found for LPEI 5.0 and 9.0. This means that every cell that has taken up polyplexes with labeled DNA exhibits DNA not only in the cytosol, but also in the nucleus. Using LPEI 2, a polymer that leads to very low transfection efficiency, significantly fewer nuclei have taken up polyplexes compared to whole cells. But this method and the determination of the mean fluorescence intensity do not provide information about the number of polyplexes that are located in whole cells and nuclei. The mean fluorescence intensity just gives an indication that the number of intracellular polyplexes increases with the MW and NP ratio and, because there seems to be a limit in the mean fluorescence intensity of nuclei, that only a certain amount of DNA can reach the nuclei. We suggest that larger polyplexes remain in the cytosol due to their size; only portions of the larger polyplexes reach the nucleus, while smaller polyplexes may enter the nucleus intact. The precise mechanism of entry of polyplexes into the cell nuclei is as yet unexplained. Endolysosomal vesicles may be a vehicle for the transport of small polyplexes to the nuclear membrane. However, the size of polyplexes, respectively the MW of LPEI, may play a major role in nuclear uptake.

In summary, we first showed that we can control the transfection efficiency by the MW of the polymer and the NP ratio and that a certain chain length of LPEI is necessary for efficient

gene delivery. Moreover, we could prove our hypothesis that low MW LPEIs allow for a high transfection efficiency accompanied by a low cytotoxicity. In conclusion, our study suggests LPEIs with low MW as promising candidates for non-viral gene delivery, because they are very efficient and significantly less toxic than their higher MW counterparts. The endolysosomolytic activity and ability to cross the nuclear membrane are major prerequisites for the high transfection efficiency.

References

1. Tatum EL. Molecular biology, nucleic acids, and the future of medicine. *Perspect Biol Med* 1966; **10**: 19-32.

2. Sadelain M. Insertional oncogenesis in gene therapy: how much of a risk? *Gene Ther* 2004; **11**: 569-573.

3. Marshall E. What to do when clear success comes with an unclear risk? *Science* 2002; **298**: 510-511.

4. Wightman L, Kircheis R, Rossler V, Carotta S, Ruzicka R, Kursa M, Wagner E. Different behavior of branched and linear polyethylenimine for gene delivery in vitro and in vivo. *J Gene Med* 2001; **3**: 362-372.

5. Wiseman JW, Goddard CA, McLelland D, Colledge WH. A comparison of linear and branched polyethylenimine (PEI) with DCChol/DOPE liposomes for gene delivery to epithelial cells in vitro and in vivo. *Gene Ther* 2003; **10**: 1654-1662.

6. Godbey WT, Wu KK, Mikos AG. Poly(ethylenimine) and its role in gene delivery. *J Control Release* 2001; **60**: 149-160.

7. Boussif O, Zanta MA, Behr JP. Optimized galenics improve in vitro gene transfer with cationic molecules up to 1000-fold. *Gene Ther* 1996; **3**: 1074-1080.

8. Abdallah B, Hassan A, Benoist C, Goula D, Behr JP, Demeneix BA. A powerful nonviral vector for in vivo gene transfer into the adult mammalian brain: polyethylenimine. *Hum Gene Ther* 1996; **7**: 1947-1954.

9. Boussif O, Lezoualc'h F, Zanta MA, Mergny MD, Scherman D, Demeneix B, Behr J. A versatile vector for gene and oligonucleotide transfer into cells in culture and in vivo: polyethylenimine. *Proc Natl Acad Sci U S A* 1995; **92**: 7297-7301.

10. Sonawane ND, Szoka FC, Verkman AS. Chloride accumulation and swelling in endosomes enhances DNA transfer bypolyamine-DNA polyplexes. *J Biol Chem* 2003; **278**: 44826-44831.

11. Godbey WT, Wu KK, Mikos AG. Size matters: molecular weight affects the efficiency of poly(ethylenimine) as a gene delivery vehicle. *J Biomed Mater Res* 1999; **45**: 268-275.

12. Godbey WT, Wu KK, Mikos AG. Poly(ethylenimine)-mediated gene delivery affects endothelial cell function and viability. *Biomaterials* 2000; **22**: 471-480.

13. Lungwitz U, Breunig M, Blunk T, Goepferich A. Synthesis and application of low molecular weight linear polyethylenimines for non-viral gene delivery. *Proceedings of the annual meeting of the German Pharmaceutical Society* 2004; P T25: 157.

14. Kunath K, Von Harpe A, Fischer D, Petersen H, Bickel U, Voigt K, Kissel T. Low-molecular-weight polyethylenimine as a non-viral vector for DNA delivery: comparison of physicochemical properties, transfection efficiency and in vivo distribution with high-molecular-weight polyethylenimine. *J Control Release* 2003; **89**: 113-125.

15. Ogris M, Steinlein P, Kursa M, Mechtler K, Kircheis R, Wagner E. The size of DNA/transferrin-PEI complexes is an important factor for gene expression in cultured cells. *Gene Ther* 1998; **5**: 1425-1433.

16. Brunner S, Furtbauer E, Sauer T, Kursa M, Wagner E. Overcoming the nuclear barrier: cell cycle independent nonviral gene transfer with linear polyethylenimine or electroporation. *Mol Ther* 2002; **5**: 80-86.

17. Goula D, Benoist C, Mantero S, Merlo G, Levi G, Demeneix BA. Polyethylenimine-based intravenous delivery of transgenes to mouse lung. *Gene Ther* 1998; **5**: 1291-1295.

18. Ferrari S, Moro E, Pettenazzo A, Behr JP, Zacchello F, Scarpa M. ExGen 500 is an efficient vector for gene delivery to lung epithelial cells in vitro and in vivo. *Gene Ther* 1997; **4**: 1100-1106.

19. Bragonzi A, Boletta A, Biffi A, Muggia A, Sersale G, Cheng SH, Bordignon C, Assael BM, Conese M. Comparison between cationic polymers and lipids in mediating systemic gene delivery to the lungs. *Gene Ther* 1999; **6**: 1995-2004.

20. Goula D, Becker N, Lemkine GF, Normandie P, Rodrigues J, Mantero S, Levi G, Demeneix BA. Rapid crossing of the pulmonary endothelial barrier by polyethylenimine/DNA complexes. *Gene Ther* 2000; **7**: 499-504.

21. Ciftci K, Levy RJ. Enhanced plasmid DNA transfection with lysosomotropic agents in cultured fibroblasts. *Int J Pharm* 2001; **218**: 81-92.

22. Bowman EJ, Siebers A, Altendorf K. Bafilomycins: a class of inhibitors of membrane ATPases from microorganisms, animal cells, and plant cells. *Proc Natl Acad Sci U S A* 1988; **85**: 7972-7976.

23. Breunig M, Lungwitz U, Klar J, Kurtz A, Blunk T, Goepferich A. Polyplexes of polyethylenimine and per-n-methylated polyethylenimine-cytotoxicity and transfection efficiency. *J Nanosci Nanotechnol* 2004; **4**: 512-520.

24. Wrobel I, Collins D. Fusion of cationic liposomes with mammalian cells occurs after endocytosis. *Biochim Biophys Acta* 1995; **1235**: 296-304.

25. Murphy RF, Powers S, Verderame M, Cantor CR, Pollack R. Flow cytofluorometric analysis of insulin binding and internalization by Swiss 3T3 cells. *Cytometry* 1982; **2**: 402-406.

26. Wattiaux R, Wattiaux-De Coninck S, Rutgeerts MJ, Tulkens P. Influence of the injection of a sucrose solution on the properties of rat-liver lysosomes. *Nature* 1964; **203**: 757-758.

27. Anji A, Shaik KA, Kumari M. Effect of ethanol on lipid-mediated transfection of primary cortical neurons. *Ann N Y Acad Sci* 2003; **993**: 95-102.

28. Godbey WT, Barry MA, Saggau P, Wu KK, Mikos AG. Polyethylenimine-mediated transfection: a new paradigm for gene delivery. *J Biomed Mater Res* 2000; **51**: 321-328.

29. Merdan T, Kunath K, Fischer D, Kopecek J, Kissel T. Intracellular processing of poly(ethylene imine)/ribozyme complexes can be observed in living cells by using confocal laser scanning microscopy and inhibitor experiments. *Pharm Res* 2002; **19**: 140-146.

30. Lemieux B, Percival MD, Falgueyret JP. Quantitation of the lysosomotropic character of cationic amphiphilic drugs using the fluorescent basic amine Red DND-99. *Anal Biochem* 2004; **327**: 247-251.

31. Preston RA, Murphy RF, Jones EW. Assay of vacuolar pH in yeast and identification of acidification-defective mutants. *Proc Natl Acad Sci U S A* 1989; **86**: 7027-7031.

32. Krasowska A, Chmielewska L, Luczynski J, Witek S, Sigler K. The dual mechanism of the antifungal effect of new lysosomotropic agents on the saccharomyces cerevisiae RXII strain. *Cell Mol Biol Lett* 2003; **8**: 111-120.

33. Brissault B, Kichler A, Guis C, Leborgne C, Danos O, Cheradame H. Synthesis of linear polyethylenimine derivatives for DNA transfection. *Bioconjug Chem* 2003; **14**: 581-587.

34. Goula D, Remy JS, Erbacher P, Wasowicz M, Levi G, Abdallah B, Demeneix BA. Size, diffusibility and transfection performance of linear PEI/DNA complexes in the mouse central nervous system. *Gene Ther* 1998; **5**: 712-717.

35. Kichler A, Leborgne C, Coeytaux E, Danos O. Polyethylenimine-mediated gene delivery: a mechanistic study. *J Gene Med* 2001; **3**: 135-144.

36. Bieber T, Meissner W, Kostin S, Niemann A, Elsasser HP. Intracellular route and transcriptional competence of polyethylenimine-DNA complexes. *J Control Release* 2002; **82**: 441-454.

37. Wattiaux R, Laurent N, Wattiaux-De Coninck S, Jadot M. Endosomes, lysosomes: their implication in gene transfer. *Adv Drug Deliv Rev* 2000; **41**: 201-208.

Chapter 3

Mechanistic Insights into Linear Polyethylenimine - mediated Gene Transfer

Miriam Breunig[1], Uta Lungwitz[1], Renate Liebl[1], Birgit Obermayer[2], Juergen Klar[2], Torsten Blunk[1], Achim Goepferich[1]

[1] Department of Pharmaceutical Technology, University of Regensburg, Universitaetsstrasse 31, 93040 Regensburg, Germany

[2] Department of Physiology, University of Regensburg, Universitaetsstrasse 31, 93040 Regensburg, Germany

To be submitted

Abstract

Background

We recently debuted a variety of linear polyethylenimines (LPEIs) with relatively low molecular weights ranging from 1.0 to 9.5 kDa as polymeric carriers for nucleic acid delivery. The highest transfection efficiency (about 44%) was obtained with LPEI 5.6 kDa, while the cytotoxicity remained low. In order to explore conceptual aspects for further optimization of polymer-based gene delivery and to gain a more complete insight into LPEI-mediated gene transfer, the kinetics of the uptake as well as the intracellular stability and transport of plasmid DNA and LPEI - polyplexes were investigated in CHO-K1 cells. Furthermore, as the ionic strength of the polyplex formation medium and the presence of serum during the transfection process strongly influence the size of polyplexes, we evaluated their impact on the transfection efficacy and cytotoxicity.

Methods

The transfection efficiencies and cytotoxicities of a series of LPEI - polyplexes formed in media with varying ionic strengths were compared in CHO-K1 cells in the presence and absence of serum with flow cytometry. The uptake and stability of the LPEI - polyplexes were assessed by flow cytometry and confocal laser scanning microscopy, respectively. Furthermore, real-time PCR was used to determine the absolute amount of intact plasmid DNA after internalization of polyplexes.

Results and Conclusions

In summary, we did not determine a correlation between the uptake, stability of polyplexes or plasmid DNA and the transfection efficiency. Therefore, we conclude that these mechanisms only contribute to a negligible extent to the high efficacy of certain LPEIs. This means that we have a very robust system for transfection that is widely independent of external influences and suitable for routine transfection experiments. Furthermore, as the ionic strength and culture medium favor the superiority of certain polyplexes, a more detailed knowledge of the polyplex structure and composition and their influence on the transfection efficiency would be a further step towards the optimization of PEI-based delivery systems.

Introduction

Technologies for gene delivery have advanced significantly over the past decade. However, no delivery system that is both safe and highly efficient has been introduced so far. Viral vectors are very efficient at transferring genes into mammalian cell, but are also accompanied by severe safety risks, namely immunogenicity and mutagenesis [1,2]. Therefore, interest in using polymers as gene carriers is growing as they may help to overcome the problems associated with viruses. Currently, in order to further enhance their efficacy and meet the requirements of idealized non-viral gene delivery systems, polymers are designed with tailor-made structures and chemical properties.

Due to its excellent efficacy, polyethylenimine (PEI) has gained some prominence compared to other non-viral gene delivery systems. It is capable of condensing DNA into polyplexes, allowing for cellular access and uptake of the nucleic acid. Once the polyplexes enter the endo-lysosomal compartment, PEI protects the DNA from degradation and guides it efficiently into the cytoplasm [3-6]. The final step in this process is the translocation of DNA to the nucleus for gene expression [7,8]. PEI exists as a branched polymer (BPEI), and in its linear form (LPEI), which has been shown to have a superior transfection efficiency and cell viability relative to BPEI-based transfection systems [9-12]. We have recently introduced a variety of LPEIs with molecular weights (MWs) ranging from 1.0 to 9.5 kDa [13]. The transfection efficiency of these LPEI - polyplexes can be altered by varying the MW and the amount of the polymer available for polyplex formation. The highest transfection efficiency (about 44%) was obtained with LPEI 5.6 kDa, while the cytotoxicity remained low. We proposed that the endo-lysosomolytic escape capacity and ability to cross the nuclear membrane are major prerequisites for the high transfection efficiency of LPEI - polyplexes.

For a rational design and further optimization of the PEI-based delivery vectors, it would be desirable to elucidate the biophysical interactions of existing polyplexes with cells in detail. Besides the endo-lysosomal escape and nuclear entry, the uptake of polyplexes is also an important step in the transfection process. Unfortunately, it seems nearly impossible to contol the uptake of unmodified polyplexes in cell culture systems, usually a higher amount than necessary for gene expression is taken up by cells, which also contributes to a significant part to the high cytotoxicity of certain polyplexes. Furthermore, the impact of the intracellular stability of polyplexes and plasmid DNA on the transfection efficacy has been investigated only in few studies so far.

Therefore, we chose three LPEI derivatives with MWs of 9.0, 5.0 and 2.0 kDa as carriers and addressed the uptake, intracellular stability and transport of plasmid DNA and polyplexes, in search of differences that could explain their varying transfection efficiencies. These three polymers were chosen because they have the same structure, but differed in their MW, transfection efficiency and cell viability: Polyplexes containing LPEI 9.0 kDa are capable of a high transfection efficiency, but are also quite cytotoxic. In contrast, the high efficacy of LPEI 5.0 kDa is accompanied by minimal cytotoxicity, while both the transfection efficiency and cytotoxicity of polyplexes formed with LPEI 2.0 kDa are very low [13]. Furthermore, as the ionic strength of the medium used during polyplex formation and the presence or absence of serum during the transfection process strongly influence the size of the polyplexes, we evaluated their influence on the transfection efficacy.

With these investigations, we intended to determine the robustness of our LPEI-based gene delivery system and whether LPEI - polyplexes are candidates for routine transfection experiments. Furthermore, this study strove to gain a more complete insight into LPEI-mediated gene transfer in order to compile a rational concept to further improve the efficacy of polymer-based nucleic acid delivery systems.

Materials and Methods

All materials were purchased from Sigma-Aldrich Chemie GmbH (Germany) unless otherwise stated.

Cell culture

CHO-K1 cells (ATCC No. CCL-61) were grown in 75 ml culture flasks in a 5% CO_2 atmosphere at 37°C as adherent culture to 90% confluence before seeding. Culture medium consisted of Ham´s F-12 supplemented with 10% FBS (Biochrom AG, Germany).

Non-viral carriers

LPEI derivates with MWs of 9.0, 5.0 and 2.0 kDa were synthesized by ring-opening polymerization of 2-ethyl-2-oxazoline and acidic hydrolysis of the corresponding poly(2-ethyl-2-oxazoline) as previously described [14]. In the following, the notation of polymers was made without the unit kDa, for example LPEI 9.0 represents LPEI with a MW of 9.0 kDa. When indicated, polymers were labeled with 6-TAMRA-succinimidyl ester (Molecular Probes, The Netherlands) as described [13].

Plasmid isolation and labeling

Plasmid encoding enhanced green fluorescent protein (EGFP) (pEGFP-N1, Clontech, Germany) was used as reporter gene in this study. Plasmid was isolated from E. coli using a Qiagen Plasmid Maxi Kit (Qiagen, Germany) according to the supplier´s protocol. When indicated, plasmid DNA was stained with the intercalating dye YOYO-1 (Molecular Probes, The Netherlands). The labeling reaction was carried out with a molar ratio of 1 dye molecule per 320 base pairs at room temperature in the dark.

Preparation of polyplexes

Plasmid DNA/LPEI complexes were prepared at NP ratios (ratio of nitrogens in polymer to phosphates in DNA) of 6, 12, 18, 24 and 30. Polyplexes were formed by diluting a mixture of 2 µg DNA and appropriate amount of polymer solution to 50 µl with 150 mM sodium chloride or 5% glucose. The resulting LPEI - polyplexes were incubated for 20 minutes at room temperature before use. The polyplexes are labeled such that LPEI 9.0 – polyplexes indicates that the plasmid DNA was complexed with LPEI 9.0.

In vitro transfection and cytotoxicity experiments

For gene transfer studies, CHO-K1 cells were grown in 24-well plates at an initial density of 38,000 cells per well. 18 hours after plating, the culture medium was removed, cells were washed with PBS (Invitrogen, Germany) and 900 µl serum-free or -containing medium was added (transfection medium). Thereafter, the prepared polyplexes were added to the cells. After 4 hours, the medium was replaced with 1 ml of culture medium. 48 hours later, cells were prepared for flow cytometry analysis. Floating cells were collected and combined with adherent cells after trypsinization. The pooled cells were washed twice with PBS, resuspended in 500 µl PBS and propidium iodide was added at a concentration of 1 µg / ml to half of the samples. Measurements were taken on a FACSCalibur (Becton Dickinson, Germany) using CellQuest Pro software (Becton Dickinson, Germany) and WinMDI 2.8 (©1993-2000 Joseph Trotter). EGFP positive cells were detected using a 530/30 nm band-pass filter, whereas the propidium iodide emission was measured with a 670 nm longpass filter. Logarithmic amplification of EGFP and propidium iodide emission in green and red fluorescence was obtained with 20,000 cells counted for each sample. In a density plot representing forward scatter against sideward scatter, whole cells were gated out and depicted in two-parameter dot plots of EGFP versus propidium iodide for data analysis. The EGFP

positive region corresponds to the transfection efficiency, while the fraction of propidium iodide negative cells was used as a measure of cell viability [15].

Cellular uptake of polyplexes

YOYO-1 - labeled DNA was used to monitor the polyplex delivery for all three polymer MWs. 50,000 CHO-K1 cells per well were seeded in a 24-well plate and then treated as described in the previous section, but detached after transfection for 6 hours. Trypsin (Invitrogen, Germany) and PBS were supplemented with 20 mM sodium azide (Merck KGaA, Germany) to prevent further particle uptake and remove surface-bound polyplexes [13,16,17]. The percentage of cells that had internalized polyplexes was determined by the number of YOYO-1 positive cells by flow cytometry. YOYO-1 was excited with a 488 nm argon laser and detected with a 530/30 bandpass filter. The mean fluorescence intensity of those cells that had taken up polyplexes served an indirect measure of the number of internalized polyplexes [13].

Intracellular trafficking of polyplexes - confocal laser scanning microscopy (CLSM)

A Zeiss Axiovert 200 M microscope coupled to a Zeiss LSM 510 scanning device (Carl Zeiss Co. Ltd., Germany) was used for CLSM experiments. The inverted microscope was equipped with a Plan – Apochromat 63x and Plan – Neofluar 100x objective. Cells were plated in an 8 – well Lab-Tek^{TM} Chambered Coverglass (Nunc GmbH & Co. KG, Germany) at an initial density of 35,000 cells / chamber in a volume of 400 µl culture medium. To maintain a pH of 7.4, 20 mM HEPES was supplemented to the medium. After 18 hours, polyplexes were added and imaging commenced immediately in each well at 37°C. The thickness of the optical sections was between 0.7 and 1.2 µm.

For the estimation of intracellular disintegration of polyplexes, TAMRA-labeled LPEI 9.0 or 5.0 and YOYO-1 - labeled DNA were used. YOYO-1 – labeled DNA was excited with a 488 nm argon laser and fluorescence was detected using a 505 – 530 nm band-pass filter, whereas the TAMRA – labeled LPEI was excited at 543 nm and recorded with a 560 nm longpass filter. Images were taken in the multitracking modus. A lot of green, red, and yellow spots, i.e. free plasmid DNA, free polymer, and polyplexes, respectively, were scored for each condition from about 25 images.

For the detection of polyplexes in endocytotic vesicles of the cell, polyplexes were marked with TAMRA-labeled LPEI 9.0 or 5.0 and YOYO-1 -labeled DNA, while FM4-64 was added

to highlight the vesicles. An argon laser with 488 nm was used to excite YOYO-1 and FM4-64; the fluorescence was imaged using a 505 - 530 nm bandpass filterand a 650 nm longpass filter, respectively. TAMRA-labeled LPEI was excited at 543 nm and the fluoresecence was recorded with a 560 - 615 nm bandpass filter. Images were taken in the multitracking modus. Before each measurement, a sample with one label only was used to adjust the gain of the photomultiplier tubes to eliminate cross-talk. Images were then acquired with constant microscope settings. The intensity profile of the fluorescence emission was examined to identify a colocalization of LPEI and plasmid DNA with FM4-64 positive vesicles.

Isolation of plasmid DNA from whole cells and quantification by real-time PCR

After 6 hours of transfection and subsequent to washing with PBS, the intracellular plasmid DNA of attached cells was isolated according to the following procedure: Cells were resuspended in a buffer containing 50 mM Tris-HCl, 10 mM EDTA and 100 µg/ml Rnase A. Thereafter, the same volume of lysis solution (200 mM NaOH, 1% SDS) was added for 5 minutes at room temperature. The reaction was stopped by neutralization with 3 M potassium acetate (pH 5.5). After 15 minutes at 4°C, the sample was centrifuged at 12,000 rpm for 25 minutes. Plasmid DNA was precipitated from the supernatant, washed with 70% ethanol and resuspended in H_2O. A portion of each sample was subjected to agarose gel electrophoresis.
Real-time PCR was performed in a Light Cycler (Roche Applied Biosciences, Germany). The diluted template isolated from cells as described above was mixed with PCR master mix consisting of QuantiTect™ SYBR® Green PCR (Qiagen, Germany) and 10 pmol primer pairs (MWG Biotech GmbH, Germany). The forward primer (5´-ACG TAA ACG GCC ACA AGT TC-3´) and the reverse primer (5´- AAG TCG TGC TGC TTC ATG TG-3´) amplified a 187-bp fragment of the pEGFP-N1 plasmid. The absolute amount of target nucleic acid was determined with pEGFP-N1 as an external standard. The amplification program consisted of 1 cycle at 95°C for 15 min, followed by 45 cycles with a denaturing phase at 95°C for 15 s, an annealing phase of 20 s at 58°C, and an elongation phase at 72°C for 20 s. A melting curve analysis was performed in order to verify specifity and identify the PCR products. The protein content of the samples was determined with a Bradford assay [18].

In vitro transcription / translation assay

The functionality of plasmid DNA complexed to LPEI was determined using the TNT® quick coupled transcription/translation system (Promega, Germany). The kit's control vector, SP6, was transformed into the E. coli strain JM109 (Promega, Germany). The transformed cells

were expanded in LB broth medium supplemented with ampicillin and plasmid DNA was isolated as described above. The in vitro transcription/translation reaction with LPEI - polyplexes or plasmid DNA was performed according to the supplier´s protocol. Luciferase expression was determined using the luciferase assay system (Promega, Germany); the luminescence was measured by photon counting (Lumat LB 9507, Berthold, Germany).

Statistical analysis

All measurements were collected (n = 3 to 6) and expressed as means ± standard deviation (SD). Single factor of variance (ANOVA) was used in conjunction with a multiple comparison test (Tukey test) to assess the statistical significance.

Results

Transfection efficiency and cell viabilty

The transfection efficiency of polyplexes formed with LPEI 9.0, 5.0 or 2.0 and plasmid DNA was evaluated in CHO-K1 cells (Figure 1).

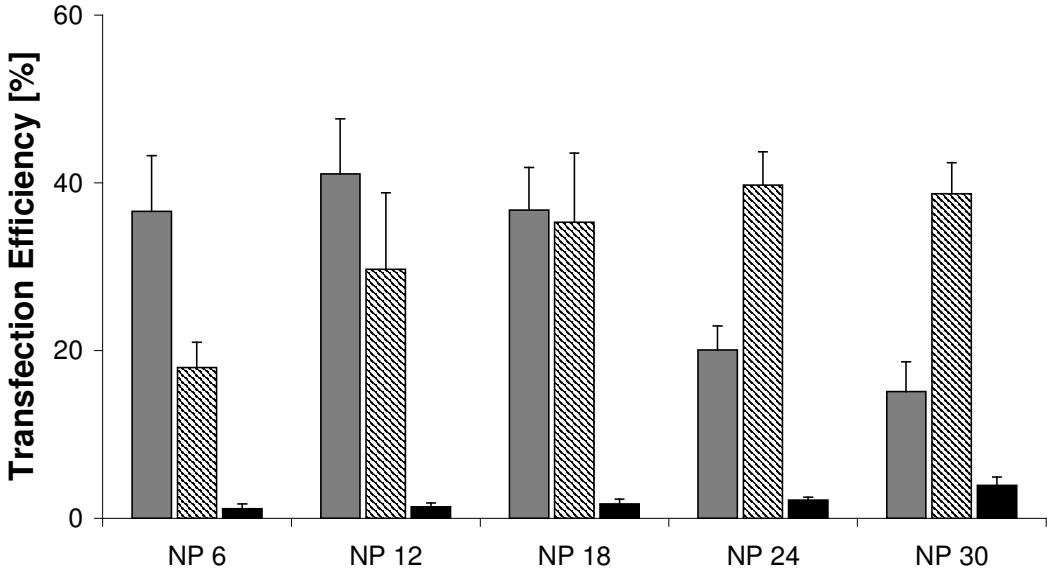

Figure 1: Transfection efficiency of LPEI 9.0 (■), 5.0 (▨) and 2.0 (■) complexed with pEGFP-N1 as reporter gene in CHO-K1 cells as determined by flow cytometry. Polyplexes were formed in 150 mM sodium chloride and the 4 hour incubation period was carried out in serum-free culture conditions. Experiments were performed in duplicate; values represent the EGFP positive cells as means ± SD of one representative experiment (n=6).

As reported previously, the efficacy could be increased with the polymer MW and the amount of polymer available for polyplex formation to a certain point, while the NP ratio for the optimal gene expression decreased with the MW of LPEI in polyplexes [13].

When introducing LPEIs with low MW, the transfection efficiency was examined for polyplexes formed in 150 mM sodium chloride solution and cells were kept in serum-free culture conditions during the 4 hour incubation period with polyplexes (Figure 1). By forming the polyplexes in salt-free medium (5% glucose instead of 150 mM sodium chloride) or using serum-containing transfection medium, the efficacy of certain polyplexes could be strongly influenced. Figure 2 shows that at certain NP ratios LPEI 9.0 - polyplexes formed in glucose and incubated in serum-free transfection medium were superior to other conditions tested. The transfection efficiency was maximized at a value of 52.38 ± 6.01% at NP 12, while the higher efficacy was also accompanied by a higher cell viability (Figure 3).

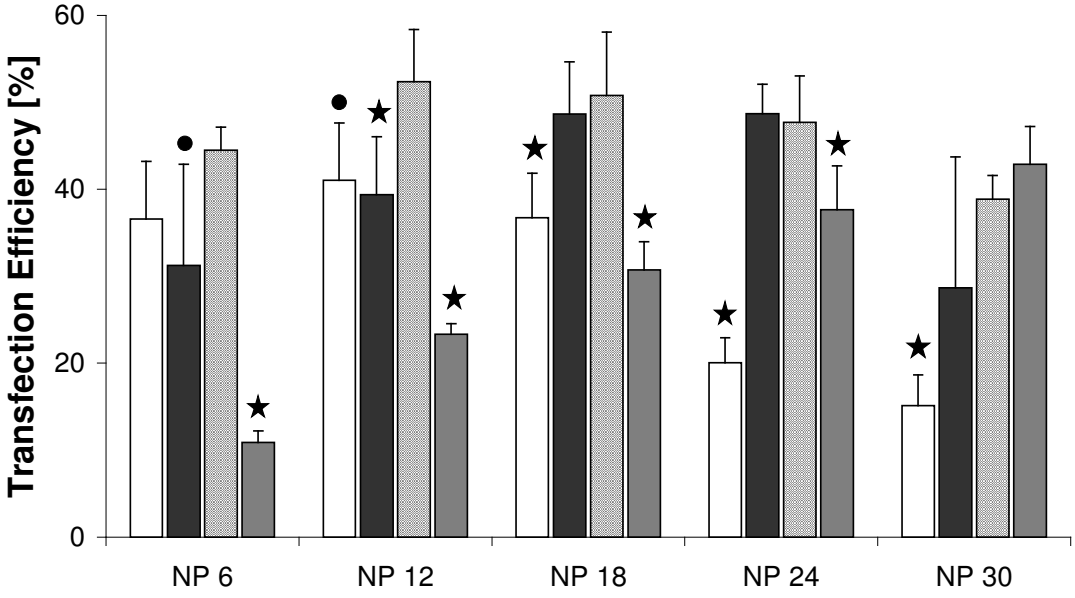

Figure 2: Transfection efficiency of LPEI 9.0 complexed with pEGFP-N1 as reporter gene in CHO-K1 cells as determined by flow cytometry. Polyplexes were formed in 150 mM sodium chloride or 5% glucose and the 4 hour incubation period was carried out in serum-free (150 mM sodium chloride: □ or 5% glucose: ▨, respectively) and –containing culture conditions (150 mM sodium chloride: ■ or 5% glucose: ▩, respectively). Experiments were performed in duplicate; values represent the EGFP positive cells as means ± SD of one representative experiment (n=6). Transfection efficiency is at the same NP ratio significantly lower compared to transfection efficiency of polyplexes formed in glucose and *incubated in serum-free transfection medium as denoted by ✦ ($p < 0.01$) or by ● ($p < 0.05$).*

When transfecting cells with LPEI 9.0 - polyplexes that were built in glucose in serum-containing medium, much higher NP ratios were necessary to yield the efficiencies possible under other conditions (Figure 2), although the cell viability was not affected by the NP ratio under these conditions (Figure 3).

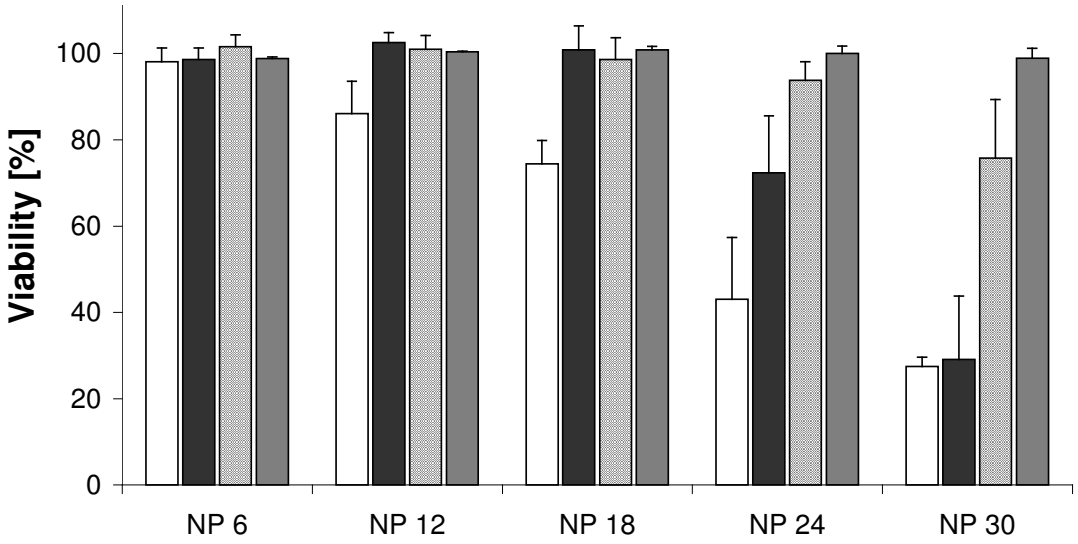

Figure 3: Relative viability of CHO-K1 cells after treatment with LPEI 9.0 - polyplexes at various NP ratios. Polyplexes were formed in 150 mM sodium chloride or 5% glucose and the 4 hour incubation period was carried out in serum-free (150 mM sodium chloride: □ or 5% glucose: ▨, respectively) and –containing culture conditions (150 mM sodium chloride: ■ or 5% glucose: ▩, respectively). Experiments were performed in duplicate, values are means ± SD of one representative experiment (n=3).

Using LPEI 5.0 in polyplexes, the transfection efficiency was higher in serum-free culture conditions irrespective of the medium used for polyplex formation (Figure 4). The effect of glucose - polyplexes on the transfection efficiency as achieved with LPEI 9.0 could not be observed. Similar tendencies as for LPEI 5.0 were obtained for LPEI 2.0, but the overall efficacy was much lower (data not shown).

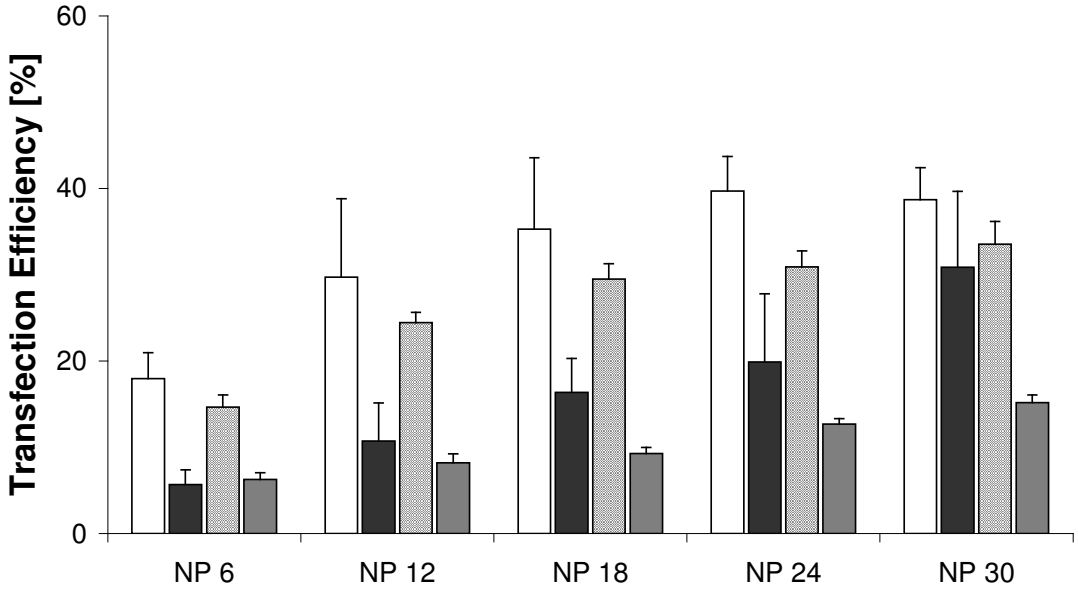

Figure 4: Transfection efficiency of LPEI 5.0 complexed with pEGFP-N1 as reporter gene in CHO-K1 cells as determined by flow cytometry. Polyplexes were built in 150 mM sodium chloride or 5% glucose and the 4 hour incubation period was carried out in serum-free (150 mM sodium chloride: □ or 5% glucose: ▨, respectively) and –containing culture conditions (150 mM sodium chloride: ■ or 5% glucose: ▩, respectively). Experiments were performed in duplicate; values represent the EGFP positive cells as means ± SD of one representative experiment (n=6).

Uptake of polyplexes

The uptake of complexes of LPEI 9.0, 5.0 and 2.0 and YOYO-1-labeled DNA in 150 mM sodium chloride was evaluated by measuring the cell-associated fluorescence after incubation in serum-free transfection medium (Figure 5). The number of fluorescent cells upon internalization of polyplexes increased with the NP ratio. No statistically significant differences were found between LPEIs at the same NP ratio, which implies that the number of cells that have taken up polyplexes is independent of the MW of LPEI.

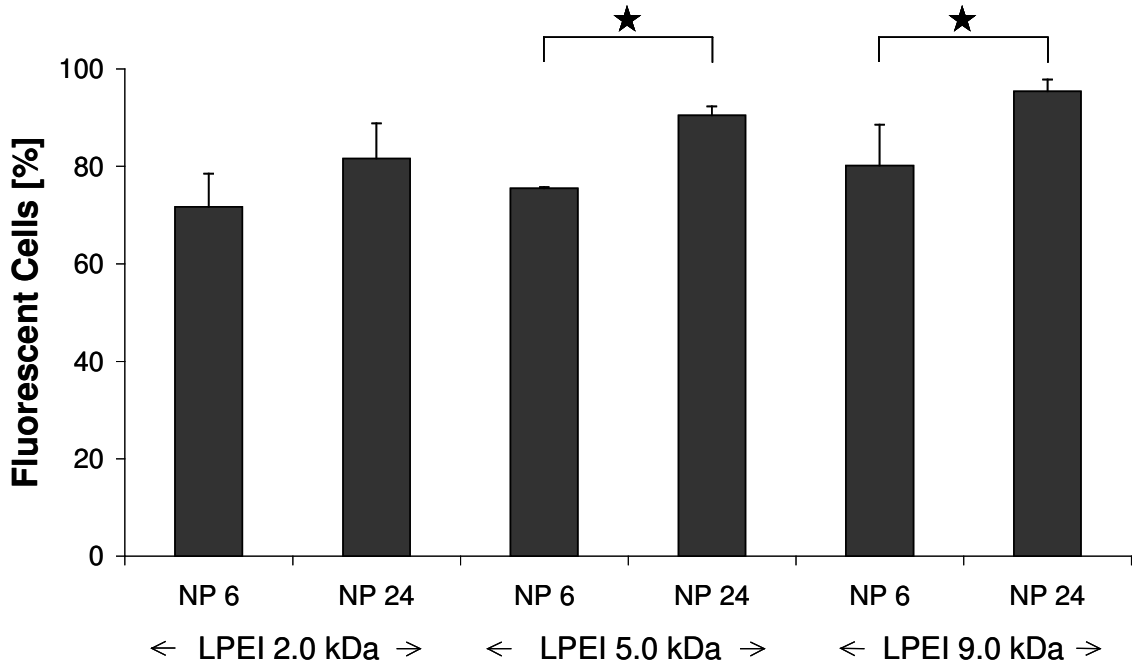

Figure 5: Uptake of polyplexes built in 150 mM sodium chloride with LPEIs of different MW as indicated in the legend. Fluorescent cells express the percentage of CHO-K1 cells that show a fluorescence due to intracellular YOYO-1 – labeled DNA. Statistically significant differences between the NP ratios of a certain polymer are denoted by ★ ($p < 0.05$). Experiments were performed in duplicate, values are means ± SD of one representative experiment (n=3).

The mean fluorescence intensity from those cells that have taken up polyplexes also increased with the NP ratio (Figure 6). No difference could be measured between LPEI 5.0 and 9.0 at the same NP ratio, but both polymers entailed a statistically significant higher mean fluorescence intensity compared to LPEI 2.0.

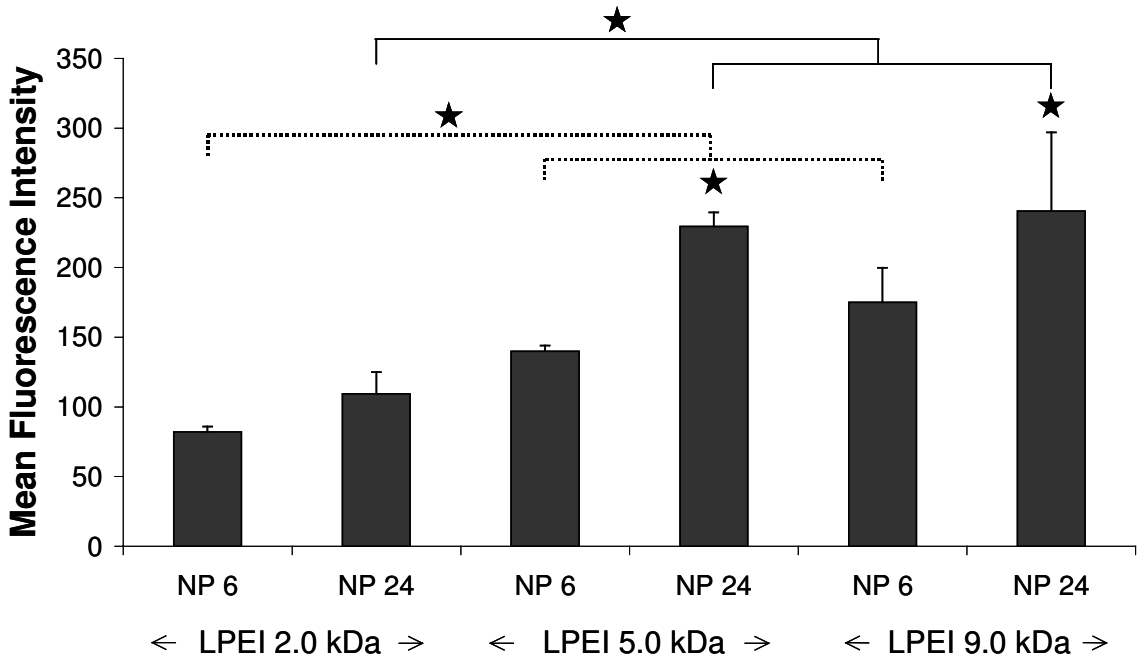

Figure 6: The mean fluorescence intensity is represented from those cells that have incorporated YOYO-1 - labeled DNA complexed with LPEI as indicated in the legend. Statistically significant differences between the NP ratios of a certain polymer or a certain NP ratio of various polymers are denoted by ★ ($p < 0.01$). Experiments were performed in duplicate, values are means ± SD of one representative experiment (n=3).

When fabricating the polyplexes in glucose solution or incubating in serum-containing culture conditions, the results were not statistically significantly different (data not shown).

Intracellular polyplex stability and transport

Polyplexes were double-labeled to investigate by CLSM whether they remained intact or disintegrated inside cells. DNA was labeled with YOYO-1 and depicted in green, whereas TAMRA-labeled LPEIs 9.0 or 5.0 (Figure 7 or 8, respectively; LPEI 2.0 was not tested) were represented by red dots. Polyplexes that were not internalized aggregated during the incubation time to large clusters. Over 95% of these extracellular polyplexes exhibited a mixture of colors representing polyplexes consisting of polymer and DNA and indicating that polyplexes were not dissociating. The smaller intracellular polyplexes could be divided into red, green and yellow dots, corresponding to polymer only, DNA only and intact polyplexes, indicating that at least a portion of the polyplexes dissociated. Polyplexes were considered to be intact even if the visual overlap of green and red was minimal.

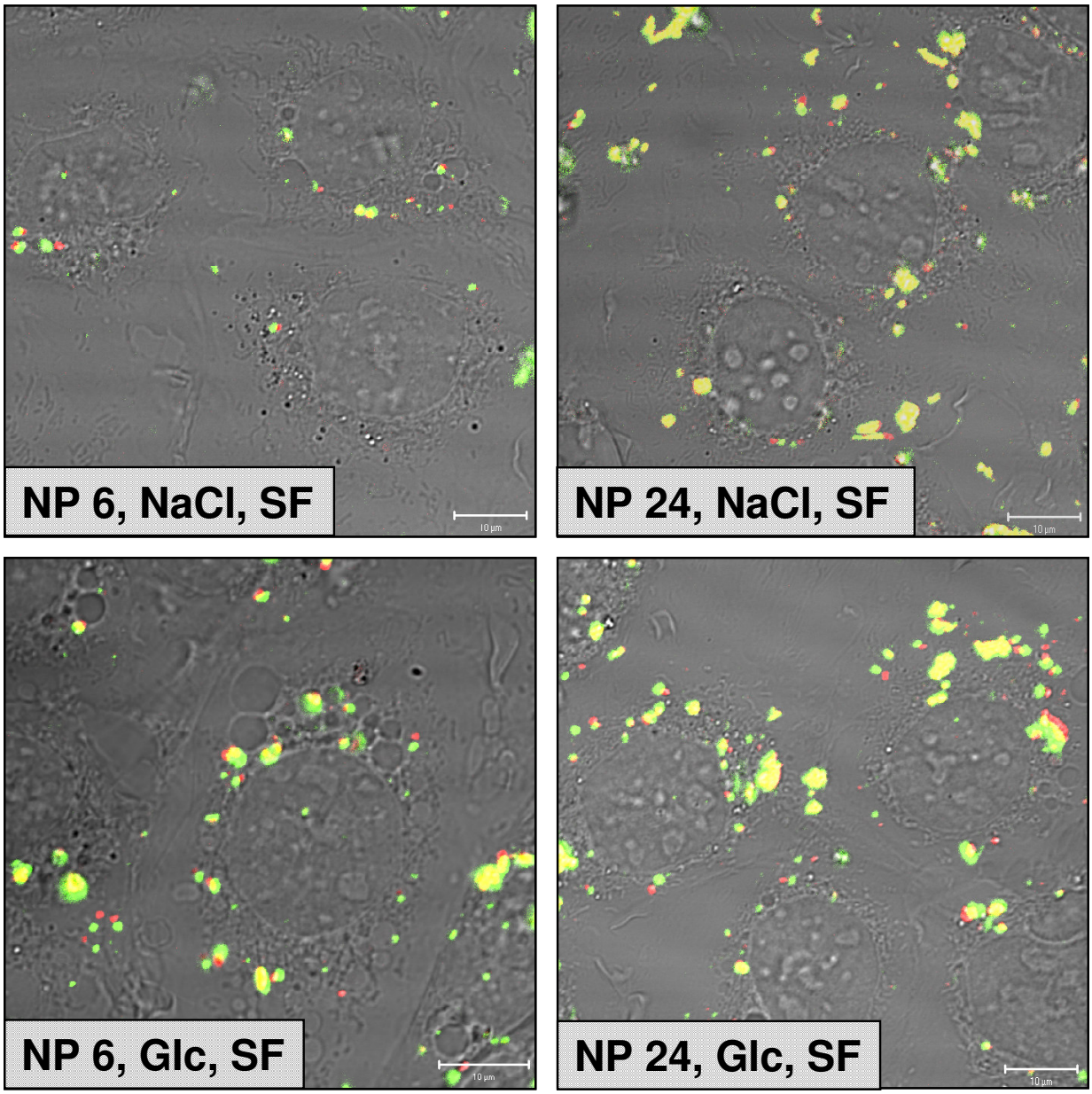

Figure 7: Double labeled LPEI 9.0 – polyplexes at NP 6 or 24 built in 150 mM sodium chloride (NaCl) or 5% glucose (Glc) solution, DNA is depicted in green, the polymer is represented by red dots and intact polyplexes by yellow dots. The 4 hour incubation period was carried out in serum-free (SF) culture medium. The confocal images were recorded after 6 hours internalization, representative images shown correspond to the superposition of phase-contrast image and the merge of green and red fluorescence images. Each bar indicates 10 µm.

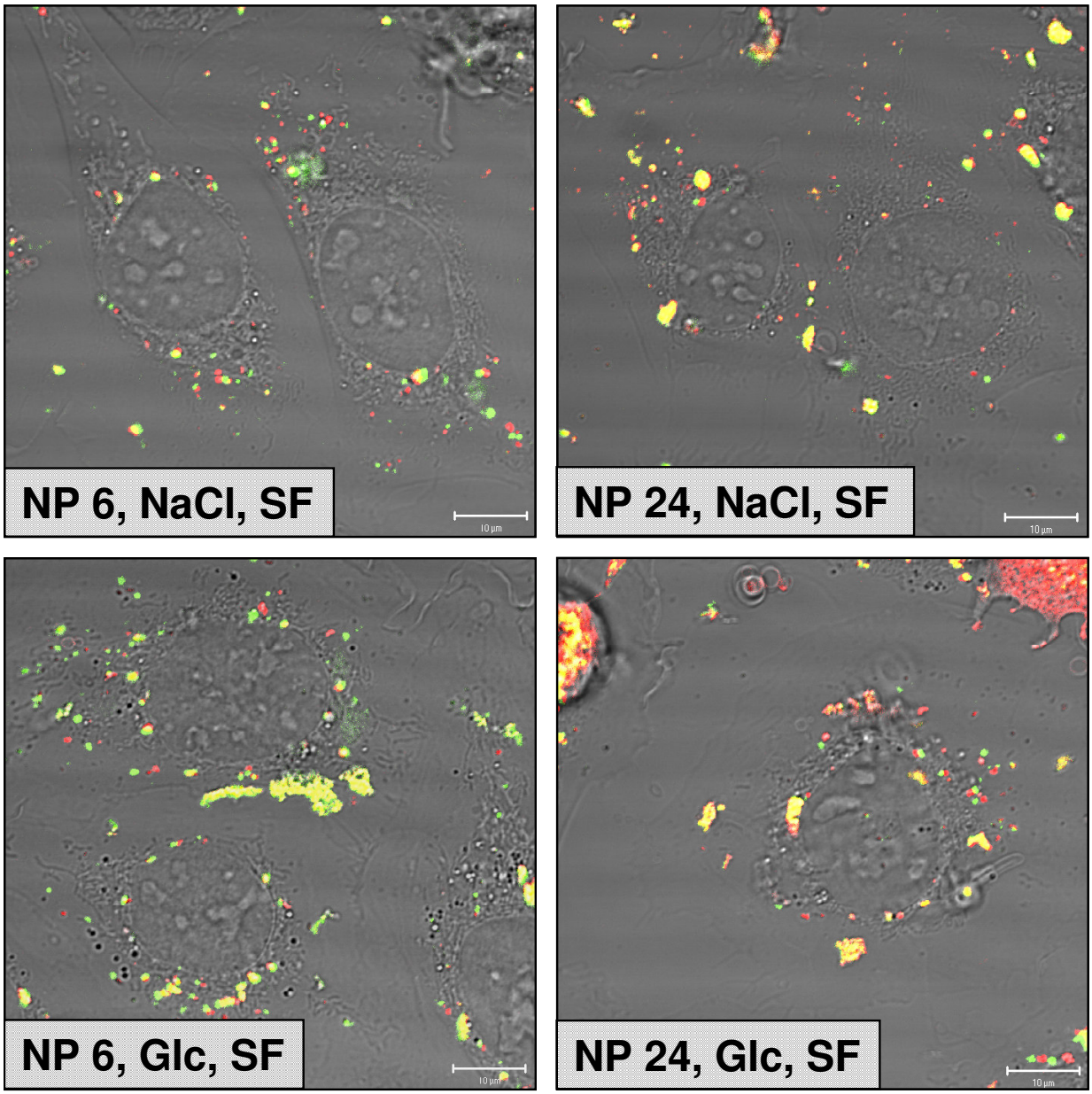

Figure 8: Double labeled LPEI 5.0 – polyplexes at NP 6 or 24 built in 150 mM sodium chloride (NaCl) or 5% glucose (Glc) solution, DNA is depicted in green, the polymer is represented by red dots and intact polyplexes by yellow dots. The 4 hour incubation period was carried out in serum-free (SF) culture medium. The confocal images were recorded after 6 hours internalization, representative images shown correspond to the superposition of phase-contrast image and the merge of green and red fluorescence images. Each bar indicates 10 µm.

No visual differences in the proportion of intact to dissociated polyplexes could be determined when changing the polymer, the medium used for polyplex fabrication or the NP ratio. To support the images with data, a certain number of green, red and yellow spots were scored and expressed as relative number of all spots (Figure 9).

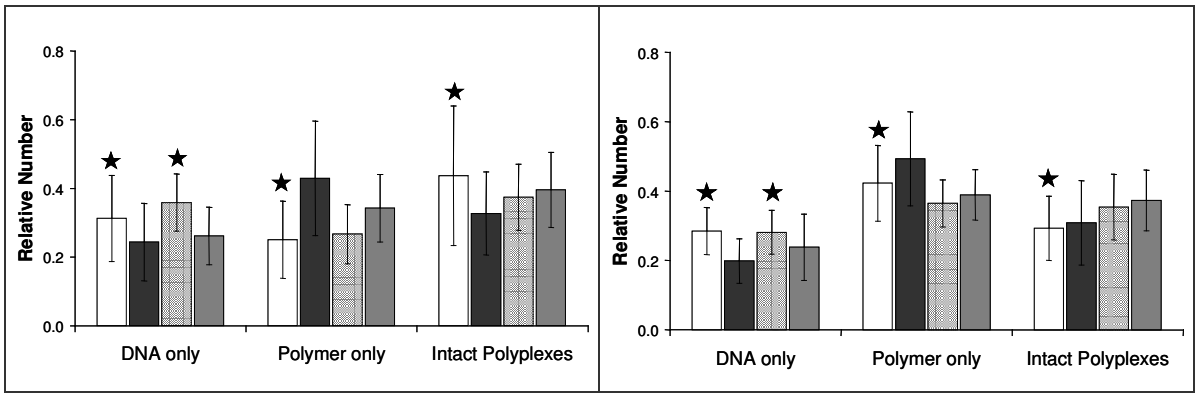

Figure 9: Estimation of dissociation of LPEI 9.0 – polyplexes (left) and LPEI 5.0 – polyplexes (right). Polyplexes were either built in 150 mM sodium chloride or 5% glucose at NP 6 (□ or ▨) and 24 (■ or ▩, respectively). Green, red, and yellow spots, i.e. free plasmid DNA, free polymer, and polyplexes, respectively, were scored for each condition from about 25 images. Statistically significant pairs of one polyplex formation medium are denoted by ★ ($p<0.01$).

No striking differences could be found between LPEI 9.0 or 5.0 in polyplexes. Free DNA slightly decreased with an increase in the NP ratio, at the same time the amount of free polymer increased, but only significantly when polyplexes were built in sodium chloride. The most prominent point to mention was the slightly higher amount of free LPEI 5.0 compared to LPEI 9.0. To estimate the amount of intact intracellular polyplexes the assumption was made that free DNA and polymer arise from polyplex dissociation in a proportion 1:1 (which is not completely correct, because it is not known if DNA and polymer participate in polyplex formation in this proportion). A calculated amount of about 60-70% polyplexes were still intact after 6 hours; they were detected both in the cytosol and the nucleus [13]. In serum-containing-culture conditions the images were similar (data not shown).

CLSM images indicate that a portion of intracellular polyplexes disintegrate. However, it remains ambigous whether polymer and DNA are then transported in separate endo-lysosomal vesicles or the dissociation may occur after endo-lysosomal release in the cytosol. Furthermore, some polyplexes were still intact even after they have reached the nuclear compartment. To elucidate the intracellular transport of plasmid DNA and LPEI, endocytotic vesicles were additionally labeled with the fluorescent dye FM4-64. Spots in confocal images were depicted in ochre, green and red indicating the vesicles, plasmid DNA and LPEI, respectively (Figure 10). After an incubation time of 2 hours (Figure 10, left), two different patterns were visible: on the one hand a merging of the three colors suggesting a localization of intact polyplexes in endocytotic vesicles (arrow) and on the other hand a merging of the three colors coexisting with a red color representing polyplexes in endocytotic vesicles from which the polymer may be escaping (stars). After 5 hours (Figure 10, right), the number of

vesicles with polyplexes as content decreased, while the number of vesicles from which the polymer appeared to escape and the plasmid DNA to remain (star) seemed to increase. Additionally, free polymer could be detected in the cytosol (open arrowhead), and plasmid DNA that was still colocalized with the FM4-64 labeled vesicles (triangle).

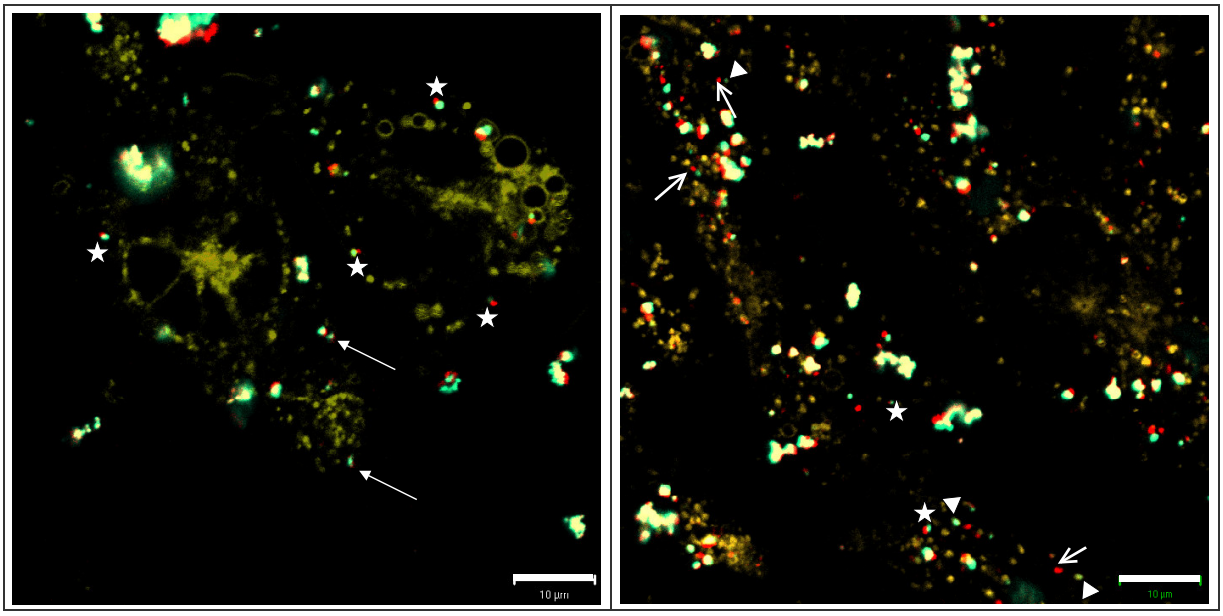

Figure 10: Intracellular localization of polyplexes with regard to endocytotic vesicles that were labeled with the fluorescent dye FM4-64 and depicted in ochre. The plasmid DNA was labeled with YOYO-1, LPEI 5.0 with TAMRA and depicted in green and red, respectively. CLSM images were taken after 2 (left) and 5 (right) hours. The intensity profile of the fluorescence emission was examined to identify a colocalization. The arrow indicates a colocalization of plasmid DNA and LPEI with the vesicles, the star denotes vesicles from which the polymer appeared to escape and the plasmid DNA to remain, polymer freely dispersed in the cytosol is denoted by an open arrowhead, while plasmid DNA that remained in the vesicles is denoted by triangles. Each bar indicates 10 µm.

Intracellular plasmid DNA stability

The intracellular stability of plasmid DNA was examined by electrophoresis of cellular extracts. Intact plasmid DNA could be detected when cells were transfected in the presence or absence of serum with LPEI 9.0 -, 5.0 - and 2.0 - polyplexes built in 150 mM sodium chloride or 5% glucose (Figure 11). The extracted material showed the relaxed and supercoiled plasmid forms, indicating that the nucleic acid has not been intracellularly processed. No short DNA fragments were visible in the gel, which implies that plasmid DNA that has been degraded must have been completely degraded or the amount of any linear remnants was below the detection limit. Plasmid DNA that did not migrate in the gel (plasmid DNA that remained in the pockets) was complexed with cellular components that have not been released by the cellular extraction procedure.

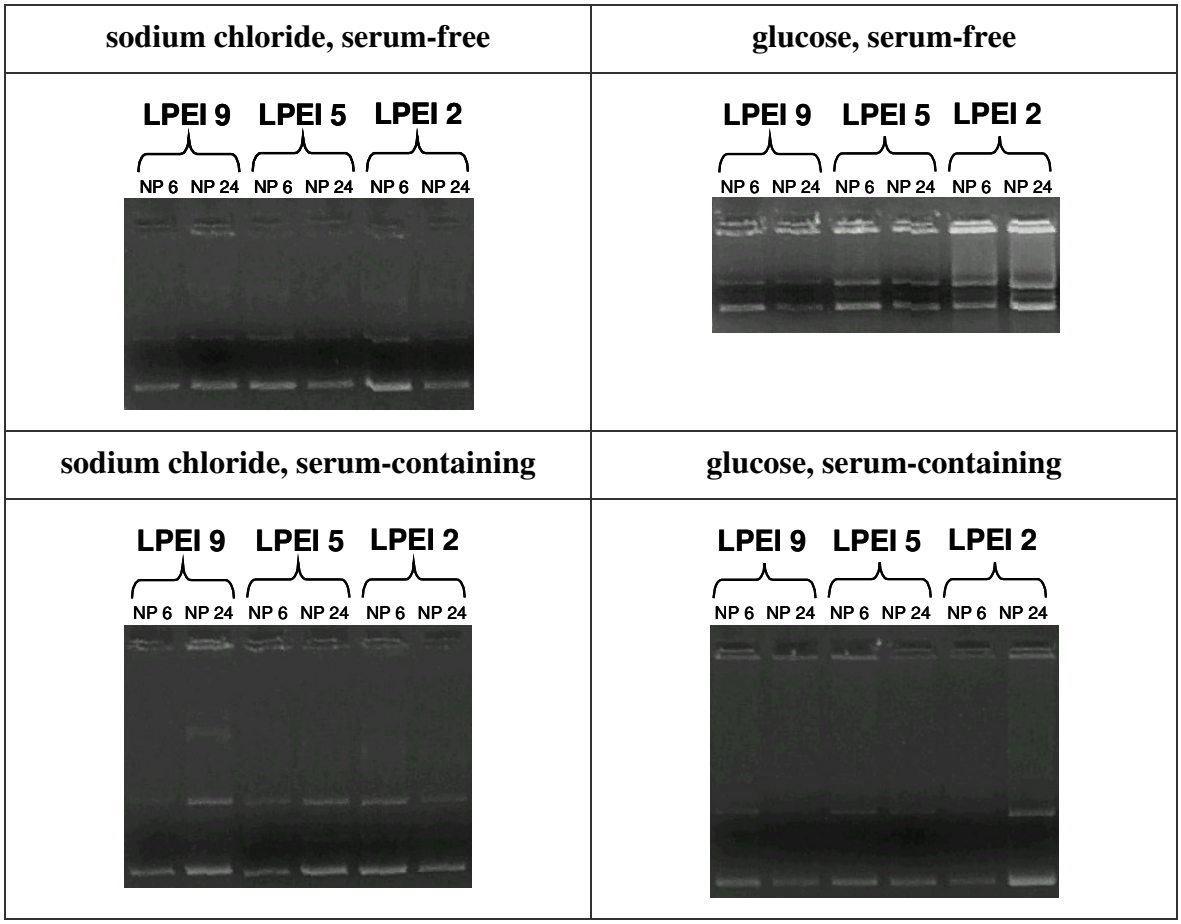

Figure 11: Agarose gel electrophoresis of plasmid DNA isolated from CHO-K1 cells upon 6 hours of transfection with LPEI 9.0, 5.0 and 2.0 at NP 6 or 24. Polyplexes were formed in 150 mM sodium chloride or 5% glucose and the 4 hour incubation period was carried out in serum free- or -containing culture conditions. The relaxed (top) and supercoiled (bottom) form of plasmid DNA were visible. Plasmid DNA that did not migrate was still complexed with cellular components and hence remained in the pockets.

Any differences in the intensity of the bands in the gel that arise due to complexation with a certain LPEI type, the NP ratio or the culture conditions could not be quantified. Furthermore, the images represent only the absolute amount of isolated DNA, but the toxicity, especially of LPEI 9.0, also has to be taken into account. Therefore, the isolated plasmid DNA was quantified by real-time PCR and normalized to the total protein (Figure 12).

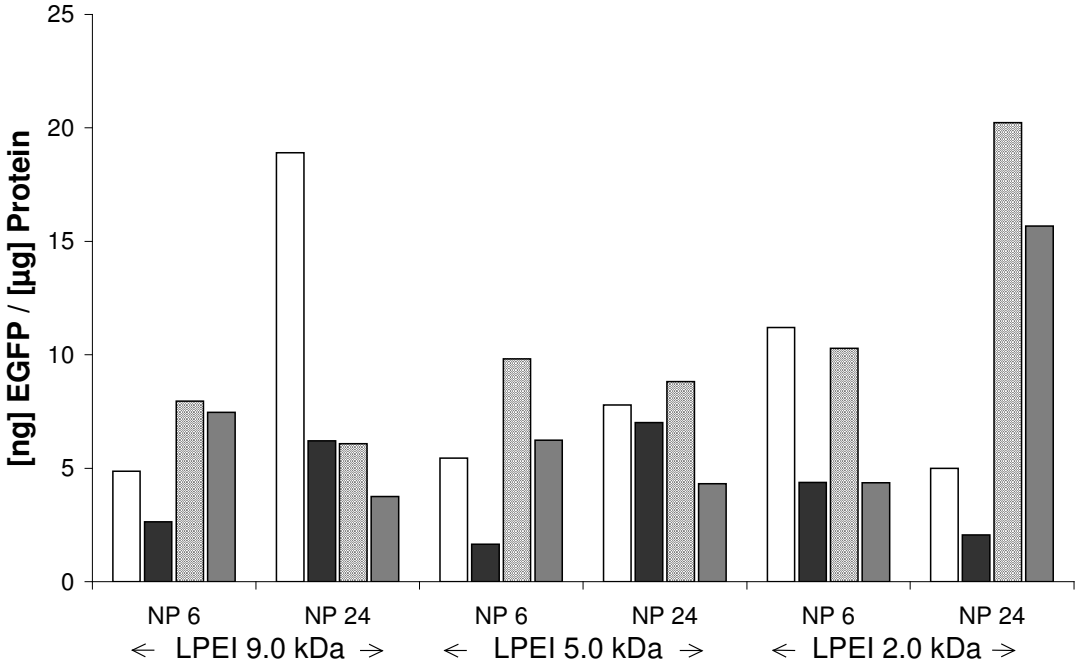

Figure 12: Amount of plasmid DNA / protein isolated after 6 hours of transfection with LPEI 9.0, 5.0 or 2.0 as carriers. Polyplexes were built in 150 mM sodium chloride or 5% glucose and the 4 hour incubation period was carried out in serum-free (150 mM sodium chloride: □ or 5% glucose: ▨, respectively) and –containing culture conditions (150 mM sodium chloride: ■ or 5% glucose: ▩, respectively). The absolute amount of target nucleic acid was determined with pEGFP-N1 as an external standard in a Light Cycler, while the protein content was determined with a Bradford assay.

The results could be divided in two groups with different patterns: Applying LPEI 9.0 - and 5.0 - polyplexes, the amount of intact plasmid DNA increased with the NP ratio when polyplexes were built in 150 mM sodium chloride, but decreased when polyplexes were built in 5% glucose. For LPEI 2.0 - polyplexes, the results were reversed. When LPEI 9.0 at NP 24 (sodium chloride, serum-free) and LPEI 2.0 at NP 24 (glucose, serum-free and -containing) were used as carriers, the amount of intact plasmid DNA was much higher compared to other conditions tested. Based on the amount of DNA used in the transfection process, only about 1/6 to 1/3 could be detected intracellularly and intact after 6 hours. The majority of the plasmid DNA used in the experiments was either not internalized or was intracellularly degraded.

Plasmid DNA accessibility for transcription

In CLSM pictures, DNA that was still complexed by LPEI was detected in the nucleus. Earlier studies revealed that transcription is not impaired when BPEI 25 kDa is closely attached to the template DNA [4]. To test this for our LPEI derivatives, we used the cell free

assay TNT® quick coupled transcription/translation system to determine the functionality of plasmid DNA complexed to LPEIs of various MW (Figure 13). The luciferase expression was reduced by nearly three-fold when plasmid DNA was complexed to LPEI 2.0 compared to plasmid DNA alone. A further decrease could be measured when using LPEI with higher MW, but there was no correlation between the MW of the polymer and the luciferase expression. Nevertheless, intracellular polyplexes are not as closely compacted as the polyplexes tested in this assay. After having been in contact with culture medium or cells, the polyplexes dissociate at least in part and hence, the accessibility of plasmid DNA for enzymes of the transcription machinery may be higher.

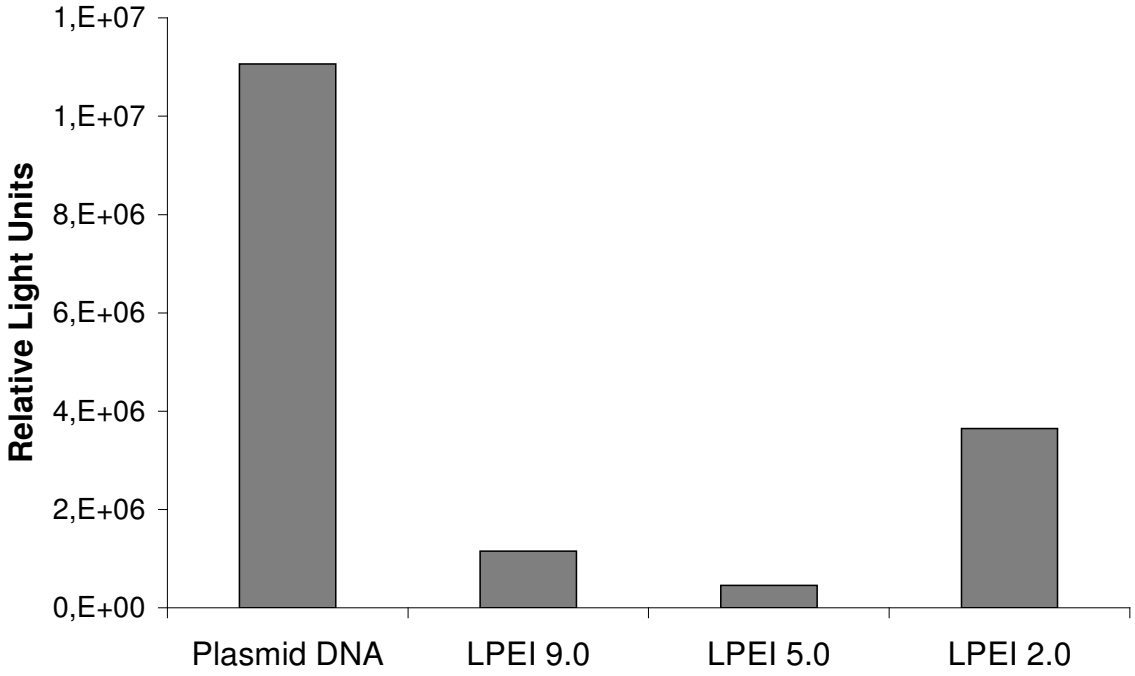

Figure 13: The functionality of plasmid DNA complexed to LPEI 9.0, 5.0 and 2.0 was accessed by the cell free assay TNT® quick coupled transcription/translation system. Plasmid DNA alone was used as a control. The luciferase expression as relative light units was determined using the luciferase assay system.

Discussion

In order for non-viral gene delivery systems to become real substitutes for viral carriers, their transfection efficiency must be improved. We introduced a variety of LPEIs that achieve a relatively high transfection efficiency (about 44%) without significant toxicity *in vitro* [13]. In our opinion, LPEI - polyplexes provide a good basis for the further optimization of polymer-based nucleic acid delivery systems. Therefore, in order to better understand the transfection mechanism, we strove to elucidate the interaction of LPEI – polyplexes with their

environment in detail. We suggested that the endo-lysosomal escape capacity and nuclear entry are major prerequisites for the high transfection efficiency of certain LPEIs. In this study, we investigated the possible correlation of the uptake, intracellular stability of plasmid DNA or polyplexes and the transfection efficiency when using LPEI 9.0, 5.0 or 2.0 in polyplexes. Furthermore, the influence of the ionic strength of the polyplex formation medium and the presence of serum during the transfection process was evaluated.

Especially LPEI 9.0 - polyplexes positively influenced the transfection efficiency and cell viability when polyplexes were formed in salt-free medium and the transfection process was carried out in the absence of serum, the transfection efficiency yielded a value of about 53%. It is known that the ionic strength of the medium for polyplex formation greatly influences the size of the complexes [19]. Generating LPEI - polyplexes in 150 mM sodium chloride or 5% glucose entails either very large (> 1 µm) or small (about 200 - 300 nm) polyplexes, respectively [14]. However, as our confocal images show, once in contact with the culture medium (serum-free or –containing) the glucose-polyplexes also tended to grow and the differences in the size seemed to equalize. Therefore, we conclude that the MW of LPEI and the medium for polyplex formation only minorly influence the size of LPEI - polyplexes in culture medium and that the fabrication procedure is a very robust method for building LPEI - polyplexes. Furthermore, it is reported that PEI/DNA polyplexes interact with various plasma proteins during incubation [5,20,21]. This may be also true for LPEI – polyplexes and after having been in contact with cells in serum-free culture medium, LPEI 9.0 – polyplexes built in glucose may have structural advantages for a high transfection efficacy. As the knowledge of the structure of polyplexes is still fragmentary, more interest should be focused on their formation and composition.

Changing the culture conditions or the medium for polyplex formation did not significantly influence the uptake of polyplexes. However, LPEI 5.0 and 9.0 increased the number of polyplexes in cells compared to the lower MW LPEI. As it is known that only one of 1000 uncomplexed plasmid DNA copies is efficiently translocated from the cytoplasm to the nucleus [22], it it clear that an excess of polyplexes is needed in the cytosol for efficient gene delivery. But this amount has not been determined yet, and therefore, it is difficult conclude whether the higher amount of plasmid DNA taken up after complexation with LPEI 9.0 or 5.0 has a benefit, and hence is one of the reasons for the higher efficacy compared to LPEI 2.0. On the other hand, plasmid DNA stability after application of LPEI 2.0 - polyplexes was similar or even higher than the to higher MW derivatives and therefore, the lower amount of polyplexes taken up may not impair the transfection efficiency considerably.

At least a portion of polyplexes was separated after uptake, but some intact polyplexes were also detected in the nucleus. LPEI may probably escape earlier from the endocytotic vesicles compared to plasmid DNA, while plasmid DNA may be transported further towards the nucleus in the endocytotic vesicles. This dissociation is an important point when considering that the transcriptional / translational activity of plasmid DNA is strongly reduced by a close interaction of polyplexes as simulated by the TNT® assay. The better accessibility of plasmid DNA in LPEI 2.0 - polyplexes may be due to a poor compaction of plasmid DNA by low MW polymers [23], which is also supported by the slightly larger size of LPEI 2.0 - polyplexes compared to LPEI 5.0 or 9.0 in cell free conditions [14]. The differences in polyplex disintegration between LPEI 9.0 and 5.0 were only marginal, other than the fact that a higher amount of free LPEI 5.0 was detected in the cytosol. The higher proportion of free polymer in cytosol could result from a better endo-lysosomal escape capacity of LPEI 5.0.

The examination of the plasmid DNA stability after a transfection incubation of 6 hours revealed that LPEIs are able to protect plasmid DNA to a large extent from the degradation by nucleases. It was surprising that the complexation with LPEI 2.0, a LPEI derivative that is only capable of a very low gene transfer efficiency, resulted in an enhanced stability of plasmid DNA under certain conditions. The fabrication method, respectively the ionic strength, did not impair the stability of plasmid DNA with regards to the transfection efficiency. Considering that there is likely an excess of polyplexes inside the CHO-K1 cells, DNases may be saturated by plasmid DNA and hence, further plasmid DNA degradation may be prevented.

In summary, our LPEI-based nucleic acid delivery system is very robust and excellent for routine transfection experiments. The high transfection efficiency of certain LPEI - polyplexes probably arises from a balance of endo-lysosomal escape capacity, nuclear transport and cytotoxicity [13]. In contrast, the cellular uptake of polyplexes built with various LPEIs, their intracellular disintegration and the stability of plasmid DNA do not influence the transfection efficiency considerably. As the structure of polyplexes significantly influences the transfection efficiency and cytotoxicity, a more detailed insight into polyplex assembling would be helpful for a further optimization of PEI-based delivery systems.

References

1. Sadelain M. Insertional oncogenesis in gene therapy: how much of a risk? *Gene Ther* 2004; **11**: 569-573.

2. Marshall E. What to do when clear success comes with an unclear risk? *Science* 2002; **298**: 510-511.

3. Behr JP. Gene transfer with synthetic cationic amphiphiles: prospects for gene therapy. *Bioconjug Chem* 1994; **5**: 382-389.

4. Bieber T, Meissner W, Kostin S, Niemann A, Elsasser HP. Intracellular route and transcriptional competence of polyethylenimine-DNA complexes. *J Control Release* 2002; **82**: 441-454.

5. Ogris M, Steinlein P, Kursa M, Mechtler K, Kircheis R, Wagner E. The size of DNA/transferrin-PEI complexes is an important factor for gene expression in cultured cells. *Gene Ther* 1998; **5**: 1425-1433.

6. Wattiaux R, Laurent N, Wattiaux-De Coninck S, Jadot M. Endosomes, lysosomes: their implication in gene transfer. *Adv Drug Deliv Rev* 2000; **41**: 201-208.

7. Godbey WT, Wu KK, Mikos AG. Tracking the intracellular path of poly(ethylenimine)/DNA complexes for gene delivery. *Proc Natl Acad Sci U S A* 1999; **96**: 5177-5181.

8. Brunner S, Furtbauer E, Sauer T, Kursa M, Wagner E. Overcoming the nuclear barrier: cell cycle independent nonviral gene transfer with linear polyethylenimine or electroporation. *Mol Ther* 2002; **5**: 80-86.

9. Goula D, Becker N, Lemkine GF, Normandie P, Rodrigues J, Mantero S, Levi G, Demeneix BA. Rapid crossing of the pulmonary endothelial barrier by polyethylenimine/DNA complexes. *Gene Ther* 2000; **7**: 499-504.

10. Goula D, Benoist C, Mantero S, Merlo G, Levi G, Demeneix BA. Polyethylenimine-based intravenous delivery of transgenes to mouse lung. *Gene Ther* 1998; **5**: 1291-1295.

11. Bragonzi A, Boletta A, Biffi A, Muggia A, Sersale G, Cheng SH, Bordignon C, Assael BM, Conese M. Comparison between cationic polymers and lipids in mediating systemic gene delivery to the lungs. *Gene Ther* 1999; **6**: 1995-2004.

12. Ferrari S, Moro E, Pettenazzo A, Behr JP, Zacchello F, Scarpa M. ExGen 500 is an efficient vector for gene delivery to lung epithelial cells in vitro and in vivo. *Gene Ther* 1997; **4**: 1100-1106.

13. Breunig M, Lungwitz U, Liebl R, Fontanar C, Klar J, Kurtz A, Blunk T, Goepferich A. Gene delivery with low molecular weight linear polyethylenimines. *J Gene Med* 2005; **7**: 1287-1298.

14. Lungwitz U, Breunig M, Blunk T, Goepferich A. Synthesis and application of low molecular weight linear polyethylenimines for non-viral gene delivery. *Proceedings of the annual meeting of the German Pharmaceutical Society* 2004; P T25: 157.

15. Breunig M, Lungwitz U, Klar J, Kurtz A, Blunk T, Goepferich A. Polyplexes of polyethylenimine and per-n-methylated polyethylenimine-cytotoxicity and transfection efficiency. *J Nanosci Nanotechnol* 2004; **4**: 512-520.

16. Wrobel I, Collins D. Fusion of cationic liposomes with mammalian cells occurs after endocytosis. *Biochim Biophys Acta* 1995; **1235**: 296-304.

17. Murphy RF, Powers S, Verderame M, Cantor CR, Pollack R. Flow cytofluorometric analysis of insulin binding and internalization by Swiss 3T3 cells. *Cytometry* 1982; **2**: 402-406.

18. Bradford MM. A rapid and sensitive method for the quantitation of microgram quantities of protein utilizing the principle of protein-dye binding. *Anal Biochem* 1976; **72**: 248-254.

19. Wightman L, Kircheis R, Rossler V, Carotta S, Ruzicka R, Kursa M, Wagner E. Different behavior of branched and linear polyethylenimine for gene delivery in vitro and in vivo. *J Gene Med* 2001; **3**: 362-372.

20. Tang GP, Zeng JM, Gao SJ, Ma YX, Shi L, Li Y, Too H-P, Wang S. Polyethylene glycol modified polyethylenimine for improved CNS gene transfer: effects of PEGylation extent. *Biomaterials* 2003; **24**: 2351-2362.

21. Ogris M, Brunner S, Schuller S, Kircheis R, Wagner E. PEGylated DNA/transferrin-PEI complexes: reduced interaction with blood components, extended circulation in blood and potential for systemic gene delivery. *Gene Ther* 1999; **6**: 595-605.

22. Pollard H, Remy JS, Loussouarn G, Demolombe S, Behr JP, Escande D. Polyethylenimine but not cationic lipids promotes transgene delivery to the nucleus in mammalian cells. *J Biol Chem* 1998; **273**: 7507-7511.

23. McKenzie DL, Kwok KY, Rice KG. A potent new class of reductively activated peptide gene delivery agents. *J Biol Chem* 2000; **275**: 9970-9977.

Chapter 4

Fluorescence Resonance Energy Transfer: Evaluation of the Intracellular Stability of Polyplexes

Miriam Breunig, Uta Lungwitz, Renate Liebl, Achim Goepferich

Department of Pharmaceutical Technology, University of Regensburg,
Universitaetsstrasse 31, 93040 Regensburg, Germany

To be submitted

Abstract

The investigation of intracellular mechanisms of non-viral nucleic acid delivery systems has attracted great impetus for the improvement of their efficacy. Especially the intracellular release of the nucleic acid from the non-viral carrier system may be a relevant criterion for the high transfection efficiency of certain polymers. Therefore, we evaluated fluorescence resonance energy transfer (FRET) in combination with confocal laser scanning microscopy or flow cytometry as tool to determine the intracellular disintegration of polyplexes built with plasmid DNA and linear polyethylenimine in living CHO-K1 cells. In microscopy, which allowed for an observation of polyplexes within single cells, sensitized emission measurement and acceptor photobleaching have been tested towards quantitative FRET analysis. In contrast, the whole cell population was analyzed by the flow cytometry-based method. We suggest that FRET is a useful tool in order to evaluate the intracellular disintegration of polyplexes built with various polymers.

Introduction

In order for non-viral nucleic acid delivery systems to become a real alternative to viral vectors, the transfection efficiency must be substantially increased. Due to its relatively high efficiency, polyethylenimine (PEI), available in both branched (BPEI) and linear (LPEI) forms, has gained some prominence compared to other non-viral gene delivery systems. PEI is capable of condensing DNA into polyplexes, allowing for the cellular uptake of DNA. Once the polyplexes enter the endo-lysosomal compartment, PEI guides the minimally degraded DNA into the cytoplasm and finally to the nucleus to be transcribed [1-4]. To further optimize the transfection efficiency of PEI-based delivery systems, it would be useful to investigate the interactions of polyplexes with cells and the intracellular mechanisms involved in the transfection process.

Some of the unique properties of PEI include its efficient condensation and protection of DNA extracellularly and its capability to release the DNA, even if only partially, intracellularly. For the investigation of the interaction of plasmid DNA and polymer, both components of polyplexes have been labeled with fluorescent dyes and observed by confocal laser scanning microscopy (CLSM) [5,31] (see also Chapter 3). However, investigations are often hampered by the limited spatial resolution of conventional widefield fluoresence microscopy. The application of a fluorescence resonance energy transfer (FRET) -based technique would allow for more precise distance measurements in the range of 1-10 nm.

So far, only two studies have utilized a FRET-based approach for the determination of the complexation state of intracellular polyplexes: Itaka *et al.* made observations concerning the condensation of double labeled plasmid DNA in intracellular polyplexes [6]. The conformational change of plasmid DNA after condensation with polymer, which would lead to a change in the distance between two fluorescent molecules attached to plasmid DNA, was detected. For analyzing FRET the fluorescence intensity ratio of the fluorescent dyes was calculated at each pixel and an image in grey scale was created to express the ratios. A decrease in the FRET efficiency of plasmid DNA in LPEI - polyplexes due to disintegration was observed after intracellular uptake, while plasmid DNA retained high FRET efficiency in BPEI - polyplexes indicating that the DNA was kept in a condensed state. However, the selection of the filter set in this measurement enables a cross-talk of the selected dyes that is not considered during the calculation of the ratio images. Nevertheless, the method can be applied in the described case, because the molar ratio of the two fluorescent dyes is constant. Similarly, Kong *et al.* observed the decondensation of BPEI - polyplexes within cells, when

plasmid DNA and BPEI were separately labeled with Alexa Fluor 488 and rhodamine, respectively [7]. The degree of energy transfer within the polyplexes was evaluated by the ratio between the average intensity of Alexa Fluor 488 and rhodamine emission at a given location. Unfortunately, a possible cross-talk and varying concentrations of fluorescent dyes in polyplexes were not considered. In conclusion, while both experimental designs are interesting, neither approach was state-of-the-art for the determination of a FRET efficiency. Therefore, we evaluated whether various methods for the investigation of FRET described in literature are applicable to determine the stability of intracellular LPEI - polyplexes. To this end, each component of the polyplexes, i.e. polymer and plasmid DNA, was labeled with a fluorescent dye and FRET was measured using both microscopy and flow cytometry.

Theory of FRET and measuring techniques

FRET is a process by which a fluorophore (the donor) in an excited state transfers its energy to a neighboring molecule (the acceptor) by non-radiative dipole-dipole interaction [8-11]. One of the most important factors influencing the efficiency of energy transfer is the distance between the donor and acceptor dye molecules (Figure 1). Energy transfer within the 1-10 nm distance range correlates well with the macromolecular dimension [12] and is, therefore, capable of resolving distances much shorter than the inherent diffraction limit of conventional microscopy.

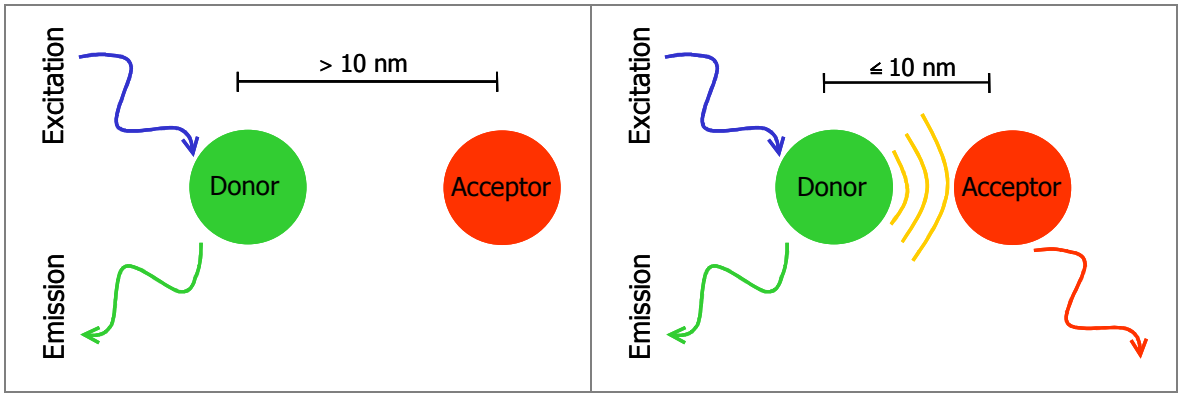

Figure 1: FRET is the non-radiative transfer of photon energy from an excited fluorophore (the donor) to another fluorophore (the acceptor) when both are located within close proximity (1-10 nm) (adapted from [13]).

When FRET occurs, there is a net gain in the energy of emission by the acceptor at the expense of the fluorescence emitted from the donor (donor quenching); this process is called sensitized emission (Figure 2).

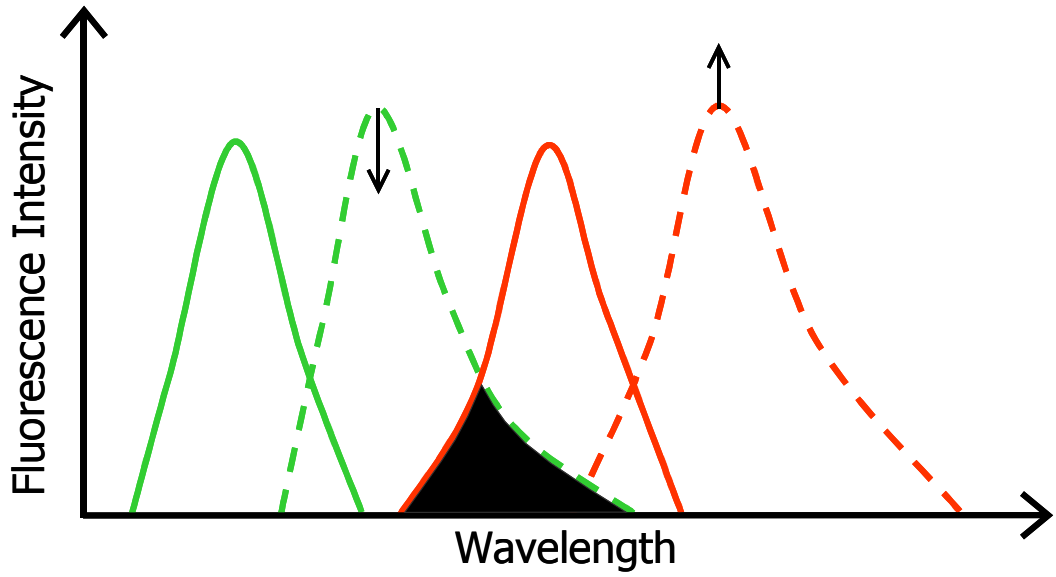

Figure 2: Fluorescence excitation and emission spectra of a FRET donor - acceptor pair. The spectra from left to right represent: donor excitation (solid line), donor emission (dashed line), acceptor excitation (solid line) and acceptor emission (dashed line). Sensitized emission requires the excitation of the donor and then the detection of the acceptor emission. Upon FRET the donor emission decreases (↓), while the acceptor emission increases (↑). The gray region indicates the overlap of the donor emission spectrum and the absorption spectrum of the acceptor

For FRET to occur efficiently:

1. The donor must have a high quantum yield.
2. The emission spectrum of the donor must overlap with the absorption spectrum of the acceptor (Figure 2).
3. The donor and acceptor molecules must be in close proximity (typically 1-10 nm).
4. The absorption and emission moments and their separation vector must be appropriately aligned.

According to the theory of Förster the transfer efficiency (E) is defined as the probability of decay of the excited donor molecules due to energy transfer as compared to the total number of decay events, and is given by (for reviews, see [14,15]):

(1) $$E = \frac{k_T}{k_T + k_F + k_D},$$

where k_T is of the rate constant of the transfer process, k_F is the rate constant of fluorescence emission of the donor, and k_D is the sum of the rate constants of all other de-excitation processes of the donor.

The rate of energy transfer (k_T) can also be expressed by:

(2) $$k_T = \text{const}\, k_F\, J\, n^{-4}\, R^{-6}\, \kappa^2 ,$$

where R is the distance between the donor and acceptor molecules, and κ^2 is an orientation factor describing the relative orientation of the donor's emission dipole and the acceptor's absorption dipole in space. The overlap integral J represents the degree of overlap between the donor fluorescence spectrum and the donor absorption spectrum, n is the refractive index of the medium.

Furthermore, E depends on the inverse sixth power of the distance between the donor and the acceptor, and hence quickly decreases with an increase of R:

(3) $$E = \frac{R^{-6}}{R^{-6} + R_0^{-6}} ,$$

where R_0 is the characteristic separation distance of each dye pair, defined as the distance at which the probability of energy transfer is 50%.

From equations (1), (2) and (3) the rate k_T of energy transfer is also defined by:

(4) $$k_T = \frac{1}{\tau}\left(\frac{R_o}{R}\right)^6 ,$$

where τ is the donor lifetime in the absence of the acceptor. As the fluorescence lifetime of a fluorophore is the characteristic time that a molecule exists in the excited state prior to returning to the ground state, time-resolved FRET measurements can be used to perform experiments with greater accuracy.

As with any proper fluorescence measurement, to be quantitative FRET methods have to account for 'bleed-through' in excitation, when the donor is excited by the excitation wavelength of the acceptor, and 'cross-talk' in emission detection, when the emission of a donor also contributes to the signal measured in a setup for acceptor detection, and vice versa.

FRET associated with cells can be measured by different means, the two most common methods being microscopy and flow cytometry. While a whole cell population can be analyzed by flow cytometry, the distribution of FRET events within a single cell can be elucidated using fluorescence microscopy. In microscopy, two main approaches have been established towards quantitative FRET analysis: sensitized emission measurement and acceptor photobleaching.

Sensitized emission in microscopy

Sensitized emission is the most common approach towards quantitative FRET. It requires the excitation of the donor and the detection of light emitted by either the donor and/or the acceptor in the presence of the other fluorophore. When FRET occurs, the intensity of donor emission is decreased and that of the acceptor emission is increased. Various methods have been applied to measure FRET from changes in donor and acceptor emission [16-19]. In the following, three different methods for the quantitative determination of sensitized emission in CLSM reported in literature are described [17-19] (the measurements are performed with a softwaretool from Carl Zeiss Co. Ltd., Germany [13]). For each measurement at least three samples are required; the donor (*d*) and acceptor (*a*) controls and the experimental sample (*f*). Furthermore, a combination of three filter sets for the detection of the donor fluorescence (*D*), the acceptor fluorescence due to direct excitation (*A*) or due to FRET (*F*) is used for the measurement of each sample.

The calculation of three different FRET values for sensitized emision is possible, (i) *Fc* (FRET corrected), (ii) *Fn* (FRET net) and (iii) *NF* (normalized FRET). In the following equations, the uppercase letter denotes the filter set and the lowercase letter indicates which fluorophores are present in the specimen (as described above in brackets), for example *Fd* indicates that the donor is labeled (*d*) and the donor fluorophore is excited and the emission is detected in the acceptor channel (*F*).

(i) The method according to *Youvan et al.* (calculation of *Fc*) simply determines a FRET intensity image corrected by the cross-talk and background intensity, but is not normalized for the concentration of the donor and acceptor [19]. This means that the FRET values are proportional to the donor and acceptor concentration and that high *Fc* numbers occur when high concentration of donor and acceptor are present:

$$(5) \qquad Fc = Ff - \left[\frac{Fd}{Dd} \cdot Df\right] - \left[\frac{Fa}{Aa} \cdot \mathrm{Af}\right].$$

Fd/Dd is a measure for the ratio of donor signal detected in the donor channel and emission crosstalk of donor signal detected in the FRET channel. *Fa/Aa* is a measure for the ratio of the acceptor signal detected in the acceptor channel and excitation crosstalk of acceptor signal detected in the FRET channel. The terms *Df* and *Af* correlate with the donor and acceptor concentration, respectively. Thus, the FRET value *Ff* can be corrected by the direct contribution of the donor and acceptor, their cross-talk and concentration, namely *Donor corr* and *Acceptor corr*, to get *Fc* according to Youvan *et al.*:

(6) $$Fc = Ff - [Donor\ corr] - [Acceptor\ corr].$$

(ii) According to Gordon *et al.* (*Fn*) the image resulting from calculation of *Fc* should be additionally normalized to the donor and acceptor signals [17]. This method may be of special interest when structures with low intensities are investigated. However, it also overcompensates for concentration, resulting in FRET values that are inversely proportional to the concentration:

(7) $$Fn = \frac{Ff - [Donor\ corr] - [Acceptor\ corr]}{G \cdot Fd \cdot Fa}.$$

(iii) In the analysis described by Xia *et al.* (*NF*), the corrected FRET image is divided by the square root of the product of donor and acceptor [18]. Hence, the FRET efficiency should be constant and independent of the local concentration of donor and acceptor.

(8) $$NF = \frac{Ff - [Donor\ corr] - [Acceptor\ corr]}{\sqrt{G \cdot Fd \cdot Fa}}.$$

Acceptor photobleaching in microscopy

Another approach to detect FRET by microscopy is acceptor photobleaching [16,20-24]. The donor is excited and its emission is detected before and after acceptor photobleaching. After the acceptor is bleached or chemically destroyed, the donor signal increases since no energy transfer to the acceptor is possible. Such an increase in fluorescence following bleaching is particularly diagnostic of FRET, because fluorescence normally decreases following a bleach. An advantage of acceptor photobleaching is that corrections are not necessary because an increase in donor fluorescence cannot be related to acceptor bleed-through.

For the measurement, a FRET positive and negative control and the spectral references are required. In a time series with about 2 to 5 pre bleach images, the acceptor should be bleached to about 20% and imaging should continue after bleaching. The FRET efficiency *E* is calculated from photobleaching kinetics of the donor in the presence and absence of the acceptor in pixels or regions of interest (ROIs) using the following equation [24]:

(9) $$E = \frac{F_{Donor\ \max} - F_{Donor\ \min}}{F_{Donor\ \max}}.$$

Linear regression of the fluorescence intensity of the donor F_{Donor} versus acceptor $F_{Acceptor}$ allows for the determination of $F_{Donor\,\max}$, while $F_{Donor\,\min}$ is obtained as average value of the fluorescence intensity of the donor from a time series of about 2-10 pre bleach images.

FRET measurements in flow cytometry

Flow cytometry enables the statistical analysis of the distribution of FRET events in a cell population. In addition to the controls needed for microscopy, an additional sample of unlabeled cells is required to account for the cell autofluorescence [15,25,26].

In the following equations it is assumed that the donor fluorescence is excited with a 488 nm laser line and detected at 530 nm and a laser emitting light of 635 nm is used to excite the acceptor which is recorded at 670 nm. Sensitized acceptor emission is detected with excitation at 488 nm and emission at 670 nm.

The simplest approach to measure energy transfer would be to determine the decrease in the fluorescence of the donor in the presence of the acceptor. Donor quenching (*ET*) can be calculated from mean fluorescence intensity of flow cytometry measurements according to [32]:

$$(10) \qquad ET = \frac{F_{1,0}(488,530) - F_{1,1}(488,530)}{F_{1,0}(488,530)} ,$$

where $F_{d,a}$ (x,y) represents the mean fluorescence intensity obtained in the absence (d=0) or presence (d=1) of a donor, in the absence (a=0) or presence (a=1) of an acceptor after excitation at x nm and detection at y nm.

The acceptor sensitized emission is expressed by the energy transfer parameter (ET_p):

$$(11) \qquad ET_p = \frac{F_{1,1}(488,670) - \frac{F_{1,1}(488,530)}{a} - \frac{F_{1,1}(635,670)}{b}}{F_{1,1}(488,670)} .$$

The factors a and b are used to correct by the direct contribution of donor and acceptor in samples with donor or acceptor labeled only, respectively:

$$(12) \qquad a = \frac{F_{1,0}(488,530)}{F_{1,0}(488,670)} \text{ and}$$

$$(13) \qquad b = \frac{F_{0,1}(635,670)}{F_{0,1}(488,670)} .$$

These calculations provide a single mean FRET efficiency for the whole cell population. However, sensitized emission can also be applied to calculate the distribution of the transfer efficiency on a cell-by-cell basis. Szollossi and co-workers reported the technical details and computer-based methods for calculation of the FRET efficiency in various papers [15,25,27-29]:

Briefly, a correction factor α, which represents the correction due to the different detectability of the donor and acceptor fluoresence, is determined by the following formula:

$$\alpha = \frac{F_{0,1}(488,670) \cdot r_{\text{Donor}} \cdot \varepsilon_{\text{Donor, 488}}}{F_{1,0}(488,530) \cdot r_{\text{Acceptor}} \cdot \varepsilon_{\text{Acceptor, 488}}} . \quad (14)$$

The numerical value of α is determined from the fluorescence intensities of cells saturated with either donor or acceptor label. Furthermore, the molar extinction coefficients ε and the conjungate-to-dye ratio r are required.

The sensitized emission has to be corrected for the direct contribution of the donor. The S_1 correction factor is determined from cells labeled with donor only and calculated using the following formula:

$$S_1 = \frac{F_{1,0}(488,670)}{F_{1,0}(488,530)} . \quad (15)$$

The sensitized emission has also to be corrected by the contribution of the acceptor which may suboptimally be excited at 488 nm. The correction factor S_2 is determined from cells with acceptor labeled only:

$$S_2 = \frac{F_{0,1}(488,670)}{F_{0,1}(635,670)} . \quad (16)$$

Furthermore, the acceptor emission is corrected for the direct contribution of the donor which may suboptimally be excited by 635 nm. The S_3 correction factor is determined from cells labeled with donor only and is calculated as follows:

$$S_3 = \frac{F_{1,0}(635,670)}{F_{1,0}(488,530)} . \quad (17)$$

Thereafter, an intermediate value A is calculated using the following formula:

$$A = \frac{1}{\alpha}\left[\frac{F_{1,2}(488,670) - S_2 \cdot F_{1,2}(635,670)}{\left(1 - \frac{S_3 \cdot S_2}{S_1}\right) \cdot F_{1,2}(488,530)} - S_1 \right] . \quad (18)$$

The FRET efficiency E can be finally obtained by the following formula:

$$E = \frac{A}{1+A} . \quad (19)$$

Materials and methods

Plasmid DNA labeling

When indicated, plasmid DNA (pEGFP-N1, Clontech) was either covalently labeled with Alexa Fluor 488 according to the manufacturer´s protocol (ULYSIS Nucleic acid labeling kit, Molecular Probes, The Netherlands) or stained with the intercalating dye YOYO-1 (Molecular Probes, The Netherlands). The labeling reaction with YOYO-1 was carried out with a molar ratio of 1 dye molecule per 320 base pairs at room temperature in the dark.

Non-viral carriers

LPEI with a MW of 5.0 kDa was synthesized as previously described [30]. When indicated, the polymer was labeled with 6-TAMRA-succinimidyl ester or Alexa Fluor 633 (both Molecular Probes, The Netherlands) as described [31]. In the following, the notation of LPEI was made without the unit kDa.

Preparation of polyplexes

Plasmid DNA / LPEI complexes were prepared at NP ratios (ratio of nitrogens in polymer to phosphates in DNA) of 6, 18 or 30 in 150 mM sodium chloride as described [31]. In the following, the notation of polyplexes was made without the unit kDa; LPEI 5.0 – polyplexes indicates that polyplexes were built with LPEI 5.0.

CLSM experiments

A Zeiss Axiovert 200 M microscope coupled to a Zeiss LSM 510 scanning device (Carl Zeiss Co. Ltd., Germany) was used for CLSM experiments. The inverted microscope was equipped with a Plan - Apochromat 63x objective. CHO-K1 cells were plated in 8 - well Lab-Tek^{TM} Chambered Coverglass (Nunc GmbH & Co. KG, Germany) at an initial density of 35,000 cells / chamber in a volume of 400 µl culture medium. 20 mM HEPES was added to the medium to maintain a pH of 7.4. After 18 hours, polyplexes were added and measurements were directly performed in each well at 37°C. The thickness of the optical sections was between 0.7 and 1.2 µm.

Sensitized emission

FRET values for sensitized emission were calculated with the FRET Macro software tool from Carl Zeiss Co. Ltd. (Germany). The specimens used to acquire the raw data were: CHO-

K1 cells incubated with polyplexes at NP 6 with donor labeled only (DNA in polyplexes labeled with YOYO-1), acceptor labeled only (LPEI 5.0 in polyplexes labeled with TAMRA) and the FRET specimen (double labeled polyplexes). The donor YOYO-1 was excited with a 488 nm argon laser and detected with a 505-530 nm bandpass filter, while TAMRA was detected with a 560 –615 nm bandpass filter after excitation with 543 nm. Each specimen was acquired in a multitrack configuration with 3 tracks: donor excitation/donor emission detection (donor track), acceptor excitation/acceptor emission detection (acceptor track) and donor excitation/acceptor emission detection (FRET track). The quantitative FRET analysis was performed according to the suppliers´ instruction. For the determination of the location of polyplexes a transmitted light image was also recorded.

Acceptor photobleaching

The acceptor photobleaching method was applied for polyplexes at NP 6 consisting of TAMRA-labeled LPEI 5.0 and Alexa Fluor 488-labeled DNA incubated with CHO-K1 cells. As controls, polyplexes with only the donor labeled were used. Images were taken in the multitracking modus with the configuration of filters for the donor and acceptor tracks without the FRET track as described above. Bleaching was conducted by scanning a region of interest 12 times using the 543 nm argon laser line at 100% intensity. Each time the whole cells were bleached to avoid unwanted fluorescence recovery after photobleaching (FRAP) effects. Before and after this bleach, Alexa Fluor 488 and TAMRA images were recorded to assess changes in donor and acceptor fluorescence. Any increase in Alexa Fluor 488 fluorescence caused by bleaching of the TAMRA acceptor could be masked by bleaching of Alexa Fluor 488 related simply to the imaging process itself. Hence, to ensure that bleaching due to imaging was minimal, the level of bleaching in each experiment was monitored by collecting Alexa Fluor 488/TAMRA image pairs before and after the bleach.

Flow cytometry

CHO-K1 cells were grown in 24-well plates at an initial density of 38,000 cells per well. 18 hours after plating, the prepared polyplexes were added to the cells. After 6 hours of transfection with polyplexes with donor labeled only (DNA in polyplexes labeled with YOYO-1), acceptor labeled only (LPEI 5.0 in polyplexes labeled with Alexa Fluor 633) and double labeled polyplexes, cells were prepared for flow cytometry analysis as described previously [31]. Untreated cells were used to determine the autofluorescence of cells. Measurements were taken on a FACSCalibur (Becton Dickinson, Germany) using CellQuest Pro software (Becton Dickinson, Germany) and WinMDI 2.8 (©1993-2000 Joseph Trotter).

YOYO-1 was excited using a 488 nm argon laser and detected with a 530 ± 30 nm bandpass filter, while Alexa Fluor 633 was excited with 635 nm and detected with a 661 ± 8 nm bandpass filter. Sensitized acceptor emission was detected with excitation at 488 nm and emission at > 670 nm.

Results and Discussion

Previous observations of double-labeled LPEI - polyplexes by CLSM indicated that polyplexes remained intact extracellularly, but once entered the cell at least a part dissociated or seemed to form loose aggregates ([31], Chapter 3). However, the evaluation of interaction of LPEI and plasmid DNA in confocal images is very time consuming and may be limited by the spatial resolution in microscopy. Therefore, FRET was introduced as tool to investigate the interaction of plasmid DNA and LPEI in polyplexes.

Sensitized emission in microscopy

For measurement of the sensitized emission of double-labeled LPEI 5.0 - polyplexes at NP 6 in CHO-K1 cells, three samples, the donor and acceptor control and the FRET sample, were analyzed. To evaluate the location of polyplexes within the cells, the calculated FRET ratio images were directly compared to an image showing both the donor and acceptor channels as well as the transmitted light channel (Figure 3 A). In this image, extracellular polyplexes were characterized by an overlay of green and red, respectively plasmid DNA and LPEI, indicating a close interaction between polymer and plasmid DNA. Some of the intracellular polyplexes seemed to disintegrate. Figures 3 B to D show the corresponding calculated FRET ratio images according to Youvan (Figure 3 B), Gordon (Figure 3 C) and Xia (Figure 3 D). The colored pixels indicate a FRET efficiency from 0 (dark blue) to 100% (white). For a direct comparison with Figure 3 A, the ratio image D according to Xia *et al.* was chosen because it is independent of the concentration of the fluorescent dyes, which is most appropriate for LPEI - polyplexes. Figure 3 B does not take the concentration of the two fluorophores into account and Figure 3 C overcompensates for the concentration.

Comparing Figures 3 A and D, extracellular polyplex aggregates were represented by colored pixels with FRET efficiencies of about 30 to 90%. The values for the FRET efficiency varied within polyplexes, indicating that the extent of interaction between polymer and plasmid DNA in extracellular polyplexes was not equally distributed. It was less time consuming to detect FRET events in intracellular polyplexes in the ratio images compared to Figure 3 A because it was not necessary to zoom into the images for a careful evaluation of each

polyplex. Polyplexes that seemed to disintegrate consisted of green, red and yellow areas, representing plasmid DNA, polymer and an overlay of both. In times when an overlay of red and green was detected in Figure 3 A, a corresponding FRET efficiency ranging from 40 to 90% was also visible in Figure 3 D, but not in areas where only a green or red fluorescence was detected. The results were reasonable and indicated that intracellular polyplexes disintegrated, but the contact between polymer and DNA was still very close in certain areas.

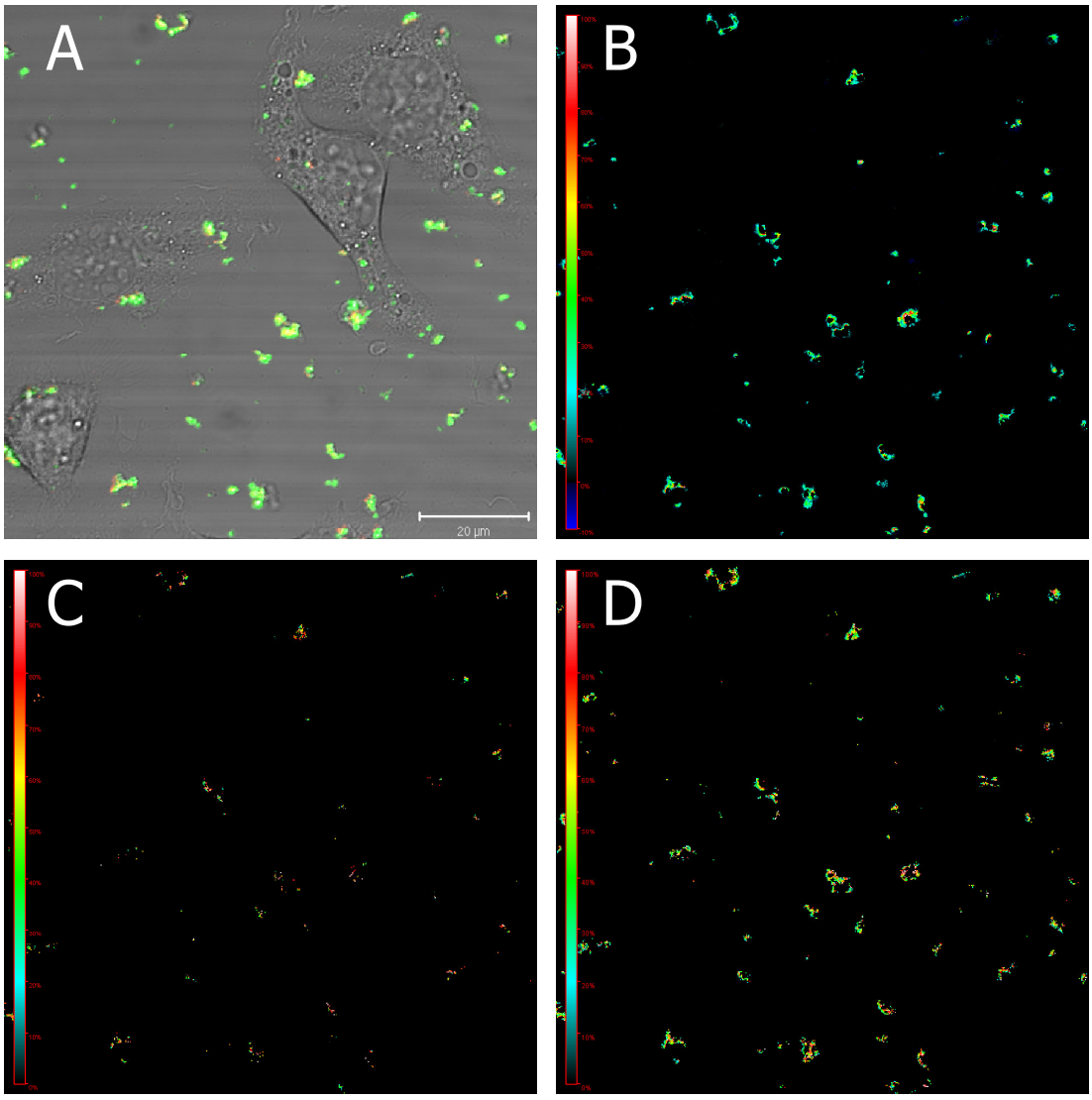

Figure 3: Sensitized emission measurements of LPEI 5.0 - polyplexes at NP 6 in CHO-K1 cells by CLSM. A: Observing double labeled LPEI - polyplexes in the multitracking mode, DNA is represented by green dots and polymer by red dots. A colocalization of both would yield a mixture color of yellow. To evaluate the location of polyplexes with regard to the cells a transmitted light image was also recorded. The bar indicates 20 µm. Figures B to D show the corresponding calculated FRET ratio images according to Youvan (B), Gordon (C) and Xia (D). The colored pixels were calculated according to [13] and indicate a FRET efficiency from 0 (dark blue) to 100% (white) as indicated by the sidebars.

Acceptor photobleaching in microscopy

Double-labeled LPEI 5.0 - polyplexes at NP 6 were used to evaluate the acceptor photobleach method. According to this procedure, if FRET occurs, photobleaching of the acceptor (TAMRA) should yield a significant increase in the fluorescence of the donor (Alexa Fluor 488). To minimize the effect of photobleaching due to imaging, images of Alexa Fluor 488 were collected at low laser intensity. The intensity of a certain number of Alexa Fluor 488 - labeled polyplexes remained nearly constant during a time series of 15 images, but sometimes also varied (about 5%) during imaging, most likely due to polyplex movements during imaging (data not shown). As a negative control, acceptor photobleaching of cells transfected with polyplexes stained with Alexa Fluor 488 alone was conducted, while larger extracellular polyplex aggregates and smaller intracellular polpylexes were evaluated. In these samples, FRET should be impossible, because the acceptor fluorophore TAMRA is absent. The fluorescence intensity decreased during imaging and bleaching, especially in smaller polyplexes (Figure 4 A, lower curve). This decrease in fluorescence intensity could be due to an unwanted bleaching of the donor or, as discussed above, due to movements of the polyplexes, the cells or even stage drift during the imaging process. Immediately after bleaching, the fluorescence intensity of larger polyplexes (Figure 4 A, upper curve) and smaller polyplexes (Figure 4 A, lower curve) seemed to remain constant.

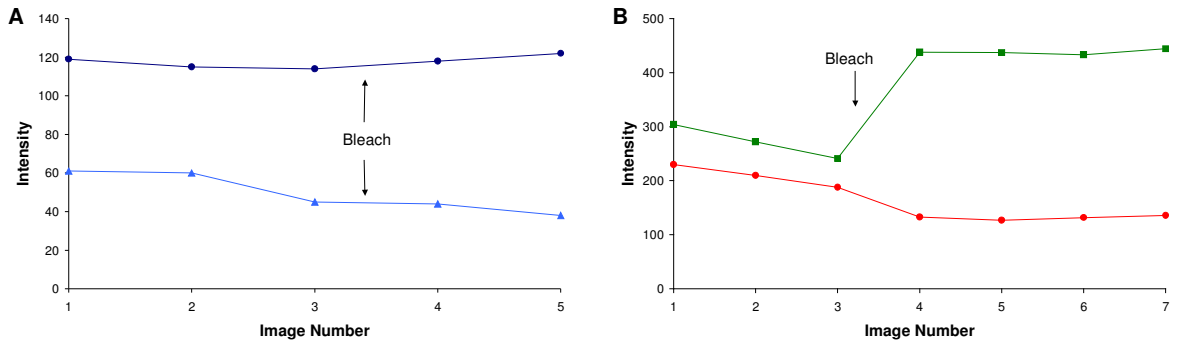

Figure 4: Acceptor photobleaching of LPEI 5.0 - polyplexes at NP 6 in CHO-K1 cells. A: As negative control cells transfected with polyplexes that were labeled with Alexa Fluor 488 alone were used. The fluorescence intensity of larger polyplexes (upper curve) and smaller polyplexes (lower curve) was quantified by averaging the fluorescence within one ROI of a certain number of polyplexes. Some bleaching due to imaging occurred at all time points except the one immediately after the bleach where constancy was detected. B: As positive control extracellular double labeled polyplexes were used. After bleaching the acceptor TAMRA (lower curve) the fluorescence of the donor Alexa Fluor 488 (upper curve) increased substantially.

As the simplest approach to evaluate whether our acceptor photobleaching protocol was feasible, the FRET efficiencies from 10 bleached extracellular polyplexes was measured and calculated as positive control. Figure 4 B shows an example of such a polyplex, after bleaching the acceptor (lower curve) the fluorescence of the donor (upper curve) substantially increased, the calculated FRET efficiency was 62.03%. This effect was reproducible for a set of 10 different polyplexes. The acceptor fluorophor TAMRA was not very effectively bleached by the applied method, but additional bleaching iterations lead to a decrease in the intensity of Alexa Fluor 488 in the negative control.

To test the intracellular polyplexes, the whole cell was bleached to avoid FRAP effects, but the intensity was calculated from a defined region containing intracellular green and red spots, respectively polyplexes. In the example shown in Figure 5, the FRET efficiency of an area containing about eight intracellular polyplexes that seemed to dissociate was calculated, it had a value of 30.5%.

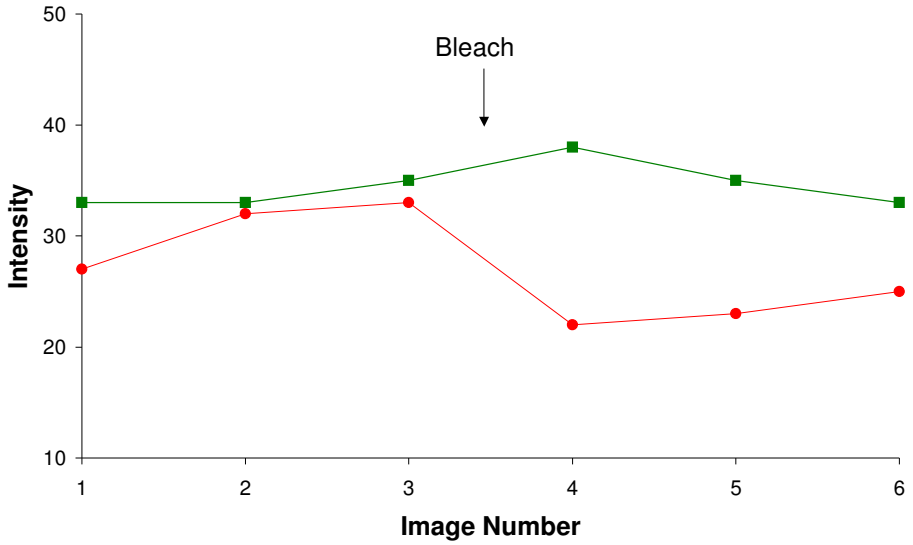

Figure 5: Acceptor photobleach of eight intracellular double labeled LPEI 5.0 - polyplexes that appeared to dissociate as shown by the fluorescence intensity of Alexa Fluor 488 (upper curve) and TAMRA (lower curve) during imaging. After bleaching the acceptor the fluorescence of the donor slightly increased.

This pattern was reproducible for intracellular polyplexes of about 10 cells. The FRET efficienies were not as high as for the positive control, indicating the interaction between polymer and plasmid DNA was not as close as in extracellular polyplexes.

However, the results were not accurate because some polyplexes, especially the smaller ones, disappeared due to drift of the stage or polyplex and cell movements (in and out of the z-stack) during the imaging and bleaching process. The acceptor photobleaching can only be applied given the fact that the time between pre- and post-bleaching is not too long to allow

for movements of or in the sample. In the samples shown, the pre and post bleach images and the bleaching itself took about 5 minutes and sample movement was visible in sequentially recorded images (data not shown). However, also image sets recorded with framewise multitracking may show a delay between the same pixel position for different channels. These problems are more pronounced in living cells compared to fixed samples. However, in our opinion, fixed samples do not reflect the situation as well as living samples, because the fixing agents alter the structure of polyplexes (data not shown). The choice of fluorescent dyes that are more readily bleached than TAMRA may help to solve the problem, but only in part.

Flow cytometry

For the evaluation of interaction between polymer and plasmid DNA in intracellular polyplexes, donor quenching of double labeled LPEI 5.0 - polyplexes (with YOYO-1 and Alexa Fluor 633) was determined (Figure 6). Donor quenching arises due to sensitized emission, but also depends on competition effects. The latter can be neglected because of a minimal bleed-through in excitation of the used FRET pair YOYO-1 and Alexa Fluor 633. The donor quenching increased with increasing NP ratio indicating an enhanced stability of polyplexes with increasing NP ratio. The enhanced stability of polyplexes may be due to more LPEI available for polyplex formation.

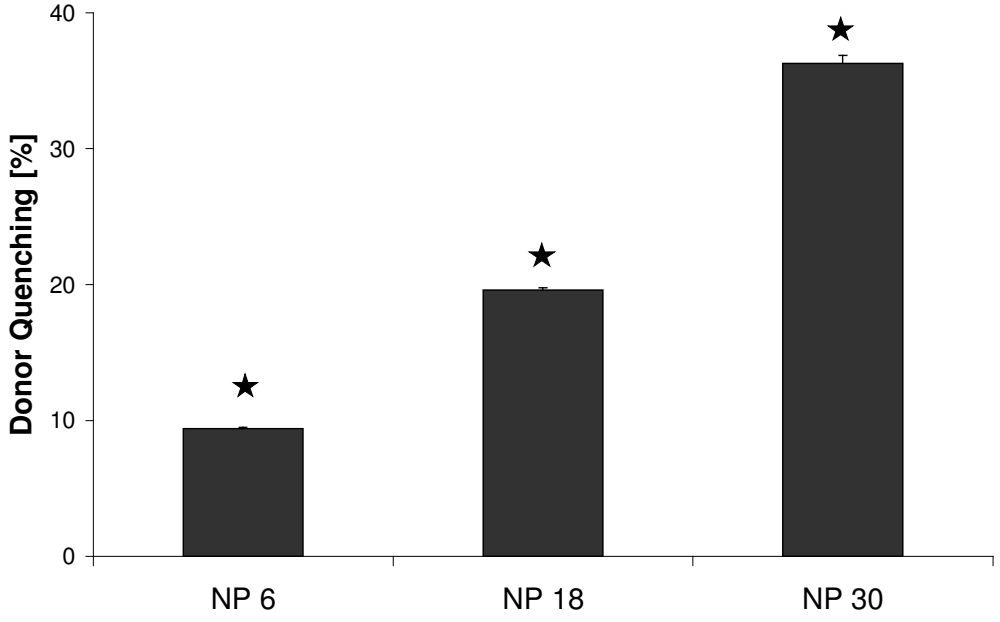

Figure 6: Donor quenching of double labeled LPEI 5.0 - polyplexes at NP 6, 18 and 30 after 6 hours of transfection as determined by flow cytometry. Statistically significant differences between NP ratios are denoted by ★ ($\alpha < 0.01$).

The FRET efficiency E on a cell-by-cell basis could not be calculated because the conjungate-to-dye ratio r (of polymer and plasmid DNA) were unknown. However, as it is most likely that the proportion of polymer to DNA is not constant in different polyplexes, donor quenching as average value for the whole cell population meets the situation better than a cell-by-cell evaluation.

Conclusions

In this study, FRET was evaluated as tool to determine the intracellular disintegration of double labeled LPEI - polyplexes in CHO-K1 cells. In microscopy, two approaches have been considered for quantitative FRET analysis: sensitized emission measurement and acceptor photobleaching. Applying the acceptor photobleach method, the results were not accurate because of movements of or in the sample during the imaging process. Therefore, we would not recommend acceptor photobleaching for this application. Sensitized emission measurement using the method according to Xia *et al.* [18] worked quite well for the determination of interaction between LPEI and plasmid DNA. Generally, we would advise caution for the investigation of interaction of polymer and plasmid DNA in living samples by FRET because of movement during the imaging process, but working with fixed cells is not an alternative because fixation agents may alter the structure of polyplexes. Furthermore, FRET occuring between two fluorescent molecules in LPEI - polyplexes was also successfully measured by flow cytometry. The advantage of the flow cytometry-based method is the analysis of a whole cell population.

With the established methods it is now possible to evaluate the intracellular stability of polyplexes built with various polymers at different NP ratios. We suggest that FRET is a useful tool in order to gain a deeper insight into LPEI-mediated gene transfer.

References

1. Behr JP. Gene transfer with synthetic cationic amphiphiles: prospects for gene therapy. *Bioconjug Chem* 1994; **5**: 382-389.

2. Bieber T, Meissner W, Kostin S, Niemann A, Elsasser HP. Intracellular route and transcriptional competence of polyethylenimine-DNA complexes. *J Control Release* 2002; **82**: 441-454.

3. Ogris M, Steinlein P, Kursa M, Mechtler K, Kircheis R, Wagner E. The size of DNA/transferrin-PEI complexes is an important factor for gene expression in cultured cells. *Gene Ther* 1998; **5**: 1425-1433.

4. Wattiaux R, Laurent N, Wattiaux-De Coninck S, Jadot M. Endosomes, lysosomes: their implication in gene transfer. *Adv Drug Deliv Rev* 2000; **41**: 201-208.

5. Goncalves C, Mennesson E, Fuchs R, Gorvel JP, Midoux P, Pichon C. Macropinocytosis of polyplexes and recycling of plasmid via the clathrin-dependent pathway impair the transfection efficiency of human hepatocarcinoma cells. *Mol Ther* 2004; **10**: 373-385.

6. Itaka K, Harada A, Yamasaki Y, Nakamura K, Kawaguchi H, Kataoka K. In situ single cell observation by fluorescence resonance energy transfer reveals fast intra-cytoplasmic delivery and easy release of plasmid DNA complexed with linear polyethylenimine. *J Gene Med* 2004; **6**: 76-84.

7. Kong HJ, Liu J, Riddle K, Matsumoto T, Leach K, Mooney DJ. Non-viral gene delivery regulated by stiffness of cell adhesion substrates. *Nat Mater* 2005; **4**: 460-464.

8. Foerster T. Energy migration and fluorescence. *Naturwissenschaften* 1946; **33**: 166-175.

9. Foerster T. Intermolecular energy transference and fluorescence. *Ann Phys [6 Folge]* 1948; **2**: 55-75.

10. Jares-Erijman EA, Jovin TM. FRET imaging. *Nat Biotechnol* 2003; **21**: 1387-1395.

11. Wu PG, Brand L. Resonance energy transfer: methods and applications. *Anal Biochem* 1994; **218**: 1-13.

12. Stryer L. Fluorescence energy transfer as a spectroscopic ruler. *Annu Rev Biochem* 1978; **47**: 819-846.

13. TASC Carl-Zeiss Jena, Geschäftsbereich AIM. 2005.

14. Szollosi J, Nagy P, Sebestyen Z, Damjanovich S, Park JW, Matyus L. Applications of fluorescence resonance energy transfer for mapping biological membranes. *Rev Mol Biotechnol* 2002; **82**: 251-266.

15. Szollosi J, Damjanovich S, Matyus L. Application of fluorescence resonance energy transfer in the clinical laboratory: routine and research. *Cytometry* 1998; **34**: 159-179.

16. Berney C, Danuser G. FRET or no FRET: a quantitative comparison. *Biophys J* 2003; **84**: 3992-4010.

17. Gordon GW, Berry G, Liang XH, Levine B, Herman B. Quantitative fluorescence resonance energy transfer measurements using fluorescence microscopy. *Biophys J* 1998; **74**: 2702-2713.

18. Xia Z, Liu Y. Reliable and global measurement of fluorescence resonance energy transfer using fluorescence microscopes. *Biophys J* 2001; **81**: 2395-2402.

19. Youvan D.C., Silva C.M., Bylina E.J., Coleman W.J., Dilworth M.R., Yang M.M. Calibration of fluorescence resonance energy transfer in microscopy using genetically engineered GFP derivatives on nickel chelating beads. *Biotechnol* 1997; **3**: 1-18.

20. Bastiaens PI, Jovin TM. Microspectroscopic imaging tracks the intracellular processing of a signal transduction protein: fluorescent-labeled protein kinaseáCábeta I. *Proc Natl Acad Sci U S A* 1996; **93**: 8407-8412.

21. Wouters FS, Bastiaens PIH, Wirtz KWA, Jovin TM. FRET microscopy demonstrates molecular association of non-specific lipid transfer protein (nsL-TP) with fatty acid oxidation enzymes in peroxisomes. *EMBO J* 1998; **17**: 7179-7189.

22. Kenworthy AK. Imaging protein-protein interactions using fluorescence resonance energy transfer microscopy. *Methods* 2001; **24**: 289-296.

23. Karpova TS, Baumann CT, He L, Wu X, Grammer A, Lipsky P, Hager GL, McNally JG. Fluorescence resonance energy transfer from cyan to yellow fluorescent protein detected by acceptor photobleaching using confocal microscopy and a single laser. *J Microsc* 2003; **209**: 56-70.

24. Amiri H, Schultz G, Schaefer M. FRET-based analysis of TRPC subunit stoichiometry. *Cell Calcium* 2003; **33**: 463-470.

25. Batard P, Szollosi J, Luescher I, Cerottini JC, MacDonald R, Romero P. Use of phycoerythrin and allophycocyanin for fluorescence resonance energy transfer analyzed by flow cytometry: advantages and limitations. *Cytometry* 2002; **48**: 97-105.

26. Sebestyen Z, Nagy P, Horvath G, Vamosi G, Debets R, Gratama JW, Alexander DR, Szollosi J. Long wavelength fluorophores and cell-by-cell correction for autofluorescence significantly improves the accuracy of flow cytometric energy transfer measurements on a dual-laser bench top flow cytometer. *Cytometry* 2002; **48**: 124-135.

27. Szollosi J, Damjanovich S, Mulhern SA, Tron L. Fluorescence energy transfer and membrane potential measurements monitor dynamic properties of cell membranes: a critical review. *Prog Biophys Mol Biol* 1987; **49**: 65-87.

28. Szollosi J, Tron L, Damjanovich S, Helliwell SH, Arndt-Jovin D, Jovin TM. Fluorescence energy transfer measurements on cell surfaces: a critical comparison of steady-state fluorimetric and flow cytometric methods. *Cytometry* 1984; **5**: 210-216.

29. Tron L, Szollosi J, Damjanovich S, Helliwell SH, Arndt-Jovin DJ, Jovin TM. Flow cytometric measurement of fluorescence resonance energy transfer on cell surfaces. Quantitative evaluation of the transfer efficiency on a cell-by-cell basis. *Biophys J* 1984; **45**: 939-946.

30. Lungwitz U, Breunig M, Blunk T, Goepferich A. Synthesis and application of low molecular weight linear polyethylenimines for non-viral gene delivery. *Proceedings of the annual meeting of the German Pharmaceutical Society* 2004; P T25: 157.

31. Breunig M, Lungwitz U, Liebl R, Fontanari C, Klar J, Kurtz A, Blunk T, Goepferich A. Gene delivery with low molecular weight linear polyethylenimines. *J Gene Med* 2005; **7**: 1287-1298.

32. Pfeiffer A, Boettcher A, Orso E, Kapinsky M, Nagy P, Bodnar A, Spreitzer I, Liebisch G, Drobnik W, Gempel K, Horn M, Holmer S, Hartung T, Multhoff G, Schuetz G, Schindler H, Ulmer AJ, Heine H, Stelter F, Schuett C, Rothe G, Szollosi J, Damjanovich S, Schmitz G. Lipopolysaccharide and ceramide docking to CD 14 provokes ligand - specific receptor clustering in rafts. *Eur J Immunol* 2001; **31**: 3153-3164.

Chapter 5

Biodegradable Polyethylenimines for Gene Delivery

Miriam Breunig[1], Uta Lungwitz[1], Renate Liebl[1], Birgit Obermayer[2], Juergen Klar[2], Achim Goepferich[1]

[1] Department of Pharmaceutical Technology, University of Regensburg, Universitaetsstrasse 31, 93040 Regensburg, Germany

[2] Department of Physiology, University of Regensburg, Universitaetsstrasse 31, 93040 Regensburg, Germany

To be submitted

Abstract

Although polyethylenimine (PEI) is one of the most successful non-viral gene delivery systems, its cytotoxicity is still a severe problem. We hypothesized that biodegradable PEIs crosslinked with disulfide bonds would maintain the efficient gene transfer, but with low cytotoxicity. Our results proved this hypothesis; the most effective biodegradable PEI was capable of 27-fold greater gene delivery than the non-degradable linear starting material. Furthermore, the maximal transfection efficiency achieved in CHO-K1 cells was with a value of about 73% much higher than the linear PEI (LPEI) derivative of similar molecular weight. Moreover, the efficacy was nearly 3-fold higher than that of branched PEI (BPEI) 25 kDa and LPEI 22 kDa, which have become benchmarks for newly synthesized polymers. It was remarkable that the cytotoxicity at NP ratios with the highest transfection efficiency was negligible compared to BPEI 25 kDa and LPEI 22 kDa. Biodegradable PEI-mediated gene delivery was dependent on intracellular reduction and could be modulated by manipulation of the number of stabilizing bonds. Confocal laser scanning microscopy revealed a longer colocalization of biodegradable PEI - polyplexes with acidic organelles compared to LPEI, which may be a prerequisite for its efficient gene delivery. In conclusion, biodegradable PEIs allow for a very high transfection efficiency accompanied by minimal cytotoxicity *in vitro* and are, therefore, a real alternative to existing polymer-based nucleic acid delivery systems.

Introduction

Despite early excitement and continued progress, there is a long way to go before non-viral gene delivery systems become a real substitute for viral vectors. One of the most successful and widely studied polymers for gene delivery reported to date is polyethylenimine (PEI). Due to their relatively high efficiency, branched PEI (BPEI) 25 kDa and linear PEI (LPEI) 22 kDa (ExGen®) have become benchmarks for other polymers, especially newly synthesized ones. PEI-based gene delivery systems work very well in many cells lines *in vitro*, but still present disappointing results in many primary cells *in vitro* and *in vivo* [1-3]. The toxicity increases with the degree of polymerization of the carrier molecule, but appears also to depend on the degree of branching. For example, by increasing the molecular weight (MW) of BPEIs, the transfection efficiency increases but is also accompanied by a high cytotoxicity [1,4]. This is not exactly true for LPEIs, the transfection efficiency also increases with the MW, but is to a certain point decoupled from cytotoxicity [5]. LPEIs have therefore been reported to be superior to BPEIs [6-9].

The acute toxicity of polycationic carriers is associated with their ability to bind non-specifically to negatively charged DNA and other biological materials. Furthermore, because the therapeutic application of transfection reagents requires a repeated use, the long-term fate of the polymeric carrier has to be considered in an organism. Therefore, high MW polymers that have superior properties to complex DNA and a stabilizing effect on polyplexes (DNA/polymer complexes) [10-14], but which can be easily degraded by the host, might help to overcome this obstacle. A popular strategy to reduce the toxicity of polyplexes is to use low MW polycations that are less cytolytic and have only a low transfecting ability [5], and crosslink them with agents that can be cleaved or activated by the intracellular environment. Such bioreversible linkages comprise esters [15-18], amides [18], orthoesters [19], imines [12,20] and disulfides [10,11,13,21-25].

Surprisingly, gene delivery using biodegradable polycations has with a few exceptions had only limited success so far [17,21,25]. The low efficiency of some biodegradable polycations may be due to their short half-life under physiological conditions and hence, reduced extracellular stability of polyplexes. Therefore, not only the biodegradability of the polymer, but also the stability of polyplexes in the extracellular environment are necessary prerequisites for efficient gene delivery. Bioreversible disulfide linkers are best suited to fulfill these demands, because they can take advantage of the high redox potential difference between the oxidazing extracellular space and the reducing intracellular environment (for

review see [26]), and therefore, they most likely allow for the release of the contained nucleic acid not until the arrival within the target cell [13,24].

Therefore, we crosslinked a LPEI derivative with a MW of 2.1 kDa with bioreversible disulfide bonds. LPEI 2.1 kDa was chosen because its polyplexes showed a minimal transfection efficiency and no cytotoxicty in a cell culture model [5]. We hypothesized that crosslinking would lead to a transfection efficiency comparable to a LPEI derivative of similar MW, but cytotoxicity as low as for LPEI 2.1 kDa.

Materials and Methods

Materials were purchased from Sigma-Aldrich Chemie GmbH (Germany) unless otherwise stated.

Cell lines and cell culture

Chinese hamster ovarian cells (CHO-K1; ATCC No. CCL-61) were grown in culture medium consisting of Ham´s F-12 supplemented with 10% FBS (Biochrom AG, Germany). The human cervical carcinoma cell line HeLa (ATCC No. CCL-2) was maintained in Dulbecco´s Medium (Invitrogen, Germany) supplemented with 10% FBS, 1 mM sodium pyruvate and 2 mM L-glutamine (both Invitrogen, Germany). The monkey kidney cell line COS-7 (ATCC No. CRL-1651) and murine kidney As.4.1 cells (ATCC No. CRL-2193) were maintained in DMEM (Invitrogen, Germany) with 4 mM L-glutamine adjusted to contain 1.5 g/L sodium bicarbonate and 4.5 g/l glucose supplemented with 10% FBS. All cells were incubated at 37°C in a 5% CO_2 humidified environment.

Non-viral carriers

Biodegradable PEIs were obtained by crosslinking LPEI with a MW of 2.1 kDa with Lomant´s reagent. The four resulting polymers had a different degree of branching and a slightly increasing MW with increasing linker/polymer proportion. The notation of the polymers was made as follows: LRx-LPEI, where x indicates the percentage of linker compared to the polymer starting material.

The notation of LPEIs was made without the unit kDa, for example LPEI 2.1 represents LPEI with a MW of 2.1 kDa (it should be annotated that LPEI 2.1 is the same polymer as LPEI 2.4 in [5], the indication of MW slightly differs because the lower one was determined by gel permeation chromatography and the higher one was estimated by ^{1}H-NMR spectroscopy).

Polymer stock solutions for LR-LPEIs, LPEIs and BPEI were prepared with 150 mM NaCl, the pH of LPEI solutions was adjusted to 7 and then filtered (0.2 µm filter, Corning GmbH, Germany). ExGen® 500 was obtained from MBI Fermentas GmbH (Germany).

Plasmid isolation and labeling

Plasmid encoding enhanced green fluorescent protein (EGFP) (Clontech, Germany) was used as reporter gene in this study. Plasmid was isolated from E. coli by using a Qiagen Plasmid Maxi Kit (Qiagen GmbH, Germany) according to the supplier´s protocol. When indicated, plasmid DNA was either covalently labeled with Alexa Fluor 546 according to the manufacturer´s protocol (ULYSIS Nucleic Acid Labeling Kit, Molecular Probes, The Netherlands) or stained with the intercalating dye YOYO-1 (Molecular Probes, The Netherlands). The labeling reaction with YOYO-1 was carried out with a molar ratio of 1 dye molecule per 320 base pairs at room temperature in the dark.

Preparation of polyplexes

Plasmid DNA/LR-LPEI or LPEI complexes were prepared at a NP ratio (nitrogens in polymer to phosphates in DNA) of 6, 12, 18, 24 and 30. Polyplexes were formed by mixing 2 µg DNA with the appropriate amount of polymer solution, while both components were diluted to 50 µl with 150 mM NaCl or 5% glucose. The resulting polyplexes were incubated for 20 minutes at room temperature before use. The notation of polyplexes was made as follows: LR1-LPEI - polyplexes expresses that polyplexes were built with LR1-LPEI. When indicated, polyplexes were incubated with dithiothreitol (DTT) at a concentration of 1 mM prior to transfection to confirm that the reduction of disulfides occurs intracellularly.

In vitro transfection and cytotoxicity experiments

For gene transfer studies, cells were grown in 24-well plates at an initial density of 38,000 – 42,000 cells per well, depending on the cell line. 18 hours after plating, the culture medium was removed, cells were washed with PBS (Invitrogen, Germany) and 900 µl serum-free or -containing medium was added (transfection medium). Thereafter, the prepared polyplexes were added to the cells. After 4-6 hours, the medium was replaced with 1 ml of culture medium. Analysis of transfection efficiency and cell viability was performed by flow cytometry 24 hours later as described previously [5,27]. Briefly, measurements were taken on a FACSCalibur (Becton Dickinson, Germany) using CellQuest Pro software (Becton Dickinson, Germany) and WinMDI 2.8 (©1993-2000 Joseph Trotter). EGFP positive cells

were detected using a 530/30 nm band-pass filter, whereas the propidium iodide emission was measured with a 670 nm longpass filter. In a density plot representing forward scatter against sideward scatter, whole cells were gated out and depicted in two-parameter dot plots of EGFP versus propidium iodide to analyse the measurements. The EGFP positive region corresponded to the transfection efficiency and the geometric mean fluorescence intensity was determined from the number of EGFP positive cells. Further, the number of propidium iodide negative cells was counted as a measure of cell viability.

Glutathione monoethyl ester (GSH MEE) was dissolved in serum-free medium and added to the cells 1 hour prior to transfection at concentrations of 1 or 5 mM. The amount of intracellular NAD(P)H of CHO-K1 cells after addition of duroquinone at concentrations of 50 or 100 µM was determined fluorometrically (excitation 340 nm and 460 nm emission) and expressed as fluorescence intensity [28,29]. The evaluation of the transfection efficiency and mean fluorescence intensity of the EGFP positive cells after addition of GSH MEE and duroquinone was performed at the indicated times by flow cytometry as described above.

Intracellular trafficking of polyplexes - confocal laser scanning microscopy (CLSM)

A Zeiss Axiovert 200 M microscope coupled to a Zeiss LSM 510 scanning device (Carl Zeiss Co. Ltd., Germany) was used for CLSM experiments. The inverted microscope was equipped with a Plan - Apochromat 63x and Plan - Neofluar 100x objective. Cells were plated in 8 – well Lab-Tek^{TM} Chambered Coverglass (Nunc GmbH & Co. KG, Germany) at an initial density of 35,000 cells / chamber in a volume of 400 µl culture medium. For maintaining a pH of 7.4, 20 mM HEPES (Invitrogen, Germany) was supplied. After 18 hours, polyplexes were added and measurements were directly performed in each well at 37°C. The thickness of the optical sections was between 0.7 and 1.2 µm.

For the investigation of the intracellular trafficking of polyplexes, LR-LPEI and YOYO-1 - labeled DNA were used. YOYO-1 was excited with a 488 nm argon laser, images were taken using a band-pass filter of 505 – 530 nm in the singletrack mode at the indicated times after the addition of the polyplexes. For the detection of polyplexes in acidic compartments of the cell, Alexa Fluor 546 - labeled plasmid DNA was applied. Polyplexes and quinacrine mustard at a concentration 10^{-6} M were added to the cells at the same point of time. Quinacrine mustard was excited at 458 nm and the fluorescence was imaged using a band-pass filter of 475 - 525 nm. Alexa Fluor - labeled DNA was excited at 543 nm and the fluoresecence was recorded with a 560 nm longpass filter. Images were taken in the multitracking modus.

Statistical analysis

All measurements were collected (n = 3 to 6) and expressed as means ± standard deviation (SD). Single factor of variance (ANOVA) was used in conjunction with a multiple comparison test (Tukey test) to assess the statistical significance.

Results

LR-LPEI - mediated gene transfer and cytotoxicity

The transfection efficiency of polyplexes formed with LR-LPEI (crosslinked with 1 to 4% linker) and plasmid DNA was evaluated in CHO-K1 cells and compared with LPEI 2.1, the starting material (Figure 1). As reported previously, the transfection efficiency of LPEI 2.1 - polyplexes was negligible and increased only slightly with increasing NP ratio [5]. A crosslinking of LPEI 2.1 with a linker/polymer proportion of 2% and higher statistically significantly increased the transfection efficiency. LR4-LPEI - polyplexes at NP 12 with a transfection efficiency of 73,60 ± 5,96% transfected 27 times more cells than the LPEI 2.1 - polyplexes. The NP ratio for the optimal gene expression decreased with the degree of branching of LR-LPEI. Furthermore, LR3-LPEI was also compared with LPEI 5.0 that had a different structure, but similar MW (Figure 1). It was remarkable that LR3-LPEI exceeded the non-degradable LPEI 5.0 - polyplexes at NP 18 nearly two fold.

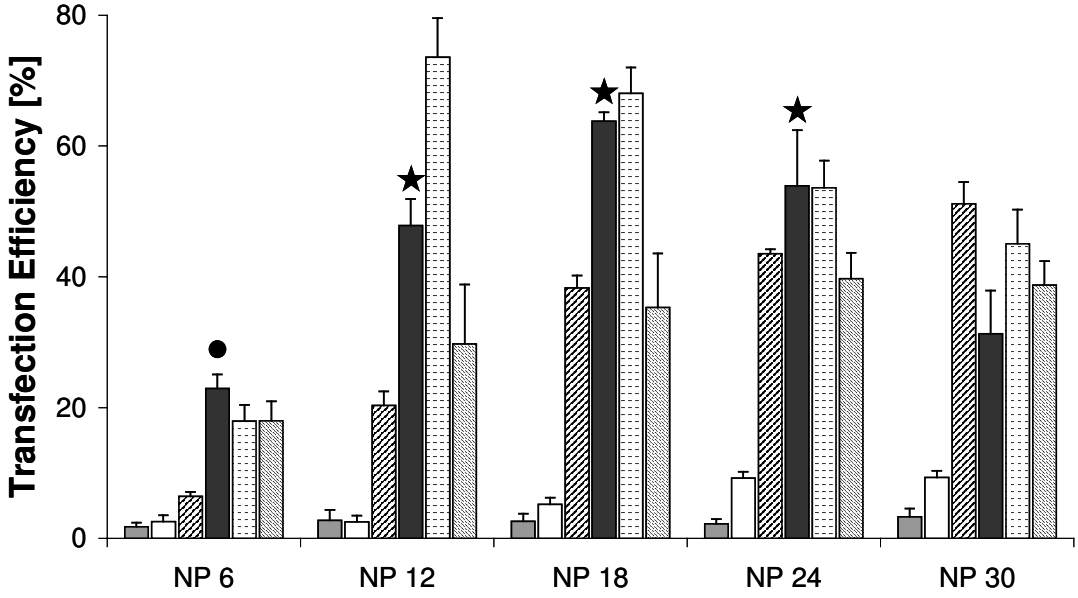

Figure 1: Transfection efficiency of LR-LPEI, crosslinked with 1% (□), 2% (▨), 3% (■) and 4% (▤) linker compared to LPEI 2.1 (■) complexed with pEGFP-N1 as reporter gene at various NP ratios in CHO-K1 cells as determined by flow cytometry. Experiments were performed in duplicate; values represent the EGFP positive cells as means ± SD of one representative experiment (n=6). Transfection efficiency of polyplexes built with LR-LPEI, crosslinked with 2 to 4% linker, was statistically significant higher ($p<0.01$, LR2-LPEI at NP 6 with $p<0.05$) compared to LPEI 2.1 and LR1-LPEI at each NP ratio tested. Further, LR3-LPEI was compared to LPEI 5.0 (▧) that has similar MW but different structure. Statistically significant differences between LPEI 5.0 and LR3-LPEI are denoted by ● ($p<0.05$) and ★ ($p<0.01$).

The cell viability was evaluated by propidium iodide staining followed by flow cytometry analysis in the same experiment [27]. Using LPEI 2.1, LR1-LPEI and LR2-LPEI in polyplexes, the cell viability seemed to be unaffected compared to untreated cells at every NP ratio tested (Figure 2). When cells were transfected with LR3-LPEI or LR4-LPEI, the cell viability slightly decreased at NP 30 or NP 24 and 30, respectively. The cell viability after transfection with LPEI 5.0 resembled that of LR3-LPEI.

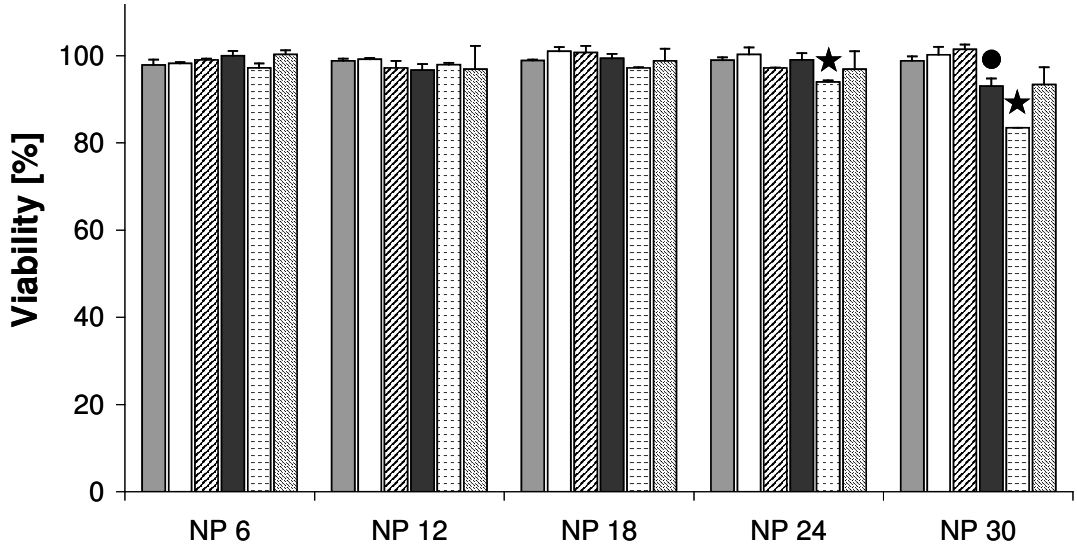

Figure 2: Relative viability of CHO-K1 cells after treatment with LR-LPEI, crosslinked with 1% (□), 2% (▨), 3% (■) and 4% (▤) linker, compared to LPEI 2.1 (▩) and LPEI 5.0 (▧) in polyplexes at various NP ratios determined with propidium iodide staining followed by flow cytometry. Experiments were performed in duplicate, values are means ± SD of one representative experiment (n=3). Cell viability statistically significant decreased compared to the treatment with same polyplexes at lower NP ratios, as indicated by ● ($p<0.05$) or by ★ ($p<0.01$).

Effect of serum and ionic strength of polyplex building medium on LR-LPEI-mediated gene transfer

It is known that the ionic strength of the formation medium affects the size and structure of PEI-based polyplexes and consequently their transfection efficiency [30]. Hence, we tested whether LR-LPEI - polyplexes built in 150 mM sodium chloride or 5% glucose could be used in the presence of 10% serum. For LR3-LPEI - polyplexes built in 150 mM sodium chloride, the number of EGFP positive cells was statistically significantly higher from NP 6 to 18 in serum-free culture condition, similar at NP 24 and finally statistically significant lower at NP 30 compared to transfection in serum-containing culture conditions (Figure 3). The efficacy of polyplexes formed in 5% glucose in serum-free transfection medium was statistically significantly higher compared to all other conditions tested. However, at the same time the cell viability also slightly decreased from about 91% at NP 6 to about 80% at NP 30 (data not shown).

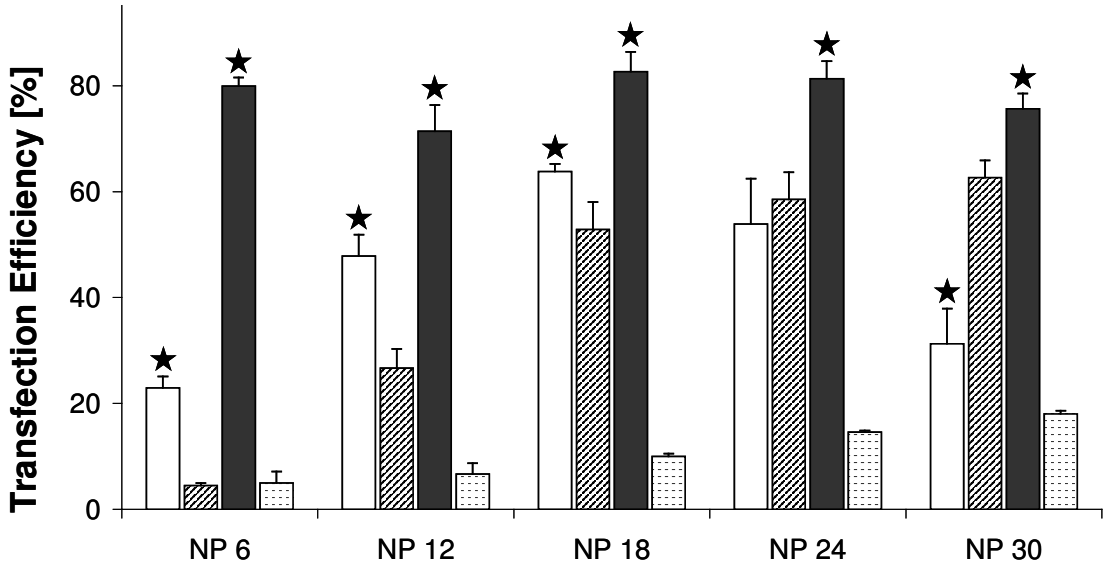

Figure 3: Transfection efficiency of LR3-LPEI, when polyplexes were built in 150 mM sodium chloride and the 4 hour incubation period was carried out in the absence or presence of serum (□ or ▨, respectively) or when polyplexes were built in 5% glucose (■ or ▩, respectively). Values represent the EGFP positive cells as means ± SD of one representative experiment (n=6). Statistically significantly different pairs are denoted by ★ (p<0.01). Transfection efficiencies of glucose-polyplexes in serum-free culture conditions were at every NP ratio statistically significant higher compared to other conditions (p<0.01).

The influencing effect of the ionic strength and culture conditions on the transfection efficiency was also observed for LR-LPEIs with another degree of branching (data not shown). However, the differences between the various conditions tested were not as remarkable and, furthermore, glucose-polyplexes were not superior to sodium chloride-polyplexes.

Response of LR-LPEI-mediated gene transfer to changes in the reducing/oxidizing environment of polyplexes and cells

After the treatment of polyplexes with DTT, the transfection efficiency of LR4-LPEI - polyplexes decreased significantly from about 75% to 60% (Figure 4). The preincubation of LPEI 5.0 - polyplexes that contained no cleavable disulfide bonds resulted only in a marginal decrease in the number of EGFP positive cells. Higher concentrations of DTT did further reduce the number of EGFP positive cells after transfection with LR4-LPEI, but did negatively influence the efficacy of LPEI 5.0 - polyplexes (data not shown).

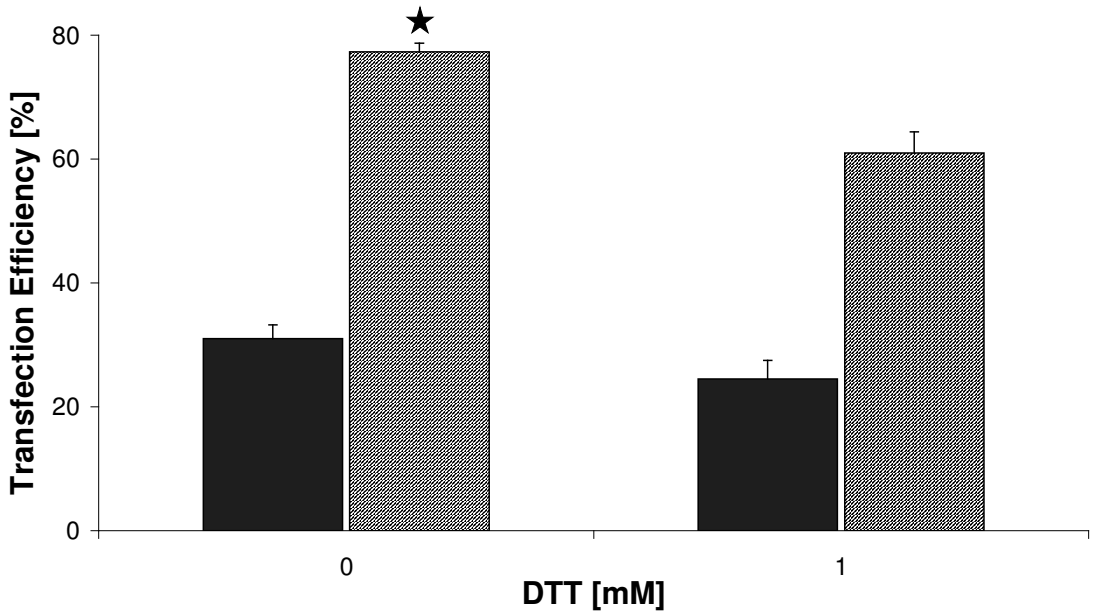

Figure 4: Transfection efficiency of LPEI 5.0 (■) - and LR4-LPEI (▨) - polyplexes at NP 18 incubated with 1 mM DTT prior to transfection compared to control conditions. Values represent the EGFP positive cells determined 24 hours post transfection by flow cytometry as means ± SD of one representative experiment (n=3). Statistically significant differences between DTT treated polyplexes and controls are denoterd by ★ ($p<0.05$).

Next, we evaluated whether changes in the intracellular NAD(P)H concentration would affect transfection. An hour before transfection, each culture was treated with duroquinone, a chemical that oxidizes NAD(P)H via a diaphorase reaction thereby lowering cellular NAD(P)H levels [28,31], which were monitored fluorometrically. As shown in Figure 5 A, the fluorescence intensity of CHO-K1 cells corresponding to the cellular level of NAD(P)H immediately decreased after the addition of duroquinone and remained low for at least 5 hours (data not shown). After 18 hours, the fluorescence intensity of duroquinone treated cells increased again to values comparable to the control, indicating that the cells may have a mechanism to adjust their NAD(P)H levels (data not shown). When transfecting cells with low NAD(P)H levels with LPEI 5.0 - polyplexes, the efficacy was not affected at either duroquinone concentration (Figure 5 B). Using LR4-LPEI - polyplexes, however, the number of transfected cells after 6 hours was significantly lower, but was similar to the control after 24 hours. The mean fluorescence intensity of EGFP positive cells after 6 hours of transfection was influenced by the addition of duroquinone using both forms of PEI in polyplexes, but for the linear form a higher concentration of duroquinone was necessary to induce a statistically significant decrease (Figure 5 C). After 24 hours, the mean fluorescence intensity of EGFP

positive cells was again similar to the controls using both linear and biodegradable PEI in polyplexes.

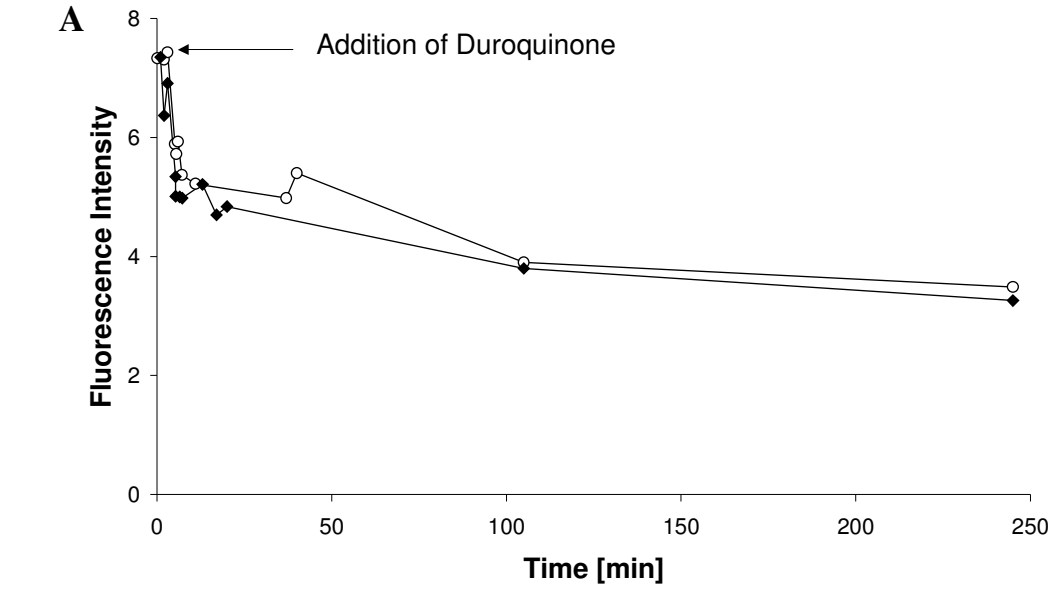

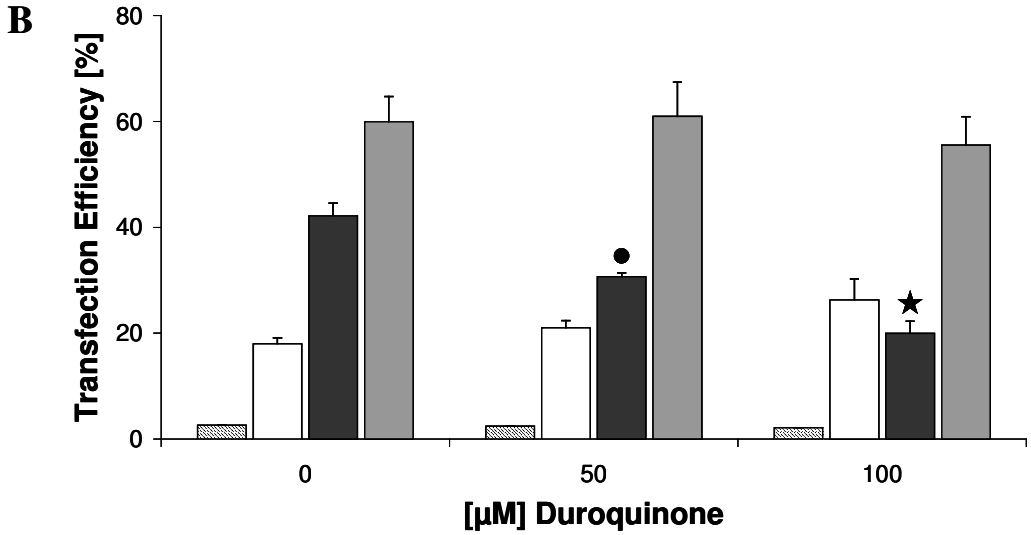

(continued on next page)

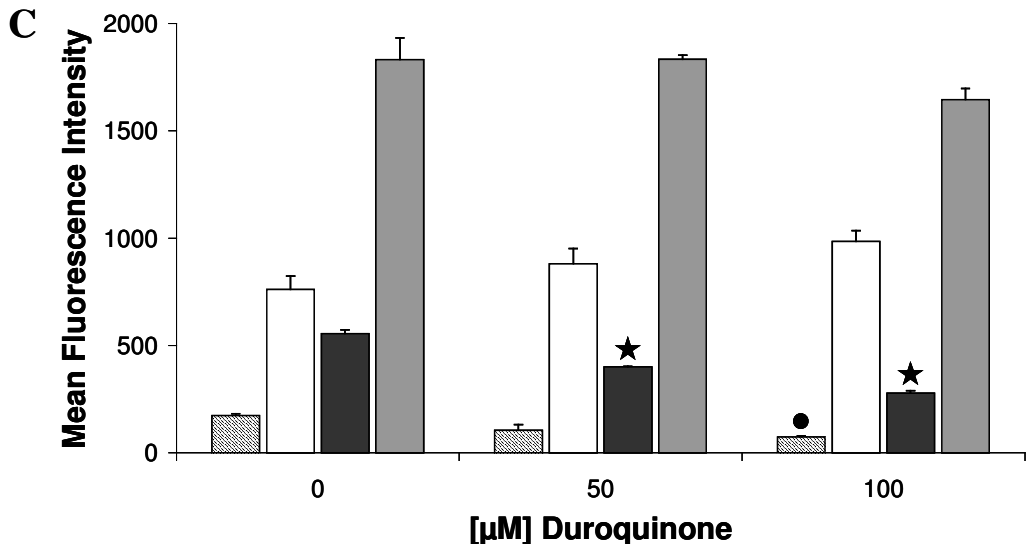

Figure 5: Effect of intracellular NAD(P)H on the transfection efficiency (B) and mean fluorescence intensity of EGFP positive cells (C). Duroquinone at a concentration of 50 or 100 µM was added to the cells one hour prior to transfection with LPEI 5.0 - polyplexes and LR4-LPEI - polyplexes at NP 12. A: Changes in the fluorescence intensity of CHO-K1 cells corresponding to the intracellular concentration of NAD(P)H after the addition of duroquinone at concentrations of 50 (○) or 100 (◆) µM. The fluorescence intensity of CHO-K1 cells resuspended in PBS buffer after trypsinization was measured fluorimetrically (340 nm excitation and 460 nm emission). B: Values represent the EGFP positive cells as means ± SD of one representative experiment (n=3) as determined by flow cytometry 6 hours (LPEI 5.0 ▨ and LR4-LPEI ■) and 18 hours (LPEI 5.0 □ or LR4-LPEI ▩; respectively) post transfection. C: Values represent the mean fluorescence intensity of EGFP positive cells as determined by flow cytometry 6 and 18 hours post transfection. Statistically significant differences compared to untreated cells are denoted by ● ($p<0.05$) or by ★ ($p<0.01$).

Enhancing the intracellular reducing conditions with glutathione (GSH) might effect the activation and hence, the efficiency of polyplexes. GSH MEE was used for this purpose, because it is effectively transported into various types of cells and converted intracellularly into GSH [32]. But boosting the intracellular GSH using GSH MEE did not further enhance the transfection efficiency of polyplexes independent of the degree of branching and hence, amount of cleavable disulfide bonds in polyplexes (Figure 6). Even higher concentrations of GSH MEE (5 mM) did not influence the number of EGFP positive cells (data not shown).

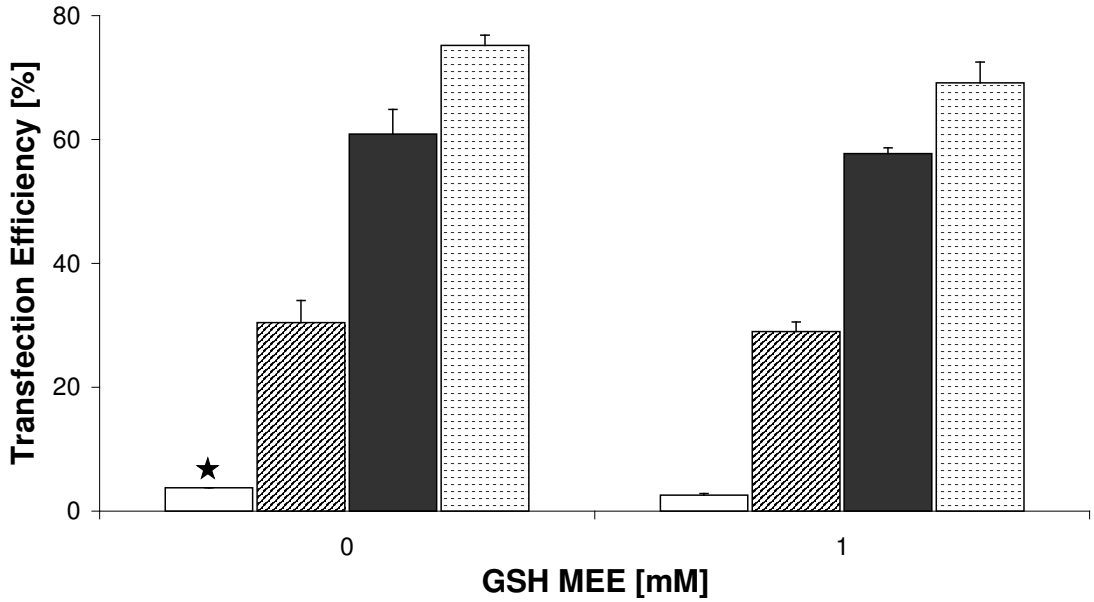

Figure 6: Influence of glutathione monoethylester (GSH MEE) at a concentration of 1 mM on the transfection efficiency of LR-LPEI, crosslinked with 1% (□), 2% (▨), 3% (■) and 4% (▤) linker, complexed with plasmid DNA at NP 18 compared to controls after 24 hours. Values represent the EGFP positive cells as means ± SD of one representative experiment (n=4). Statistically significant pairs are denoted by ★ (p<0.05).

Evaluation of LR-LPEI - mediated gene transfer in various cell lines

The next step was to evaluate the polyplexes formed with crosslinked LPEI in a number of cell lines (Figure 7). Regarding CHO-K1, COS-7 and HeLa cells, the optimal NP ratio for the transfection was different, but the maximum value was in the same range. The cell viability was as favorable in the other cell lines as it was in the CHO-K1 cells, with the exception of 5% more dead cells in COS-7 at NP 18 to 30 (data not shown). The performance of LR3-LPEI - polyplexes in As4.1 cells was much lower, but the cell viability was not affected by the transfection process (data not shown).

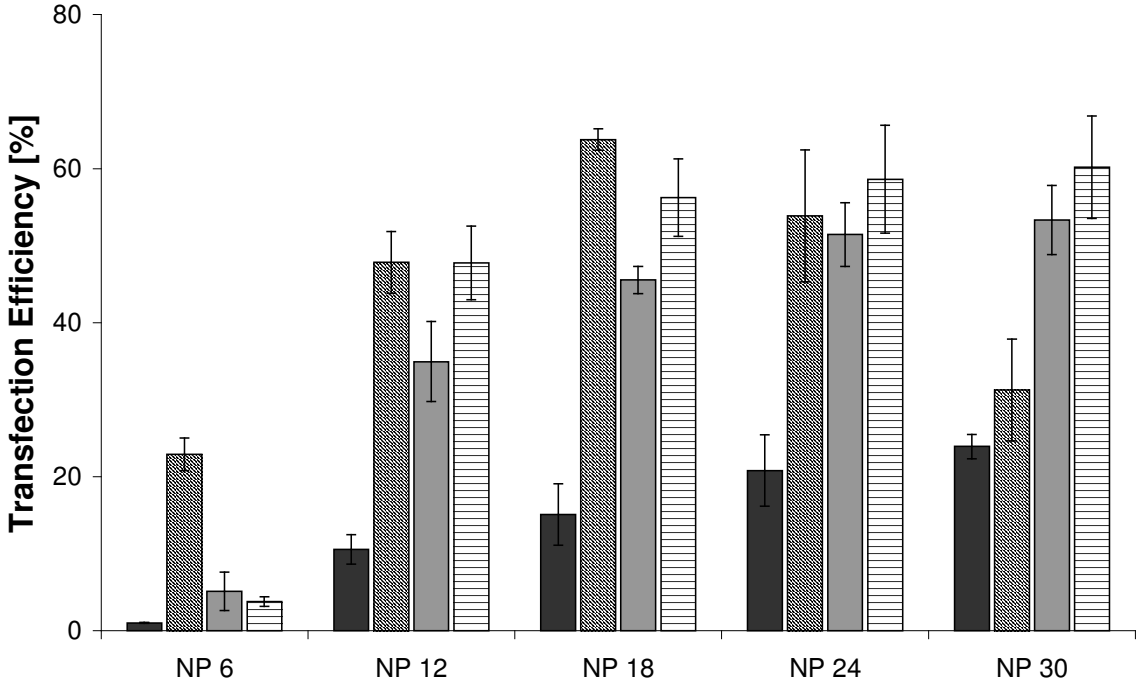

Figure 7: Transfection efficiency of LR3-LPEI complexed with pEGFP-N1 in As4.1 (■), CHO-K1 (▨), COS-7(□) and HeLa (▤) cells at various NP ratios as determined by flow cytometry. Values represent the EGFP positive cells as means ± SD of one representative experiment (n=4).

Uptake and lysosomal localization of LR-LPEI - polyplexes

The uptake of LR-LPEI - polyplexes into CHO-K1 cells and their shape was evaluated by CLSM during incubation over 8 hours (Figure 8 A) using plasmid DNA in polyplexes labeled with YOYO-1. The first polyplexes were detected inside CHO-K1 cells after one hour (data not shown). With further incubation, polyplexes were dispersed over the cytosol and in some cells polyplexes could be detected in the nucleus. The larger green dots in Figure 8 A were polyplex aggregates that were not taken up by cells. Intracellular polyplexes were more round compared to extracellular polyplexes. It was remarkable that cells showed a strong green fluorescence due to EGFP production only after five hours (data not shown, but see also Figure 5).

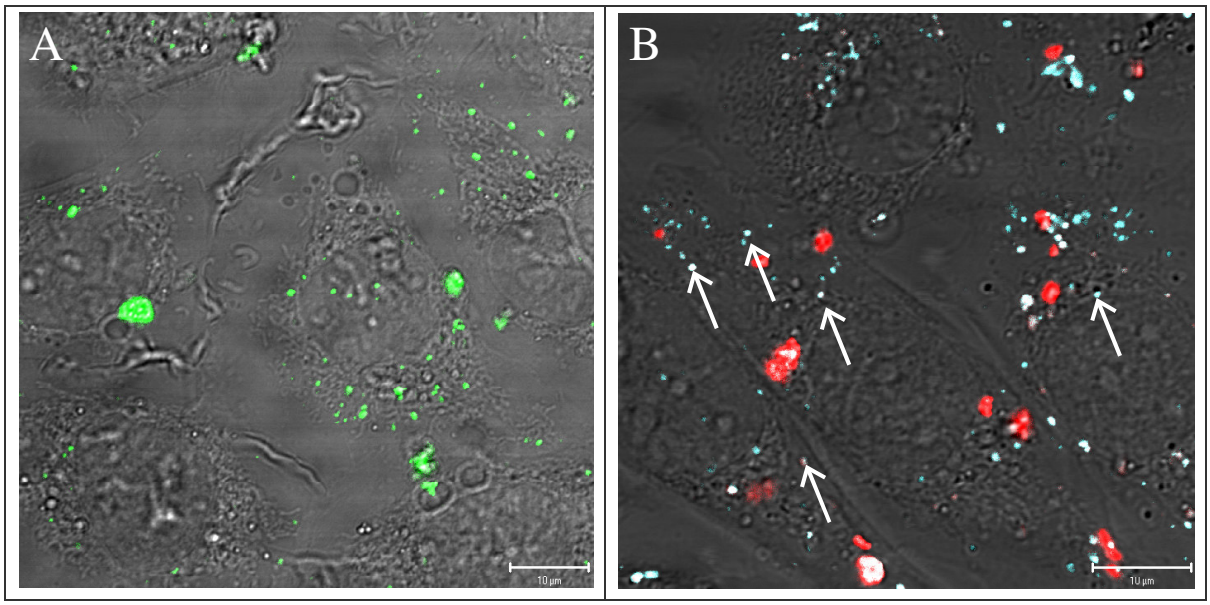

Figure 8: Observation of LR3-LPEI - polyplexes at NP 18 in CHO K1 cells five hours post transfection by CLSM. A: Uptake of polyplexes when plasmid DNA was labeled with YOYO-1 (green). Intracellular polyplexes were dispersed over the cytosol. B: Tracking Alexa 546-labeled DNA (red) and acidic vesicles (turquoise). A mixture of both colors indicates a close proximity. Most polyplexes were colocalized with acidic vesicles, some examples are indicated by an arrow. Pictures are an overlay of transmitted light and fluorescence images. Each bar indicates 10 µm.

CLSM was also used to verify whether acidic vesicles and polyplexes ever colocalized (Figure 8 B). A merge of acidic organelles and polyplexes would yield a combination color of turquoise and red. Most of the polyplexes taken up by CHO-K1 cells were colocalized with the acidic organelles through the whole observation time (Figure 8 A, arrow). The larger red dots were again polyplex aggregates that were not taken up by cells.

Comparison with BPEI 25 kDa and LPEI 22 kDa

Finally, the biodegradable PEIs were compared to BPEI 25 kDa and LPEI 22 kDa, the gold standards in the field of polymer-based nucleic acid delivery. The most effective polymer in the series of biodegradable PEIs, LR4-LPEI, far exceeded the efficacy of BPEI 25 kDa and LPEI 22 kDa (Figure 9). It was outstanding that, in contrast to BPEI and LPEI (data not shown), the high transfection efficiency was not associated with a reduction in cell viability.

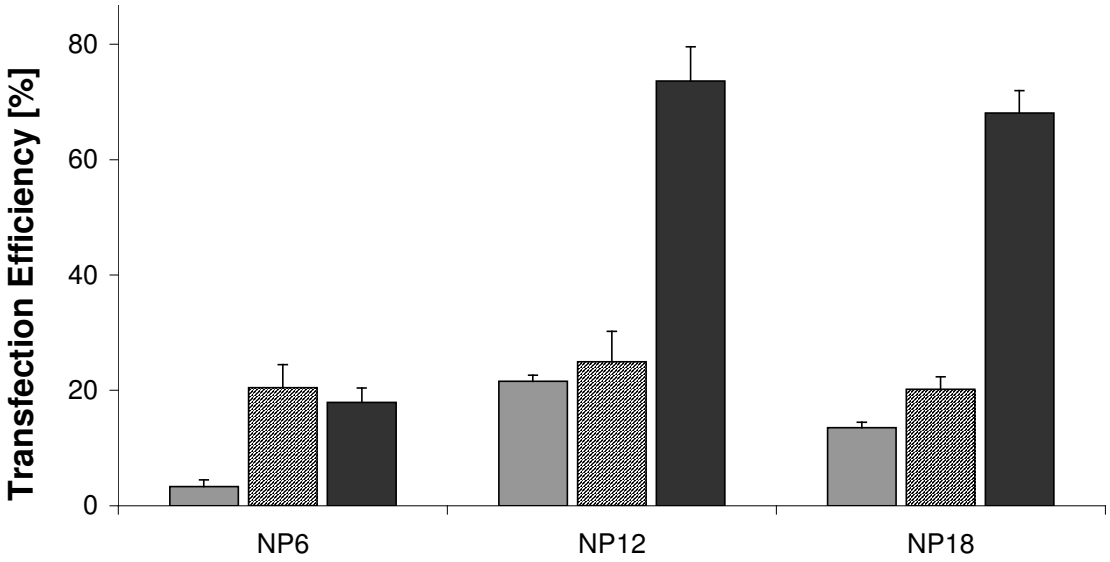

Figure 9: Transfection efficiency of BPEI 25 kDa (□), LPEI 22 kDa (▨) and LR4-LPEI (■) complexed with pEGFP-N1 as reporter gene at NP 6 to 18 in CHO-K1 cells as determined by flow cytometry. Values represent the EGFP positive cells as means ± SD of one representative experiment (n=4 or 6).

Discussion

In this study we proved our hypothesis that a bioreversible crosslinking of low MW LPEIs would raise the polymer´s efficacy due to the higher MW and hence transfection efficiency, while the biodegradable linkages would undergo intracellular breakdown and therefore not be toxic. LR4-LPEI exhibited a gene transfer activity greater than either BPEI 25 kDa or LPEI 22 kDa, some of the most effective polymers for gene transfection reported to date. Moreover, the cell viability was nearly unaffected after the transfection process. Furthermore, it is remarkable that many EGFP positive cells could be detected already after 6 hours of incubation with polyplexes. However, the mean fluorecence intensity of these EGFP positve cells was much lower compared to 24 hours, indicating that the translation had just begun. The early transcription/translation of EGFP has not been observed for LPEI – polyplexes. It is unclear why certain LR-LPEIs are more effective than the non-degradable form of similar MW. Perhaps the polymer degradation may facilate the unpacking and hence, easier transcription [33].

Disulfides were designed to exploit the differences in the degradation potential at different locations within and upon cells providing a clear opportunity to design vectors that are stable in the plasma but unstable within the endo-lysosomal compartment or cytoplasm. The concentration of extracellular GSH (estimated 1–2 µM) is usually 100 to 1000 times less than intracellular GSH and hence favors the maintenance of disulfide bonds. The majority of GSH

in cells is usually found in the cytosol; estimated GSH levels in the cells are 1–11 mM. Some organelles, however, such as the nucleus, appear to have their own GSH pools [26,34]. A simulated activation of polyplexes with DTT in the extracellular space decreased the transfection efficiency, which implies that the integrity of polyplexes is necessary for effective delivery. The decrease may be ascribed to the formation of shorter polymer chains that show a reduced gene transfer ability [5]. Higher concentrations of DTT for preincubation further decreased LR-LPEI-mediated gene transfer, but also influenced the efficiency of LPEI - polyplexes. This may be due to the fact that the structure and hence the transfection efficiency of polyplexes is responding to changes in the ionic strength during the formation and content of the culture medium. Pretreatment of CHO-K1 cells with GSH MEE to increase the cellular GSH pool [35] did not improve the gene expression of LR-LPEI - polyplexes. The level of GSH in CHO-K1 cells appears to be sufficient to activate the carriers at the tested NP ratios irrespective of the proportion of the disulfide linker. Furthermore, NAD(P)H also participates in the intracellular activation of LR-LPEI - polyplexes. Lower intracellular NAD(P)H levels reduced not only the number of EGFP positive cells, but also the amount of EGFP. Therefore, from literature and our results we conclude, that the polyplexes may at least partially undergo a GSH- and NAD(P)H-dependent reduction inside the cell [25,29,36]. It is not completely clear in which compartment of the cell the disulfide cleavage occurs, but most likely within the endolysomal compartment or in the cytoplasm. A cleavage in the early endosome probably plays a minor role because it is thought to be devoid of reducing activity [37-39]. It is also possible that the disulfide bonds are broken in the lysosomes, because a prolonged colocalization of plasmid DNA with acidic vesicles was observed.

By generating polyplexes in salt-free (5% glucose) or -containing (150 mM sodium chloride) medium and transfecting in serum-free or -containing culture conditions, we could show that the transfection ability of some of the LR-LPEI - polyplexes used for gene transfer is strongly influenced by these conditions. Wagner *et al.* hypothesized that this effect may be due to different polyplex stability and growth [30]. When examining the CLSMs pictures, it is clear that polyplex size has to be controlled and optimized. Therefore, in future studies the focus should not only be based on novel polymers, but also on techniques for polyplex building and understanding the polyplex structure - transfection ability relationship.

Concluding, we identified biodegradable PEI-based polyplexes that are superior to other polymer-based non-viral gene delivery systems reported so far. Our study proved the hypothesis that polyplexes with very high gene tranfer percentages, that are decoupled from cytotoxicity, could be produced using biodegradable PEIs. The efficacy of the most effective

LR-LPEI was nearly 3-fold higher than branched BPEI 25 kDa or LPEI 22 kDa, while the cytotoxicity of the biodegradable PEI - polyplexes was negligible. LR-LPEI-mediated gene delivery was dependent on intracellular reduction and could be modulated by manipulation of the number of stabilizing bonds. Moreover, the functionality of LR-LPEI could be demonstrated in various cell lines.

Therefore, we suggest that LR-LPEIs are a real substitute for existing polymer- and PEI-based nucleic acid delivery systems. The next step will be to test the capacity of biodegradable LR-LPEIs to transfect primary cells *in vitro*.

References

1. Godbey WT, Wu KK, Mikos AG. Size matters: molecular weight affects the efficiency of poly(ethylenimine) as a gene delivery vehicle. *J Biomed Mater Res* 1999; **45**: 268-275.

2. Tan PH, Beutelspacher SC, Wang YH, McClure MO, Ritter MA, Lombardi G, George AJT. Immunolipoplexes: an efficient, nonviral alternative for transfection of human dendritic cells with potential for clinical vaccination. *Mol Ther* 2005; **11**: 790-800.

3. Moghimi SM, Symonds P, Murray JC, Hunter AC, Debska G, Szewczyk A. A two-stage poly(ethylenimine)-mediated cytotoxicity: implications for gene transfer/therapy. *Mol Ther* 2005; **11**: 990-995.

4. Kunath K, Von Harpe A, Fischer D, Petersen H, Bickel U, Voigt K, Kissel T. Low-molecular-weight polyethylenimine as a non-viral vector for DNA delivery: comparison of physicochemical properties, transfection efficiency and in vivo distribution with high-molecular-weight polyethylenimine. *J Control Release* 2003; **89**: 113-125.

5. Breunig M, Lungwitz U, Liebl R, Fontanari C, Klar J, Kurtz A, Blunk T, Goepferich A. Gene delivery with low molecular weight linear polyethylenimines. *J Gene Med* 2005; **7**: 1287-1298.

6. Goula D, Benoist C, Mantero S, Merlo G, Levi G, Demeneix BA. Polyethylenimine-based intravenous delivery of transgenes to mouse lung. *Gene Ther* 1998; **5**: 1291-1295.

7. Ferrari S, Moro E, Pettenazzo A, Behr JP, Zacchello F, Scarpa M. ExGen 500 is an efficient vector for gene delivery to lung epithelial cells in vitro and in vivo. *Gene Ther* 1997; **4**: 1100-1106.

8. Bragonzi A, Boletta A, Biffi A, Muggia A, Sersale G, Cheng SH, Bordignon C, Assael BM, Conese M. Comparison between cationic polymers and lipids in mediating systemic gene delivery to the lungs. *Gene Ther* 1999; **6**: 1995-2004.

9. Goula D, Becker N, Lemkine GF, Normandie P, Rodrigues J, Mantero S, Levi G, Demeneix BA. Rapid crossing of the pulmonary endothelial barrier by polyethylenimine/DNA complexes. *Gene Ther* 2000; **7**: 499-504.

10. Oupicky D, Carlisle RC, Seymour LW. Triggered intracellular activation of disulfide crosslinked polyelectrolyte gene delivery complexes with extended systemic circulation in vivo. *Gene Ther* 2001; **8**: 713-724.

11. Trubetskoy VS, Loomis A, Slattum PM, Hagstrom JE, Budker VG, Wolff JA. Caged DNA does not aggregate in high ionic strength solutions. *Bioconjug Chem* 1999; **10**: 624-628.

12. Adami RC, Rice KG. Metabolic stability of glutaraldehyde cross-linked peptide DNA condensates. *J Pharm Sci* 1999; **88**: 739-746.

13. McKenzie DL, Kwok KY, Rice KG. A potent new class of reductively activated peptide gene delivery agents. *J Biol Chem* 2000; **275**: 9970-9977.

14. Ward CM, Read ML, Seymour LW. Systemic circulation of poly(L-lysine)/DNA vectors is influenced by polycation molecular weight and type of DNA: differential circulation in mice and rats and the implications for human gene therapy. *Blood* 2001; **97**: 2221-2229.

15. Park MR, Han KO, Han IK, Cho MH, Nah JW, Choi YJ, Cho CS. Degradable polyethylenimine-alt-poly(ethylene glycol) copolymers as novel gene carriers. *J Control Release* 2005; **105**: 367-380.

16. Ahn CH, Chae SY, Bae YH, Kim SW. Biodegradable poly(ethylenimine) for plasmid DNA delivery. *J Control Release* 2002; **80**: 273-282.

17. Forrest ML, Koerber JT, Pack DW. A degradable polyethylenimine derivative with low toxicity for highly efficient gene delivery. *Bioconjug Chem* 2003; **14**: 934-940.

18. Thomas M, Ge Q, Lu JJ, Chen J, Klibanov AM. Cross-linked small polyethylenimines: while still nontoxic, deliver DNA efficiently to mammalian cells in vitro and in vivo. *Pharm Res* 2005; **22**: 373-380.

19. Masson C, Garinot M, Mignet N, Wetzer B, Mailhe P, Scherman D, Bessodes M. pH-sensitive PEG lipids containing orthoester linkers: new potential tools for nonviral gene delivery. *J Control Release* 2004; **99**: 423-434.

20. Kim YH, Park JH, Lee M, Kim YH, Park TG, Kim SW. Polyethylenimine with acid-labile linkages as a biodegradable gene carrier. *J Control Release* 2005; **103**: 209-219.

21. Gosselin MA, Guo W, Lee RJ. Efficient gene transfer using reversibly cross-linked low molecular weight polyethylenimine. *Bioconjug Chem* 2001; **12**: 989-994.

22. Dauty E, Remy JS, Blessing T, Behr JP. Dimerizable cationic detergents with a low cmc condense plasmid DNA into nanometric particles and transfect cells in culture. *J Am Chem Soc* 2001; **123**: 9227-9234.

23. Dauty E, Remy JS, Zuber G, Behr JP. Intracellular delivery of nanometric DNA particles via the folate receptor. *Bioconjug Chem* 2002; **13**: 831-839.

24. Kwok KY, Park Y, Yang Y, McKenzie DL, Liu Y, Rice KG. In vivo gene transfer using sulfhydryl crosslinked PEG-peptide/glycopeptide/DNA co-condensates. *J Pharm Sci* 2003; **92**: 1174-1185.

25. Read ML, Bremner KH, Oupicky D, Green NK, Searle PF, Seymour LW. Vectors based on reducible polycations facilitate intracellular release of nucleic acids. *J Gene Med* 2003; **5**: 232-245.

26. Schafer FQ, Buettner GR. Redox environment of the cell as viewed through the redox state of the glutathione disulfide/glutathione couple. *Free Radic Biol and Med* 2001; **30**: 1191-1212.

27. Breunig M, Lungwitz U, Klar J, Kurtz A, Blunk T, Goepferich A. Polyplexes of polyethylenimine and per-n-methylated polyethylenimine-cytotoxicity and transfection efficiency. *J Nanosci Nanotechnol* 2004; **4**: 512-520.

28. Chernyak BV, Dedov VN, Chernyak VY. Ca2+-triggered membrane permeability transition in deenergized mitochondria from rat liver. *FEBS Lett* 1995; **365**: 75-78.

29. Balakirev M, Schoehn G, Chroboczek J. Lipoic acid-derived amphiphiles for redox-controlled DNA delivery. *Chem Biol* 2000; **7**: 813-819.

30. Wightman L, Kircheis R, Rossler V, Carotta S, Ruzicka R, Kursa M, Wagner E. Different behavior of branched and linear polyethylenimine for gene delivery in vitro and in vivo. *J Gene Med* 2001; **3**: 362-372.

31. Balakirev MY, Zimmer G. Gradual Changes in Permeability of Inner Mitochondrial Membrane Precede the Mitochondrial Permeability Transition. *Arch Biochem Biophys* 1998; **356**: 46-54.

32. Levy EJ, Anderson ME, Meister A. Transport of Glutathione Diethyl Ester Into Human Cells. *Proc Natl Acad Sci U S A* 1993; **90**: 9171-9175.

33. Schaffer DV, Fidelman NA, Dan N, Lauffenburger DA. Vector unpacking as a potential barrier for receptor-mediated polyplex gene delivery. *Biotechnol Bioeng* 2000; **67**: 598-606.

34. Bellomo G, Vairetti M, Stivala L, Mirabelli F, Richelmi P, Orrenius S. Demonstration of nuclear compartmentalization of glutathione in hepatocytes. *Proc Natl Acad Sci USA* 1992; **89**: 4412-4416.

35. Levy EJ, Anderson ME, Meister A. Transport of glutathione diethyl ester into human cells. *Proc Natl Acad Sci U S A* 1993; **90**: 9171-9175.

36. Carlisle RC, Etrych T, Briggs SS, Preece JA, Ulbrich K, Seymour LW. Polymer-coated polyethylenimine/DNA complexes designed for triggered activation by intracellular reduction. *J Gene Med* 2004; **6**: 337-344.

37. Collins DS, Unanue ER, Harding CV. Reduction of disulfide bonds within lysosomes is a key step in antigen processing. *J Immunol* 1991; **147**: 4054-4059.

38. Xing R, Mason RW. Design of a transferrin-proteinase inhibitor conjugate to probe for active cysteine proteinases in endosomes. *Biochem J* 1998; **336**: 667-673.

39. Saito G, Swanson JA, Lee KD. Drug delivery strategy utilizing conjugation via reversible disulfide linkages: role and site of cellular reducing activities. *Adv Drug Deliv Rev* 2003; **55**: 199-215.

Chapter 6

Limitations of Polyethylenimine-based Polyplexes

[1]Miriam Breunig, [1]Uta Lungwitz, [1]Renate Liebl, [1]Daniela Eyrich, [2]Birgit Obermayer, [3]Josef Koestler, [3]Ralf Wagner, [1]Torsten Blunk, [1]Achim Goepferich

[1] Department of Pharmaceutical Technology, University of Regensburg, Universitaetsstrasse 31, 93040 Regensburg, Germany

[2] Department of Physiology, University of Regensburg, Universitaetsstrasse 31, 93040 Regensburg, Germany

[3] Institute of Medicinal Microbiology and Hygiene, University of Regensburg, Franz-Josef-Strauss-Alle 11, 93052 Regensburg, Germany

Introduction

The need for safe and efficient nucleic acid delivery methods remains a critical obstacle to the routine clinical implementation of human gene therapy. Although virus-based delivery systems are the most efficient gene delivery systems currently available, polymeric carriers have several advantages that make them a promising alternative. Unfortunately, none of the existing polymer systems is generally acceptable for human gene therapy, primarily due to lack of efficiency. Among various cationic polymers polyethylenimines (PEIs) have emerged as the most efficient non-viral carriers for gene transfer into many cells. Although PEI-based gene delivery systems work very well in many cells *in vitro*, their gene expression is still too low for *in vivo* application.

Recently, we have introduced a variety of biodegradable PEIs that have successfully been applied for the transfection of various cell lines *in vitro* (see Chapter 5). Their efficacy was nearly by 3-fold higher than that of branched PEI (BPEI) 25 kDa and linear PEI (LPEI) 22 kDa, which have become benchmarks for newly synthesized polymers. The next step was to evaluate their gene transfer ability in human primary cells *in vitro*. Primary cells should be more representative of the *in vivo* situation than transformed cell lines and would better predict limitations to gene transfer *in vivo*. We chose two different test systems, namely denritic cells (DCs) and chondrocytes. In contrast to cell lines that are permanently dividing, DCs are terminally differentiated and non-dividing (for reviews, see [1,2]), while human chondrocytes still have the ability for proliferation [3], but their mitogenic activity is limited. Furthermore, both cell types are interesting candidates concerning a therapeutic application as described below.

The polymer-based carrier system has to navigate multiple obstacles to perform nucleic acid delivery. After condensing the DNA into polyplexes allowing for cellular uptake, the polymer should guide the nucleic acid safely through the endo-lysosomal compartment, and finally to the nucleus to be transcribed [4-7]. In cell lines, the endo-lysosomal escape and translocation to the nucleus seem to be a limiting step, but not the uptake of polyplexes [5,8,9]. In contrast, it was described that using cationic lipids as carrier systems, the uptake of plasmid DNA into differentiated primary cells severly restricts gene transfer [10,11]. Therefore, a second subject of this study was to test whether this is also true for polymers. We used the colon carcinoma cell line HT-29 as a model for 'hard-to-transfect' cells and measured the amount of internalized plasmid DNA.

Dendritic cells

DCs are unique antigen-presenting cells (APCs) with the competence to induce a primary immune response by transferring information from the outside world to the adaptive immune response (for reviews, see [2,12,13]). They originate from the bone marrow and their precursors home via the bloodstream to almost all organs, where they can be found in an immature state with high endocytotic and phagocytic capacity. This has lead to considerable interest in the application of DCs and DNA vaccines as tools for immunotherapy in the field of cancer and infectious diseases [2,14-17]. However, the development of effective DC-based vaccines requires their genetic manipulation.

The situation is rather complicated (for reviews, see [2,13]), but in short, DCs respond to DNA vaccines in two ways: by inducing both cellular and humoral immune responses. The cell-mediated immune response to DNA vaccines results from the uptake of plasmid DNA into DCs *in vitro* or *in vivo*, where the expression of the target antigen gene occurs. Fragments of the resulting proteins bind to class I MHC molecules. The presentation of these MHC-bound peptides on the cell surface stimulates CD8 T cells which are cytotoxic and have the machinery to destroy the infected cell. The humoral-mediated response occurs if the synthesized proteins are released and engulfed by APCs. In this case, the proteins are degraded in the class II pathway and presented to helper T cells. These secrete lymphokines that aid B cells to produce antibodies. A cross-priming and hence class I presentation of exogenous antigens is also possible.

DCs can be generated in sufficient numbers from circulating precursors, such as peripheral blood monocytotic cells (PBMCs) and $CD34^+$ stem cells, in the presence of cytokine cocktails [17]. Of particular interest are the more abundant $CD14^+$ PBMCs, which differentiate on culture in the presence of granulocyte-macrophage colony stimulating factor (GM-CSF) and interleukin-4 (IL-4) to immature DCs (iDCs), defined in part by their high antigen uptake. Further induction by inflammatory stimuli (for example bacterial DNA, lipopolysaccharide, double-stranded DNA) or transfection results in the expression of DC maturation markers. The mature DCs (mDCs) are more potent T cell stimulators than iDCs, but have reduced phagocytic and endocytic activities [1,2,13].

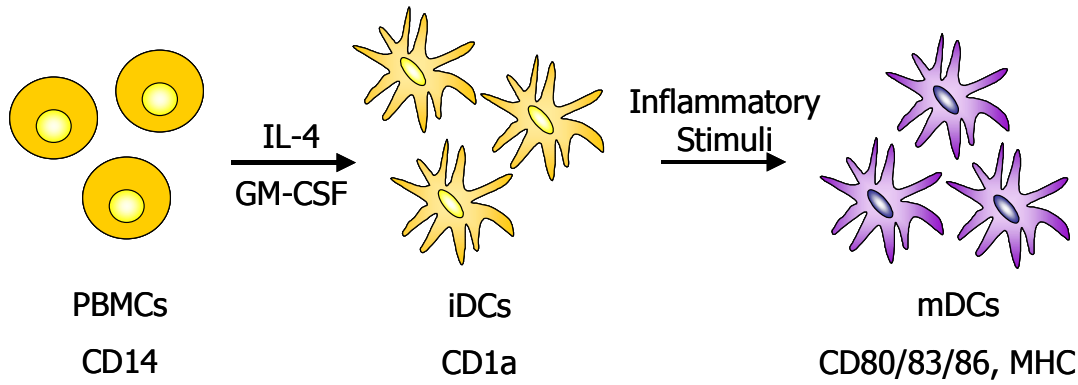

Figure 1: Generation of human DCs from peripheral blood CD14$^+$ mononuclear cells (PBMCs) when cultured in the presence of GM-CSF and IL-4. Immature DC (iDCs) can be further induced by inflammatory stimuli or transfection to mature DCs (mDCs). Human DC are characterized by the surface expression. The DC phenotype varies with different stages of maturation and differentiation. CD1a is preferentially expressed on human iDC. Antibodies to CD83 react with mDCs, which also express high levels of costimulatory molecules such as CD80 or CD86 and adhesion molecules including MHC I.

Chondrocytes

Chondrocytes populate the articular cartilage at low density. Certain concepts for repairing articular cartilage lesions employ a cell-based therapy (for review, see [18]), in which the initial healing response is, in part, mediated and dependent on signalling polypeptides. A major challenge is an appropriate delivery system for these therapeutic agents, because experiments *in vitro* and *in vivo* require relatively large, often repeated doses (for review, see [19]). Genetically engineered chondrocytes may be used as factories for the sustained protein production (for review, see [20]).

Materials and Methods

Materials were purchased from Sigma-Aldrich Chemie GmbH (Germany) unless otherwise stated.

DC preparation and cell culture

DCs were generated as desribed with slight modifications [21,22]. Briefly, PBMCs were isolated from buffy coat preparation of healthy donors by Ficoll density centrifugation (density of 1.077 g/cm^3) in Leucosep® Separation Falcon tubes (Greiner Bio-One GmbH, Germany). CD14$^+$ monocytes were enriched by magnetic cell sorting using the MACS system and MACS CD14 MicroBeads (both Milteny Biotec, Germany) according to the

manufacturer´s protocol. Monocytes were cultured for 6 days in RPMI 1640 medium containing 10% FBS, 2 mM glutamine (all Biochrom GmbH, Germany), non-essential amino acids, pyruvate, β-mercaptoethanol, penicillin/streptomycin (all Invitrogen, Germany). GM-CSF (Leucomax®) and IL-4 (Sigma, Germany) were added to the culture medium at concentrations of 500 U/ml. At days 3 and 5 culture medium was refreshed and at day 5 cells were transfected with polyplexes as desribed below.

Human chondrocytes in passage 2 were a kind gift from the HNO clinic (University of Regensburg). They were maintained in DMEM (4.5 g/l glucose) supplemented with 1% HEPES, 1% non-essential amino acids, 1% penicillin/streptomycin (all Invitrogen GmbH, Germany), 0.1 % proline, 0.1% ascorbic acid and 10% FBS (Biochrom AG, Germany).

Chinese hamster ovarian cells (CHO-K1; ATCC No. CCL-61) were grown in culture medium consisting of Ham´s F-12 supplemented with 10% FBS (Biochrom AG, Germany). HT-29 cells (ATCC No. HTB-38) were grown in McCoy´s modified 5A medium supplemented with 10% FBS. All cells were incubated at 37°C in a 5% CO_2 humidified environment.

Non-viral carriers

Biodegradable PEIs were obtained by crosslinking LPEI with a MW of 2.1 kDa [23] with Lomant´s reagent. The four resulting polymers had a different degree of branching and a slightly increasing MW with increasing linker/polymer proportion. Polymers are denoted as follows: LRx-LPEI, where x indicates the percentage of linker compared to the polymer starting material. Polymer stock solutions for LR-LPEIs were prepared with 150 mM NaCl, the pH of LPEI solutions was adjusted to 7 and then filtered (0.2 µm filter, Corning GmbH, Germany). ExGen® 500 was obtained from MBI Fermentas GmbH (Germany).

Plasmid isolation and labeling

Plasmid encoding enhanced green fluorescent protein (EGFP) (Clontech, Germany) was used as reporter gene in this study. Plasmid was isolated from E. coli by using a Qiagen Plasmid Maxi Kit (Qiagen GmbH, Germany) according to the supplier´s protocol.

When indicated, plasmid DNA was either covalently labeled with Alexa Fluor 546 according to the manufacturer´s protocol (ULYSIS Nucleic Acid Labeling Kit, Molecular Probes, The Netherlands) or stained with the intercalating dye YOYO-1 (Molecular Probes, The Netherlands). The labeling reaction with YOYO-1 was carried out with a molar ratio of 1 dye molecule per 320 base pairs at room temperature in the dark.

Preparation of polyplexes

Polyplexes were prepared at NP ratio (nitrogens in polymer to phosphates in DNA) of 6, 12, 18 and 24. Unless otherwise stated, polyplexes were formed by mixing 2 µg DNA with the appropriate amount of polymer solution and diluting to 50 µl with 150 mM NaCl. The resulting polyplexes were incubated for 20 minutes at room temperature before use. The notation of polyplexes was made as follows: LR1-LPEI - polyplexes indicates that polyplexes were formed with LR1-LPEI.

Transfection experiments

For gene transfer studies, cells were grown in 24-well plates at an initial density of 38,000 – 100,000 cells per well, depending on each cell type. The prepared polyplexes were added to cells in 900 µl serum-free or -containing medium. After 4-6 hours, the medium was replaced with 1 ml of culture medium. Analysis of transfection efficiency and cell viability was performed by flow cytometry 24 hours later as described previously [24,25]. Briefly, measurements were taken on a FACSCalibur (Becton Dickinson, Germany) using CellQuest Pro software (Becton Dickinson, Germany) and WinMDI 2.8 (©1993-2000 Joseph Trotter). EGFP positive cells were detected using a 530/30 nm band-pass filter, whereas the propidium iodide emission was measured with a 670 nm longpass filter. In a density plot representing forward scatter against sideward scatter, whole cells were gated out and depicted in two-parameter dot plots of EGFP versus propidium iodide to analyse the measurements. The EGFP positive region corresponded to the transfection efficiency. Further, the number of propidium iodide negative cells was counted as a measure of cell viability.

Intracellular trafficking of polyplexes - confocal laser scanning microscopy (CLSM)

A Zeiss Axiovert 200 M microscope coupled to a Zeiss LSM 510 scanning device (Carl Zeiss Co. Ltd., Germany) was used for CLSM experiments. The inverted microscope was equipped with a Plan - Apochromat 63x objective. Cells were plated in 8 – well Lab-Tek^{TM} Chambered Coverglass (Nunc GmbH & Co. KG, Germany) at an initial density of 35,000 cells / chamber in a volume of 400 µl culture medium. For maintaining a pH of 7.4, 20 mM HEPES (Invitrogen, Germany) was supplied. After 18 hours, polyplexes were added and measurements were directly performed in each well at 37°C. The thickness of the optical sections was between 0.7 and 1.2 µm.

For the investigation of the intracellular trafficking of polyplexes, YOYO-1 was excited with a 488 nm argon laser and images were taken using a band-pass filter of 505 – 530 nm at the indicated times after the addition of the polyplexes. Alexa Fluor 546 - labeled plasmid DNA was excited at 543 nm and the fluoresecence was recorded with a 560 nm longpass filter.

Isolation of plasmid DNA from whole cells and determination by real-time PCR

After 6 hours of transfection with LR-LPEI - polyplexes and subsequent to washing with CellScrub buffer (PEQLAB Biotechnologie GmbH, Germany), intracellular plasmid DNA of attached CHO-K1 or HT-29 cells (same initial cell density) was isolated according to the following procedure: Cells were resuspended in a buffer containing 50 mM Tris-HCl, 10 mM EDTA and 100 µg/ml Rnase A. Thereafter, the same volume of lysis solution (200 mM NaOH, 1% SDS) was added for 5 minutes at room temperature. The reaction was stopped by neutralization with 3 M potassium acetate, pH 5.5. After centrifugation at 12,000 rpm, plasmid DNA in the supernatant was precipitated, washed with 70% ethanol and resuspended in H_20. The solutions of three samples were pooled for real-time PCR.

Real-time PCR was performed in a Light Cycler (Roche Applied Biosciences, Germany). The diluted templates were mixed with PCR master mix consisting of QuantiTect™ SYBR® Green PCR (Qiagen, Germany) and 10 pmol of each primer pair. The forward primer (5´- ACG TAA ACG GCC ACA AGT TC-3´) and the reverse primer (5´- AAG TCG TGC TGC TTC ATG TG-3´) amplified a 187-bp fragment of the pEGFP-N1 plasmid. The absolute amount of target nucleic acid was determined with pEGFP-N1 as external standard. The amplification program consisted of 1 cycle at 95°C for 15 min, followed by 45 cycles with a denaturing phase at 95°C for 15 s, an annealing phase of 20 s at 58°C, and an elongation phase at 72°C for 20 s. A melting curve analysis was performed in order to verify specifity and identify the PCR products.

Results

Transfection of DCs and chondrocytes

After 5 days of cultivation in the presence of GM-CSF and IL-4, the proportion of iDCs in the whole cell population was determined to be 94% by flow cytometry after staining with fluorescein-conjugated anti-CD1a antibody. Furthermore, 24 hours after transfection, over 90% of cells exhibited the surface markers CD80 and CD86, which is indicative of a successful maturation to mDCs (data not shown).

Because of limitations in the cell source, only few conditions were tested in this experimental setup. Using LR3-LPEI for complex formation the number of EGFP positive cells increased with the amount of plasmid DNA in polyplexes to a maximum of 2.65% and the cell viability was similar compared to untreated cells. The efficacy of LPEI 22 kDa (ExGen®) resembled LR3-LPEI, but the linear polymer was by three-fold more toxic as compared to the biodegradable form of PEI.

The cytotoxicity appears to depend to a large extent on the donor of PBMCs, because the transfection efficiency of LR3-LPEI (2 µg plasmid DNA) was reproducible in three independent experiments, but the cytotoxicity only twice. In the third experiment the toxicity increased up to about 30% (data not shown).

Table 1: Transfection efficiency of LR3-LPEI or ExGen® complexed with pEGFP-N1 at NP 18 in DCs. Values represent the EGFP positive or dead cells as means ± SD (n=2).

Polyplex type	Transfection Efficiency [%]	Toxicity [%]
LR3-LPEI (1 µg plasmid DNA)	0.45 ± 0.21	6.37 ± 0.76
LR3-LPEI (2 µg plasmid DNA)	0.64 ± 0.32	8.63 ± 0.53
LR3-LPEI (3 µg plasmid DNA)	2.65 ± 0.10	13.56 ± 0.45
ExGen® (2 µg plamid DNA)	2.32 ± 0.23	28.92 ± 2.01
Untreated Cells	0.10 ± 0.05	12.73 ± 1.89

To get a better insight into the transfection process, polyplexes were fluorescently labeled and observed by CLSM during incubation with DCs. During maturation, DCs lost their charcteristic spiky arms, assumed a spherical shape and formed large colonies (Figure 2A). This process was nearly completed after three hours of transfection as observed by microscopy (data not shown). LR3-LPEI - polyplexes appeared to be associated with the surface of some round DCs, but not internalized. Presumably, the passage to the center of the

colonies was obstructed to the polyplexes. Examining the cells by 3D confocal z-image stacks, this observation could not be confirmed for certain, because it was difficult to distinguish the cell exterior from interior in transmitted light images (Figure 2 B).

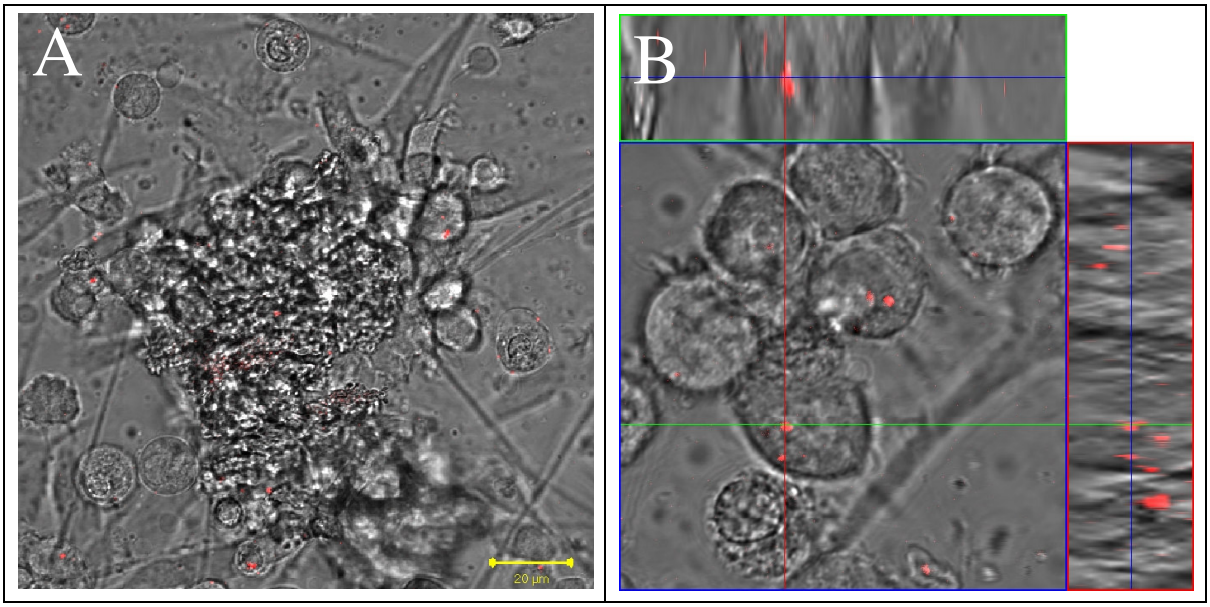

Figure 2: A: Incubation of DCs with LR3-LPEI - polyplexes at NP 18 labeled with Alexa Fluor 546 (indicated by red dots). The bar indicates 20 µm. B: The cells were examined by 3D confocal z-image stacks to evaluate the location of polyplexes with regard to the cells. Pictures are an overlay of transmitted light and fluorescence images.

Transfection of chondrocytes

Human chondrocytes were more susceptible to PEI-based transfection, but the overall efficacy was lower than in the cell lines tested in Chapter 5. The transfection efficiency could again be modulated by the NP ratio and the degree of branching of the polymer. The maximum transfection efficiency of about 9% was obtained with LR4-LPEI at NP 12 (Figure 3). The cell viability did not dip below 90% at any NP ratio tested (data not shown).

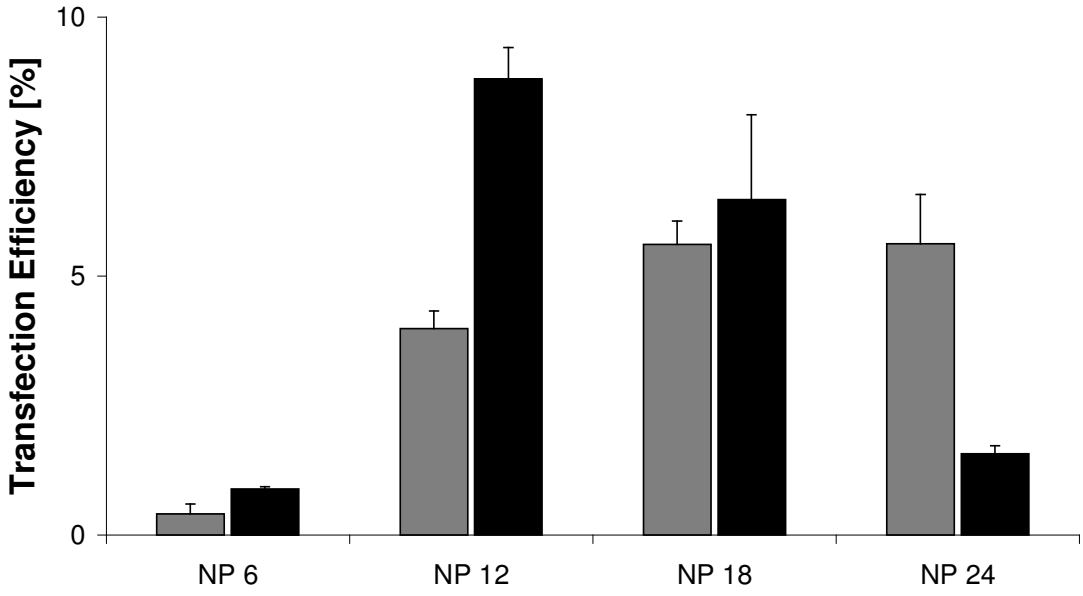

Figure 3: Transfection efficiency of LR3-LPEI (□) and LR4-LPEI (■) complexed with pEGFP-N1 at various NP ratios in human chondrocytes of passage 3. Values represent the EGFP positive cells as means ± SD (n=4).

Transfection and uptake of polyplexes in HT-29 cells

To test whether the uptake may be a limiting step in the transfection process as it is reported for certain lipids such as DMRIE-DOPE or LipofectACE® [10,11], HT-29 cells were chosen as a model because of ease of maintainance and better availability compared to DCs. The transfection efficiency seemed to increase with the degree of branching of PEI and was similar as obtained in DCs (Table 2). Furthermore, the shape of HT-29 cells is similar to that of to mDCs and at high densities they preferentially grew in colonies (images not shown).

Table 2: Transfection efficiency and cytotoxicity of various LR-LPEIs, crosslinked with 1 to 4% linker, complexed with pEGFP-N1 at NP 18 in HT-29 cells. Values represent the EGFP positive or viable cells compared to untreated cells as means ± SD of one representative experiment (n=4).

LR-LPEI type	Transfection Efficiency [%]	Toxicity [%]
LR1-LPEI	0.23 ± 0.08	10.31 ± 0.33
LR2-LPEI	0.48 ± 0.11	12.51 ± 0.52
LR3-LPEI	1.54 ± 0.15	16.88 ± 1.29
LR4-LPEI	3.66 ± 0.52	19.41 ± 1.13
Untreated Cells	0.09 ± 0.03	10.06 ± 0.88

To study the uptake in HT-29 cells, polyplexes were labeled with YOYO-1 and observed by CLSM during incubation. In CHO-K1 cells, which were used as positive control, polyplexes were dispersed over the cytosol of cells after 5 hours of incubation (Figure 4 A). The larger green dots were polyplex aggregates that were not taken up by cells. In contrast, the polyplexes seemed only losely attached to HT-29 cells as shown for DCs (Figure 4 B).

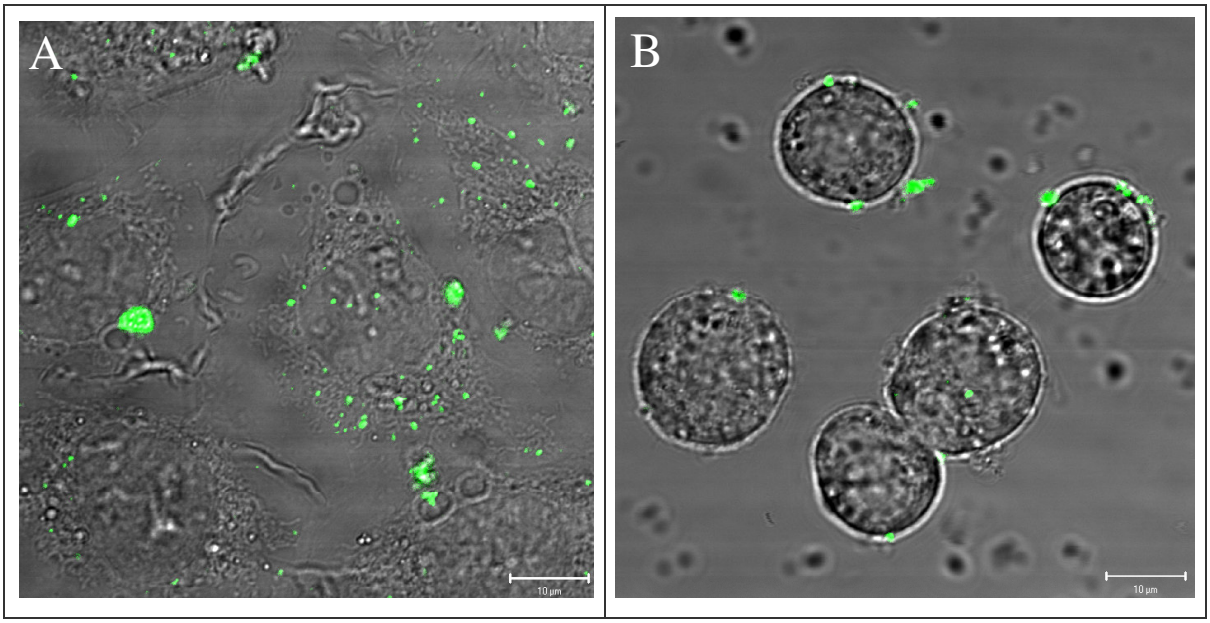

Figure 4: Uptake of LR3-LPEI - polyplexes at NP 18 labeled with YOYO-1 in CHO-K1 (A) and HT-29 (B) cells five hours post transfection as examined by CLSM five hours after transfection. Pictures are an overlay of transmitted light and fluorescence images. Each bar indicates 10 µm.

To document the CLSM images with data, plasmid DNA taken up by the cells was isolated after 6 hours and quantified by real-time PCR. As carrier molecules for plasmid DNA transfer into cells, various LR-LPEIs, crosslinked with 1 to 4% linker, were used at NP 18. Irrespective of the polymer tested, the amount of plasmid DNA isolated from CHO-K1 cells was a multiple higher compared to HT-29 cells (Figure 5).

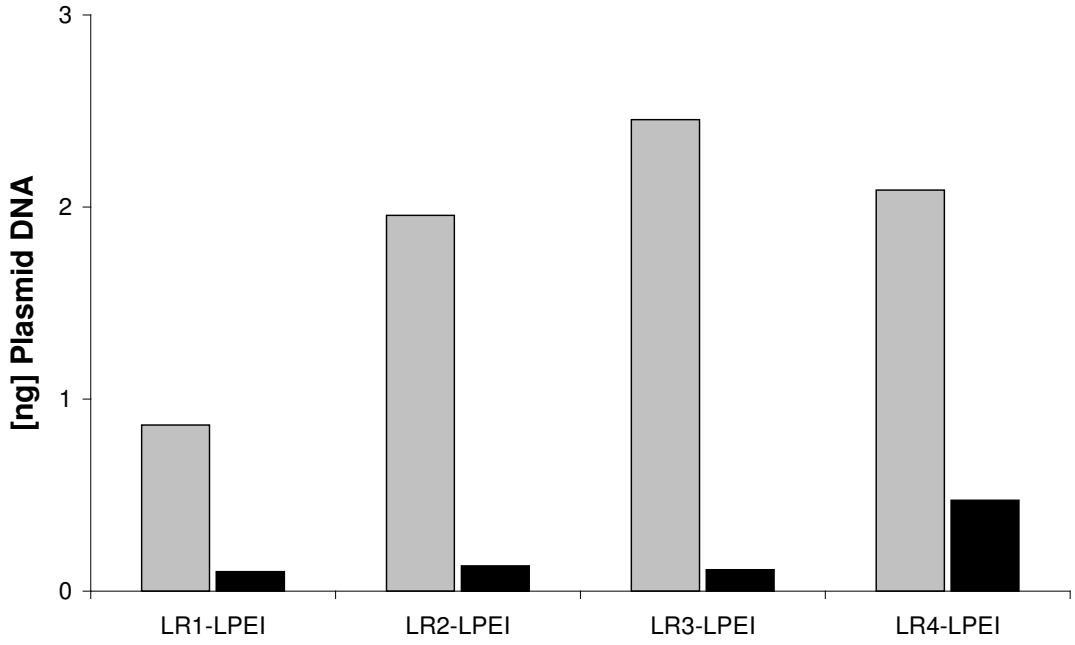

Figure 5: Plasmid DNA isolated after 6 hours of transfection from an aliquot of CHO-K1 (□) or HT-29 (■) cells with various LR-LPEI - polyplexes (as indicated in the legend) at NP 18. The absolute amount of target nucleic acid after 6 hours of transfection was determined with pEGFP-N1 as external standard in a Light Cycler.

To test the effectivity of plasmid DNA in HT-29 cells compared to CHO-K1 cells as positive control, the ratio of plasmid DNA taken up or the transfection efficiency, respectively, between CHO-K1 and HT-29 cells was calculated. The ratio of plasmid DNA taken up (CHO-K1/HT-29) varied with the polymer used for transfection (Table 3). The ratio first increased with the degree of branching of LR-LPEI, but then decreased with LR4-LPEI as carrier molecule below the ratio of LR1-LPEI. The ratio of transfection efficiency (CHO-K1/HT-29) depended also on the LR-LPEI type and was much higher than the ratio of the uptake (Table 3).

Table 3: The ratio of plasmid DNA taken up (column 2) and transfection efficiency (column 3) between CHO-K1 and HT-29 cells after transfection with various LR-LPEIs at NP 18.

LR-LPEI type	Plasmid DNA taken up (CHO-K1 / HT-29)	Transfection efficiency (CHO-K1 / HT-29)
LR1-LPEI	8.5	~ 22
LR2-LPEI	14.9	~ 80
LR3-LPEI	21.8	~ 41
LR4-LPEI	4.4	~ 19

Discussion

Substantial effort has been devoted towards the development of efficient polymers for nucleic acid delivery. Non-viral carriers are typically safer but much less efficient than viruses. In addition, many polymers still exhibit significant cytotoxicity in various cells. Biodegradable PEIs (Chapter 5) were the first delivery systems that enabled a remarkably high transfection efficiency simultaneously with a high cell viability. This study aimed at testing the functionality of biodegradable PEI - polyplexes in human primary cells, namely DCs and chondrocytes.

The transfection efficiency of biodegradable PEI-based polyplexes seemed to depend on the mitogenic activity of cells, because the number of EGFP positive cells decreased in the following order: permanently dividing cell lines (Chapter 5) > human chondrocytes > human DCs. This implies that biodegradable PEIs have improved nuclear import characteristics compared to other polymer-based delivery systems, because they are capable of transfecting non-dividing cells, but nevertheless the breakdown of the nuclear envelope favors gene transfer.

Various attemps have been undertaken in order to transfect DCs with polymer- and lipid-based gene delivery systems or even by electroporation, however, only with limited success. The amount of transfected monocyte-derived DCs did not exceed 1-5%, and was also accompanied by a high cytotoxicity [26,27]. Therefore, biodegradable PEI-based polyplexes are a good basis for further optimization because they are accompanied by a very low cytotoxicity. A first step towards this direction would be to enhance the cellular uptake of polyplexes. For example, the attachment of mannose to PEI-based polyplexes and taking advantage of receptor-mediated endocytosis slightly improved the transfection efficiency in DCs [28,29]. Furthermore, the strategy of using immunolipoplexes containing anti-CD71 or anti-CD205 monoclonal antibodies has been shown to be more effective compared to unmodified lipoplexes: up to 10% mDCs, and up to 20% iDCs could be transfected, but the cellular toxicity also ranged from 20 to 70% depending on the lipid for immunolipoplex formation [27].

The efficacy in human chondrocytes was acceptable, but can most likely be vastly improved. Using FuGENE6 (other lipid-based reagents, such as TransFast and LipofectAmine, failed to transfect chondrocytes) the transfection efficiency could be augmented from 9 up to about 40% after treatment with hyaluronidase in order to make the extracellular matrix more permeable to the transfection agent [30-34]. Therefore, future studies will test whether this is also true for biodegradable PEI - polyplexes.

DCs are expensive to maintain and not available in a high quanities, thus, HT-29 cells were used as a model to test whether the uptake is one of the limiting steps in the transfection of 'hard-to-transfect' cells. HT-29 cells were chosen because the transfection efficiency and cytotoxicity were similar to DCs and CLSM pictures indicated similar cell shape and uptake of polyplexes. Quantification of intracellular plasmid DNA in HT-29 cells revealed up to 21-fold lower levels than CHO-K1 cells that were used as positive control. For the first time, it was demonstrated that the uptake using polymers for gene delivery may be one of the limiting steps in 'hard-to-transfect' cells. Moreover, the plasmid DNA taken up by HT-29 cells was less efficient, because the ratio of the uptake (CHO-K1/HT-29) was lower than the ratio of the transfection efficiency (CHO-K1/HT-29). This is due to the fact that endo-lysosomal escape and nuclear entry are further limiting steps in non-viral gene transfer.

Concluding, for further improvement of non-viral gene delivery systems, much more effort should be made to transfer nucleic acids into 'hard-to-transfect' cells. It is our opinion that solving the problem will require the design of "intelligent" polyplexes. A first step would be to enhance their cellular uptake by attaching appropriate signalling sequences, such as the TAT peptide, to their surface [35,36]. TAT peptides derived from the HIV-1 TAT protein have been shown to facilitate intracellular delivery of proteins and small colloidal particles and also relatively large drug carriers, such as 200-nm liposomes [37].

References

1. Mellman I, Steinman RM. Dendritic cells: specialized and regulated antigen processing machines. *Cell* 2001; **106**: 255-258.

2. Banchereau J, Briere F, Caux C, Davoust J, Lebecque S, Liu YJ, Pulendran B, Palucka K. Immunobiology of dendritic cells. *Annu Rev Immunol* 2000; **18**: 767-811.

3. Tallheden T, Bengtsson C, Brantsing C, Sjoegren-Jansson E, Carlsson L, Peterson L, Brittberg M, Lindahl A. Proliferation and differentiation potential of chondrocytes from osteoarthritic patients. *Arthritis Res Ther* 2005; **7**: R560-R568.

4. Behr JP. Gene transfer with synthetic cationic amphiphiles: prospects for gene therapy. *Bioconjug Chem* 1994; **5**: 382-389.

5. Bieber T, Meissner W, Kostin S, Niemann A, Elsasser HP. Intracellular route and transcriptional competence of polyethylenimine-DNA complexes. *J Control Release* 2002; **82**: 441-454.

6. Ogris M, Steinlein P, Kursa M, Mechtler K, Kircheis R, Wagner E. The size of DNA/transferrin-PEI complexes is an important factor for gene expression in cultured cells. *Gene Ther* 1998; **5**: 1425-1433.

7. Wattiaux R, Laurent N, Wattiaux-De Coninck S, Jadot M. Endosomes, lysosomes: their implication in gene transfer. *Adv Drug Deliv Rev* 2000; **41**: 201-208.

8. Itaka K, Harada A, Yamasaki Y, Nakamura K, Kawaguchi H, Kataoka K. In situ single cell observation by fluorescence resonance energy transfer reveals fast intra-cytoplasmic delivery and easy release of plasmid DNA complexed with linear polyethylenimine. *J Gene Med* 2004; **6**: 76-84.

9. Grosse S, Aron Y, Honore I, Thevenot G, Danel C, Roche AC, Monsigny M, Fajac I. Lactosylated polyethylenimine for gene transfer into airway epithelial cells: role of the sugar moiety in cell delivery and intracellular trafficking of the complexes. *J Gene Med* 2004; **6**: 345-356.

10. Matsui H, Johnson LG, Randell SH, Boucher RC. Loss of binding and entry of liposome-DNA complexes decreases transfection efficiency in differentiated airway epithelial cells. *J Biol Chem* 1997; **272**: 1117-1126.

11. Fasbender A, Zabner J, Zeiher BG, Welsh MJ. A low rate of cell proliferation and reduced DNA uptake limit cationic lipid-mediated gene transfer to primary cultures of ciliated human airway epithelia. *Gene Ther* 1997; **4**: 1173-1180.

12. Liu YJ. Dendritic cell subsets and lineages, and their functions in innate and adaptive immunity. *Cell* 2001; **106**: 259-262.

13. Lipscomb MF, Masten BJ. Dendritic cells: immune regulators in health and disease. *Physiol Rev* 2002; **82**: 97-130.

14. Nencioni A, Brossart P. Cellular immunotherapy with dendritic cells in cancer: current status. *Stem Cells* 2004; **22**: 501-513.

15. Gregoriadis G. Genetic vaccines: strategies for optimization. *Pharm Res* 1998; **15**: 661-670.

16. Banchereau J, Schuler-Thurner B, Palucka AK, Schuler G. Dendritic cells as vectors for therapy. *Cell* 2001; **106**: 271-274.

17. Brossart P, Wirths S, Brugger W, Kanz L. Dendritic cells in cancer vaccines. *Exp Hematol* 2001; **29**: 1247-1255.

18. Caplan AI. Review: mesenchymal stem cells: cell-based reconstructive therapy in orthopedics. *Tissue Eng* 2005; **11**: 1198-1211.

19. Holland TA, Mikos AG. Advances in drug delivery for articular cartilage. *J Control Release* 2003; **86**: 1-14.

20. Palmer G, Pascher A, Gouze E, Gouze JN, Betz O, Spector M, Robbins PD, Evans CH, Ghivizzani SC. Development of gene-based therapies for cartilage repair. *Crit Rev Eukaryot Gene Expr* 2002; **12**: 259-273.

21. Romani N, Reider D, Heuer M, Ebner S, Kampgen E, Eibl B, Niederwieser D, Schuler G. Generation of mature dendritic cells from human blood An improved method with special regard to clinical applicability. *J Immunol Methods* 1996; **196**: 137-151.

22. Zhou LJ, Tedder TF. CD14+ blood monocytes can differentiate into functionally mature CD83+ dendritic cells. *Proc Natl Acad Sci U S A* 1996; **93**: 2588-2592.

23. Lungwitz U, Breunig M, Blunk T, Goepferich A. Synthesis and application of low molecular weight linear polyethylenimines for non-viral gene delivery. *Proceedings of the annual meeting of the German Pharmaceutical Society* 2004; P T25: 157.

24. Breunig M, Lungwitz U, Klar J, Kurtz A, Blunk T, Goepferich A. Polyplexes of polyethylenimine and per-n-methylated polyethylenimine-cytotoxicity and transfection efficiency. *J Nanosci Nanotechnol* 2004; **4**: 512-520.

25. Breunig M, Lungwitz U, Liebl R, Fontanari F, Klar J, Kurtz A, Blunk T, Goepferich A. Gene delivery with low molecular weight linear polyethylenimines. *J Gene Med* 2005; **7**, 1287-1298.

26. Van Tendeloo VFI, Snoeck H, Lardon F, Vanham GLEE, Nijs G, Lenjou M, Hendriks L, Van Broeckhoven C, Moulijn A, Rodrigus I, Verdonk P, Van Bockstaele DR, Berneman ZN. Nonviral transfection of distinct types of human dendritic cells: high-efficiency gene transfer by electroporation into hematopoietic progenitor- but not monocyte-derived dendritic cells. *Gene Ther* 1998; **5**: 700-707.

27. Tan PH, Beutelspacher SC, Wang YH, McClure MO, Ritter MA, Lombardi G, George AJT. Immunolipoplexes: an efficient, nonviral alternative for transfection of human dendritic cells with potential for clinical vaccination. *Mol Ther* 2005; **11**: 790-800.

28. Diebold SS, Kursa M, Wagner E, Cotten M, Zenke M. Mannose polyethylenimine conjugates for targeted DNA delivery into dendritic cells. *J Biol Chem* 1999; **274**: 19087-19094.

29. Diebold SS, Plank C, Cotten M, Wagner E, Zenke M. Mannose receptor-mediated gene delivery into antigen presenting dendritic cells. *Somatic Cell Mol Genet* 2002; **27**: 65-74.

30. Madry H, Trippel SB. Efficient lipid-mediated gene transfer to articular chondrocytes. *Gene Ther* 2000; **7**: 286-291.

31. Madry H, Kaul G, Cucchiarini M, Stein U, Zurakowski D, Remberger K, Menger MD, Kohn D, Trippel SB. Enhanced repair of articular cartilage defects in vivo by transplanted chondrocytes overexpressing insulin-like growth factor I (IGF-I). *Gene Ther* 2005; **12**: 1171-1179.

32. Trippel SB, Ghivizzani SC, Nixon AJ. Gene-based approaches for the repair of articular cartilage. *Gene Ther* 2004; **11**: 351-359.

33. Madry H, Cucchiarini M, Stein U, Remberger K, Menger MD, Kohn D, Trippel SB. Sustained transgene expression in cartilage defects in vivo after transplantation of articular chondrocytes modified by lipid-mediated gene transfer in a gel suspension delivery system. *J Gene Med* 2003; **5**: 502-509.

34. Stove J, Fiedler J, Huch K, Gunther K-P, Puhl W, Brenner R. Lipofection of rabbit chondrocytes and long lasting expression of a lacZ reporter system in alginate beads. *Osteoarthritis Cartilage* 2002; **10**: 212-217.

35. Gupta B, Levchenko TS, Torchilin VP. Intracellular delivery of large molecules and small particles by cell-penetrating proteins and peptides. *Adv Drug Deliv Rev* 2005; **57**: 637-651.

36. Tseng YL, Liu JJ, Hong RL. Translocation of liposomes into cancer cells by cell-penetrating peptides penetratin and Tat: a kinetic and efficacy study. *Mol Pharmacol* 2002; **62**: 864-872.

37. Torchilin VP, Rammohan R, Weissig V, Levchenko TS. TAT peptide on the surface of liposomes affords their efficient intracellular delivery even at low temperature and in the presence of metabolic inhibitors. *Proc Natl Acad Sci U S A* 2001; **98**: 8786-8791.

Chapter 7

Polyplexes of Polyethylenimine and Per-N-methylated Polyethylenimine – Cytotoxicity and Transfection Efficiency

Miriam Breunig[1], Uta Lungwitz[1], Juergen Klar[2], Armin Kurtz[2], Torsten Blunk[1], Achim Goepferich[1]

[1] Department of Pharmaceutical Technology, University of Regensburg, Universitaetsstrasse 31, 93040 Regensburg, Germany

[2] Department of Physiology, University of Regensburg, Universitaetsstrasse 31, 93040 Regensburg, Germany

Journal of Nanoscience and Nanotechnology 4 (2004), 512-520

Abstract

For non-viral gene delivery, the carriers for DNA transfer into cells must be vastly improved. The branched cationic polymer polyethylenimine has been described as an efficient gene carrier. However, polyethylenimine was demonstrated to mediate substantial cytotoxicity. Therefore, this study aimed at investigating per-N-methylated polyethylenimine, which is thought to have a much lower cytotoxicity due to its lower charge density. Results from a gel retardation assay and laser light scattering indicated that per-N-methylated polyethylenimine condenses DNA into small and compact nanoparticles with a mean diameter < 150 nm. Furthermore, polyplexes of polyethylenimine and per-N-methylated polyethylenimine with DNA had a positive zeta potential and the polymers protected DNA from nuclease-mediated digestion. The transfection efficiency of polyethylenimine and per-N-methylated polyethylenimine was tested in CHO-K1 cells. Using green fluorescent protein as reporter gene and flow cytometry analysis, we demonstrated that per-N-methylated polyethylenimine has a lower cytotoxicity, but also a significantly lower transfection efficiency. Using propidium iodide staining, we could additionally distinguish between viable and dead cells. At NP≥12, per-N-methylated polyethylenimine showed a much higher cell viability and the ratio of viable *and* transfected cells to dead *and* transfected cells was about 1.5 to 1.7 fold higher than for polyethylenimine. The results of cell viability from flow cytometry analysis were confirmed by the MTS assay. Using luciferase reporter gene for transfection experiments, the gene expression of per-N-methylated polyethylenimine was lower at NP 6, 12 and 18 as compared to polyethylenimine, but at NP 24 it yielded similar levels.

Introduction

In recent years, gene therapy research has become a scientific discipline with great potential for the treatment of genetic and acquired diseases, including cystic fibrosis and some cardiovascular disorders [1,2]. The basic principle of gene therapy is to deliver genetic material (DNA or RNA) to cells either to stimulate the production of lacking gene products or to turn off certain genes encoding undesirable proteins [3].

So far, viral vectors based on adenoviruses and retroviruses have been the most popular vehicles for gene transport. They have several great advantages, such as the ability to transfect cells of specific tissues and to enter cells easily and are also able to prompt the transcription machinery to produce the desired gene products. However, the safety concerns with such viral vectors are significant, as they can trigger immunogenic responses and insertional mutagenesis. In one gene therapy clinical trial, a patient died due to a severe immune response to the virus [4]. In another trial with modified retroviruses as shuttles for genes, one person developed cancer caused by the insertion of foreign DNA into his genome [5]. Therefore, non-viral delivery systems, even if they have lower transfection efficiencies, should be considered to circumvent these risks.

One non-viral gene delivery strategy involves the use of cationic polymers that can assemble with negatively charged DNA into nanoparticles. Polyethylenimine (PEI) is one of the most promising polycations currently available for non-viral gene delivery in vivo and in vitro. PEI complexes with negatively charged DNA via an electrostatic interaction into polyplexes with a mean diameter less than 150 nm [6]. The positive net charge of the complexes, arising due to an excess of polymer, allows them to bind to polyanionic components of the cell membrane, which leads to endocytosis of the nanoparticles [7]. Due to the fact that PEI is only partially protonated at physiological pH, the accumulation of polyplexes in endosomes and the subsequent degradation in endolysosomes can be avoided. The ´proton sponge mechanism´ hypothesis [8] suggests that PEI will buffer the internal pH in early and late endosomes [9]. The protonation most likely triggers a passive chloride influx, which causes osmotic swelling with subsequent endosome rupture, releasing the polyplexes into the cytoplasm. After nuclear entry of the DNA-polymer nanoparticles, the final step in this process is the transcription of the delivered gene and production of the desired gene product. Transcription efficiencies of branched PEI with a molecular weight of 25 kDa have been reported to be 10 to 20% [10].

Despite its excellent properties, however, PEI is not the ideal transfection agent. Due to its high cytotoxicity, host cell viability is strongly reduced. Both membrane permeabilization, a consequence of the high charge density, and the complexation of cellular DNA to excess polymer contribute to this cytotoxicity [10,11]. Therefore, it would be desirable to develop alternative polymers with both lower cytotoxicity and comparable transfection efficiency.
One approach to decrease the cytotoxicity of PEI is to reduce its cationic charge density. Aliphatic amines entail increasing basicity, or charge density, as follows: primary < tertiary < secondary amines (1^0, 3^0 and 2^0). Branched PEI (Figure 1, top) with a molecular weight of 25 kDa consists of 1^0, 2^0 and 3^0 amines [12]. In order to alter the charge density, we synthesized per-N-methylated polyethylenimine (mPEI, Figure 1, bottom) [13], a polycationic polymer in which all 1^0 and 2^0 amino groups of PEI are converted to 3^0 amino groups.

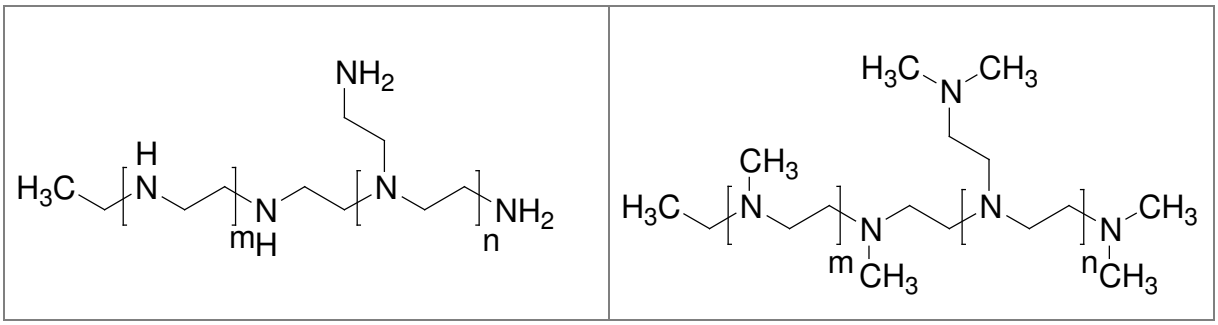

Figure 1: Structure of PEI (left) and mPEI (right).

Testing mPEI´s ability to build nanoparticles for gene delivery, we investigated its DNA complexation capacity and transfection in vitro. Our main goal was to compare the cytotoxicity of PEI and its methylated form mPEI. Further, we examined the transfection efficiency of both non-viral gene carriers with special interest in the host cell viability following transfection.

Materials and Methods

Materials

Branched PEI (M_W = 25 kDa) was used as obtained from Sigma-Aldrich (Taufkirchen, Germany). mPEI was prepared by complete reductive methylation of branched PEI (Eschweiler-Clark reaction) [13]. Spectra/Por® Biotech Membranes with a molecular weight cutoff (MWCO) of 8.000 Da were from Kleinfeld Labortechnik (Gehrden, Germany). Nutrient Mixture F-12 [Ham] (Ham´s F-12), DNase I, ethidium bromide (EtBr), propidium iodide, ampicillin and kanamycin were all purchased from Sigma-Aldrich (Taufkirchen,

Germany). pGL3-Enhancer vector, Luciferase Assay System, E. coli JM109 and CellTiter 96® AQ_{ueous} One Solution Cell Proliferation Assay were commercially obtained from Promega (Mannheim, Germany). pEGFP-N1 was from Clontech (Heidelberg, Germany). For transfection and cytotoxicity experiments, CHO-K1 cells (ATCC No. CCL-61) were used. Qiagen Plasmid Maxi Kit was from Qiagen (Hilden, Germany). Fetal bovine serum (FBS) was supplied by Biochrom KG seromed (Berlin, Germany). Agarose, PBS and LB broth medium were purchased from Invitrogen GmbH (Karlsruhe, Germany). Serva Blue G 250 was from Serva Electrophoresis GmbH (Heidelberg, Germany). 0.2 µm membrane filters were obtained from Corning GmbH (Wiesbaden, Germany). All other solvents and chemicals were purchased in analytical grade from Sigma-Aldrich (Taufkirchen, Germany).

Cell culture

CHO-K1 cells were grown in 75 ml culture flasks containing 10 ml Ham´s F-12 supplemented with 10% FBS in a 5% CO_2 atmosphere at 37°C as adherent culture to 90% confluency before seeding. Culture medium (Ham´s F-12 supplemented with FBS) was changed every 3 days and cells were passaged roughly once a week.

Non-viral carriers

PEI was used without further purification, while mPEI was dialyzed against ddH_2O using Spectra/Por® Biotech Membranes with a MWCO of 8 kDa. Both polymer stock solutions were prepared with 150 mM NaCl at a concentration, such that 1 µl would contain as much nitrogens as 2 µg plasmid DNA would have phosphates (NP ratio = 1, where NP indicates the ratio of the number of nitrogens in polymer to the number of phosphates in DNA). The pH of PEI and mPEI solution was adjusted to 7 and then the solutions were filtered through a 0.2 µm filter.

Amplification and purification of plasmid DNA

Plasmids encoding firefly luciferase (pGL3-enhancer vector) and GFP (pEGFP-N1) were used as reporter genes in this study. The plasmids were transformed into E. coli JM109 bacterial strain. The transformed cells were expanded in LB broth medium supplemented with either ampicillin for pGL3-enhancer vector or kanamycin for pEGFP-N1. Plasmids were isolated by using a Qiagen Plasmid Maxi Kit according to the supplier´s protocol. The concentration and purity of the DNA were measured by UV absorption at 260 and 280 nm.

Gel retardation assay

For evaluating the polymers´ complexation capacity, polyplexes were prepared at various NP ratios ranging from 0 to 5 in 150 mM NaCl by adding polymer solution to 1 µg reporter plasmid and incubated for 20 minutes at room temperature. The samples were loaded onto a 0.8% agarose gel in Tris-borate buffer and run at 80 V for 1.5 h. DNA was visualized with EtBr staining on a UV transilluminator.

Size and zeta potential measurements

The effective hydrodynamic diameter, polydispersity indices and zeta potential of DNA-polymer complexes were determined by using a Malvern ZetaSizer (Model 3000 HSA, Malvern Instruments GmbH, Germany). Samples were prepared at various NP ratios as follows: 10 µg plasmid DNA and the appropriate amount of polymer were each diluted in 250 µl of 50 mM NaCl / 3.3% glucose or 150 mM NaCl and mixed by vortexing. The complexes were allowed to form for 20 minutes at room temperature. After the polyplex solution was diluted to a final volume of 2 ml with ddH_2O, laser light scattering analyses were performed at 25°C with an incident laser beam of 633 nm at a scattering angle of 90°. The zeta potential of the polyplex solution was determined by measuring the electrophoretic mobility. The polyplex building and measurements were reproduced in triplicate.

DNase I digestion

The reaction compound consisted of either naked DNA or polyplexes at a NP ratio of 10, digestion buffer pH 8 (20 mM $MgSO_4$) and DNase I solution. After 3 minutes at room temperature the digestion was halted by the addition of stop solution (0.2 M EDTA, 0.7 N NaOH) [14]. The integrity of the plasmid was examined by loading the samples on a 1% alkaline agarose gel containing EtBr. The gels were run at 60 V for 1 hour.

Transfection experiments

For gene transfer studies CHO-K1 cells were grown in 24-well plates at an initial density of 40.000 cells per well. 20 hours after plating, the culture medium was replaced with 900 µl of serum-free medium. Polyplexes were prepared by mixing 50 µl of DNA (0.4 µg/µl pEGFP-N1 or pGL3-enhancer vector) and 50 µl of polymer solution. Plasmid DNA and polymer were each diluted in 150 mM NaCl unless otherwise indicated. The solutions containing the polyplexes were incubated for 20 minutes at room temperature and then added to the cells.

After 4 hours, the transfection medium (serum-free medium containing polyplexes that were not taken up by cells) was replaced with 1 ml of culture medium.

48 hours later, cells transfected with pEGFP-N1 were prepared for FACS (fluorescence activated cell sorting) analysis. Floating cells were collected and combined with trypsinized, adherent cells. The pooled cells were washed twice with 1 ml PBS, resuspended in 500 µl PBS and propidium iodide was added at a concentration of 1 µg/ml. Measurements were taken on a FACSCalibur (Becton Dickinson, Germany) using CellQuest Pro software (Becton Dickinson, Germany) and WinMDI 2.8 (©1993-2000 Joseph Trotter). GFP positive cells were detected using a 530/30 nm bandpass filter, whereas the propidium iodide emission was measured with a 670 nm longpass filter. Logarithmic amplification of GFP and propidium iodide emission in green and red fluorescence was obtained with 20.000 cells counted for each sample. Two-parameter dot plots of GFP versus propidium iodide were used to analyse the measurements (Figure 2). The GFP positive region was drawn starting above cell autofluorescence, where GFP positive cells were < 0.2%. Dot plots were thereby divided in four quadrants: For evaluating transfected *and* viable cells, respectively transfection efficiency, cells in the upper left (UL) quadrant were determined. Transfected *and* dead cells were assesed counting events in the upper right quadrant (UR), viable cells were determined by the number of propidium iodide negative cells in the upper left *and* lower left quadrants (UL, LL).

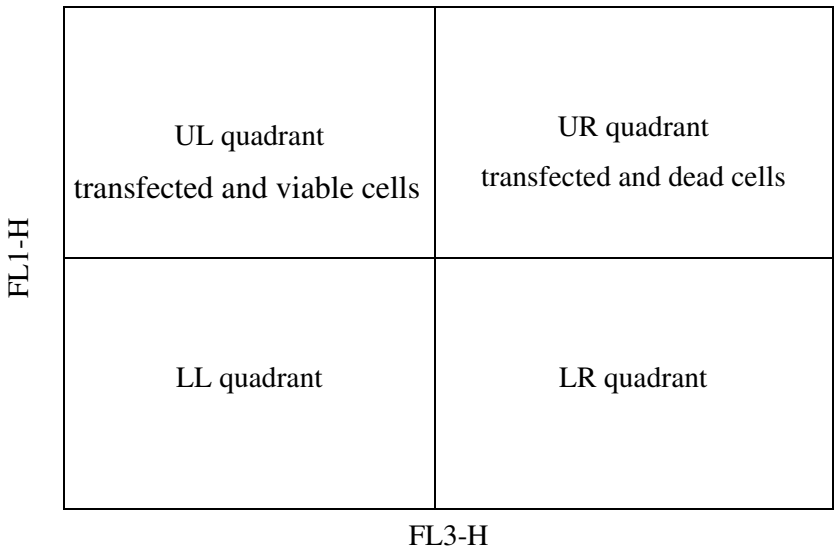

Figure 2: FACS analysis: FL3-H assessed at 670 nm represents viability, FL1-H indicates GFP fluorescence intensity at 530 nm. Transfected and *viable cells appear in the upper left (UL) quadrant, whereas transfected and dead cells appear in the upper right (UR) quadrant. Viable cells are determined by the number of propidium iodide negative cells in the upper left (UL)* and *lower left (LL) quadrants. Dead and non-transfected cells are shown in the lower right (LR) quadrant.*

Cells transfected with pGL3-enhancer vector were lysed and analysed for luciferase activity by photon counting (Lumat LB 9507, Berthold, Germany) by using the Luciferase Assay System kit according to the supplier´s protocol. Total protein content was determined by Bradford assay [15]. Results were expressed as relative light units (RLU) per mg of protein.

Cell viability

Cell viability was evaluated using the CellTiter 96® AQ_{ueous} One Solution Cell Proliferation Assay. Cells were seeded into 96-well plates at a density of 7.000 cells per well. 20 hours after seeding, polymer or prepared polyplexes (the amount of plasmid DNA was adjusted to the concentration of transfection experiments) diluted in 100 µl of serum-free medium were added to the cells, followed by incubation for 4 hours. The medium was then removed and replaced with culture medium. Cells were further incubated for 24 hours. Thereafter, 20 µl of Cell Titer 96® AQ_{ueous} One Solution containing the tetrazolium compound MTS [3-(4,5-dimethylthiazol-2-yl)-5-(3-carboxymethoxyphenyl)-2-(4-sulfophenyl)-2H-tetrazolium-inner salt] was added into each well [16,17]. After 3 hours at 37°C in a humified 5% CO_2 atmosphere the amount of soluble formazan produced by cellular reduction of MTS was quantified by recording the absorption at 490 nm (Microplate Reader, ICN-Flow, Bartolomey Labortechnik, Germany). The relative cell viability was calculated according the following equation:

Cell viability [%] = (OD_{490} sample / OD_{490} control) x 100.

OD_{490} sample represents the wells treated with polymer or polyplexes and OD_{490} control is the measurement from wells treated with culture medium only.

Statistics

Statistical significance was assessed by one-way analysis of variance (ANOVA) followed by Tukey´s post-hoc test. Significance level was set as indicated.

Results and discussion

Gel retardation assay

The capacity of PEI and mPEI to form complexes with plasmid DNA was examined in a gel retardation assay with EtBr as a probe. This assay is a first indicator for the appropriate nanoparticle composition and the NP ratio at which polyplex building occurs. The interaction of the cationic polymer and negatively charged DNA was determined by retardation of the

electrophoretic mobility of DNA and finally at a polymer excess by displacement of the intercalated dye EtBr from the double helix accompanied by a quenching of EtBr fluorescene. Figure 3 illustrates a typical result of a gel retardation assay for PEI (top) and mPEI (bottom).

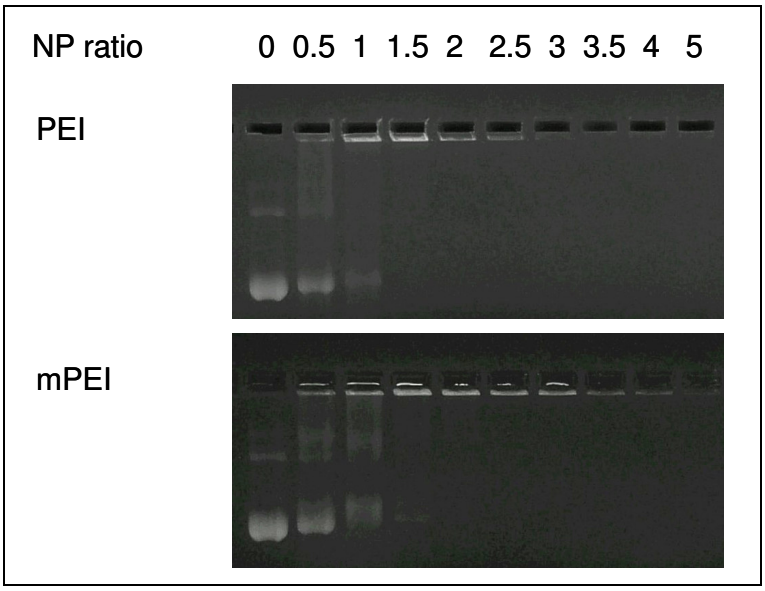

Figure 3: Plasmid DNA complexation capacity of PEI (top) and mPEI (bottom) at different NP ratios examined in a gel retardation assay. For each sample, 1 µg DNA was used and illuminated by ethidium bromide staining.

Uncomplexed DNA (denoted by NP 0 in Figure 3) migrated normally into the gel, while increasing amounts of polycationic PEI and mPEI retarded movement of the DNA through the gel as a consequence of partial neutralization. Figure 3 also shows that PEI-DNA nanoparticles are neutral at NP 2 – 2.5, as DNA did not migrate in the electric field, whereas nanoparticles with mPEI are neutralized at NP 2.5. Further increase of polymer concentration reduced the intensity of EtBr fluorescence reflecting the formation of compact nanoparticles. When PEI was used as the complexing polycation, no DNA was visible at NP 3.5; polyplexes of mPEI and plasmid DNA completely quenched EtBr fluorescence first at NP 5. These results indicate that both polymers allow a sufficient plasmid DNA complexation and that mPEI due to its lower charge density, respectively less nitrogens protonated at pH 7, forms compact nanoparticles at higher NP ratios (NP ≥ 5) than PEI (NP ≥ 3.5).

Size and zeta potential measurements

The hydrodynamic diameter of nanoparticles to be ingested by cells via endocytotic vesicles should be smaller than 150 nm [18]. Therefore, it was important to verify, whether the

reduction of cationic charge density by methylation of PEI still allowed for the formation of small nanoparticles.

The mean diameter of the polyplexes was dependent on the polymer, NP ratio and the ionic strength of the medium. When PEI was used as a nanoparticle forming agent, polyplexes built in 50 mM NaCl / 3.3% glucose were smaller than 150 nm in mean diameter at NP ratios ranging from NP 6 to 20 (Figure 4). Increasing amounts of PEI (NP ≥ 10) additionally reduced the size of the polyplexes from 150 to 100 nm. Generally, as Figure 4 shows, mPEI forms larger nanoparticles, especially at a NP ratio of 6, although at higher NP ratios (NP ≥ 8), mPEI can condense plasmid DNA into polyplexes with a mean diameter ranging from 120 – 140 nm. Laser light scattering analysis also measures a polydispersity index (PI) ranging from 0 up to 1.0 for determining the homogeneity of the size distribution. A PI of 0 denotes a completely monomodal size distribution, an inhomogenous sample with a wide distribution of nanoparticles is indicated by a PI of 1.0. With the exception of NP 6, PIs of polyplexes formed with mPEI have a lower value than the ones with PEI suggesting a narrower size distribution.

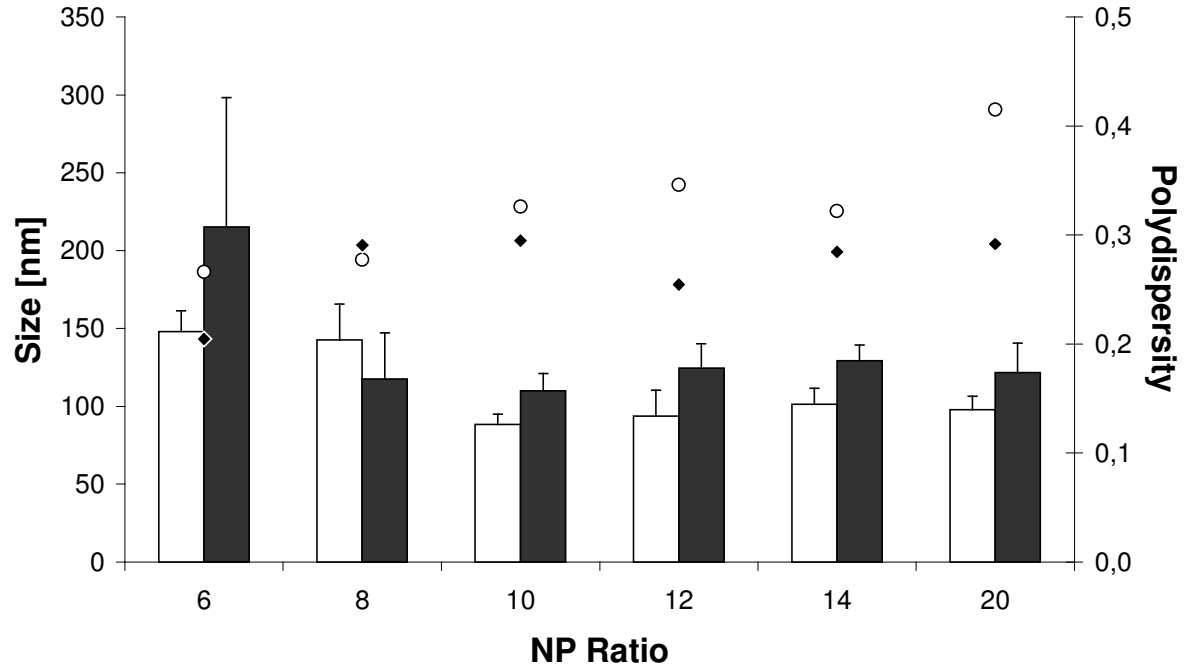

Figure 4: Effective size and polydispersity (PI) of DNA–polymer complexes formed with PEI (□ size, ○ PI) or mPEI (■ size, ◆ PI) and 10 µg plasmid DNA at various NP ratios in 50 mM NaCl / 3.3% glucose. Values are means ± SD of three independent experiments.

Investigating the influence of increasing the ionic strength of the complex formation medium, nanoparticles were produced in the same way with 150 mM NaCl instead of 50 mM NaCl / 3.3% glucose. At low NP ratios (6, 8 and 10), polyplexes with PEI and mPEI formed in 150

mM NaCl were about 50 – 100 nm larger than those formed in 50 mM NaCl / 3.3% glucose, whereas at NP ≥ 12, the higher ionic strength only increased the mean diameter about 10 – 20 nm (data not shown). Hypothetically, nanoparticles built in 50 mM NaCl / 3.3% glucose are more compact and smaller, because there are fewer free ions in solution that can interact in complex formation. Both types of polyplexes were subjected to transfection experiments (see 3.4).

Collectively, the data show that polyplexes formed with PEI and mPEI fulfill the requirement of building nanoparticles smaller than 150 nm. PEI, as compared with mPEI, forms smaller polyplexes, but in contrast the PIs of polyplexes with mPEI are lower. Despite less protonated nitrogens participating in polyplex building, mPEI allows formation of small nanoparticles.

In order to induce a successful association with the negatively charged plasma membrane and to avoid aggregation, the surface charge of polyplexes, or the zeta potential, should be positive.

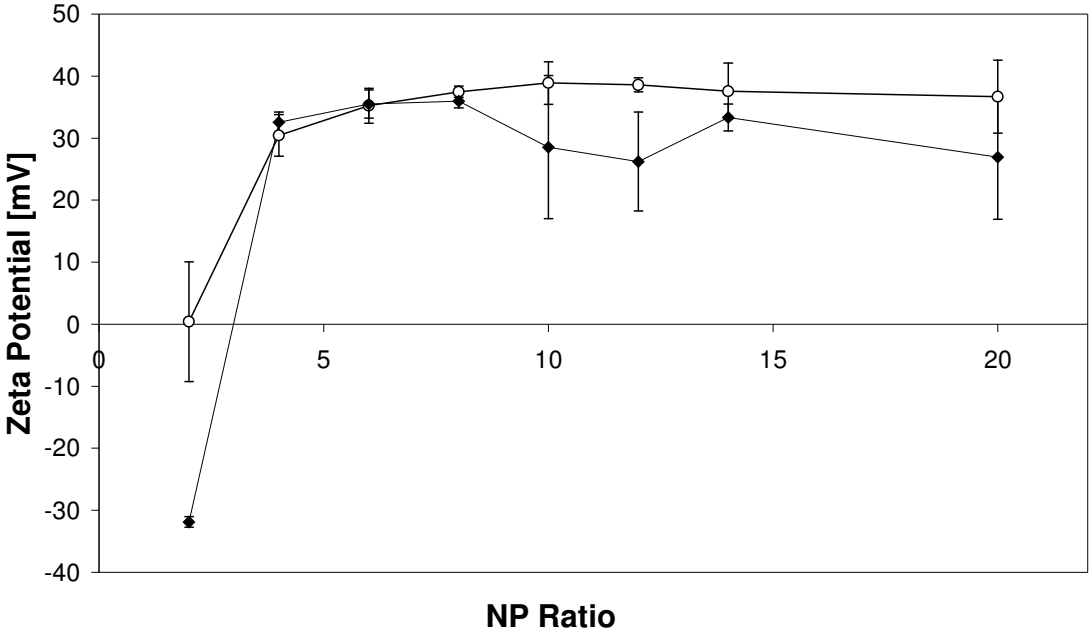

Figure 5: Zeta potential of DNA-polymer complexes formed with PEI (○) or mPEI (◆) and 10 µg plasmid DNA at various NP ratios in 50 mM NaCl / 3.3% glucose. Values are means ± SD of three independent experiments. Zeta potential of PEI-polyplexes is significantly different from mPEI-polyplexes at NP 2 ($\alpha < 0.01$).

Figure 5 shows that polyplexes of PEI are neutral at NP 2, while mPEI forms neutral polyplexes at NP 3. Hence, results of the zeta potential measurement confirmed the gel retardation assay: due to its lower basicity, mPEI is first capable of building polyplexes at higher NP ratios. With an increasing amount of polymer, the zeta potential yielded up to 30 –

40 mV. At NP ratios > 8, the values for the zeta potential of PEI-plasmid DNA plateaued; the surface charge of mPEI-DNA polyplexes slightly decreased, but the differences between the two were not considerable. Zeta potential of PEI-polyplexes is only significantly different from mPEI-polyplexes at NP 2 ($\alpha < 0.01$). To summarize, the zeta potential of PEI and mPEI polyplexes should not result in different interactions with cells.

DNase I digestion

In non-viral gene delivery, the cationic polymers not only act as a gene carrier, but they also protect plasmid DNA from degradation [14,19]. To evaluate the accessibility of the plasmid DNA to nuclease-mediated hydrolysis, complexes were exposed to DNase I [20]. Digestion was stopped by addition of an alkaline buffer that also separated the polymer-DNA nanoparticles as a consequence of deprotonation of the polymer.

Both naked DNA and DNA-polymer complexes were subjected to digestion reaction to compare stability with and without polymer. For negative control, polyplexes and DNA were used and treated in the same procedure as samples but without any enzyme units (Figure 6, lanes denoted with 1). As expected, DNA remained intact. Applying 5 enzyme units (Figure 6, lanes indicated by 2), naked DNA was digested completely, whereas DNA protected with PEI was intact. Under the same conditions, DNA complexed with mPEI was slightly degraded, as indicated by a dimmer EtBr fluorescence. Serial dilution of the enzyme was made. With 2.5 enzyme units (Figure 6, lane 3), naked DNA was still completely degraded, but DNA protected with PEI and mPEI remained intact in the same quality. Figure 6, lane 5 illustrates the samples digested with 0.005 enzyme units. At this enzyme concentration, naked DNA survived the digestion reaction.

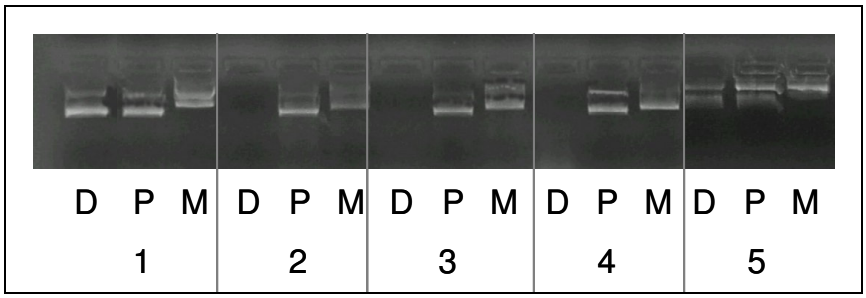

Figure 6: DNase I digestion of plasmid DNA (D) and plasmid DNA-polymer complexes illuminated by ethidium bromide staining, P indicates polyplexes formed with PEI, M indicates polyplexes formed with mPEI. The numbers denote enzyme units (U) as follows: 1 = 0 U, 2 = 5 U, 3 = 2.5 U, 4 = 1.25 U, 5 = 0.005 U.

Both PEI and mPEI are able to protect DNA from nucleases-mediated digestion, but PEI-polyplexes have a better stability to higher DNase I concentrations. Whether this difference has an effect on polyplex stability in cells is difficult to assess, due to the fact that the physiological concentration of nucleases is not known.

Transfection experiments

The in vitro transfection ability of the non-viral gene carriers PEI and mPEI was compared in CHO-K1 cells with both pEGFP-N1 encoding green fluorescent protein (GFP) and pGL3-Enhancer vector encoding firefly luciferase. For transfection experiments, NP ratios ≥ 6 were selected due to the fact that small polyplexes with a positive zeta potential are formed and because ratios ranging from 4.5 to 135 have been reported [8] previously.

The measurement of the efficiency of pEGFP-N1 delivery utilized a versatile and quantitative flow cytometry method that simultaneously elucidates the cellular state of transfected and non-transfected cells. This method combines two color fluorescence analysis of GFP and propidium iodide in one experiment. The DNA intercalator propidium iodide was used to assess plasma membrane integrity and has been established in flow cytometry for the staining of dead cells.

CHO-K1 cells were transfected with polymer-plasmid DNA nanoparticles formed at NP ratios of 6, 12, 18 and 24. Figure 7 illustrates that the transfection efficiency, i.e. the percentage of viable and transfected cells, of PEI yielded up from 9% (NP 6) to 18% at NP 12, followed by a decrease to 9% at NP 24 due to its high cytotoxicity. In contrast, mPEI showed minimal transfection ability at a NP ratio of 6. With an increasing amount of polymer, the transfection efficiency yielded up to 2.5 - 3% (NP 18). A further increase of mPEI (NP 24) did not augment the transfected *and* viable cells. Transfection efficiencies of the non-viral carrier PEI were significantly ($\alpha < 0.01$) higher than efficiencies of mPEI.

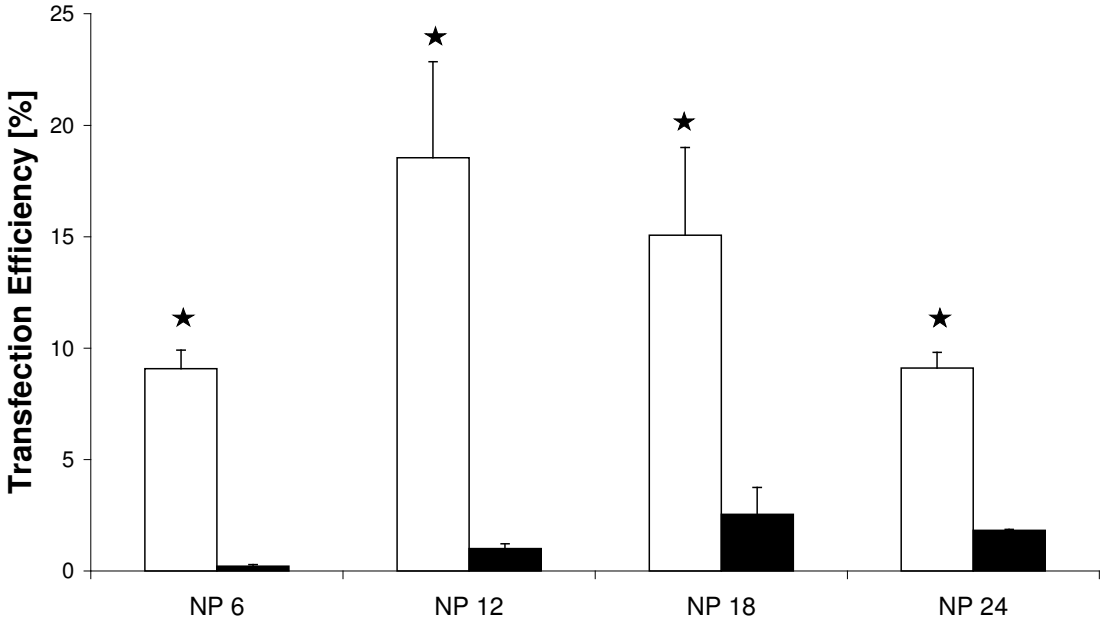

Figure 7: Transfection efficiency of the non-viral carriers PEI (□) and mPEI (■) with 2 µg pEGFP-N1 as reporter gene. Values represent the GFP positive and viable cells as means ± SD of one representative experiment (n=3). Transfection efficiencies of PEI are significantly different from mPEI, denoted by ★ ($\alpha < 0.01$).

Having a closer look to the cellular state of the transfected cells, the ratio of viable *and* transfected cells (UL quadrant) to dead *and* transfected cells (UR quadrant) was determined. For PEI and mPEI at NP 6 a ratio of 6.8 and 6.5 (Tab. 1) was obtained.

Table 1: Ratio of viable and *transfected cells (UL quadrant) to dead* and *transfected cells (UR quadrant) of the non-viral carriers PEI and mPEI assessed by flow cytometry technique with GFP as reporter gene and propidium iodide staining. Values are indicated as means ± SD of one representative experiment (n=3).*

NP	Ratio of viable *and* transfected cells to dead *and* transfected cells	
	PEI	mPEI
6	6.8 ± 0.8	6.5 ±0.8
12	4.1 ± 1.4	6.2 ± 0.3
18	2.7 ± 0.1	4.3 ± 0.6
24	2.3 ± 0.7	3.9 ± 0.4

With increasing amounts of polymer, the ratio of viable *and* transfected cells to dead *and* transfected cells decreased due to the cytotoxicity, whereas values for mPEI were 1.5 to 1.7 fold higher than for PEI. Higher ratios, i.e. more transfected *and* viable cells, for mPEI were

obtained as consequence of its lower cytotoxicity (see 3.5). The transfection efficiency of the smaller-sized polyplexes formed in reduced ionic strength medium (50 mM NaCl / 3.3% glucose) was also evaluated in CHO-K1 cells. mPEI showed a slight increase in transfection efficiency at NP 6, 12 (significantly different from polyplexes in 150 mM NaCl, $\alpha < 0.05$) and 18 of ca. 0.5 – 1.0% (data not shown) accompanied by a loss in cell viability. Polyplexes produced in 50 mM NaCl / 3.3% glucose with PEI achieved a larger number of transfected cells at NP 6 (ca. 2% higher than in 150 mM NaCl), but at higher NP ratios a decrease in transfection efficiency was observed (data not shown). As mentioned before, nanoparticles formed in 50 mM NaCl / 3.3% glucose could be more stable due to less free ions that can interact in complex formation. This stability could be responsible for higher transfection efficiencies. Interestingly, higher transfection efficiencies of the smaller nanoparticles resulted in an increased cytotoxicity with both polymers (see 3.5).

In conclusion, using pEGFP-N1 as a reporter gene, the non-viral carrier PEI shows a significantly higher transfection efficiency than mPEI at NP 6, 12, 18 and 24.

Luciferase reporter gene expression (Figure 8) confirmed the trends seen with the cationic carrier PEI when using GFP as a reporter gene: the number of RLU / mg of protein could be augmented from NP 6 to NP 12 and then decreased. With mPEI, the gene expression could be increased from NP 6 to NP 24.

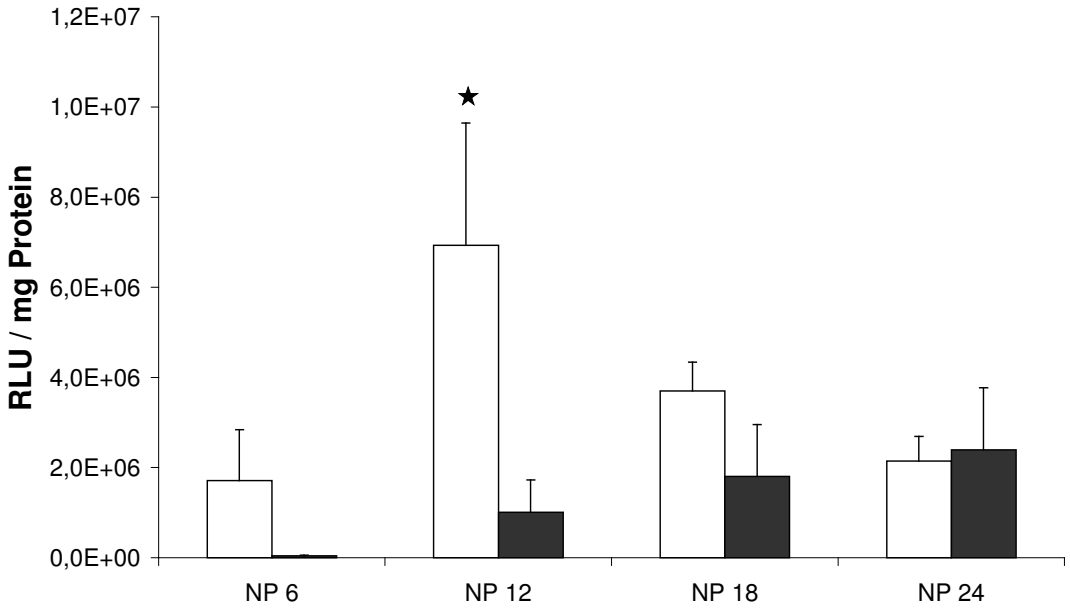

Figure 8: Luciferase reporter gene expression of the cationic carriers PEI (□) and mPEI (■) expressed as relative light units (RLU) / mg of protein. Values are means ± SD of one representative experiment (n=4). Gene expression of PEI at NP 12 is significantly different from mPEI, denoted by ★ ($\alpha < 0.01$).

In contrast to the transfection efficiency with pEGFP-N1 as reporter gene, as Figure 8 illustrates, gene expression with PEI and mPEI had nearly the same extent at NP 24. At NP 12 RLU / mg of protein of PEI-DNA complexes were significantly different from mPEI nanoparticles. These results should be considered with regard to the fact that only adherent, respectively viable cells, were analysed.

To summarize, evaluating transfection efficiency flow cytometry can be considered as more presice method.

Cell viability

Cell viability of CHO-K1 cells after treatment with DNA-polymer nanoparticles or free polymer was measured by the MTS assay. Free and complexed polymer were tested for tagging of which component contributes more to cytotoxicity.

The cytotoxicities of polyplexes formed with PEI and mPEI are presented in Figure 9. It is shown that neither type of polyplex displayed significant cytotoxicity at NP 6. Higher NP ratios of mPEI-complexes did not influence cell viability, whereas cytotoxicity increased with PEI proportion in polyplexes. The number of viable cells after treatment with DNA-PEI nanoparticles decreased to 70% at NP 24. The relative viability of cells transfected with PEI compared with mPEI was significantly lower ($\alpha < 0.01$) at NP 12, 18 and 24.

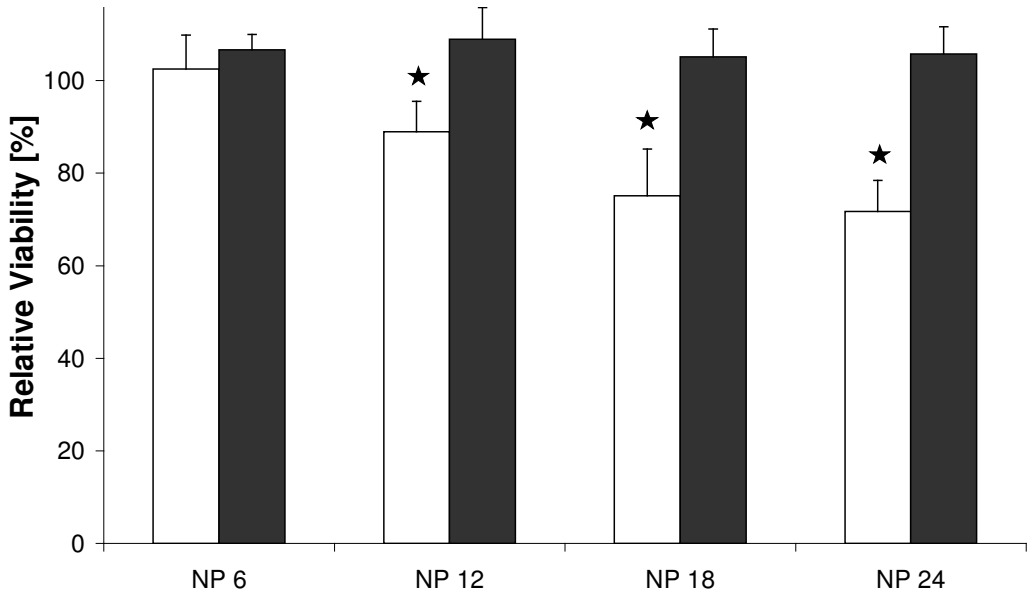

Figure 9: Relative Viability of CHO-K1 cells after treatment with DNA-PEI (□) or –mPEI (■) complexes at various NP ratios determined with the MTS assay. Values are means ± SD of one representative experiment (n=4). Relative viability of cells transfected with PEI is significantly different from mPEI at NP 12, 18 and 24, denoted by ★ ($\alpha < 0.01$).

With propidium iodide staining, we had the tool to determine the number of viable cells at the time point of flow cytometry analysis (UL *and* LL quadrants) and were also able to compare these results with data from the cell viability assay. Regarding polyplexes built in 150 mM NaCl, DNA-PEI nanoparticles reduced the fraction of viable cells from 90% at NP 6 to 60% (NP 24). In contrast, the values of viable cells after treatment with mPEI-plasmid DNA nanoparticles were without exception higher than after incubation with PEI nanoparticles (Figure 10). The number of viable cells was determined to be over 90% at NP 6 and decreased to about 80% at NP 24.

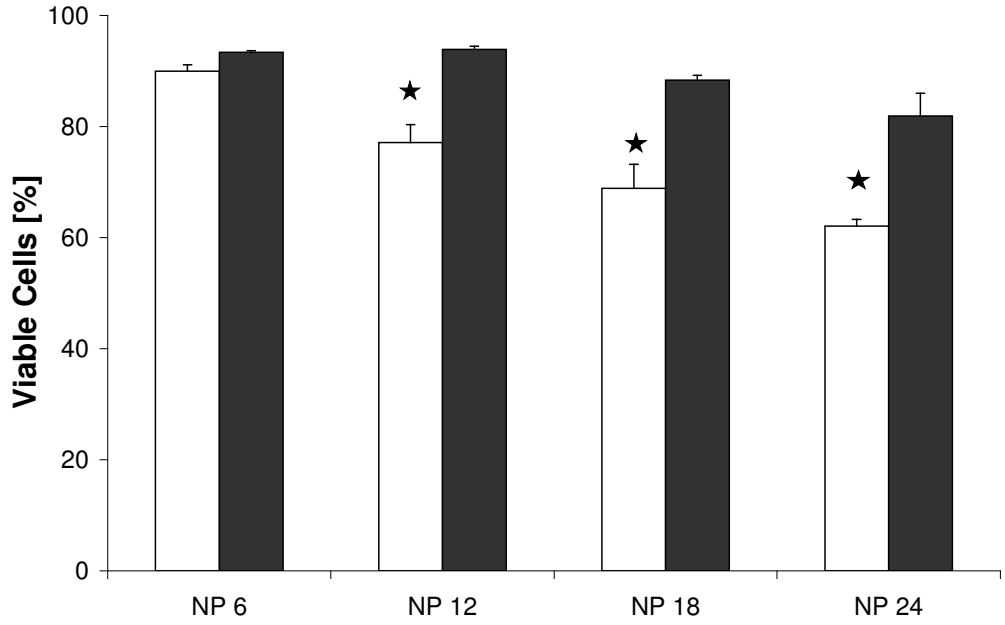

Figure 10: Viable, i.e. propidium iodide negative cell population, 48 hours post transfection with PEI (□) and mPEI (■), as assessed by flow cytometry. Propidium iodide staining is immediate in dead cells due to the loss of their membrane integrity, while live cells remain unstained. Viability of cells transfected with PEI is significantly different from mPEI at NP 12, 18 and 24, as denoted by ★ ($\alpha < 0.01$).

To summarize, the number of viable cells transfected with PEI was significantly ($\alpha < 0.01$) lower than transfected with mPEI at NP ratios of 12, 18 and 24. In comparison to polyplexes formed in 150 mM NaCl analysis of cells transfected with nanoparticles formed in 50 mM NaCl / 3.3% glucose showed a tremendous increase in cytotoxicity (data not shown). In contrast to FACS analysis, the results for the cell viability of the MTS assay were about 10% higher. The reason is that both methods have a different principle: in FACS analysis, changes in cell granularity and perforation of cell membranes are considered, whereas the MTS assay evaluates the metabolic activity. The membrane of a cell can be lysed or there can be changes

in granularity and the cell will still be metabolically active. Despite of these differences, both methods demonstrate the same trend for cell viability.

Figure 11 illustrates the value for cytotoxicity of free polymer in culture medium. Free mPEI had less toxic effects on CHO-K1 cells than PEI.

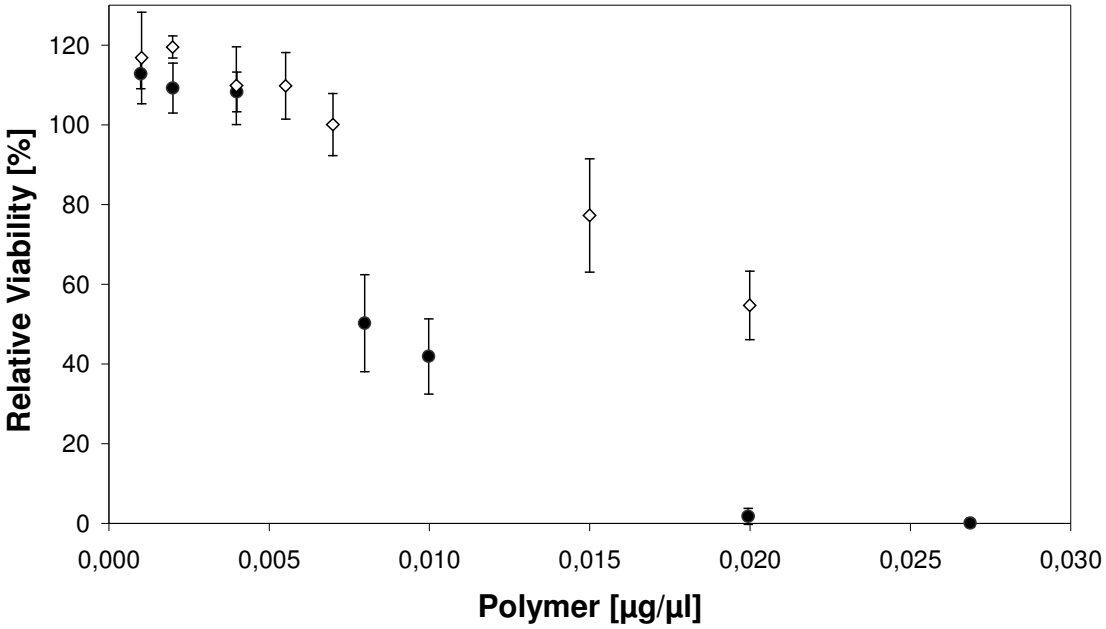

Figure 11: Relative viability as function of free PEI (●) and mPEI (◇) in culture medium. Values are means ± SD of one representative experiment (n=4).

Comparing free polymer and the same amount of polymer complexed with DNA, polymer solution displays higher values for cytotoxicity. These results are probably due to the fact that polyplex-building reduces the free function of polymer, i.e. polymer that can permeabilize cell membranes or complex cellular DNA.

Our hypothesis that mPEI is less toxic due to its lower charge density could be verified by these results.

Conclusions and Outlook

In this study we investigated the complexation capacity and transfection efficiency, with special regard to cell viability and cytotoxicity, of the cationic polymers PEI and mPEI.

Despite the reduction of the cationic charge density of PEI by methylation, and thus the presence of fewer protonated nitrogens to participate in complex formation, mPEI allowed for the building of small and compact polyplexes for non-viral gene delivery.

The results of the in vitro transfection experiments comparing the two cationic polymers were evaluated with special regard to cell viability. To summarize our results, PEI had a higher transfection efficiency than mPEI, but at NP 12, 18 and 24 the ratio of viable *and* transfected cells to dead *and* transfected cells was higher for mPEI. It can be concluded, that a higher transfection efficiency is accompanied by an increase in cytotoxicity. Transfection experiments with luciferase yielded better results for mPEI, but unfortunately this method of analysis provides no information about the cellular state.

mPEI displayed a lower cytotoxicity than PEI because of fewer nitrogens protonated at physiological pH that can permeabilize cell membranes. Our hypothesis of reducing the cyotoxicity by methylation of PEI could be confirmed.

The reason for mPEI´s lower transfection efficiency is unclear. Because the polyplex size is comparable to DNA-PEI nanoparticles, one possibility could be that mPEI is not able to buffer the pH in endosomes following by the escape of the polyplexes in cytoplasm.

For future experiments, there are different approaches possible to improve the properties of non-viral vectors for gene delivery. A better understanding in polyplex building, a process that has been poorly investigated so far, could help in the designing of novel polymers. The development of a biodegradable PEI may be one way to both maintain the transfection efficiency and also reduce the cytotoxicity. Polyamines, such as tetra-amine spermine and triamine spermidine, are naturally found in cells, thus, short fragments of PEI should display less cytotoxicity.

References

1. Ledley FD. Pharmaceutical approach to somatic gene therapy. Pharm Res 1996; 13: 1595-1614.

2. Ehsan A, Mann JM, Dzau VJ. Gene Therapy for Cardiovascular Disease and Vascular Grafts. In: Smyth Templeton N, Lasic DD, editors. Gene Therapy - Therapeutic Mechanism and Strategies. New York, Basel: Marcel Dekker, Inc., 2000: 421-438.

3. Akhtar S, Hughes MD, Khan A, Bibby M, Hussain M, Nawaz Q, Double J, Sayyed P. The delivery of antisense therapeutics. Adv Drug Deliv Rev 2000; 44: 3-21.

4. Ferber D. Gene therapy: Safer and virus-free? Science 2001; 294: 1638-1642.

5. Marshall E. What to Do When Clear Success Comes With an Unclear Risk? Science 2002; 298: 510-511.

6. Erbacher P, Remy JS, Behr JP. Gene transfer with synthetic virus-like particles via the integrin-mediated endocytosis pathway. Gene Ther 6: 138-145.

7. Labat-Moleur F, Steffan A-M, Brisson C, Perron H, Feugeas O, Furstenberger P, Oberling F, Brambilla E, Behr J-P. An electron microscopy study into the mechanism of gene transfer with lipopolyamines. Gene Ther 1996; 3: 1010-1017.

8. Boussif O, Lezoualc'h F, Zanta MA, Mergny MD, Scherman D, Demeneix B, Behr J. A versatile vector for gene and oligonucleotide transfer into cells in culture and in vivo: polyethylenimine. Proc Natl Acad Sci U S A 1995; 92: 7297-7301.

9. Alberts B, Bray D, Lewis J, et al. Molecular Biology of the Cell. Third Edition ed. New York & London: Garland Publishing, Inc., 1994, p.622.

10. Godbey WT, Wu KK, Mikos AG. Poly(ethylenimine)-mediated gene delivery affects endothelial cell function and viability. Biomaterials 2000; 22: 471-480.

11. Helander IM, Alakomi HL, Latva-Kala K, Koski P. Polyethyleneimine is an effective permeabilizer of Gram-negative bacteria. Microbiology (Reading, UK) 1997; 143: 3193-3199.

12. Godbey WT, Wu KK, Mikos AG. Poly(ethylenimine) and its role in gene delivery. J Control Release 2001; 60: 149-160.

13. Lungwitz U, Breunig M, Blunk T, Goepferch A. Synthesis of per-N-methylated polyethylenimine as a novel non-viral vector for gene delivery. Arch. Pharm. Pharm. Med. Chem. 335, Suppl. 1, 115: 2002.

14. Godbey WT, Barry MA, Saggau P, Wu KK, Mikos AG. Polyethylenimine-mediated transfection: a new paradigm for gene delivery. J Biomed Mater Res 2000; 51: 321-328.

15. Bradford MM. A rapid and sensitive method for the quantitation of microgram quantities of protein utilizing the principle of protein-dye binding. Anal Biochem 72: 248-254.

16. Mosmann T. Rapid colorimetric assay for cellular growth and survival: application to proliferation and cytotoxicity assays. J Immunol Methods 65: 55-63.

17. Cory AH, Owen TC, Barltrop JA, Cory JG. Use of an aqueous soluble tetrazolium/formazan assay for cell growth assays in culture. Cancer Commun 3: 207-212.

18. Alberts B, Bray D, Lewis J, et al. Molecular Biology of the Cell. Third Edition ed. New York & London: Garland Publishing, Inc., 1994, p. 618.

19. Barry ME, Pinto-Gonzalez D, Orson FM, McKenzie GJ, Petry GR, Barry MA. Role of endogenous endonucleases and tissue site in transfection and CpG-mediated immune activation after naked DNA injection. Human Gene Ther 1999; 10: 2461-2480.

20. Reitz M, Lober G, Kleemann P, Dick W. Secretion of neutral and acid DNases in cultivated human lymphocytes after incubation with DNA; possible consequences for inhalation anesthesia. Z Naturforsch [C] 50: 419-424.

Chapter 8

Summary and Conclusions

Summary

With recent advances in molecular biology and the sequencing of the human genome, nucleic acids are expected to engage a pivotal position in the development of novel therapeutic concepts. The basic principle of nucleic acid delivery is to influence cellular functions either to stimulate or turn off the production of certain proteins. Furthermore, nucleic acid delivery is also increasingly utilized in basic research in order to gain a more complete comprehension of distinct cellular functions. So far, there are two common approaches towards nucleic acid delivery: the transfer of the genetic information using viral vectors or non-viral methods, such as wrapping of DNA to synthetic gene vehicles and physical principles [1-5]. Although viral vectors are very effective and are capable of many of the required tasks for efficient gene transfer, their broad use is limited by severe safety risks [6,7]. Therefore, non-viral delivery systems such as lipids, polymers or gene gun and electroporation are gaining growing attention. This work focused on the use of polymers as vehicles for nucleic acid delivery.

Several important design criteria and characteristics towards effective polymer-based systems have been identified so far and, among various polymers, polyethylenimine (PEI) has become a gold standard for nucleic acid delivery [8]. The processing of DNA with the polymer to particles, the so-called polyplexes, their engulfment into cells and intracellular fate are being intensively investigated. Furthermore, the efficacy of polyplexes is being improved by exploiting particular cellular mechanisms and signal sequences are attached to polyplexes in order to steer them to certain intracellular organelles, especially the nucleus (Chapter 1). The relatively high transfection efficiency of branched PEI (BPEI) -based delivery systems is seriously afflicted by the cytotoxicity of the polymer. In contrast, the linear form (LPEI) has a particularly high gene expression accompanied by a lower cytotoxicity, but nevertheless the transfection efficiency of LPEI 22 kDa (ExGen®) cannot be enhanced beyond a certain limit due to cytotoxicity.

Towards the development of optimal non-viral transfer systems and before polymer-based delivery systems may come into clinics, fundamental questions concerning their efficacy, cytotoxicity and interaction with the environment have to be resolved. Therefore, the ultimate goal of this thesis was to identify strategies towards effective PEI-based delivery systems with low cytotoxicity for *in vitro* use.

The first objective was to overcome the frequent restriction that high transfection efficiency is limited by the cytotoxicity of the non-viral carrier. Therefore, we explored the potential of utilizing LPEIs with a molecular weight (MW) ranging from 1.0 to 9.5 kDa to overcome this limitation (Chapter 2). This study showed that the transfection efficiency of LPEI - polyplexes in CHO-K1 cells as a model cell line could be altered by varying the MW and the amount of polymer available for polyplex formation. It was striking that the transfection efficiency with certain low MW LPEI derivatives was much higher compared to the commercially available LPEI 22 kDa within the same test system: in addition, the maximal transfection efficiency of about 44%, obtained with LPEI 5.6 kDa at NP 18, was accompanied by minimal cytotoxicity. By using LPEI 5.0 kDa and smaller in polyplexes, the transfection efficiency could be increased without affecting the cell viability. Furthermore, we could show that a MW greater than 1.0 kDa is necessary for gene expression. As observed by confocal laser scanning microscopy (CLSM) and demonstrated by the addition of lysosomotropic agents, LPEI - polyplexes have an impressive endo-lysosomal escape capacity. Additionally, LPEIs may also help the plasmid DNA to overcome the nuclear membrane, thereby enhancing the gene transfer. This study envisioned the decoupling of transfection efficiency from cytotoxicity and demonstrated that LPEIs with low MW are more efficient and significantly less toxic than their high MW counterparts in CHO-K1 cells *in vitro*.

A follow-up study focused on the uptake and intracellular stability of various LPEI - polyplexes and plasmid DNA in order to investigate differences relevant for their efficacy. Furthermore, the influence of the ionic strength of the polyplex formation medium and presence of serum during the transfection process on the transfection efficiency was evaluated (Chapter 3). Generating the LPEI - polyplexes in 150 mM sodium chloride or 5% glucose produces either very large (>1 µm) or small (about 200 – 300 nm) polyplexes, respectively [9,10]. But once in contact with culture medium, the differences seemed to equalize. This means that the size of the resulting polyplexes is not susceptible to varying ionic strength in culture medium during the fabrication procedure. However, the transfection efficiency of LPEI 9.0 kDa, but not of derivatives with lower MW, was significantly influenced by the ionic strength: the fabrication of polyplexes in 5% glucose following transfection in serum-free culture conditions remarkably enhanced the transfection efficiency compared to other conditions tested. The reason for this phenomenon is unclear and has to be further elucidated, most likely the polyplex assembly may favor the superiority of these polyplexes.

The overall amount of polyplexes taken up by cells was slightly higher when polyplexes were built with LPEIs of 5.0 and 9.0 compared to 2.0 kDa, but independent of the polyplex

formation medium and the culture conditions during the transfection process. However, the higher number of intracellular polyplexes using LPEI 5.0 or 9.0 kDa as carrier systems did not entail a higher amount of plasmid DNA intracellularly available for transfection. Furthermore, we did not determine a correlation between the disintegration of polyplexes inside cells, the stability of plasmid DNA and the transfection efficiency. This means that we have a very robust system for LPEI-based nucleic acid delivery that is widely independent of external influences and suitable for routine transfection experiments. The high transfection efficiency of certain LPEI - polyplexes probably arises due to a balance of endo-lysosomal escape capacity, nuclear transport and cytotoxicity.

The application of fluorescence imaging technology has demonstrated the capability for real-time measurements in the field of non-viral gene delivery in order to investigate the interaction of polyplexes with their environment. However, due to the resolution limit of a light microscope, it remains possible that fluorescently labeled molecules observed are colocalized without being associated. Techniques such as fluorescence resonance energy transfer (FRET) provide the opportunity for a better resolution in the distance range of 1-10 nm [11,12]. Hence, we evaluated whether FRET is a valuable tool to determine the intracellular disintegration of double labeled LPEI - polyplexes in CHO-K1 cells by CLSM (Chapter 4). In microscopy, allowing for the evaluation of the distribution of FRET events whithin a single cell, two approaches have been tested towards quantitative FRET analysis, sensitized emmision measurement and acceptor photobleaching. Results from the acceptor photobleach method were not accurate due to movements of or in the sample during the imaging and bleaching process. Sensitized emission measurement using the method according to Xia et al. [13] worked quite well for the determination of interaction between LPEI and plasmid DNA. The results confirmed images recorded by conventional CLSM: A fraction of the intracellular polyplexes disintegrated, but at certain areas the contact between polymer and DNA was still very close. Furthermore, FRET occuring between a donor and an acceptor molecule of double labeled LPEI - polyplexes was also measured by flow cytometry. The advantage of the flow cytometry-based method is the analysis of a whole cell population. As indicated by a decrease in the donor quenching, the stability of intracellular polyplexes built with LPEI 5.0 kDa seemed to be enhanced with increasing NP ratio. In summary, the interaction of polymer and plasmid DNA in living cells have to be carefully addressed by FRET-based techniques because of movements of or in the sample during the imaging process. We suggest that FRET is a valuable tool in order to gain a deeper insight into LPEI-mediated gene transfer.

If polyplexes are applied once in vivo, the long-term fate of the polymeric carrier has to be considered in an organism. Therefore, high MW polymers that have superior properties to complex DNA and a stabilizing effect on polyplexes, but which can be easily degraded by the host, might help to overcome this obstacle. We hypothesized that a bioreversible crosslinking of low MW LPEIs would raise the polymer's efficacy due to the higher MW and hence transfection efficiency, while the biodegradable linkages would undergo intracellular breakdown and hence minimize toxicity. In detail, various biodegradable PEIs, namely LR-PEIs, were investigated concerning their transfection efficiency and cytotoxicity (Chapter 5). The biodegradable polymers had a different degree of branching and a slightly increasing MW with increasing linker/polymer proportion. LPEI 2.1 kDa was chosen as starting material for crosslinking because its polyplexes showed a minimal transfection efficiency and no cytotoxicty in a cell culture model (Chapter 2). We expected that crosslinking would lead to a transfection efficiency comparable to a LPEI derivative of the higher MW, but cytotxicity as low as for LPEI 2.1 kDa. Our results proved the hypothesis: the most effective LR-PEI was capable of gene delivery in 27-fold more cells than the non-degradable starting material and moreover, the maximum transfection efficiency achieved in CHO-K1 cells had a value of about 73%, which is much higher than that of the LPEI derivative of similar MW. These biodegradable PEIs can be counted among the most effective polymer-based gene delivery vehicles, because the efficacy was nearly 3-fold higher than with BPEI 25 kDa and LPEI 22 kDa, to which newly synthesized polymers are usually compared. LR-PEI-mediated gene delivery was dependent on intracellular reduction and could be modulated by manipulation of the number of stabilizing bonds. CLSM revealed a longer colocalization of biodegradable PEI- polyplexes with acidic organelles compared to LPEI - polyplexes. In summary, we identified biodegradable PEI-based polyplexes that are superior to existing polymer-based gene delivery systems.

After biodegradable PEI-based polyplexes had successfully been applied for the transfection of various cell lines *in vitro*, the next step was to evaluate their gene transfer ability in human primary cells and in a 'hard-to-transfect' cell line (Chapter 6). Primary cells should be more representative of the *in vivo* situation than transformed cell lines and would better predict limitations to gene transfer *in vivo*. We chose two different test systems, denritic cells (DCs) and chondrocytes. In contrast to cell lines that are permananetly dividing, DCs are terminally differentiated and non-dividing, while human chondrocytes still have the ability for proliferation, but their mitogenic activity is limited. In DCs the transfection efficiency was nearly negligible and also accompanied by a remarkable toxicity. According to confocal

images, the uptake of polyplexes seemed to be one of the limiting steps in the transfection process. Human chondrocytes were more susceptible to PEI-based transfection, but the efficacy was much lower compared to the cell lines tested in Chapter 5. In HT-29 cells, a 'hard-to-transfect' cell line, the gene transfer was as low as in DCs, the uptake besides other reasons such as nuclear entry, has been demonstrated to be a limiting step in the transfection process.

Last mentioned, we showed that the PEI backbone is a necessary prerequisite for efficient polymer-based gene delivery. The investigation of per-N-methylated PEI relvealed that the polymer is still capable of condensing plasmid DNA into polyplexes, but the resulting polyplexes lost their functionality in most instances (Chapter 7). This may be due to the fact that per-N-methylated PEI lost its most prominent feature: the high cationic charge density, which is postulated to be significantly responsible for efficient gene delivery [8].

Conclusions

In conclusion, this thesis successfully demonstrated strategies towards very efficient PEI-based nucleic acid delivery systems with low cytotoxicity. By comprehensively evaluating modifications in the structure of existing PEI derivatives it was possible to overcome the frequent restriction that a high transfection efficiency is accompanied by high cytotoxicty. To this end, we introduced LPEIs with low MW and biodegradable PEIs that are far more efficient and substantially less toxic in cell lines *in vitro* than other polymer-based systems reported in literature. Furthermore, these polymer-based systems are easy to handle and the transfection procedure is reproducible and independent of external influences.

Polyplexes are challenged by numerous biological barriers on their way to the nucleus. We strove to gain more insight into the knowledge of interaction of polyplexes with these obstacles.

The PEI-based systems presented here could be an excellent basis for future studies directed at the transfection of primary cells *in vitro*. A key step will be the development of PEI-based polyplexes with tailored structure-composition-properties that react to specific changes of their environment to enhance the cellular and nuclear entry.

References

1. Han So, Mahato RI, Sung YK, Kim SW. Development of biomaterials for gene therapy. *Mol Ther* 2000; **2**: 302-317.

2. De Smedt SC, Demeester J, Hennink WE. Cationic polymer based gene delivery systems. *Pharm Res* 2000; **17**: 113-126.

3. Mehier-Humbert S, Guy RH. Physical methods for gene transfer: improving the kinetics of gene delivery into cells. *Adv Drug Deliv Rev* 2005; **57**: 733-753.

4. Duzgunes N, Tros de Ilarduya C, Simoes S, Zhdanov RI, Konopka K, Pedroso de Lima MC. Cationic liposomes for gene delivery: Novel cationic lipids and enhancement by proteins and peptides. *Curr Med Chem* 2003; **10**: 1213-1220.

5. Liu D, Ren T, Gao X. Cationic transfection lipids. *Curr Med Chem* 2003; **10**: 1307-1315.

6. Marshall E. What to do when clear success comes with an unclear risk? *Science* 2002; **298**: 510-511.

7. Sadelain M. Insertional oncogenesis in gene therapy: how much of a risk? *Gene Ther* 2004; **11**: 569-573.

8. Boussif O, Lezoualc'h F, Zanta MA, Mergny MD, Scherman D, Demeneix B, Behr J. A versatile vector for gene and oligonucleotide transfer into cells in culture and in vivo: polyethylenimine. *Proc Natl Acad Sci U S A* 1995; **92**: 7297-7301.

9. Wightman L, Kircheis R, Rossler V, Carotta S, Ruzicka R, Kursa M, Wagner E. Different behavior of branched and linear polyethylenimine for gene delivery in vitro and in vivo. *J Gene Med* 2001; **3**: 362-372.

10. Lungwitz U, Breunig M, Blunk T, Goepferich A. Synthesis and application of low molecular weight linear polyethylenimines for non-viral gene delivery. *Proceedings of the annual meeting of the German Pharmaceutical Society* 2004; P T25: 157.

11. Jares-Erijman EA, Jovin TM. FRET imaging. *Nature Biotechnol* 2003; **21**: 1387-1395.

12. Foerster T. Intermolecular energy transference and fluorescence. *Ann Phys [6 Folge]* 1948; **2**: 55-75.

13. Xia Z, Liu Y. Reliable and global measurement of fluorescence resonance energy transfer using fluorescence microscopes. *Biophys J* 2001; **81**: 2395-2402.

Appendix

Abbreviations

^{1}H-NMR	proton nuclear magnetic resonance
ANOVA	analysis of variance
APC	antigen presenting cell
As4.1	cell line from the murine kidney
ATP	adenosine triphosphate
bp	base pair
BPEI	branched PEI
CD	cluster of differentiation
CHO-K1	chinese hamster ovarian cell line
CLSM	confocal laser scanning microscopy
CMV	cytomegalovirus
CO_2	carbon dioxide
COS-7	monkey kidney cell line
Da	Dalton
DC	dendritic cell
DMEM	Dulbecco`s modified eagle`s medium
DMSO	dimethyl sulfoxide
DNA	deoxyribonucleic acid
DNase	deoxyribonuclease
DTS	DNA nuclear targeting sequences
DTT	dithiotreitol
E	the energy transfer efficiency of a FRET pair
EDTA	ethylendiaminetetraacetic acid
EGFP	enhanced green fluorescent protein
ET	the energy transfer efficiency of a FRET pair expressed by donor quenching
EtBr	ethidium bromide
ET_p	the energy transfer parameter of a FRET pair
FACS	fluorescence activated cell sorting
FBS	fetal bovine serum
Fc	FRET corrected
FCS	fluorescence correlation spectroscopy

FISH	fluorescent in situ hybridzation
FM4-64	N-(3-triethylammoniumpropyl)-4-(6-(4-(diethylamino)phenyl)hexatrienyl)pyridinium dibromide
Fn	FRET net
FRET	fluorescence resonance energy transfer
GFP	green fluorescent protein
Glc	glucose
GM-CSF	granulocyte-macrophage colony stimulating factor
GSH MEE	glutathione monoethyl ester
Ham´s F-12	Nutrient Mixture F-12
HeLa	human cervical carcinoma cell line
His-PLL	histidylated PLL
HIV	human immunodeficiency virus
HT-29	human colorectal adenocarcinoma cell line
iDC	immature DC
IL-4	interleukine-4
J	the overlap integral
κ^2	the orientationof the transition moments of the donor and acceptor molecules of a FRET pair
kDa	kilo Dalton
k_T , k_F, k_D	various rate constants describing decay events of the donor molecules of a FRET pair
LL quadrant	lower left quadrant
LPEI	linear PEI
LR-LPEI	biodegradable PEI
LR quadrant	lower right quadrant
mDC	mature DC
MHC	major histocompatibility complex
mPEI	per-N-methylated PEI
MTS	[3-(4,5-dimethylthiazol-2-yl)-5-(3-carboxymethoxyphenyl)-2-(4-sulfophenyl)-2H-tetrazolium-inner salt]
MW	molecular weight
MWCO	molecular weight cut off
n	the refractive index

NF	normalized FRET
NLS	nuclear localization signal
NPC	nuclear pore complex
NP ratio	the ratio of nitrogens in polymer to phosphates in DNA
PAM	polyamidoamine
PBMC	peripheral blood monocytotic cell
PBS	phosphate-buffered saline
PCR	polymerase chain reaction
pDEAEMA	poly(diethylaminoethyl methylacrylate)
PEI	poly(ethylenimine)
pEGFP-N1	plasmid encoding EGFP
pGL3-enhancer vector	plasmid encoding firefly luciferase
PI	polydispersity index
PLL	poly(L-lysine)
PNA	peptide nucleic acid
PTDs	protein transduction domains
R	the distance between the FRET dye pair
R_0	the characteristic separation distance of every FRET dye pair defining where the probability of energy transfer is 50%.
RLU	relative light units
RNA	ribonucleic acid
rpm	rotations per minute
ROI	region of interest
SDS	dodium dodecyl sulfate
SF	serum free
SV40	simian virus 40
τ	the lifetime of a fluorophore
TAMRA	tetramethylrhodamine
Tris buffer	tris(hydroxymethyl)aminomethane buffer
UL quadrant	upper left quadrant
UR quadrant	upper right quadrant
UV	ultraviolett light or irradiation

Curriculum Vitae

Name:	Miriam Annemone Breunig
Date of birth:	September 14, 1976
Place of birth:	Buchen, Odenwald
Nationality:	German
Martial status:	Single

Education

09/83 – 07/87	Elementry School: Grundschule, Mudau
09/87 – 06/96	Grammer School: Burghardt-Gymnasium, Buchen
06/96	University-entrance diploma (Abitur)

Professional Training

10/96 – 10/00	Studies of Pharmacy: Ruprecht Karls University, Heidelberg
10/97	Practical Training: Scherer GmbH, Eberbach (Department: Analytics)
04/99 – 05/99	Practical Training: BASF AG, Ludwigshafen (Department: Galenics)
08/99 – 09/99	Practical Training: Knoll GmbH, Ludwigshafen (Department: Quality control)
11/00 – 04/01	Pharmaceutical Traineeship: Knoll GmbH, Ludwigshafen (Department: Quality control)
05/01 – 10/01	Pharmaceutical Traineeship: Mozart Apotheke, Oftersheim
12/01	Acquisition of the licence to practise as pharmacist
01/02 - today	PhD program at the Department of Pharmaceutical Technology of the University of Regensburg

List of Publications

Publications

1. Breunig M, Lungwitz U, Klar J, Kurtz A, Blunk T, Goepferich A: Polyplexes of polyethylenimine and per-n-methylated polyethylenimine-cytotoxicity and transfection efficiency. Journal of Nanoscience and Nanotechnology **4** (2004): 512-520 (Chapter 7).
2. Drotleff S, Lungwitz U, Breunig M, Dennis A, Blunk T, Tessmar J, Goepferich A. Biomimetic polymers in pharmaceutical and biomedical sciences. European Journal of Pharmaceutics and Biopharmaceutics 2004; **58**: 385-407
3. Lungwitz U, Breunig M, Blunk T, Gopferich A. Polyethylenimine-based non-viral gene delivery systems. European Journal of Pharmaceutics and Biopharmaceutics 2005; **60**: 247-266.
4. Breunig M, Lungwitz U, Liebl R, Fontanari C, Klar J, Kurtz A, Blunk T, Goepferich A. Gene delivery with low molecular weight linear polyethylenimines. Journal of Gene Medicine 2005; **7**: 1287-1298 (Chapter 2).

Conference Abstracts

1. Breunig M, Lungwitz U, Klar J, Kurtz A, Blunk T, Goepferich A: Gene delivery with modified polyethylenimine. DPHG Jahrestagung, Berlin, Germany (2002).
2. Lungwitz U, Breunig M, Blunk T, Goepferich A: Synthesis of per-N-methylated polyethylenimine as a novel non-viral vector for gene delivery. DPHG Jahrestagung, Berlin, Germany (2002).
3. Breunig M, Lungwitz U, Klar J, Kurtz A, Blunk T, Goepferich A: Gene delivery with non-toxic per-N-methylated PEI / DNA polyplexes. Controlled Release Society, Glasgow, Scotland (2003).
4. Breunig M, Lungwitz U, Klar J, Kurtz A, Blunk T, Goepferich A: Per-N-methylated polyethylenimine as non-viral carrier for gene delivery with low cytotoxicity. American Chemical Society, New York, USA (2003).
5. Breunig M, Lungwitz U, Klar J, Kurtz A, Blunk T, Goepferich A: A Novel method for the simultaneous determination of the transfection efficiency and cytotoxicity in non-viral gene delivery. Arbeitsgemeinschaft für Pharmazeutische Verfahrenstechnik, Nuernberg, Germany (2004).

6. Breunig M, Lungwitz U, Klar J, Kurtz A, Blunk T, Goepferich A: Transfection efficiency and cytotoxicity of low molecular weight linear polyethylenimines in vitro. Controlled Release Society German Chapter Annual Meeting, Heidelberg, Germany (2004).
7. Lungwitz U, Breunig M, Drotleff S, Knerr R, Blunk T, Goepferich A: Low molecular weight linear polyethylenimines for non-viral transfection. Controlled Release Society German Chapter Annual Meeting, Heidelberg, Germany (2004)
8. Lungwitz U, Breunig M, Blunk T, Goepferich A: Synthesis and application of low molecular weight linear polyethylenimines for non-viral gene delivery. Proceedings of the annual meeting of the Austrian, Czech and German Pharmaceutical Societies, Regensburg, Germany (2004).
9. Lungwitz U, Breunig M, Blunk T, Goepferich A: Low molecular weight linear polyethylenimines for non-viral gene delivery. Society for Biomaterials Conference: Biomaterials in Regenerative Medicine: The Advent of Combinatio, Philadelphia, Pennsylvania, USA (2004).
10. Breunig M, Lungwitz U, Liebl R, Klar J, Kurtz A, Blunk T, Goepferich A: Low molecular weight linear polyethylenimines as promising vehicles for non-viral gene delivery. American Association of Pharmaceutical Scientists, Baltimore, USA (2004).
11. Breunig M, Lungwitz U, Blunk T, Tessmar J, Goepferich A. Drug and Gene Delivery for Tissue Engineering Applications, 4th Annual Meeting of the European Tissue Engineering Society, Munich, Germany (2005).
12. Breunig M, Lungwitz U, Liebl R, Klar J, Obermayer B, Blunk T, Goepferich A. Mechanistic Insights into linear polyethylenimine – mediated gene trasnfer. European Society of Gene Therapy, Prague, Czech Republic (2005).

Award

Controlled Release Society German Chapter Annual Meeting (2004) Oral Presentation

Acknowledgements

Mein besonderer Dank gilt

Herrn Prof. Göpferich für das Thema, für die kontinuierliche Unterstützung und vor allem für seinen Enthusiasmus beim Fortgang der Arbeit. Die zahlreichen Diskussionen und Gespräche waren sehr wertvoll. Weiterhin möchte ich mich für die Förderung zur Teilnahme an nationalen und internationalen Kongressen bedanken.

Uta Lungwitz für die Synthese der Polymere, die außerordentlich fruchtbare Zusammenarbeit bei unserem Projekt und die zahlreichen kritischen und wertvollen Diskussionen.

Renate Liebl für die überaus engagierte Zusammenarbeit und intensive Unterstützung bei unserem Projekt.

Dr. Jürgen Klar für die umfassende Hilfestellung und das Einarbeiten in die Zellkultur, die Transfektion und bei weiteren Problemen. Birgit Obermayer danke ich für die wertvollen Tipps und die Unterstützung bei der rt-PCR. In diesem Zusammenhang möchte ich Herrn Prof. Armin Kurtz danken, der diese Zusammenarbeit ermöglicht hat (Institut für Physiologie, Universität Regensburg).

Allison Dennis (Department of Biomedical Engineering, Georgia Institute of Technology, Atlanta, USA) für die gewissenhafte und konstruktive Durchsicht zahlreicher Manuskripte einschließlich dieser Arbeit.

Claudia Fontanari für ihre Mitarbeit während ihrer Diplomarbeit an unserem Institut.

Prof. Ralf Wagner und Dr. Josef Köstler für die Hilfe und das Einarbeiten in die Dendritenzellkultur (Institut für Mikrobiologie, Klinikum Universität Regensburg).

Dr. Gero Brockhoff (Pathologie, Klinikum Universität Regensburg) für die Einführung in Mehrfarbmessungen am FACS.

Weiterhin möchte ich mich recht herzlich bedanken bei

Bernhard Appel, Andrea Blaimer, Dr. Torsten Blunk, Ferdinand Brandl, Sigrid Drotleff, Daniela Eyrich, Dr. Claudia Fischbach, Lydia Frommer, Dr. Michael Hacker, Robert Knerr, Stefan Kolb, Dr. Esther Lieb, Angelika Maschke, Liane Öttl, Edith Schindler, Florian Sommer, Dr. Jörg Teßmar, allen derzeitigen und ehemaligen Kolleginnen und Kollegen und Stella Schreiner für die konstruktive Zusammenarbeit, ihre Diskussionsfreudigkeit und Unterstützung in vielfältigen Belangen sowie die außerfachlichen Gespräche und Aktivitäten.

Abschießend gilt mein tiefer Dank meinen Eltern, meiner Schwester Esther und Peter Feldmeier, die mir diesen Weg ermöglicht und mich auf ihm bestärkt und unterstützt haben!